ARTIC ATMOSPHERIC NOISE AND PROPAGATION STUDIES. PART A. ARCTIC SFERIC DATA-- AUGUST 1958 TO MARCH 1969

A. L. Whitson

Stanford Research Institute

Prepared for:

Air Force Cambridge Research Laboratories

February 1960

CONTRACT AF 19(604)-2

ARCTIC ATMOSPHERIC NOISE AND PROPAGATION STUDIES
Part A: Arctic Sferic Data--August 1958 to March 1959

By: A. L. Whitson

Prepared for:

AIR FORCE CAMBRIDGE RESEARCH CENTER
LAURENCE G. HANSCOM FIELD

AIR RESEARCH AND DEVELOPMENT COMMAND
BEDFORD, MASSACHUSETTS

Unclassified

Security Classification

DOCUMENT CONTROL DATA - R&D

(Security classification of title, body of abstract and indexing annotation must be entered when the overall report is classified)

1. ORIGINATING ACTIVITY *(Corporate author)*
Stanford Research Institute
Menlo Park, California

2a. REPORT SECURITY CLASSIFICATION
Unclassified

2b. GROUP

3. REPORT TITLE
ARCTIC ATMOSPHERIC NOISE AND PROPAGATION STUDIES
PART A: ARCTIC SFERIC DATA - AUGUST 1958 TO MARCH 1959

4. DESCRIPTIVE NOTES *(Type of report and inclusive dates)*
Scientific Final.

5. AUTHOR(S) *(First name, middle initial, last name)*
A. L. Whitson

6. REPORT DATE	7a. TOTAL NO. OF PAGES	7b. NO. OF REFS
February 1960	202	33

8a. CONTRACT OR GRANT NO.	9a. ORIGINATOR'S REPORT NUMBER(S)
AF19(604)-2409	
b. PROJECT, TASK, WORK UNIT NOS. 4662	
c. DOD ELEMENT n/a	9b. OTHER REPORT NO(S) *(Any other numbers that may be assigned this report)* AFCRC-TR-60-118(A)
d. DOD SUBELEMENT n/a	

10. DISTRIBUTION STATEMENT
Approved for public release; distribution unlimited

11. SUPPLEMENTARY NOTES	12. SPONSORING MILITARY ACTIVITY
TECH, OTHER	Air Force Cambridge Research Laboratories (LI) L. G. Hanscom Field Bedford, Massachusetts 01730

13. ABSTRACT From August 1958 through March 1959 Stanford Research Institute operated sferic monitoring stations at Fairbanks, Alaska, at Thule, Greenland, and at St. Johns, Newfoundland to record sferic 3- to 30-kc waveforms, direction of arrival, and rates of occurrence of sferics, and atmospheric noise levels from 12 to 30 kc.

Large amounts of the above data have been recorded. Also, uniformly distributed samples of the data have been analyzed to determine sferic amplitude and direction-of-arrival distributions, sferic waveform types, sferic ELF content, sferic source locations in all portions of the Northern Hemisphere, and RMS atmospheric noise levels as functions of time of day and season. In addition, the application of the data collected to the better understanding of VLF propagation and of the influence of geophysical phenomena are discussed.

The preliminary results of this analysis have been published in eight Monthly Data-Summary Bulletins and seven Monthly Data-Summary Bulletin Supplements, Sferic Source Locations.

The equipment used has been described in Technical Report 1 on this contract "SRI Sferic Monitoring System" ASTIA No. AD214947.

I

Details of illustrations in this document may be better studied on microfiche

DD FORM 1 NOV 65 1473

Unclassified

Security Classification

14. KEY WORDS	LINK A		LINK B		LINK C	
	ROLE	WT	ROLE	WT	ROLE	WT

AFCRC-TR-60-118(A)

FEBRUARY 1960

ARCTIC ATMOSPHERIC NOISE AND PROPAGATION STUDIES

Part A: Arctic Sferic Data—August 1958 to March 1959

By: A. L. Whitson

SRI Project 2418

Prepared for:

AIR FORCE CAMBRIDGE RESEARCH CENTER
LAURENCE G. HANSCOM FIELD

AIR RESEARCH AND DEVELOPMENT COMMAND
BEDFORD, MASSACHUSETTS

CONTRACT AF 19(604)-2409

APPROVED:

E. A. Post, Manager
Radio and Weather Sciences Laboratory

D. R. Scheuch, Assistant Director
Division of Engineering Research

Copy No. 33

II

ABSTRACT

From August 1958 through March 1959 Stanford Research Institute operated sferic monitoring stations at Fairbanks, Alaska, at Thule, Greenland, and at St. Johns, Newfoundland to record sferic 3- to 30-kc waveforms, direction of arrival, and rates of occurrence of sferics, and atmospheric noise levels from 12 to 30 kc.

Large amounts of the above data have been recorded. Also, uniformly distributed samples of the data have been analyzed to determine sferic amplitude and direction-of-arrival distributions, sferic waveform types, sferic ELF content, sferic source locations in all portions of the Northern Hemisphere, and RMS atmospheric noise levels as functions of time of day and season. In addition, the application of the data collected to the better understanding of VLF propagation and of the influence of geophysical phenomena are discussed.

The preliminary results of this analysis have been published in eight Monthly Data-Summary Bulletins and seven Monthly Data-Summary Bulletin Supplements, Sferic Source Locations.

The equipment used has been described in Technical Report 1 on this contract "SRI Sferic Monitoring System" ASTIA No. AD 214947.

PREFACE

This is the first part of a two-part Final Report. Part B is published separately with a classification of SECRET-RESTRICTED DATA. The work recorded in this Final Report was sponsored by the Air Research and Development Command, Air Force Cambridge Research Center, under Contract AF 19(604)-2409.

CONTENTS

ABSTRACT iii
PREFACE v
LIST OF ILLUSTRATIONS xi
LIST OF TABLES xv

I INTRODUCTION 1

A. Purpose 1
B. Method of Approach 1
C. Data Forms 2
D. Scope of This Report 5

II CONCLUSIONS 8

III SFERIC RATES AND AMPLITUDE DISTRIBUTIONS 10

A. Diurnal Variations in Sferic Rate 10
B. Monthly Variations in Sferic Rate 14
C. Sferic Amplitude Distributions 14
D. Direction-of-Arrival Variations 21

IV WAVEFORM TYPES 22

A. Waveform Classification 22
B. Distribution of Waveform Types 22

V RMS ATMOSPHERIC NOISE 29

A. RMS Noise Measurements 29
B. Diurnal Variation of RMS Noise Level 29
C. Monthly Variation of RMS Noise Level 29
D. RMS Noise Spectrum Variations 33

VI LOCATION OF ACTIVITY 34

A. Source Location of Individual Sferics 34
B. Storm Center Locations 43
C. Thunderstorm Days 43

VII ELF FROM SFERICS 45

A. VLF/ELF Ratio 45
B. A Note Concerning ELF Propagation 51

VIII SOME OBSERVATIONS ON VLF PROPAGATION 54

A. Relative Received Peak Amplitude 54
B. Propagation Over Specific Arctic Paths 54
C. Atmospheric Noise Spectrum 58
D. VLF Station Reception 58

IX CORRELATION WITH GEOPHYSICAL DATA 59

A. Solar Influence 59
B. Sunspot Number and Magnetic Index 59
C. Solar Flares 59

Acknowledgment 63

Appendix A--Installation 65
1. Site Selection 67
2. Fairbanks, Alaska 67
3. Thule, Greenland 69
4. St. Johns, Newfoundland 71

Appendix B--Available Sferic Data 73
1. Introduction 75
2. Waveform and DF Film 75
3. Integrated DF Film 83
4. Events Counter 83
5. Scanning Receiver 83
6. Miscellaneous Data 84

Appendix C--Calibration and Performance Measurements 85
1. Introduction 87
2. Vertical Antenna Effective Height 87
3. Calibration Circuit 89
4. Waveform and DF Film 91
5. Events Counter 92
6. Scanning Receiver 92
7. Time Standard 92
8. Sferic Amplitude Corrections 94
9. Direction-of-Arrival Corrections 97
10. Scanning Receiver Amplitude Corrections 97

Appendix D--Amplitude and Direction-of-Arrival Distributions . . 101

Appendix E--Event Counters 121

Appendix F--RMS Noise Spectrum - 12 to 30 kc 141

Appendix G--Integrated DF 163

Appendix H--Direction-of-Arrival Accuracy 179

Appendix I--Waveform and DF Film IBM Format 185

Bibliography 189

ILLUSTRATIONS

Fig.	I-1	Waveform and DF Film Sample	3
Fig.	I-2	Integrated DF Film Sample	4
Fig.	I-3	Scanning Receiver Sample Records	6
Fig.	III-1	Diurnal Sferic Rate in Quarter GMT Days at Fairbanks, Alaska--September 1958 to March 1959.	11
Fig.	III-2	Diurnal Sferic Rate in Quarter GMT Days at Thule, Greenland--September 1958 to March 1959	12
Fig.	III-3	Diurnal Sferic Rate in Quarter GMT Days at St. Johns, Newfoundland--September 1958 to March 1959.	13
Fig.	III-4	Monthly Sferic Rate at Fairbanks Alaska--August 1958 to March 1959	15
Fig.	III-5	Monthly Sferic Rate at Thule, Greenland--September 1958 to March 1959.	16
Fig.	III-6	Monthly Sferic Rate at St. Johns, Newfoundland--August 1958 to March 1959	17
Fig.	III-7	Winter Sferic Amplitude Distribution, Fairbanks, Alaska	18
Fig.	III-8	Winter Sferic Amplitude Distribution, Thule, Greenland	19
Fig.	III-9	Winter Sferic Amplitude Distribution, St. Johns, Newfoundland	20
Fig.	IV-1	Sferic Waveform Classifications.	23
Fig.	IV-2	Monthly Waveform Types, Fairbanks, Alaska--August 1958 to March 1959	25
Fig.	IV-3	Monthly Waveform Types, Thule, Greenland--September 1958 to March 1959.	26
Fig.	IV-4	Monthly Waveform Types, St. Johns, Newfoundland--August 1958 to March 1959	27
Fig.	V-1	Diurnal RMS Noise Level Variation, January 1959.	30
Fig.	V-2	RMS Noise Level at 0300, 0900, 1500, and 2100 Hours GMT--August 1958 to March 1959.	31
Fig.	V-3	Monthly RMS Noise Level, August 1958 to March 1959	32
Fig.	VI-1	Identification of Individual Sferics	35
Fig.	VI-2	Sferic Activity, September 1958	36
Fig.	VI-3	Sferic Activity, October 1958	37
Fig.	VI-4	Sferic Activity, November 1958	38
Fig.	VI-5	Sferic Activity, December 1958	39
Fig.	VI-6	Sferic Activity, January 1959	40
Fig.	VI-7	Sferic Activity, February 1959	41
Fig.	VI-8	Sferic Activity, March 1959	42
Fig.	VI-9	Diurnal Variation in Sferic Activity at the Sferic Source	44

Preceding page blank

Fig. VII-1 Distribution of VLF/ELF Ratio, St. Johns, Newfoundland--January 1959. 47
Fig. VII-2 Diurnal Variation of VLF/ELF Ratio, St. Johns, Newfoundland--January 1959. 48
Fig. VII-3 Diurnal Variation of ELF Polarity, St. Johns, Newfoundland--January 1959. 49
Fig. VII-4 Distribution of VLF/ELF Ratio, Thule, Greenland--September 1958 50
Fig. VII-5 VLF/ELF Ratio as Function of Signal Amplitude, Thule, Greenland--September 1959. 52
Fig. VII-6 ELF Waveforms 53

Fig. VIII-1 Relative Received Peak Amplitude Geographic Distribution 55
Fig. VIII-2 Sferic Propagated Along Fairbanks-Thule Path 56
Fig. VIII-3 Sferic Propagated Along St. Johns-Thule Path 57

Fig. IX-1 Scanning Receiver Data During Solar Flare, 13 October 1958 61

Fig. A-1 Installation at Fairbanks, Alaska. 68
Fig. A-2 Installation at Thule, Greenland 70
Fig. A-3 Installation at St. Johns, Newfoundland. 72

Fig. B-1 Film Operating Schedule--August 1958 to November 1958 76
Fig. B-2 Film Operating Schedule--December 1958 to March 1959 77

Fig. C-1 Vertical Antenna Equivalent Height 88
Fig. C-2 Simplified Calibration Circuit 90
Fig. C-3 Sferic System Frequency Response 93
Fig. C-4 Measurement of Timing Accuracy, 12 November 1958 . . . 95
Fig. C-5 Time Measurement Accuracy 96
Fig. C-6 Scanning Receiver Calibration at 10 μv per meter . . . 98

Fig. D-1 Sferic Amplitude Distribution--August 1958 104
Fig. D-2 Sferic Amplitude Distribution--September 1958. 105
Fig. D-3 Sferic Amplitude Distribution--October 1958. 106
Fig. D-4 Sferic Amplitude Distribution--November 1958 107
Fig. D-5 Sferic Amplitude Distribution--December 1958 108
Fig. D-6 Sferic Amplitude Distribution--January 1959. 109
Fig. D-7 Sferic Amplitude Distribution--February 1959 110
Fig. D-8 Sferic Amplitude Distribution--March 1959 111
Fig. D-9 Direction-of-Arrival Distribution--August 1958 112
Fig. D-10 Direction-of-Arrival Distribution--September 1958. . . 113
Fig. D-11 Direction-of-Arrival Distribution--October 1958. . . . 114
Fig. D-12 Direction-of-Arrival Distribution--November 1958 . . . 115
Fig. D-13 Direction-of-Arrival Distribution--December 1958 . . . 116
Fig. D-14 Direction-of-Arrival Distribution--January 1959 . . . 117
Fig. D-15 Direction-of-Arrival Distribution--February 1959 . . . 118
Fig. D-16 Direction-of-Arrival Distribution--March 1959 119

Fig. E-1 Sferics per Second at Fairbanks, Alaska--
December 1958 124
Fig. E-2 Sferics per Second at Fairbanks, Alaska--
January 1959 125
Fig. E-3 Sferics per Second at Fairbanks, Alaska--
February 1959. 126
Fig. E-4 Sferics per Second at Fairbanks, Alaska--
March 1959 127
Fig. E-5 Sferics per Second at Thule, Greenland--
September 1958 128
Fig. E-6 Sferics per Second at Thule, Greenland--
October 1958 129
Fig. E-7 Sferics per Second at Thule, Greenland--
November 1958. 130
Fig. E-8 Sferics per Second at Thule, Greenland--
January 1959 131
Fig. E-9 Sferics per Second at Thule, Greenland--
February 1959. 132
Fig. E-10 Sferics per Second at Thule, Greenland--
March 1959 133
Fig. E-11 Sferics per Second at St. Johns, Newfoundland--
August and September 1958 134
Fig. E-12 Sferics per Second at St. Johns, Newfoundland--
October 1958. 135
Fig. E-13 Sferics per Second at St. Johns, Newfoundland--
November 1958 136
Fig. E-14 Sferics per Second at St. Johns, Newfoundland--
December 1958. 137
Fig. E-15 Sferics per Second at St. Johns, Newfoundland--
January 1959 138
Fig. E-16 Sferics per Second at St. Johns, Newfoundland--
March 1959 139

Fig. F-1 RMS Noise Spectrum at Fairbanks, Alaska--
October 1958 144
Fig. F-2 RMS Noise Spectrum at Fairbanks, Alaska--
November 1958. 145
Fig. F-3 RMS Noise Spectrum at Fairbanks, Alaska--
December 1958. 146
Fig. F-4 RMS Noise Spectrum at Fairbanks, Alaska--
January 1959 147
Fig. F-5 RMS Noise Spectrum at Fairbanks, Alaska--
February 1959. 148
Fig. F-6 RMS Noise Spectrum at Fairbanks, Alaska--
March 1959 149
Fig. F-7 RMS Noise Spectrum at Thule, Greenland--
September 1958 150
Fig. F-8 RMS Noise Spectrum at Thule, Greenland--
October 1958 151
Fig. F-9 RMS Noise Spectrum at Thule, Greenland--
November 1958. 152

Fig. F-10 RMS Noise Spectrum at Thule, Greenland--
December 1958 153
Fig. F-11 RMS Noise Spectrum at Thule, Greenland--
January 1959 154
Fig. F-12 RMS Noise Spectrum at Thule. Greenland--
February 1959. 155
Fig. F-13 RMS Noise Spectrum at Thule, Greenland--
March 1959. 156
Fig. F-14 RMS Noise Spectrum at St. Johns, Newfoundland--
September 1958 157
Fig. F-15 RMS Noise Spectrum at St. Johns, Newfoundland--
October 1958. 158
Fig. F-16 RMS Noise Spectrum at St. Johns, Newfoundland--
November 1958. 159
Fig. F-17 RMS Noise Spectrum at St. Johns, Newfoundland--
December 1958 160
Fig. F-18 RMS Noise Spectrum at St. Johns, Newfoundland--
January 1959 161
Fig. F-19 RMS Noise Spectrum at St. Johns, Newfoundland--
February and March 1959. 162

Fig G-1 Ten Min. Integrated DF,Fairbanks, Alaska--
25-26 September 1958 166
Fig. G-2 Ten Min. Integrated DF,Thule, Greenland--
25-26 September 1958--10 mv/m. 167
Fig. G-3 Ten Min. Integrated DF, St. Johns, Newfoundland--
25-26 September 1958--100 mv/m. 168
Fig. G-4 Ten Min. Integrated DF, Fairbanks, Alaska--
13-14 November 1958--10 mv/m 169
Fig. G-5 Ten Min. Integrated DF, Thule, Greenland--
13-14 November 1958--10 mv/m 170
Fig. G-6 Ten Min. Integrated DF, St. Johns, Newfoundland--
13-14 November 1958--10 mv/m 171
Fig. G-7 Ten Min. Integrated DF, Fairbanks, Alaska--
13-14 January 1959--10 mv/m 172
Fig. G-8 Ten Min. Integrated DF, Thule, Greenland--
13-14 January 1959--10 mv/m 173
Fig. G-9 Ten Min. Integrated DF, St. Johns, Newfoundland--
13-14 January 1959--10 mv/m 174
Fig. G-10 Ten Min. Integrated DF, Fairbanks, Alaska--
14-15 March 1959--10 mv/m 175
Fig. G-11 Ten Min. Integrated DF, Thule, Greenland--
14-15 March 1959-- 30 mv/m 176
Fig. G-12 Ten Min. Integrated DF, St. Johns, Newfoundland--
14-15 March 1959--10 mv/m. 177

TABLES

Table	IV-1	Percentage of Waveforms in Each Classification During Each Quarter of the GMT Day	24
Table	VII-1	VLF/ELF Ratio Data	46
Table	B-1	Daily Waveform and DF Film Schedule, 21 August 1958 to 30 September 1958	78
Table	B-2	Daily Waveform and DF Film Schedule, 1 October 1958 to 31 October 1958	79
Table	B-3	Daily Waveform and DF Film Schedule, 1 November 1958 to 3 January 1959	80
Table	B-4	Daily Waveform and DF Film Schedule, 4 January to 28 February 1959	81
Table	B-5	Daily Waveform and DF Film Schedule, 1 March to 31 March 1959	82
Table	H-1	Closing Angle	182
Table	H-2	VLF Station DF Data	183

ARCTIC SFERIC DATA--AUGUST 1958 to MARCH 1959

I INTRODUCTION

A. Purpose

The investigation of atmospheric noise (sferics) started around the turn of the century and has continued in all parts of the world since that time. Sferics have been observed to determine atmospheric noise levels, the nature of VLF propagation, the location of thunderstorms, and solar effects upon the ionosphere.* With few exceptions, these investigations have been made with systems designed to observe sferic phenomena at relatively close ranges and at middle latitudes. It was the goal of this project to gather consistent, reliable, detailed, all-season data on atmospheric noise (sferic) phenomena in the entire Northern Hemisphere by a single system, located in the Arctic.

Stanford Research Institute, under contract to AFCRC, designed and operated a sferic monitoring net with stations at Fairbanks, Alaska, at Thule, Greenland, and at St. Johns, Newfoundland,** to collect diurnal and seasonal sferic data in the entire Northern Hemisphere, and to investigate VLF propagation in the Arctic. The monitoring stations were in operation from August 1958 through March 1959.

B. Method of Approach

Since the nature and magnitude of sferics that could be received in the Arctic were unknown, the data recording systems had to be capable of a wide range of operating modes. This capability was achieved by designing special equipment made up of several flexible sub-systems that could be used separately or in combination.[1] The system was used seven days a week to collect large amounts of sferic data at various operating conditions.***

Analysis was made on selected samples of data. These samples were then combined and averaged and were presented in preliminary form in eight Monthly Data-Summary Bulletins. All data collected have been cataloged and are available in their original form at the contracting agency.

---

* The Bibliography, p. 189, contains a list of publications on VLF research

** See Appendix A for a description of the installations

[1] The system used is described in Technical Report 1, "SRI Sferic Monitoring System," ASTIA No. AD-214947 of this contract.

*** See Appendix B for operating schedule

C. Data Forms

Sferic data were collected in the following forms. The names given here to the various data forms will be used throughout this and subsequent reports.

1. Waveform and DF Film

Atmospheric noise (sferic) waveforms, as received on an omnidirectional vertical antenna, were amplified by a receiver having a 3- to 30-kc bandwidth and applied (without detection or frequency translation) to a triggered, two-speed sweep on one beam of a dual-beam oscilloscope. The sweep speeds used were one millisecond for the first half of the sweep and ten milliseconds for the last half of the sweep. Triggering of the oscilloscope sweep was from the positive or negative peak amplitude of individual sferics that exceeded a pre-set triggering level (threshold). This triggering level could easily be changed by a 10-db step attenuater receiver-gain adjustment. The waveform receiver and display system was linear over a 20-db amplitude range.

In addition to the sferic waveform display, the instantaneous direction of arrival of the individual sferic signal was displayed on the second beam of the oscilloscope. Crossed loops and two receivers identical to the waveform receiver were used. The DF display was Z-axis-modulated with the first 300 microseconds of the signal from the waveform receiver to obtain a triggered DF display that contained sense information.

A continuous-motion 35mm camera with a film speed of one inch per second* recorded the signals displayed on the oscilloscope. In addition, a clock and timing lights within the camera were driven from a battery-operated time standard synchronized to the Bureau of Standards Radio Station, WWV, to place Greenwich Mean Time (GMT) on the 35mm photographic film. Figure I-1 shows a typical waveform-and-DF-film sample that contains three sferic waveforms and their indicated direction of arrival.

2. Integrated DF Film

The system described above which was used to record waveform and direction-of-arrival information simultaneously on film was also used to obtain only direction-of-arrival data. The waveform trace of the dual beam oscilloscope was turned off and a camera film drive system was used, which allowed the film to stand still for an interval of from one minute to one hour and record the direction-of-arrival of all sferics that exceeded the system threshold during the interval. At the end of each interval, the time was marked on the film and the film was advanced approximately one inch to record the next interval. These film records are called integrated DF film since each film frame records the integrated direction-of-arrival distribution of sferic activity for the interval chosen. Figure I-2 shows a sample of integrated DF film with two frames

*Film speeds of 1/8, 1/4, 1/2, 1, 2, 4, and 8 inches per second were available. Normal operation used 1 inch per second.

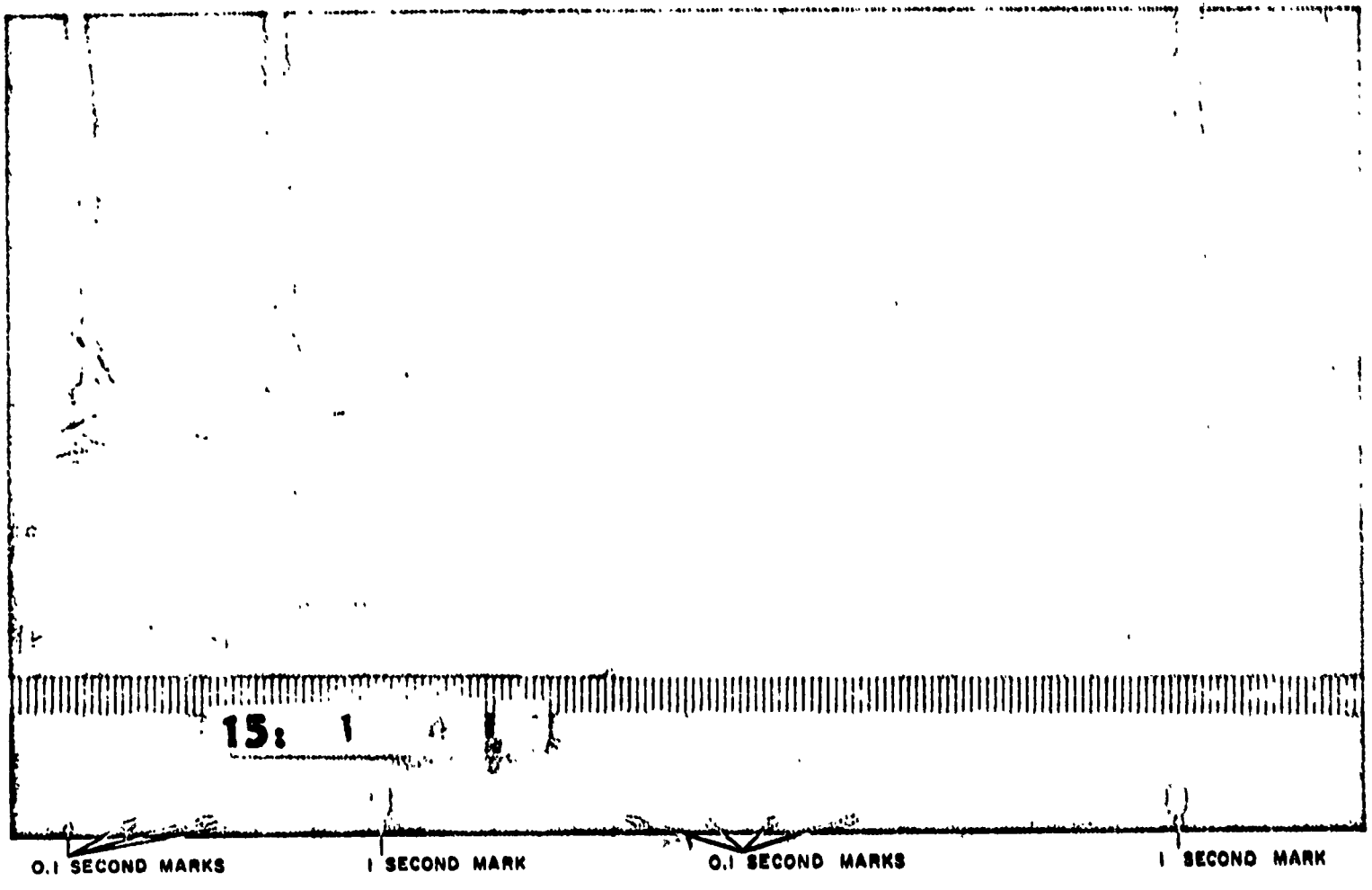

FIG. I-1
WAVEFORM AND DF FILM SAMPLE

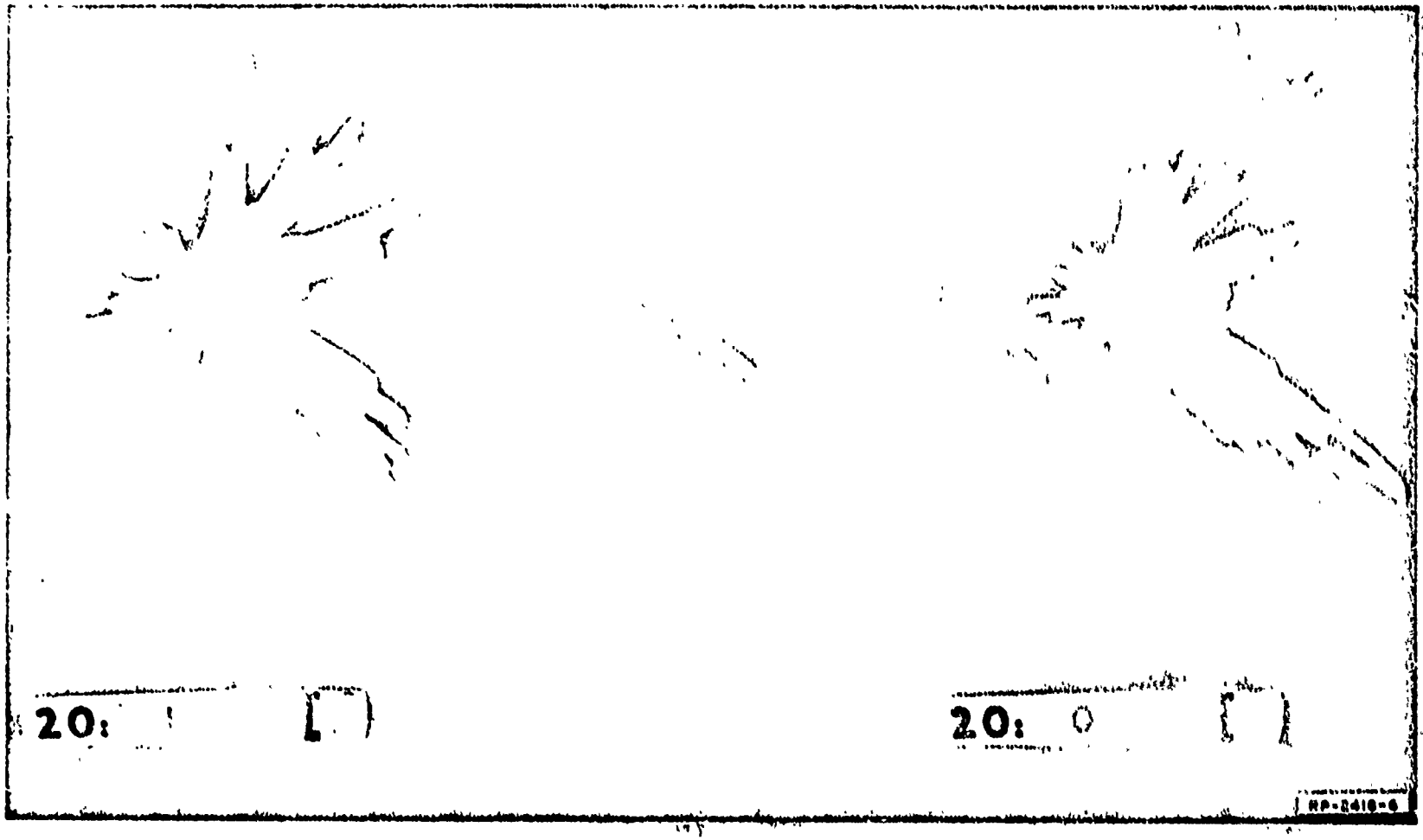

FIG. I-2
INTEGRATED DF FILM SAMPLE

of data. Four sferics occurred during film transit. The integrating interval used in Fig. I-2 is approximately 3 minutes 15 seconds, as can be seen from the timing record.

3. Events Counters

Sferic rates were recorded by amplifying the 3- to 30-kc spectrum from the vertical antenna and triggering electromechanical counters having pre-set thresholds. Four 20-db fixed-gain amplifiers and counters were placed in cascade to continuously record the number of sferics exceeding fixed thresholds. The thresholds used were four consecutive field strengths selected from 1, 10, 100, 1,000, and 10,000 millivolts per meter, center-to-peak.

Four sets of four counters per set were switched sequentially onto the amplifiers to record the number of sferics exceeding each of four thresholds for each quarter GMT day (00-06, 06-12, 12-18, and 18-24 hours GMT). The counts on these counters were recorded daily by the station operator, and provided the omnidirectional sferic rate data.

4. Scanning Receiver

A scanning receiver with a 100-cycle bandwidth and a pen recorder were used to record the omnidirectional RMS noise and signal level in the 12- to 30-kc frequency band. The receiver scanned from 12 to 30 kc and back to 12 kc in one hour. The system dynamic range extended from 3 microvolts to 1 volt, and the recording system was linear in db. Tuning frequency and a 25-kc calibration signal were also recorded. Figure I-3 shows two typical scanning receiver records. The RMS noise spectrum from 12 to 30 kc is shown, as is the RMS level of all VLF stations received in the 12- to 30-kc frequency band.

5. VLF/ELF Waveforms

The ELF component of sferic waveforms was occasionally recorded on 35mm film with the waveform and DF film system described in Part C-1 by changing the band-shaping filters in the waveform receiver to have a 10-cycle to 30-kc pass band.

D. Scope of this Report

More data were collected than it was economically feasible to analyze. In addition, the analyzed data cannot be presented in their entirety in any reasonable manner. Therefore, preliminary processing of the analyzed data was necessary. In general, this preliminary processing summarized the analyzed data into quarter-GMT-day intervals for comparisons between the various data forms. These analyzed data are presented in the Appendices without interpretation, in the hope that they will be useful to other investigators for future analysis. The Appendices and this Introduction constitute a sferic data-summary report that can be used without reference to the body of the report. The Introduction and

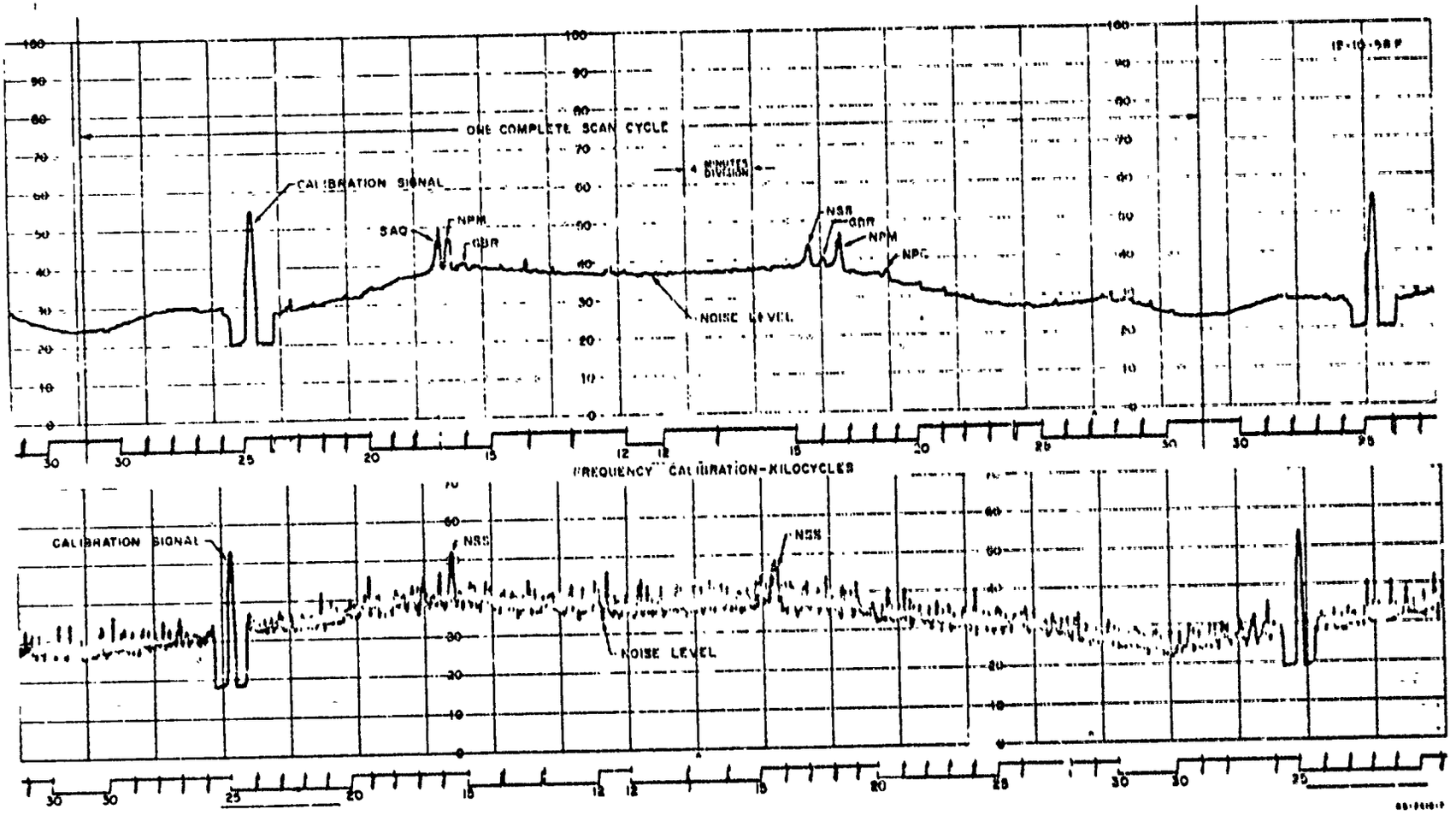

FIG. 1-3

SCANNING RECEIVER SAMPLE RECORDS

Appendices A, B, C, H, and I define the system characteristics that are applicable to understanding the data forms presented. Appendices D, E, F, and G present the waveform and DF film, integrated DF film, event counts, and scanning receiver data that have been analyzed, with a brief description of the analysis method used for each data type. A Bibliography is also appended, which lists related publications that describe, in general, VLF and sferic research activities.

The body of this report presents discussions based upon data averages from the Appendices and, thus, presents the over-all results and not specific detailed data. Sferic rates, waveform types, RMS noise, and location-of-activity data from the Appendices are averaged to show month-to-month variations and diurnal variations. In addition, a limited amount of VLF-ELF waveform data is presented and VLF propagation and the influence of geophysical data on sferic activity are briefly discussed.

This report presents all sferic data analyzed and published in the Monthly Data-Summary Bulletins, except for individual sferic source-location data. Source-location data were too bulky to present in any reasonable manner, and are available in the Monthly Data-Summary Bulletins.

II CONCLUSIONS

The operation of a three-station sferic monitoring net in the Arctic to record sferic activity in all parts of the Northern Hemisphere has resulted in large amounts of sferic data. Portions of these data have been analyzed to demonstrate the capability of the equipment and techniques; the results of the analysis are presented in this report.

The amplitude distributions of sferics received at Fairbanks, Thule, and St. Johns from September 1958 through March 1959 have been determined as a function of quarter GMT days and for each month. These distributions show that in the Northern Hemisphere during the winter, the month-to-month variation in the rate of sferics exceeding a specific field strength decreases as the latitude of the receiving station increases. This is equivalent to stating that, as the average distance from the world storm centers to the receiving station is increased, the time variation in sferic rate is decreased and that the total number of lightning strokes in the world is more or less constant with time. Thus, at Fairbanks and Thule one sferic amplitude distribution can be used to describe the received sferic rates for the entire Northern Hemisphere winter. A sferic rate exceeding 10 millivolts per meter at Fairbanks and Thule is about one sferic per second and decreases to about 0.01 sferic per second at 100 millivolts per meter. The sferic rate at St. Johns is approximately 10 sferics per second at 10 millivolts per meter and 0.5 sferic per second at 100 millivolts per meter.

Sferics have been received from all portions of the Northern Hemisphere. Approximately 3,200 individual sferics have been located as to geographic source. The source location data and data from received direction-of-arrival distributions correlate with reported thunderstorm-day contours throughout the world. In addition, the diurnal variation of sferic activity has been determined and shows that for any geographical location in the middle latitudes, local sferic activity is a minimum in the local morning and is a maximum during the local night for the winter months.

Atmospheric noise amplitude spectrum in the 12- to 30-kc frequency band has been determined for the three receiving stations for 0300, 0900, 1500, and 2100 hours GMT. These data indicate that atmospheric noise level is closely dependent upon frequency. Noise amplitudes tend to be a maximum at approximately 15 kc, with a lesser maximum at 25 kc, for the Fairbanks and Thule receiving stations. Once again the variation in atmospheric noise level is less when the receiving station is farther from the world thunderstorm centers.

Some data on the ELF component of sferics are presented in the form of the peak-to-peak amplitude ratio of the VLF to ELF received components. This ratio has a mean value of less than 10 and is approximately log-normally distributed. The VLF/ELF ratio increases with received amplitude of the VLF component and decreases with range from the sferic source to the receiving station.

The sferic data collected at the Fairbanks, Thule, and St. Johns sferic monitoring stations contain data on VLF propagation in the Arctic. This research program did not include any studies of the data to determine VLF propagation characteristics. However, from sferics propagated along the Thule-Fairbanks and Fairbanks-Thule path, it is indicated that propagation attenuation is dependent upon the direction of propagation. In addition, direction-of-arrival measurements on various keyed-CW VLF stations indicate that the variation in direction of arrival (i.e., DF error) is a minimum when the propagation path is aligned with the earth's magnetic field. Additional analysis of the sferic data collected, including spectrum analysis of sferic waveforms propagated over known Arctic paths, would give VLF propagation attenuation characteristics as functions of frequency and path alignment with the earth's magnetic field.

As stated earlier, only a portion of the sferic data collected has been analyzed. A large portion of this unanalyzed body of raw data contains additional data that would better define sferic activity in the Northern Hemisphere for the winter months. Many additional source locations of sferics could be determined. Analysis of the scanning receiver records for all hours of the day would define, in detail, the 12 to 30 kc atmospheric noise amplitude spectrum as received in the Arctic. All data collected have, however, been cataloged and stored for future reference and analysis.

The operation of a three-station sferic monitoring net in the Arctic has provided a good statistical description of Northern Hemisphere winter sferic activity. The operation of such a system during the summer months would supplement the data and provide a description of sferic activity for all seasons. However, such operation was not possible within the limitations of this contract.

III SFERIC RATES AND AMPLITUDE DISTRIBUTIONS

A. Diurnal Variations in Sferic Rate

Sferic rate is defined as the number of sferics per second that exceed a fixed field strength (threshold). Thus, omnidirectional sferic rate is a function of time of day, season, geographic location of the receiving station, and other possible unknowns such as sunspot number, magnetic index, aurora, etc. The sferic rate data from the waveform and DF film and from the events counter, as presented in Appendices D and E, respectively, show sferic rate as a function of time of day, season, and geographic location of the receiving station. The diurnal sferic rate variations obtained from data presented in Appendices D and E for Fairbanks, Thule, and St. Johns are shown in Figs. III-1, III-2, and III-3. The figures show the monthly average sferic rate for each quarter GMT day* as a function of threshold in millivolts per meter, center to peak. The solid circles are data from the events counter, and the open circles are data from waveform and DF film. For example, at St. Johns for November 1958, Fig. III-3 shows the average sferics per second at 100 millivolts per meter center to peak are 0.50 for 00-06 GMT, 0.60 for 06-12 GMT, 0.25 for 12-18 GMT, and 0.36 for 18-24 GMT (all from the events counter data), and 0.18 for 00-06 GMT, 0.51 for 06-12 GMT, 0.11 for 12-18 GMT, and 0.11 for 18-24 GMT (all from the waveform-and-DF-film data).

The data in Figs. III-1, III-2, and III-3 are omnidirectional sferic rates and represent data for the entire Northern Hemisphere. During the winter the Northern Hemisphere is in darkness for much of the time, so that daily variations related to daylight or darkness are not distinguishable. However, if GMT quarter days are converted to approximate local time at each receiving station (GMT minus 10 hours for Fairbanks and GMT minus 4 hours for Thule and St. Johns) then the diurnal variations at the three stations do tend to show a weak correlation. In local time at each receiving station, the 00-06 GMT interval for Fairbanks corresponds approximately to the 18-24 GMT interval for Thule and St. Johns.

---

*GMT (Greenwich Mean Time) is used throughout this report, Quarter GMT days are 00-06, 06-12, 12-18 and 18-24 hours GMT.

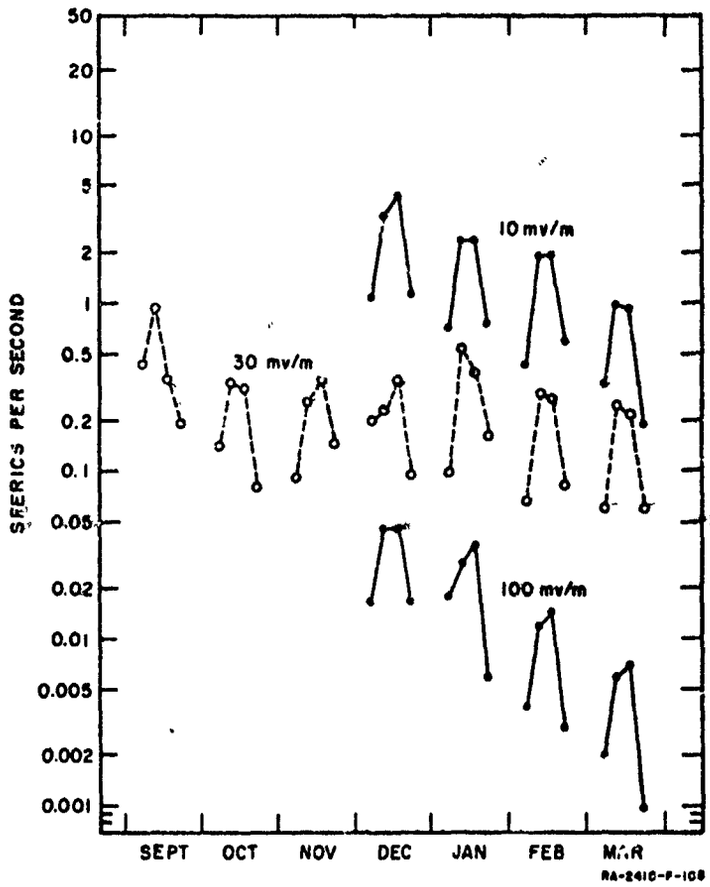

FIG. III-1

DIURNAL SFERIC RATE IN QUARTER GMT DAYS AT FAIRBANKS, ALASKA — SEPTEMBER 1958 TO MARCH 1959

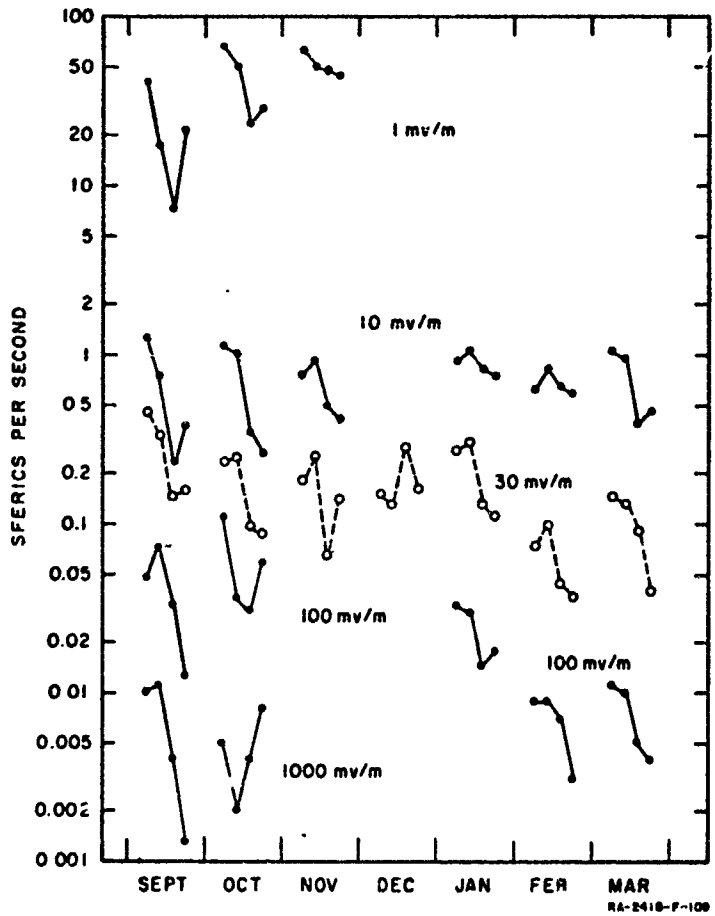

FIG. III-2

DIURNAL SFERIC RATE IN QUARTER GMT DAYS AT THULE, GREENLAND — SEPTEMBER 1958 TO MARCH 1959

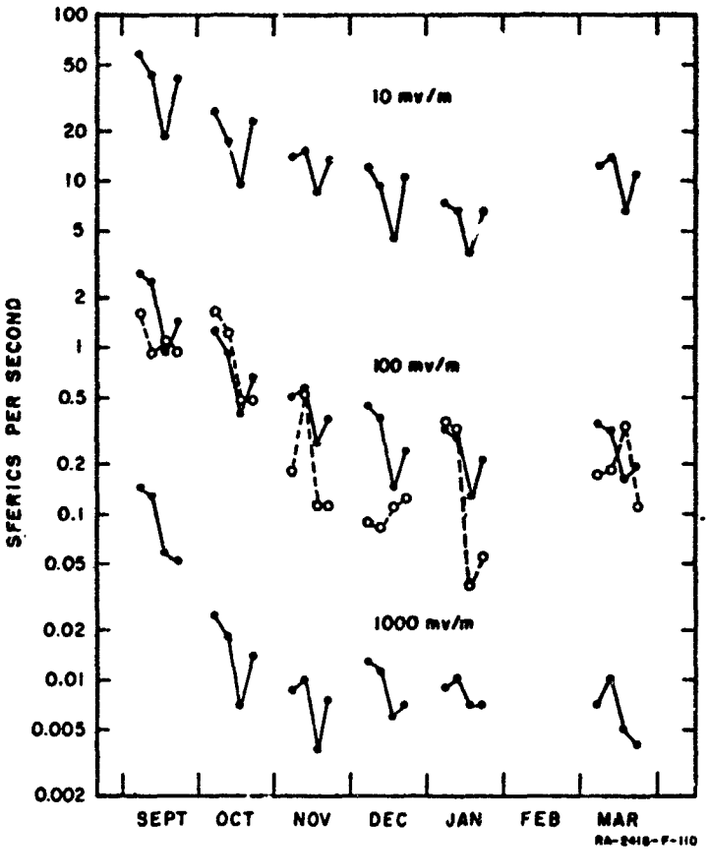

FIG. III-3

DIURNAL SFERIC RATE IN QUARTER GMT DAYS AT ST. JOHNS, NEWFOUNDLAND — SEPTEMBER 1958 TO MARCH 1959

The waveform and DF film represents samples of sferic data. These samples were scheduled* to obtain data for all hours of the GMT day over a 12-day period. The events counter continuously recorded sferic-rate data. The lack of correlation between the sferic rates obtained from the two data recording systems could be due to the influence of day-to-day variations in the waveform-and-DF-film data. Thus, the events counter data are preferred for diurnal variation in sferic rate (solid circles on Figs. III-1, III-2, and III-3).

B. Monthly Variations in Sferic Rate

The average month-to-month variations in sferic rate for Fairbanks, Thule, and St. Johns are shown in Figs. III-4, III-5, and III-6, respectively. The data for these figures were obtained from Figs. III-1, III-2, and III-3. The solid-line histograms represent events counter data, and the dashed-line histograms represent waveform-and-DF-film data. For example, one can see from Fig. III-6 that at St. Johns, for November 1958, the average number of sferics per second at 100 millivolts per meter, center to peak is 0.42 from the events counter data and 0.25 from the waveform-and-DF-film data.

The data presented in Figs. III-4, III-5, and III-6 show that from September 1958 through March 1959, the variation in average sferic rate is relatively small (3 or 4 to 1) for Fairbanks and Thule and is no greater than 10 to 1 for St. Johns. The variation in sferic rate increases as sferic monitoring station latitude decreases. This is equivalent to saying that during the Northern Hemisphere winter, sferic activity is centered in the Southern Hemisphere and that monitoring sferic activity at great distances from the major sferic source centers tends to give a constant average monthly sferic rate. The variation in average monthly sferic rate increases as the monitoring stations approach the storm centers.

C. Sferic Amplitude Distributions

The data presented so far in this section indicate that an average sferic amplitude distribution for each Arctic receiving station would, on the average, define sferic rate activity for any particular time during the Northern Hemisphere winter. (Amplitude distribution is herein defined as sferic rate versus threshold.) The solid line curves in Figs. III-7, III-8, and III-9 show the average winter sferic amplitude distributions for Fairbanks, Thule, and St. Johns. These curves are averages from the September 1958 through March 1959 amplitude distributions in Appendix D, which were obtained from waveform and DF film.

---

* See Appendix B for schedule used.

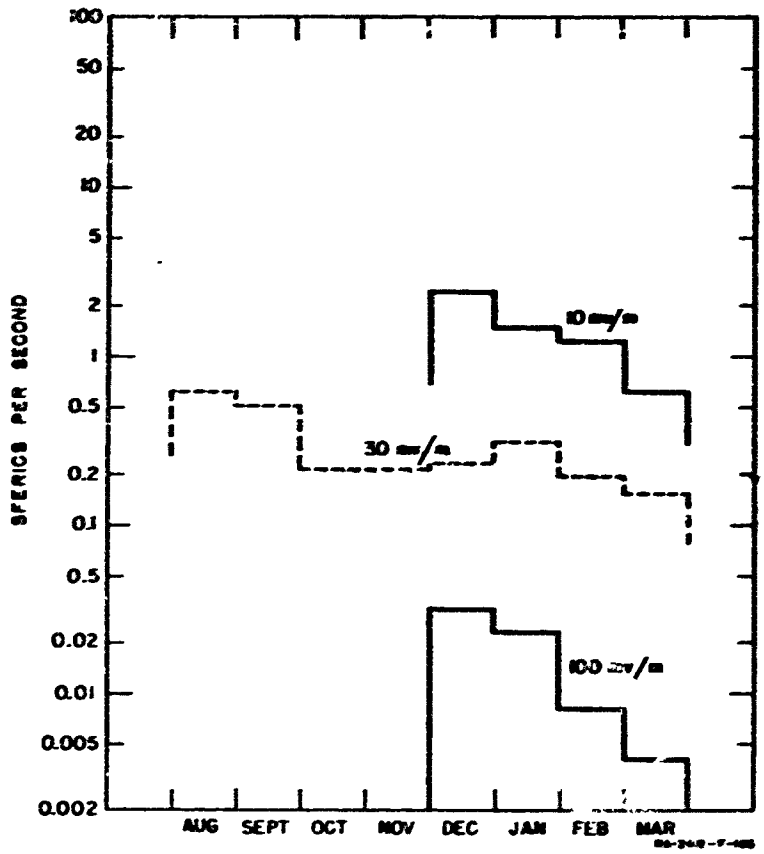

FIG. III-4

MONTHLY SFERIC RATE AT FAIRBANKS, ALASKA
AUGUST 1958 TO MARCH 1959

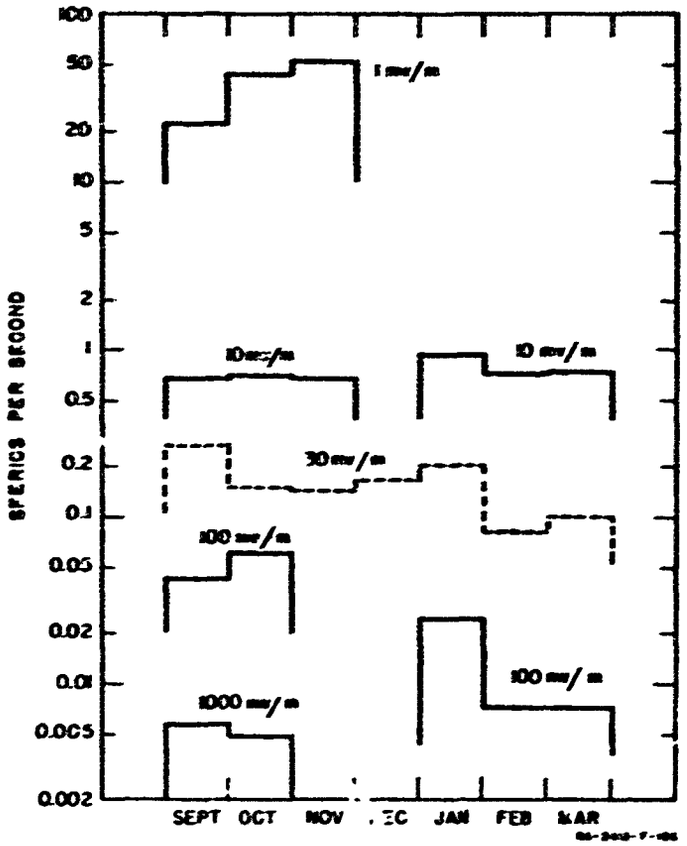

FIG. III-5

MONTHLY SFERIC RATE AT THULE, GREENLAND
SEPTEMBER 1958 TO MARCH 1959

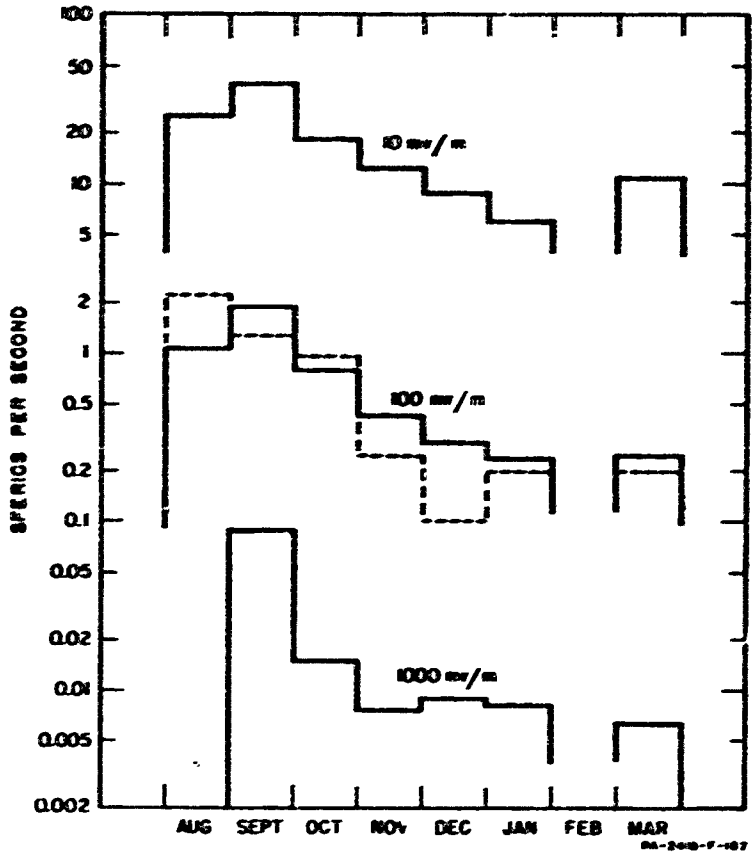

FIG. III-6

MONTHLY SFERIC RATE AT ST. JOHN., NEWFOUNDLAND
AUGUST 1958 TO MARCH 1959

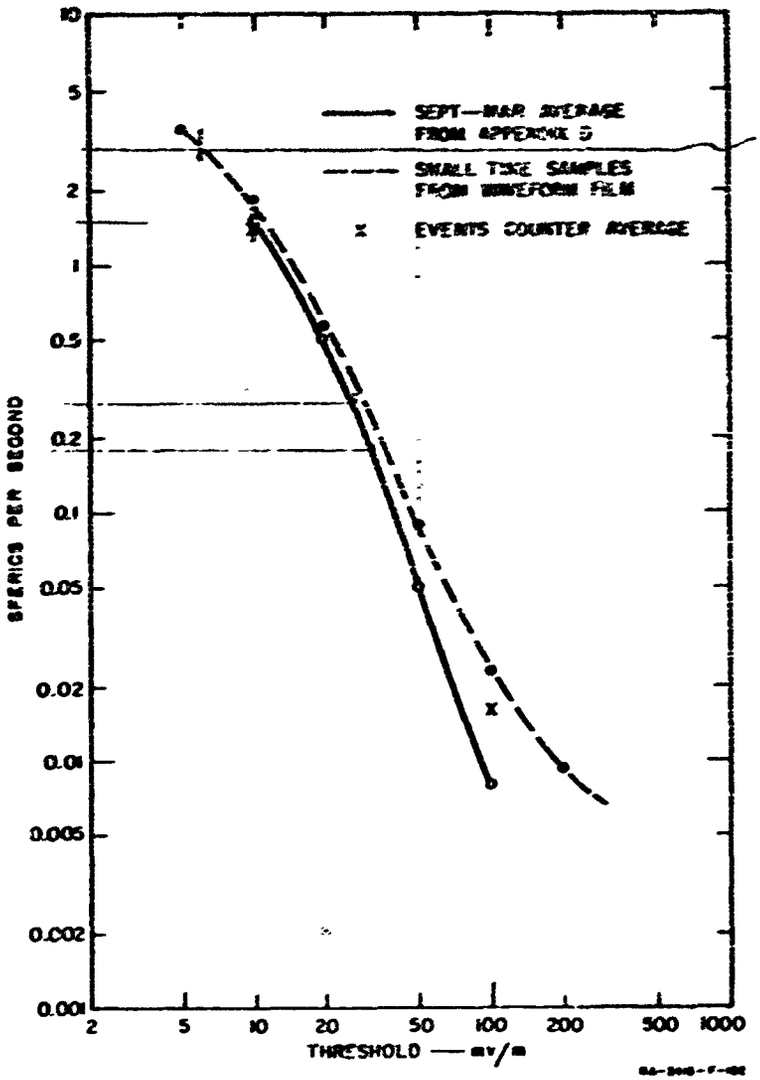

FIG. III-7

WINTER SFERIC AMPLITUDE DISTRIBUTION, FAIRBANKS, ALASKA

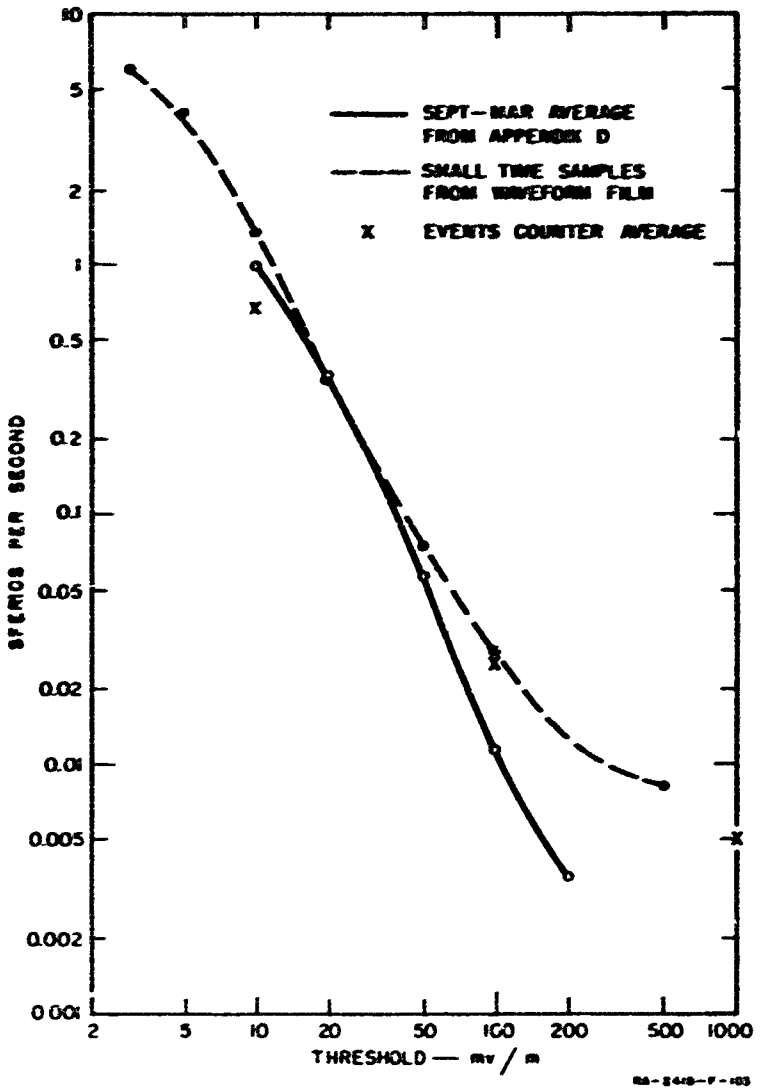

FIG. III-8

WINTER SFERIC AMPLITUDE DISTRIBUTION, THULE, GREENLAND

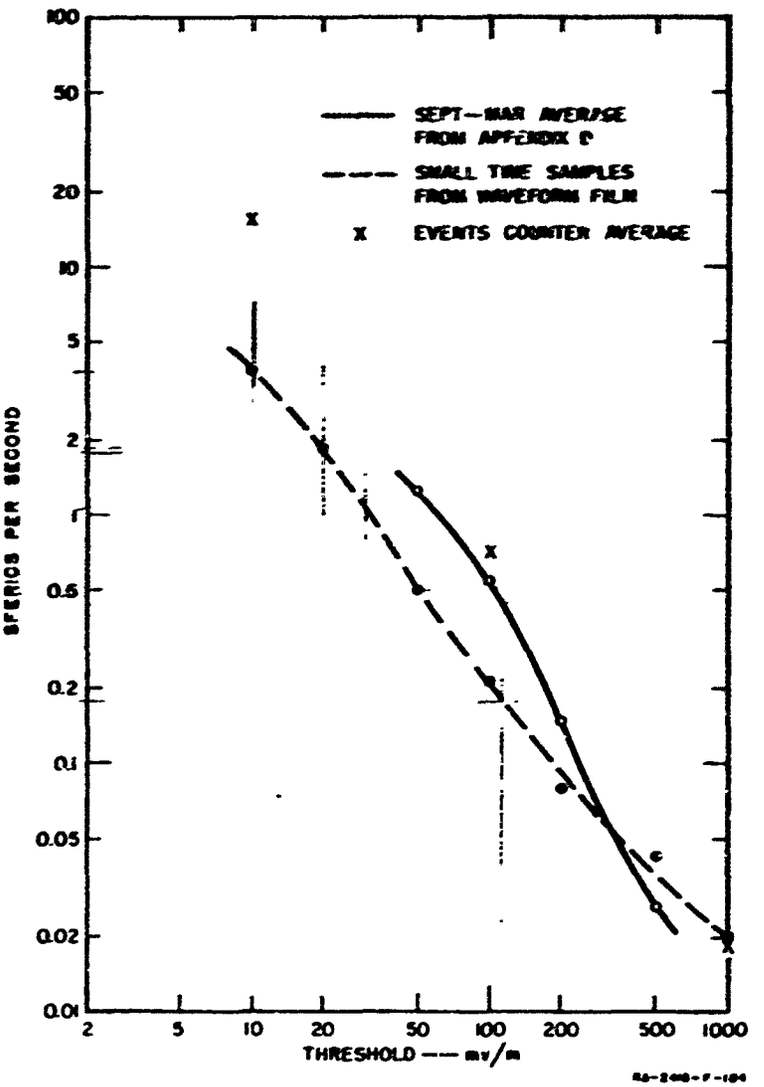

FIG. III-9

WINTER SFERIC AMPLITUDE DISTRIBUTION, ST. JOHNS, NEWFOUNDLAND

In addition to the sferic rate data obtained from waveform and DF film that are presented in Appendix D, other short-time samples of waveform and DF film have been analyzed to determine sferic rates at other thresholds. These samples were normally taken from one day's data each month. The poor statistical time distribution of these small samples prevented their inclusion in Appendix D, but they are averaged and shown as dashed-line curves on Figs. III-7, III-8, and III-9. The average sferic rates from the events counter are shown by the symbol X on Figs. III-7, III-8, and III-9.

The data presented on Figs. III-7, III-8, and III-9 from the various data recording systems are in good agreement with each other. These curves can be used to obtain a typical winter sferic rate for Fairbanks, Alaska, for Thule, Greenland, and for St. Johns, Newfoundland. Specific sferic rate data must be obtained from the Appendices. Figures III-7, III-8, and III-9 apply for the range of thresholds shown. Extrapolation of these curves is not possible from the data collected.

D. Direction of Arrival Variations

In Figs. III-1 through III-9, omnidirectional sferic rate data are presented. In Appendix D (Figs. D-8 through D-16) the direction-of-arrival distributions from the waveform-and-DF-film data are shown. The direction-of-arrival distributions and amplitude distributions shown in Appendix D can be used with some success to obtain diurnal and monthly variations of sferic rate for any particular sector for each sferic monitoring station.

IV WAVEFORM TYPES

A. Waveform Classifications

The sferics recorded on the waveform and DF film were analyzed for waveform type. The waveform classifications were designated, Type 1 (ordinary--all waveforms not included in other designations), Type 2 (smooth--having at least six smooth half-cycles with a smoothly rising and falling envelope), Type 3 (peaky--a repetitive pattern of three or four spikes or pulses), Type 4 (precursor with sferic--a ragged waveform for about one millisecond followed by a sferic), Type 5 (precursor without sferic), and Type 9 (quasi-CW--an approximate sinusoid). Types 1, 2, 3, 4, and 9 are shown in Fig. IV-1.

The waveform classifications tend to indicate range. That is, Types 3, 4, and 5 are characteristic of sferics at short ranges since, in general, precursors and individual pulses from different sky waves can be seen only at close range. Type 2 (smooth) is characteristic of propagation over long ranges, and Type 1 (ordinary) is characteristic of medium-range propagation. This statement of waveform type as a function of range is only approximate; individual exceptions can always be found.

B. Distribution of Waveform Types

The results of the waveform type analysis from the waveform and DF film are tabulated in Table IV-1 (in percent) for Fairbanks, Thule, and St. Johns. Four percentages are given for each month, one for each quarter of the GMT day.

The waveform type data shown in Table IV-1 were averaged for each month and for each receiving station and are shown in Figs. IV-2, IV-3, and IV-4 as histograms. Here waveform types are totaled together for long range (Type 2, smooth), medium range (Type 1, ordinary), and short range (all other types). Quasi-CW is included with the short-range types, since the percentage of this type are small. The quasi-CW waveform type is a "whistler" signal and does not fall into a range classification as listed above.

Several facts are evident from Figs. IV-2, IV-3, and IV-4. Short-range sferics are in a minority, which is normal for monitoring stations at high northern latitudes during the Northern Hemisphere winter. St. Johns shows a slightly higher percentage of short-range activity, since it is at the lowest latitude. Long-range sferics (smooth) show an increase in percentage during mid-winter when

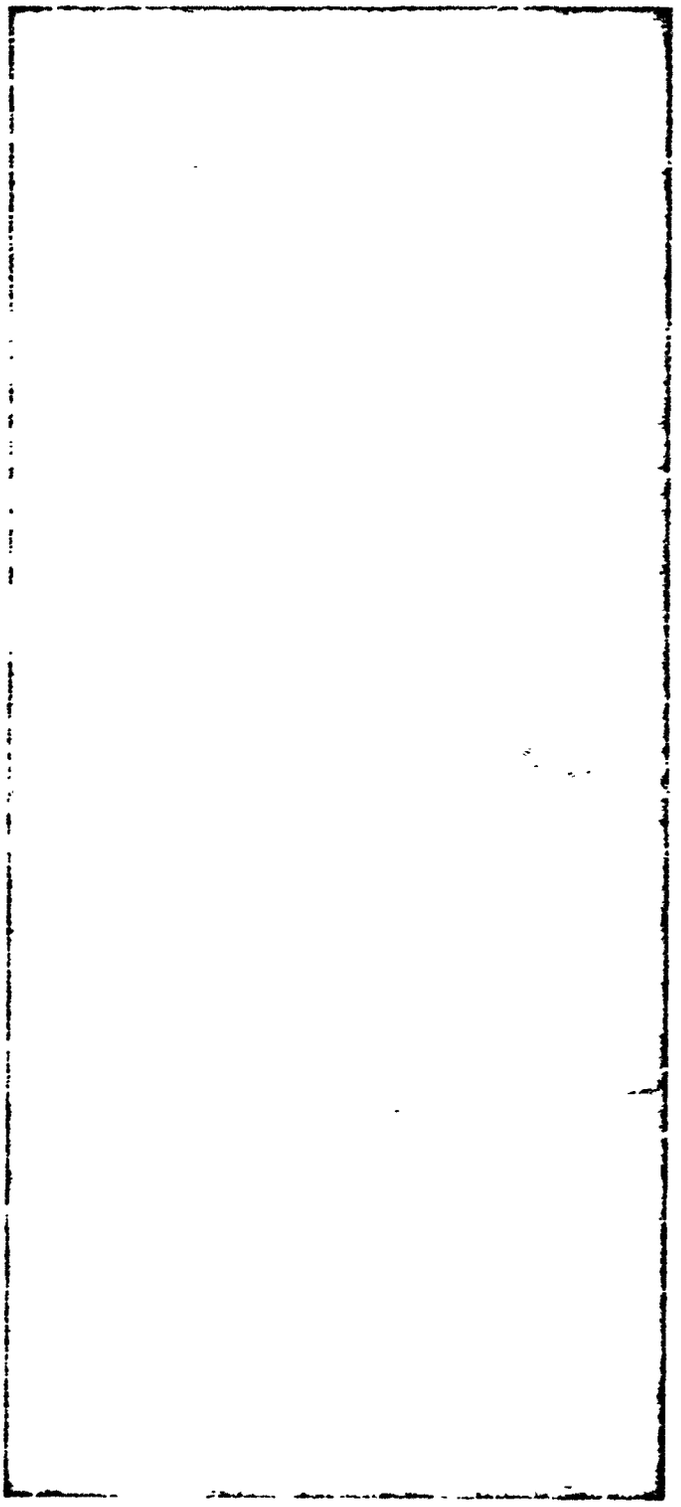

FIG. IV-1

SFERIC WAVEFORM CLASSIFICATIONS

Table IV-1

PERCENTAGE OF WAVEFORMS IN EACH CLASSIFICATION DURING EACH QUARTER OF THE GMT DAY

Month	Quarter of the GMT Day	Fairbanks, Alaska						Thule, Greenland						St. John, Nfld.					
		Waveform Type						Waveform Type						Waveform Type					
		1	2	3	4	5*	9	1	2	3	4	5*	9	1	2	3	4	5*	9
August 1958	00-06	73	26	**	**	**	1	No data						50	37	13	**	**	0
	06-12	74	25	**	**	**	1	No data						77	20	3	**	**	0
	12-18	69	31	**	**	**	0	No data						No data					
	18-24	74	22	**	**	**	4	No data						No data					
September 1958	00-06	71	25	1	0	3	0	69	25	3	1	2	0	76	19	5	**	**	0
	06-12	71	23	1	1	4	0	No data						67	29	4	**	**	0
	12-18	50	41	0	2	7	0	49	42	5	1	3	0	58	31	4	3	4	0
	18-24	61	32	1	0	4	2	69	20	3	4	4	0	60	34	4	1	1	0
October 1958	00-06	58	37	2	3	--	0	54	39	5	2	--	0	84	12	4	0	--	0
	06-12	66	24	9	1	--	0	56	38	5	1	--	0	67	26	7	0	--	0
	12-18	75	18	5	2	--	0	44	46	9	1	--	0	38	56	6	0	--	0
	18-24	56	38	5	1	--	0	56	39	4	1	--	0	46	52	2	0	--	0
November 1958	00-06	50	42	7	1	--	0	36	62	2	0	--	0	80	7	13	0	--	0
	06-12	65	27	7	1	--	0	69	28	3	0	--	0	84	4	12	0	--	0
	12-18	78	13	8	1	--	0	38	60	2	0	--	0	73	13	14	0	--	0
	18-24	51	36	12	1	--	0	38	56	6	0	--	0	76	19	5	0	--	0
December 1958	00-06	25	71	4	0		0	30	56	6	3		0	64	20	16	0		0
	06-12	53	44	3	0	--	0	17	75	3	3	--	2	64	24	11	1	--	0
	12-18	44	54	2	0	--	0	16	75	8	1	--	0	46	47	6	0	--	1
	18-24	30	70	0	0	--	0	6	86	8	0	--	0	47	48	5	0	--	0
January 1959	00-06	40	49	10	1	--	0	40	52	7	0	--	1	76	15	9	0	--	0
	06-12	71	22	7	0	--	0	36	61	2	1	--	0	72	23	5	0	--	0
	12-18	74	18	8	0	--	0	26	74	0	0	--	0	39	57	4	0	--	0
	18-24	37	48	15	0	--	0	43	54	0	2	--	1	46	50	4	0	--	0
February 1959	00-06	42	54	4	0	--	0	58	31	10	1	--	0	No data					
	06-12	64	31	5	0	--	0	63	32	5	0	--	0	No data					
	12-18	60	35	4	1	--	0	58	38	4	0	--	0	No data					
	18-24	34	57	9	0	--	0	60	33	6	1	--	0	No data					
March 1959	00-06	38	57	5	0	--	0	64	31	5	0	--	0	83	11	5	1	--	0
	06-12	62	30	8	0	--	0	61	32	5	2	--	0	71	16	13	0	--	0
	12-18	72	17	10	0	--	1	38	52	8	0	--	2	55	28	16	1	--	0
	18-24	24	69	17	0	--	0	45	49	4	2	--	0	50	45	4	1	--	0

*After September, the Type 5 classification was eliminated and waveforms were classified Type 3.

** Classification was not established for these.

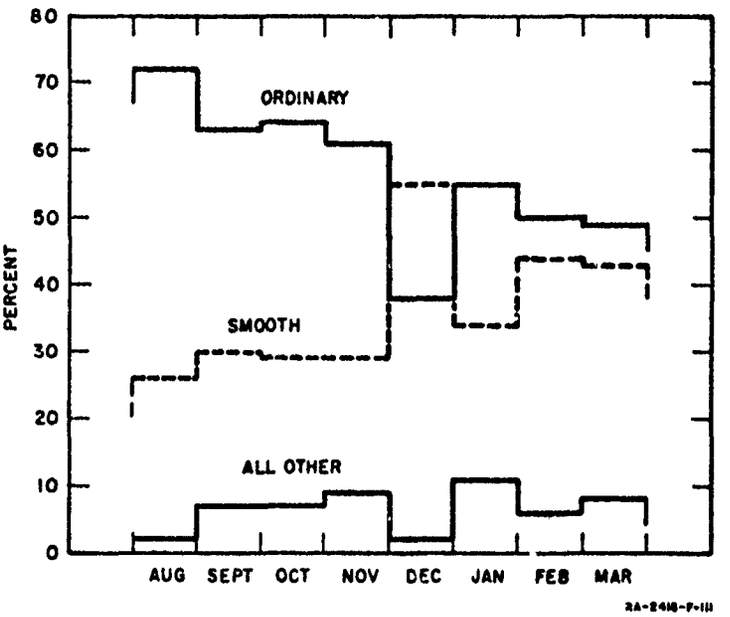

FIG. IV-2

MONTHLY WAVEFORM TYPES, FAIRBANKS, ALASKA
AUGUST 1958 TO MARCH 1959

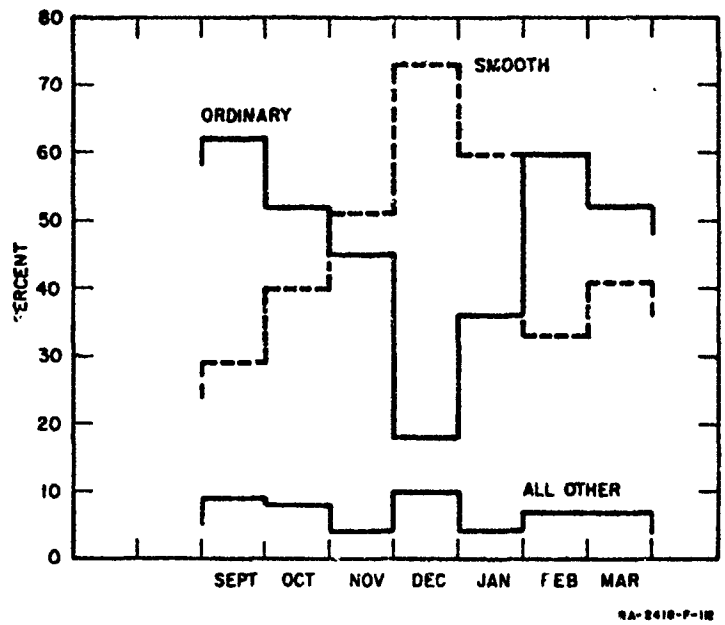

FIG. IV-3

MONTHLY WAVEFORM TYPES, THULE, GREENLAND
SEPTEMBER 1958 TO MARCH 1959

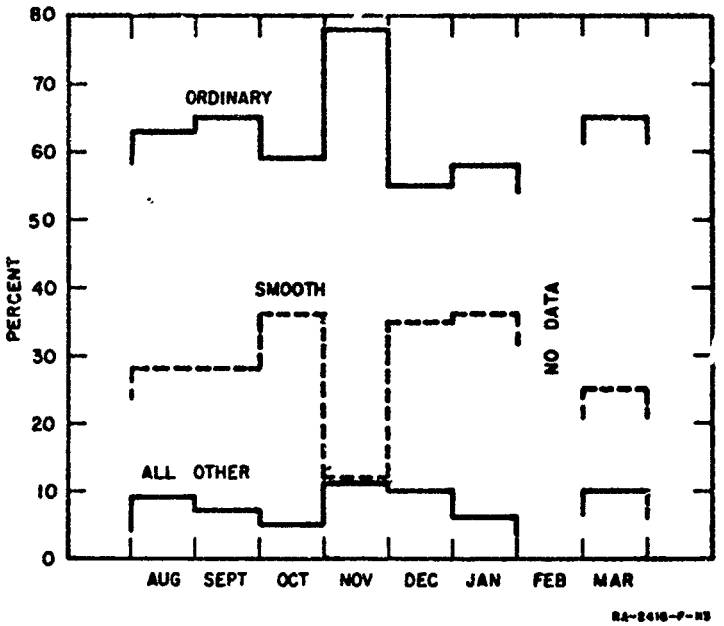

FIG. IV-4

MONTHLY WAVEFORM TYPES, ST. JOHNS, NEWFOUNDLAND
AUGUST 1958 TO MARCH 1959

activity is at maximum range. The percentage of sferics in each type might have been predicted for the monitoring sites used, since the major sferic source centers are generally known by location and seasons.

V RMS ATMOSPHERIC NOISE

A. RMS Noise Measurements

The RMS atmospheric noise level was recorded at Fairbanks, Alaska, at Thule, Greenland, and at St. Johns, Newfoundland, in the 12- to 30-kc frequency band by a scanning receiver with a 100-cycle bandwidth. The scanning receiver tuned from 12 to 30 kc and back to 12 kc in one hour, and the output of the receiver was recorded on a pen recorder. Root-mean-square noise level, as a function of frequency from 12 to 30 kc, at 0300, 0900, 1500, and 2100 hours GMT is presented in Appendix F as half-month averages and minimum-maximum values for each sferic monitoring station.

B. Diurnal Variation of RMS Noise Level

The scanning receiver recorded RMS atmospheric noise level in a 100-cycle bandwidth on a 24-hour-a-day schedule. Each scanning cycle lasted one hour, so that each frequency from 12 to 30 kc was scanned and recorded twice per hour. Figure V-1 shows the 12- and 24-kc RMS atmospheric noise levels for a 24-hour period on 24 January 1959, as recorded at Fairbanks, Thule, and St. Johns. In addition, the 12- and 24-kc averages from Appendix F for 0300, 0900, 1500, and 2100 hours GMT are shown. Figure V-1 demonstrates that the RMS atmospheric noise data presented in Appendix F can be used to present the general diurnal variation in RMS atmospheric noise. This diurnal variation in RMS noise level is shown in Fig. V-2 which shows the monthly average RMS noise level at 15 and 25 kc for 0300, 0900, 1500, and 2100 hours GMT as received at all three sites. The noise levels at 15 and 25 kc were chosen as two arbitrary frequencies in the 12- to 30-kc scanning frequency range to present the diurnal variation in RMS atmospheric noise.

C. Monthly Variation of RMS Noise Level

The monthly RMS noise levels at 15 kc and 25 kc were averaged from the data presented in Fig. V-2 and are shown in Fig. V-3 as histograms for Fairbanks, Thule, and St. Johns. Each monthly average was obtained from the averages at 0300, 0900, 1500, and 2100 hours GMT. It can be seen in Fig. V-3 that variation in RMS noise level and average noise level both decrease with an increase in receiving location latitude which is equivalent to an increase in distance from sferic activity. This variation in noise level is compatible with the variation in sferic rate. Thule, Greenland, with no local sferic activity, has a fairly constant noise level for the months shown, while Fairbanks, Alaska, and St. Johns, Newfoundland, show an increased variation that is smoothly varying for the months shown.

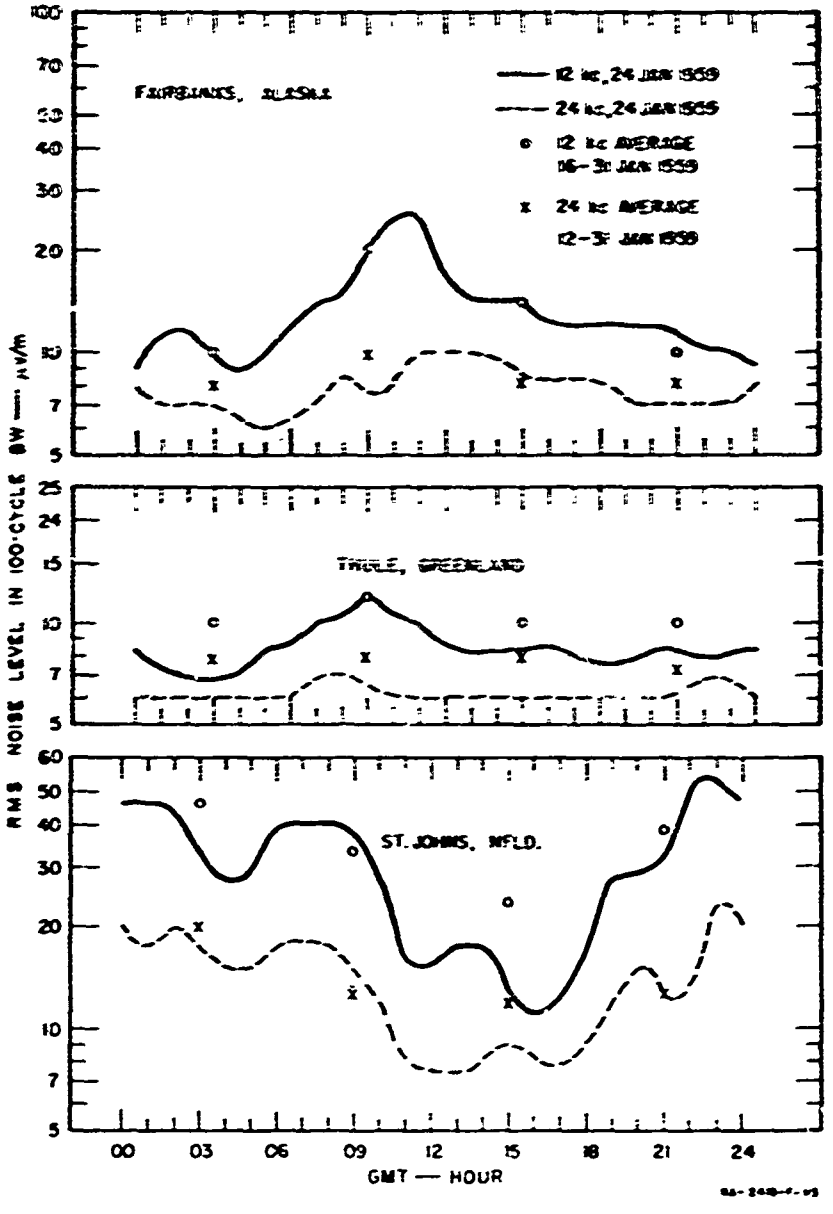

FIG. V-1

DIURNAL RMS NOISE LEVEL VARIATION, JANUARY 1959

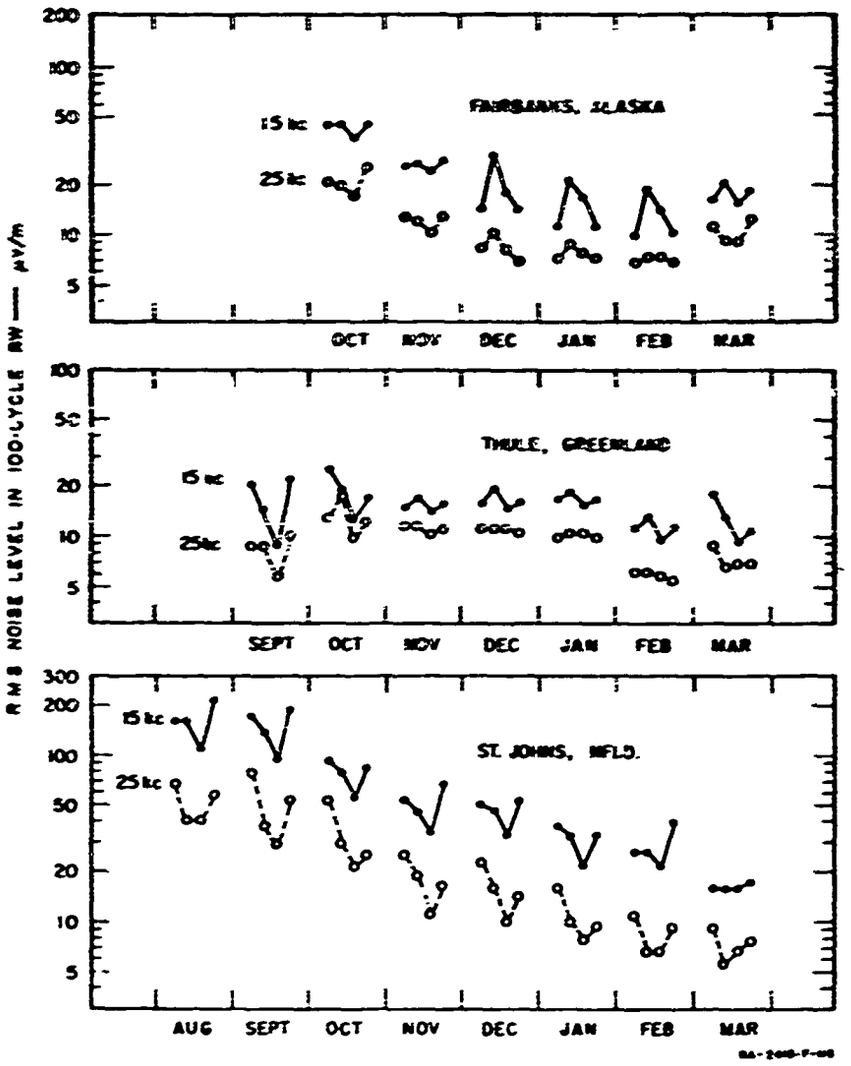

FIG. V-2

RMS NOISE LEVEL AT 0300, 0900, 1500, AND 2100 HOURS GMT
AUGUST 1958 TO MARCH 1959

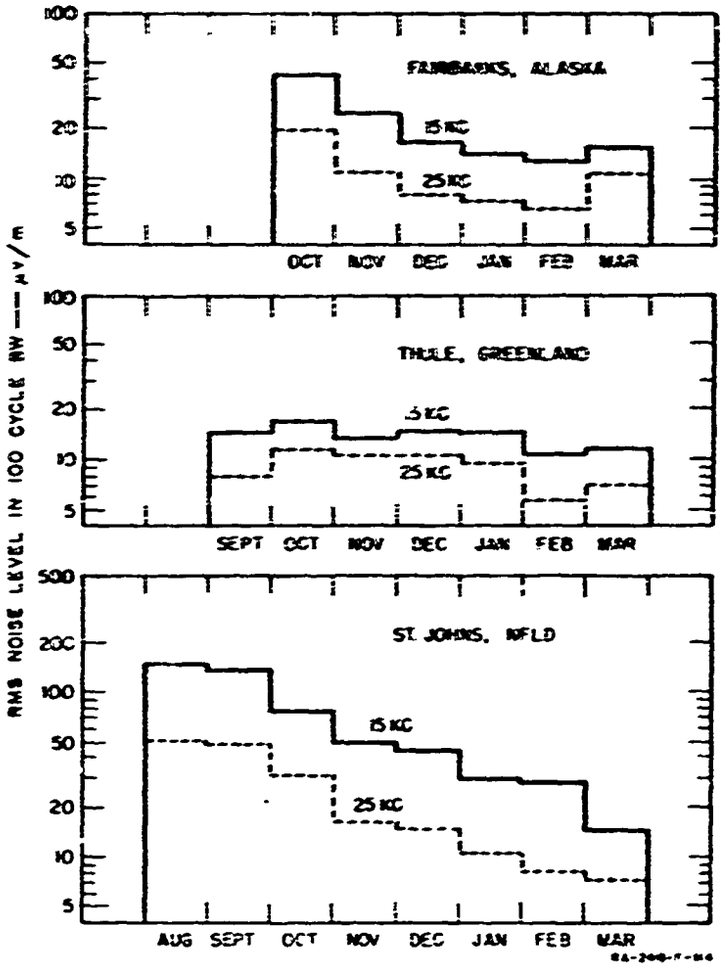

FIG. V-3

MONTHLY RMS NOISE LEVEL, AUGUST 1958 TO MARCH 1959

D. RMS Noise Spectrum Variations

As stated above, the scanning receiver recorded atmospheric noise level in a 100-cycle bandwidth as a function of frequency from 12 to 30 kc. In general the shape of the noise spectrum varied as a function of time of day, season, and receiving-station location. This spectrum variation can be seen by comparing the variations in the 15- and 25-kc noise levels shown in Fig. V-2 and V-3. Once again there is less difference between the 15- and 25-kc noise levels as the latitude of the receiving station increases.

Figures V-2 and V-3 do not present a clear picture of RMS noise spectrum variations, but do indicate the general trend. For RMS noise spectrum details see Appendix F.

VI LOCATION OF ACTIVITY

A. Source Location of Individual Sferics

The waveform and DF films collected at Fairbanks, Thule, and St. Johns were analyzed to determine the source location of individual sferics using direction of arrival at two or more receiving stations. Recognition of the same sferic at all stations was based upon the following:

(1) The time recording system used could be read to one-millisecond accuracy as is shown in Appendix C. This time accuracy was sufficient to verify source location using arrival times.

(2) Sferics often arrive in groups as shown in Fig. VI-1. The elapsed time between adjacent sferics in these groups identifies a particular group at each receiving station. Sferics 1, 2, and 4 have identical received time distributions at all three receiving stations. Sferic 3 was not received at Fairbanks.

(3) Individual sferics were found that had similar characteristics at all three receiving stations. Sferic 4 in Fig. VI-1 is an example. This sferic shows a sizable waveform following the initial sferic pulse.

The source locations of individual sferics were obtained by aligning in time the waveform and DF films from Fairbanks, Thule, and St. Johns, and recording the direction of arrival of those sferics that were received at Thule and at either or both of the other two stations. This procedure was used since Thule was the center station in the three-station network and all sferics received at Thule from the major world storm centers had a high probability of being received at one or both of the other two stations. The time patterns and waveform characteristics were sufficient in many instances to correct for occasional gross time errors caused by equipment failures or operator mistakes.

Approximately 3,200 sferics source locations* were obtained for the months of September 1958 through March 1959. These sferics were located in all areas of the Northern Hemisphere. The shaded areas in Figs. VI-2 through VI-8 show the areas by months where individual sferics were located using waveform and DF film. These shaded areas cannot be used as an indication of the magnitude of sferic activity for each month because the sample periods are not equal and are not uniformly distributed throughout the GMT day. In addition, the threshold levels used during

*Sferic source locations and their received amplitudes are not listed in this report because this information has been published in seven Monthly Sferic Data-Summary Bulletin Supplements, Sferic Source Locations, September 1958 through March 1959, Contract AF 19(604)-2409

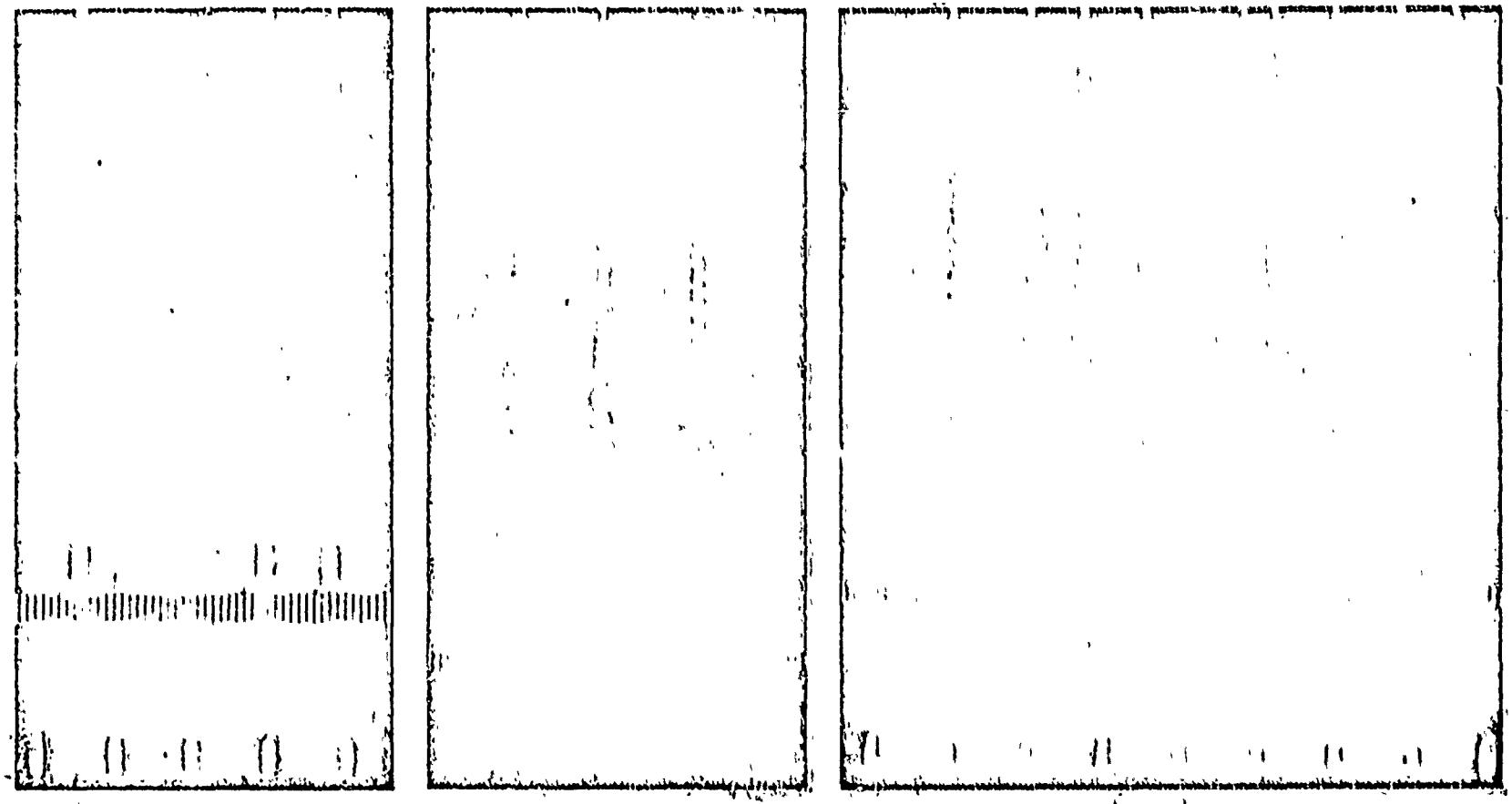

FIG. VI-1
IDENTIFICATION OF INDIVIDUAL SFERICS

THUNDERSTORM DAYS, SEPTEMBER

THUNDERSTORM DAYS, SEPTEMBER

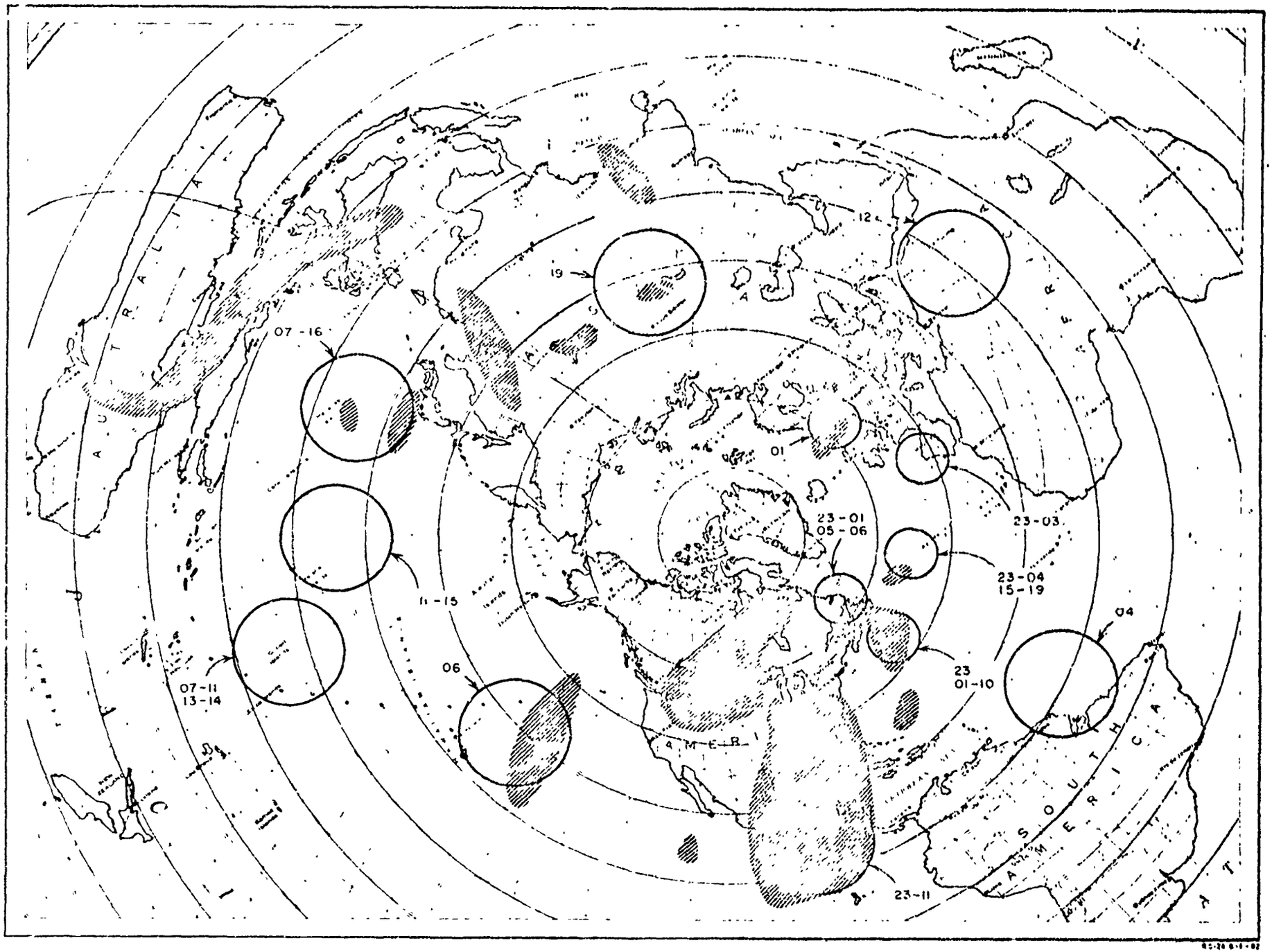

FIG. VI-2 SFERIC ACTIVITY, SEPTEMBER 1958

THUNDERSTORM DAYS, OCTOBER

THUNDERSTORMS, 2AM TO 8AM OCTOBER

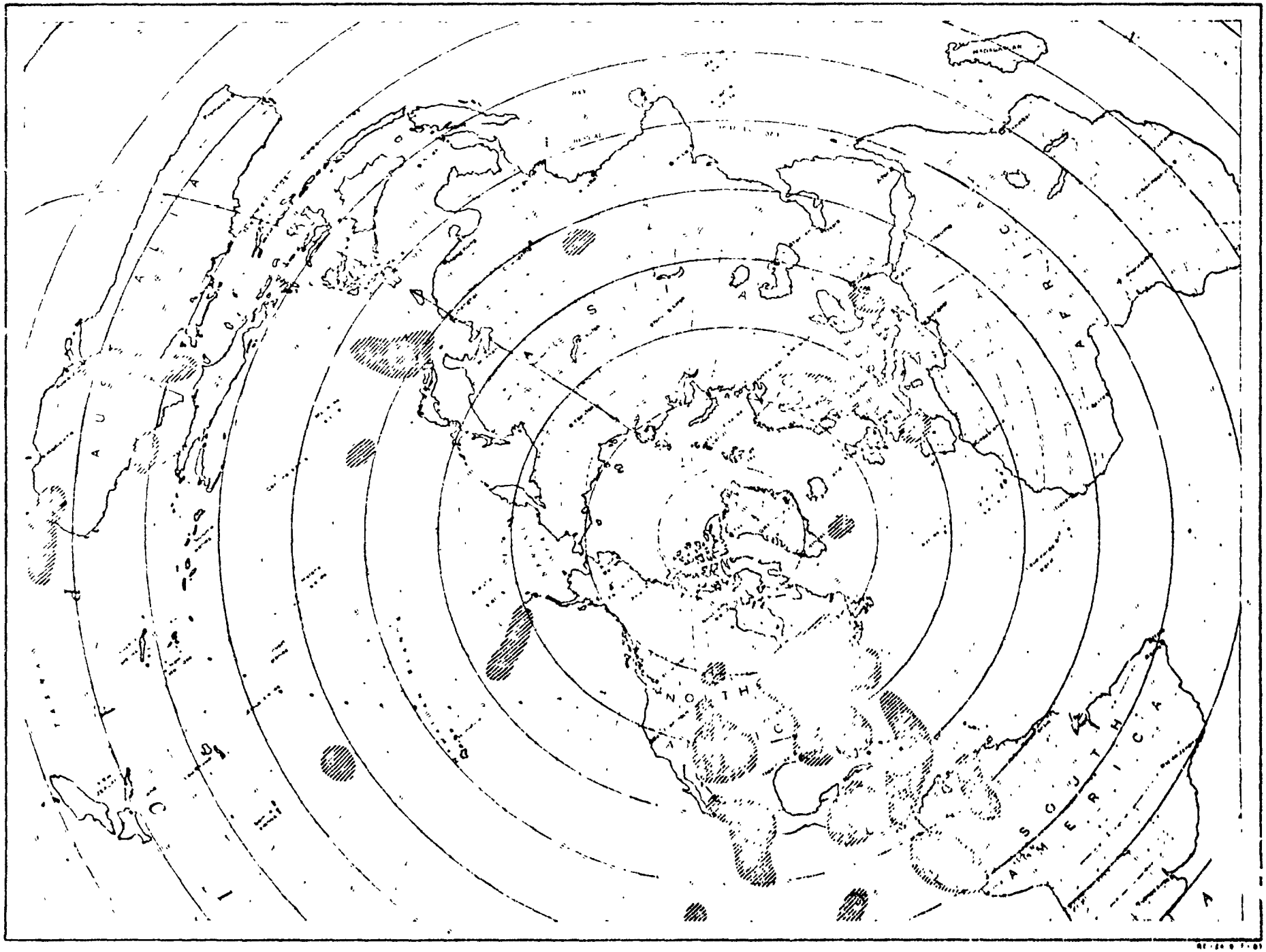

FIG. VI-3 SFERIC ACTIVITY, OCTOBER 1958

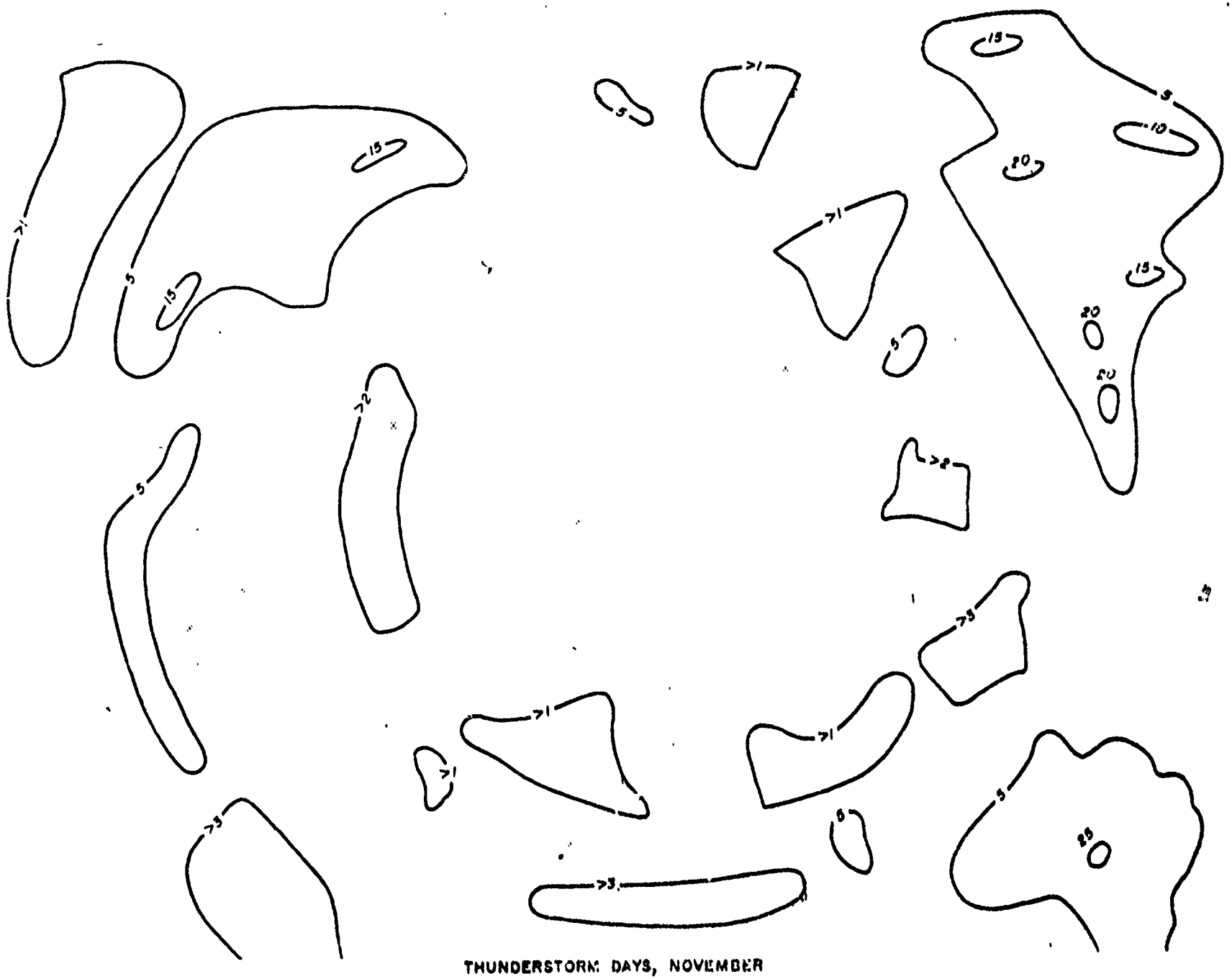

THUNDERSTORM DAYS, NOVEMBER

THUNDERSTORM DAYS, NOVEMBER

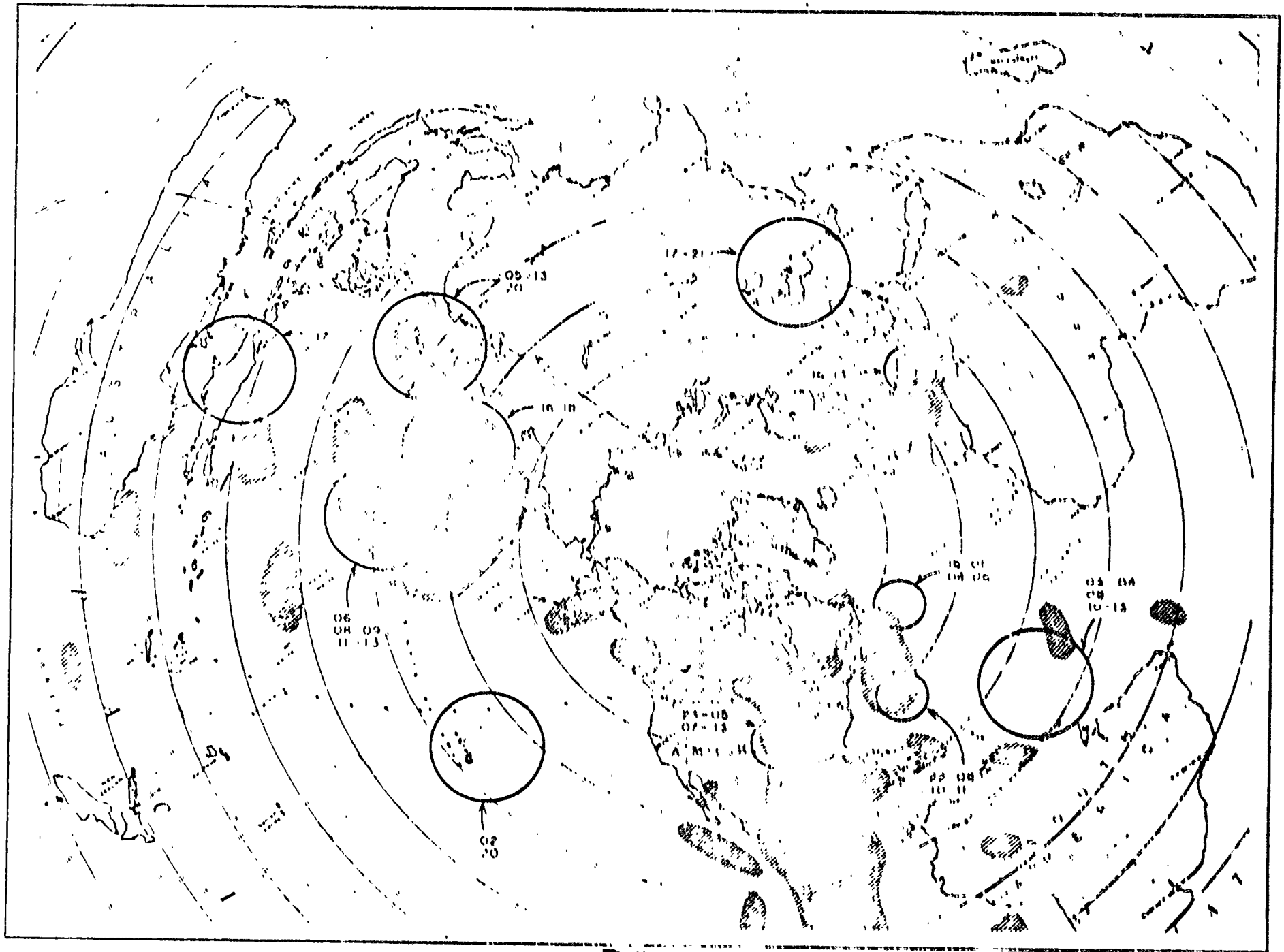

FIG. VI-4 SFERIC ACTIVITY, NOVEMBER 1958

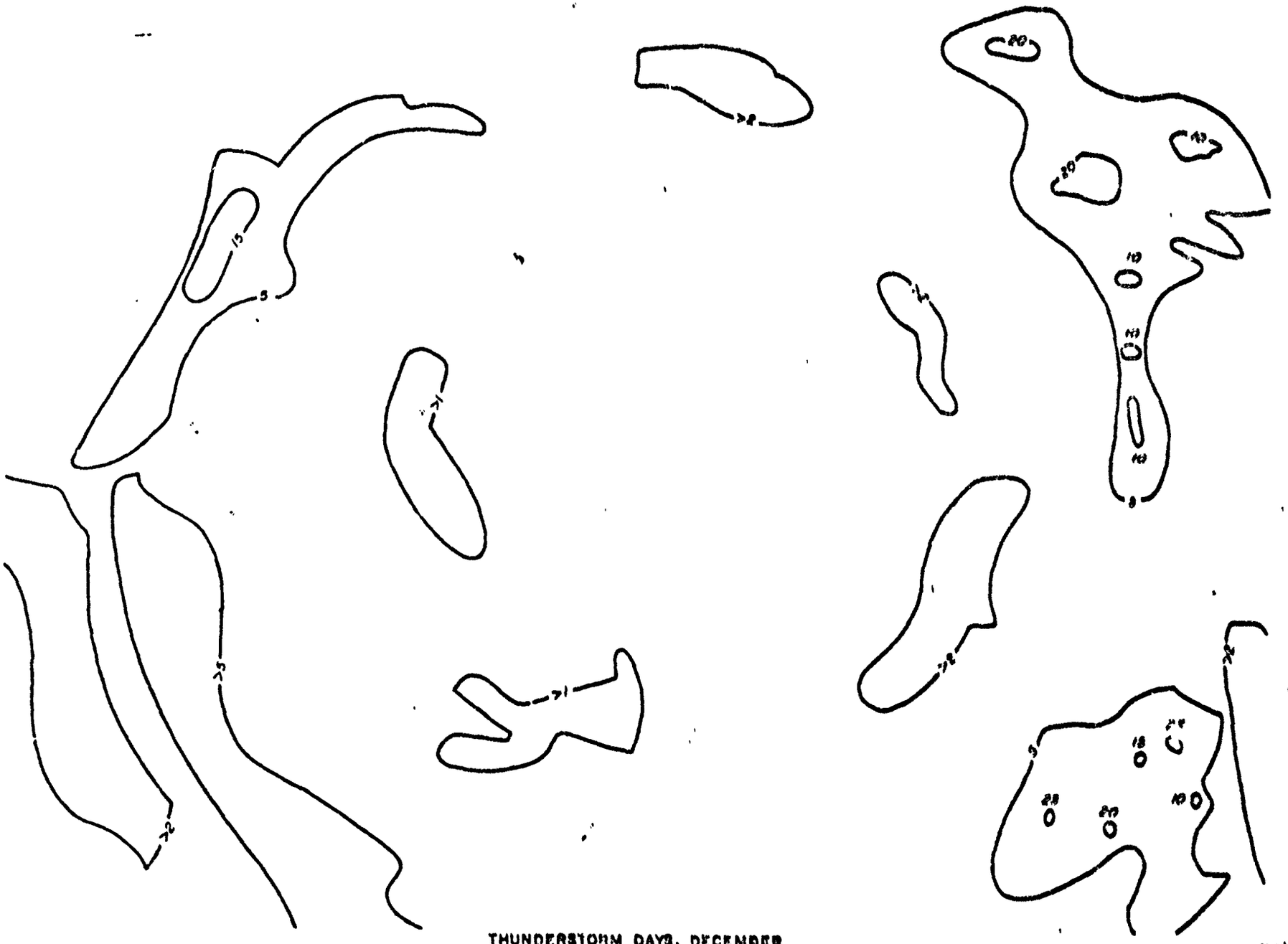

THUNDERSTORM DAYS, DECEMBER

THUNDERSTORM DAYS: DECEMBER

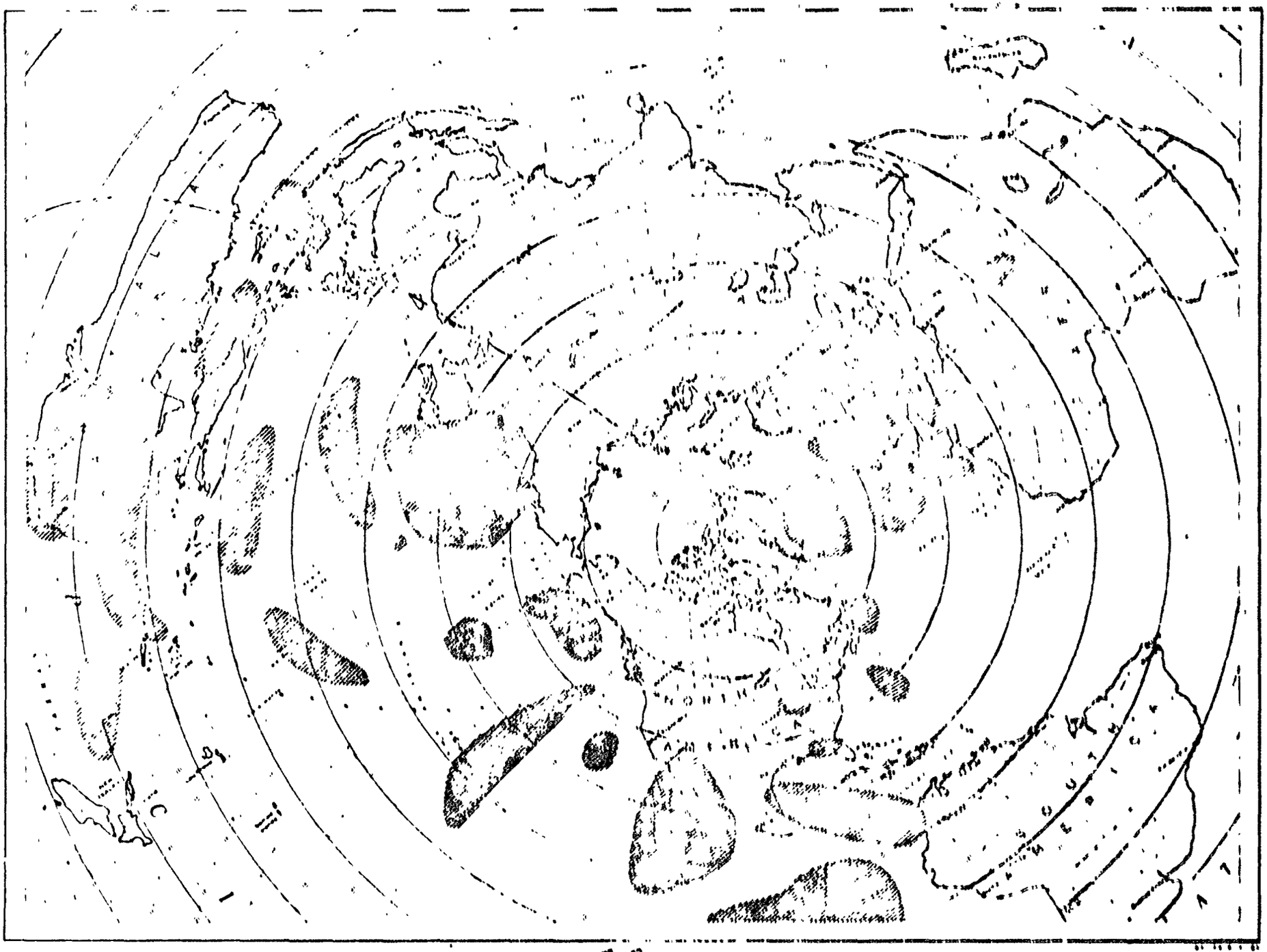

FIG. VI-5 SFERIC ACTIVITY, DECEMBER 1958

THUNDERSTORM DAYS, JANUARY

THUNDERSTORM DAYS, JANUARY

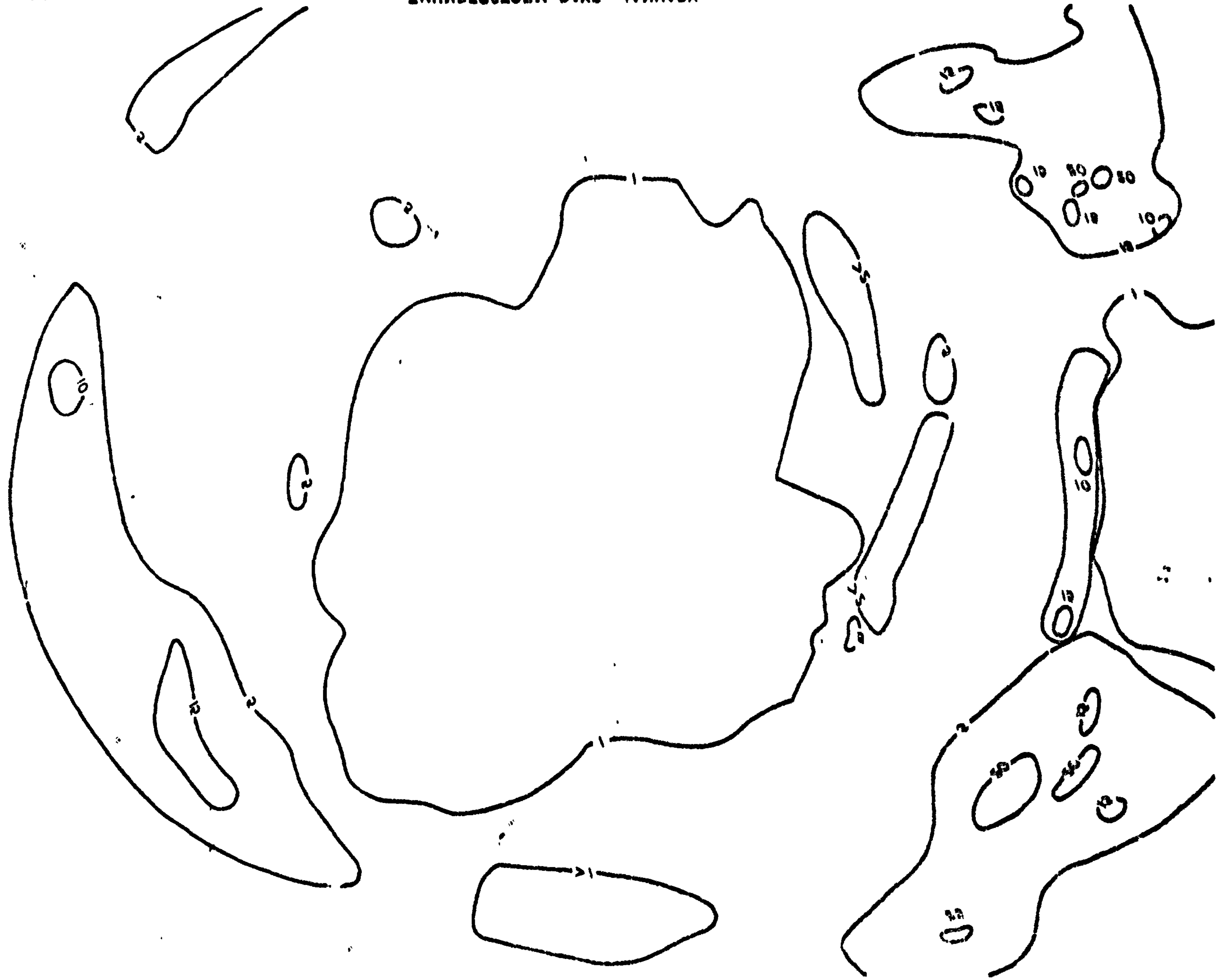

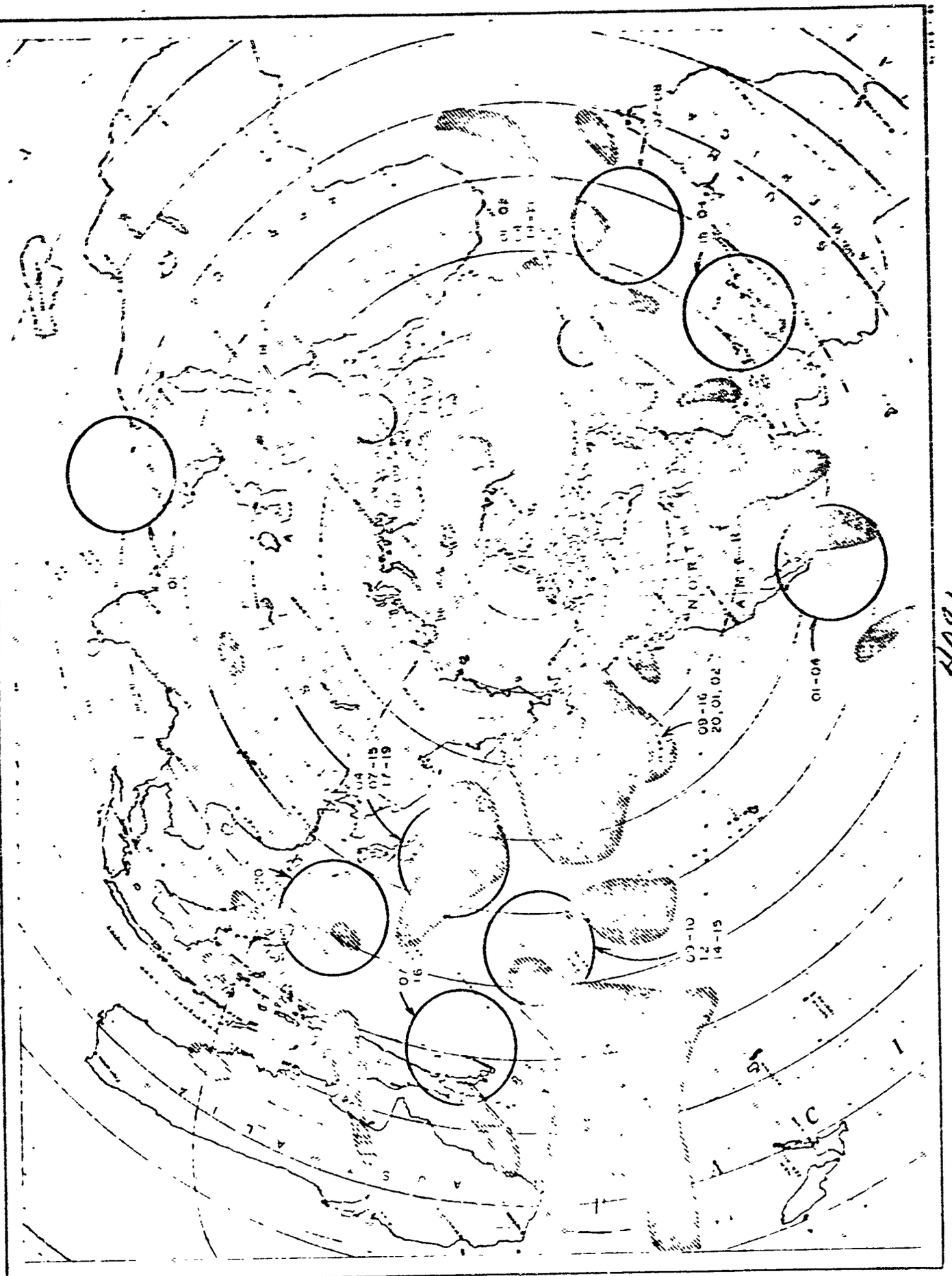

FIG. VI-6 SFERIC ACTIVITY, JANUARY 1959

THUNDERSTORM DAYS, FEBRUARY

THUNDERSTORM DAYS: FEBRUARY

THUNDERSTORM DAYS, FEBRUARY

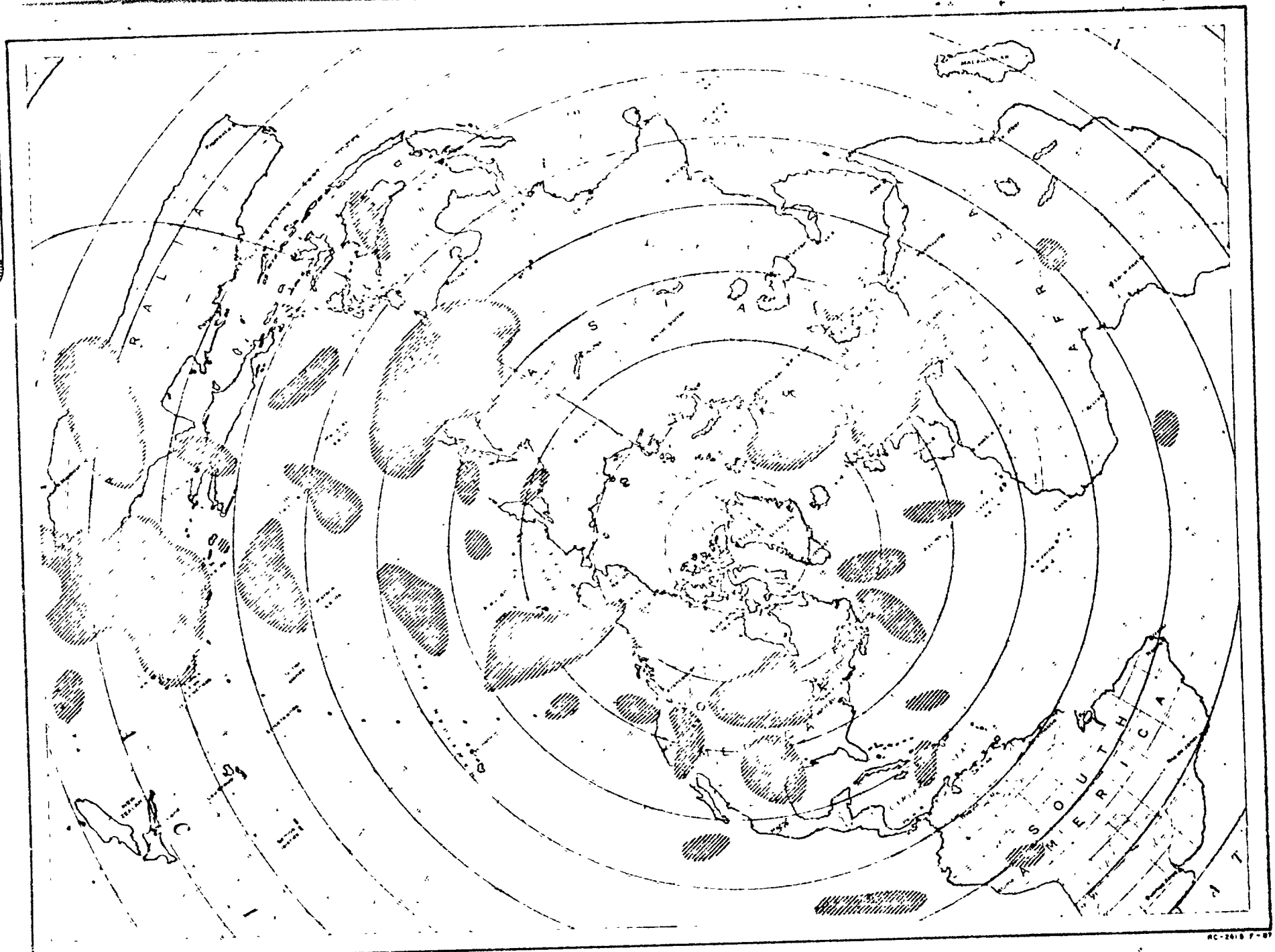

FIG. VI-7 SFERIC ACTIVITY, FEBRUARY 1959

THUNDERSTORM DAYS, MARCH

THUNDERSTORM DAYS, MARCH

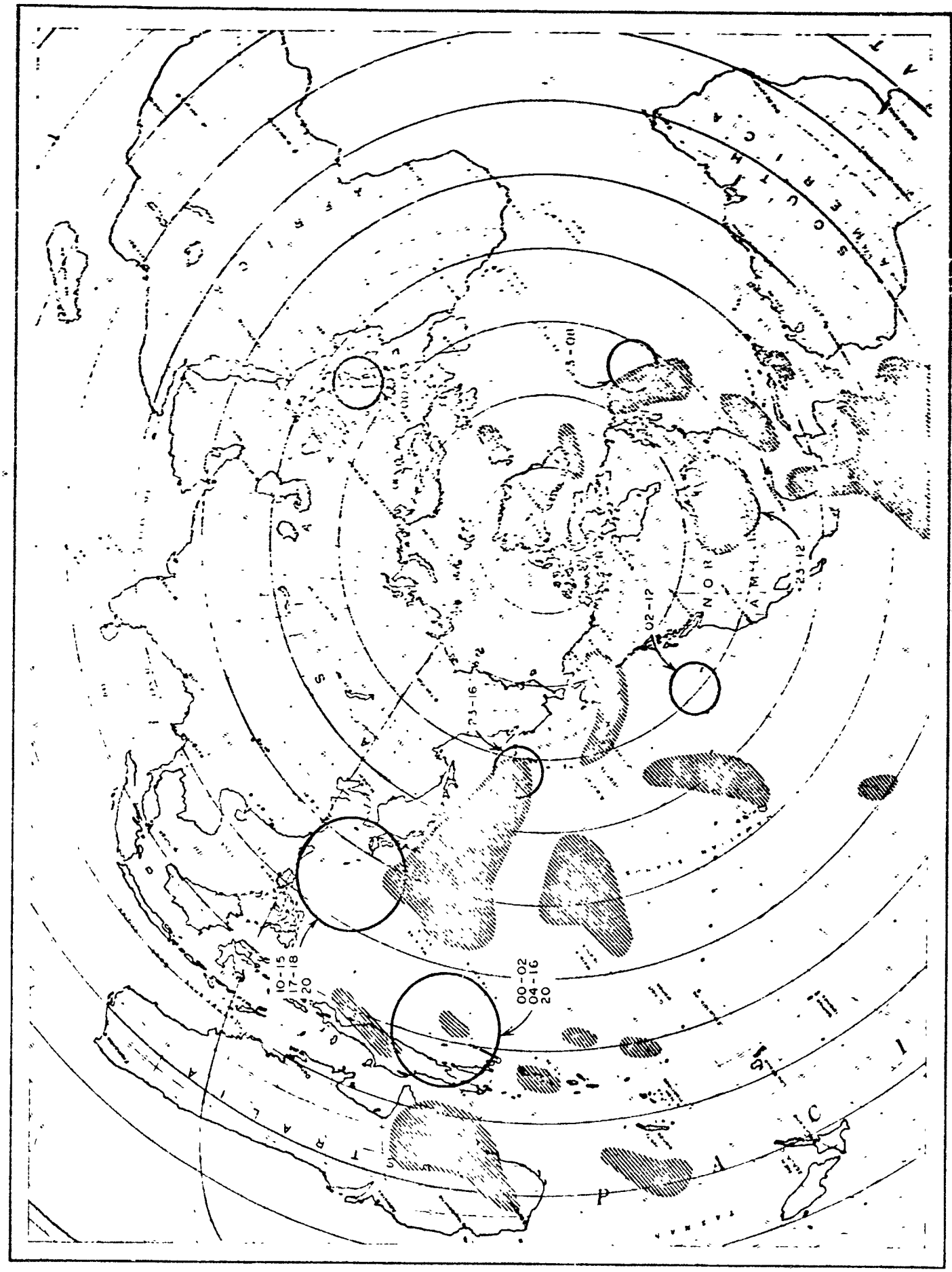

FIG. VI-8 SFERIC ACTIVITY, MARCH 1959

September and October 1958 were not adjusted to optimize the probability of receiving the same sferic at all three receiving stations.

B. Storm Center Locations

In addition to locating individual sferics from the waveform and DF film, the integrated DF films for September and November 1958 and January and March 1959 were used to locate storm centers as a function of time of day.* These storm centers were located from the geographical intersections of the DF lobes for each hour each month and are shown as circles of Figs. VI-2, VI-4, VI-6, and VI-8. The time in hours GMT is shown for each storm center. For example, off the coast of Japan in September 1958, thunderstorms occurred between 0700 and 1600 hours GMT. The circles on Figs. VI-2, VI-4, VI-6, and VI-8 do not necessarily represent a true picture of sferic storm centers since only those sferics within a limited amplitude range were recorded and since, using lobe intersections, there is a possibility that near storms hide distant storms.

The integrated-DF film data shown in Fig. VI-2, VI-4, VI-6, and VI-8 show sferic activity for each storm center as a function of time-of-day in GMT hours. These data have been converted into local time at each storm center and averaged to obtain the diurnal variation in sferic activity as is shown in Fig. VI-9. Figure VI-9 shows relative sferic activity for winter for any one geographic location in the Northern Hemisphere as a function of local time. Sferic activity is a minimum between 0400 and 1000 local time and increases to a maximum at 2000 local time with virtually all activity ceasing after 0400, local time. The relatively large activity during local night, in particular 0000 to 0400, agrees with other winter data [2] on thunderstorm activity. In normal summertime, maximum activity should occur in late afternoon, and minimum activity after midnight.

C. Thunderstorm Days

World thunderstorm days[3] have been recorded for years and data on average thunderstorm days in the form of contours are shown on Figs. VI-2 through VI-8 as overlays to show the correlation between sferic activity as determined by the SRI Sferic Monitoring System and reported thunderstorm days.

---

*The integrated DF films used here are shown in Appendix G

[2] "Thunderstorm Rainfall," Hydrometeorological Report 5, U.S. Army Engineer Waterways Experiment Station, Vicksburg, Mississippi

[3] "World Distribution of Thunderstorm Days," WMO/OMM-21, TP-21, World Meteorological Organization, Geneva, Switzerland (1956)

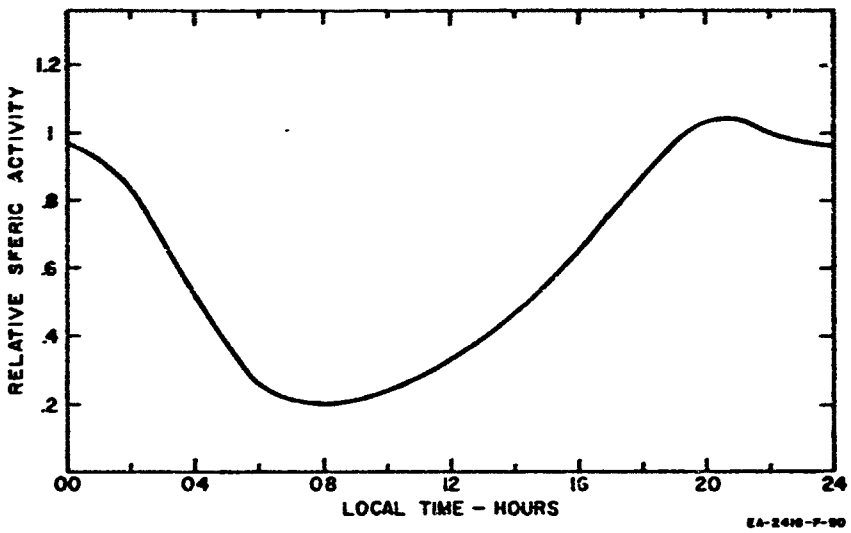

FIG. VI-9

DIURNAL VARIATION IN SFERIC ACTIVITY AT THE SFERIC SOURCE

VII ELF FROM SFERICS

It is well known that lightning strokes emit sferics with frequency components in the ELF band (below 1 kc). Sferic waveforms were recorded on waveform and DF film at various times with a system bandwidth of 10 cps to 30 kc. This section presents sferic ELF data collected at Thule, Greenland, and at St. Johns, Newfoundland.

A. VLF/ELF Ratio

Sferic ELF content can be measured as the peak-to-peak amplitude ratio of the VLF component to the ELF component. This measurement is referred to as the VLF/ELF ratio. ELF sferic waveform film was analyzed* for this ratio as indicated in Table VII-1 for September 1958 at Thule, and January 1959 at St. Johns. The VLF/ELF ratio was classified as positive or negative depending upon the initial polarity of ELF component. For sferics with a VLF component near the system threshold, it was not always possible to determine the initial polarity of the ELF component. Sferics in this class were classified as "unknown polarity."

The SRI Sferic Monitoring System has a dynamic recording range of 20 db above VLF threshold amplitude. Thus, VLF/ELF ratios greater than about 20 (ELF less than 1/2 VLF threshold amplitude) were not readable and were classified as "no ELF." This limitation tends to accentuate the number of sferics in the "no ELF" classification.

The VLF/ELF ratio data from St. Johns were collected in January 1959 at a VLF threshold of 30 mv/m. Samples were obtained throughout the GMT day. The distribution of the VLF/ELF ratio of all ELF sferics observed at St. Johns is shown in Fig. VII-1. The distribution is approximately log normal with a mean of 6.56 and a median of 5.9. The mean VLF/ELF ratios as a function of time of day for positive and negative polarities are shown in Fig. VII-2. VLF/ELF ratio is fairly constant for local nighttime and increases and becomes slightly erratic during the local daytime.

Figure VII-3 shows the percentage of sferics with positive, negative, and no ELF as a function of time of day at St. Johns. Sferics with positive ELF predominate.

Figure VII-4 shows the distribution of the VLF/ELF ratio at Thule for the various thresholds listed in Table VII-1. All sferics with ELF components are shown with no differentiation as to polarity since the data in Table VII-1 show that the percentage of sferics in each classification is independent of sferic VLF amplitude (threshold).

---

*The propagation velocity for ELF is less than that for VLF, and at large distances from the sferic source the ELF pulse is time separated from the VLF pulse. Thus, VLF and ELF components were separable on the film records.

TABLE VII-1 VLF/ELF Ratio Data

LOCATION AND DATE	VLF THRESHOLD MV/M	TOTAL SFERICS	PERCENT OF TOTAL SFERICS				MEAN VLF/ELF RATIO		
			POSITIVE	NEGATIVE	UNKNOWN POLARITY	NO ELF	POSITIVE	NEGATIVE	ALL*
Thule, Greenland September 1958	1	180+	≈65	≈10			1.65	1.07	1.88
	3	607	61.8	14.0	12.4	11.8	3.22	3.76	3.38
	10	163	59.5	19.2	14.1	17.2	4.23	3.26	4.08
	30	388	53.9	13.9	12.6	19.6	5.62	5.96	5.69
	100	72	56.9	11.2	15.2	16.7	4.76	5.19	4.83
	All$^{\Phi}$	1410	58.7	13.2	12.8	15.3	3.69	4.11	3.86
St. Johns, Newfoundland January 1959	30	774	23.4	26.1	17.2	33.3	6.63	5.96	6.79
	100	48+	≈27	≈21			5.61	6.71	6.10

*Including sferics with unknown ELF polarity

+Recorded only sferics with positive or negative ELF. Percentage is based on other data and is approximate.

$^{\Phi}$Not including the 180 sferics at 1 mv/m

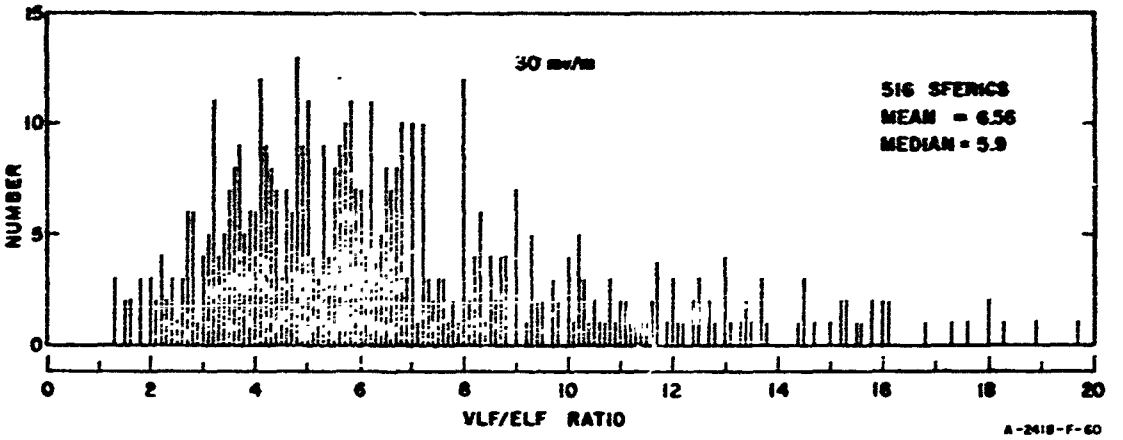

FIG. VII-1

DISTRIBUTION OF VLF/ELF RATIO, ST. JOHNS, NEWFOUNDLAND
JANUARY 1959

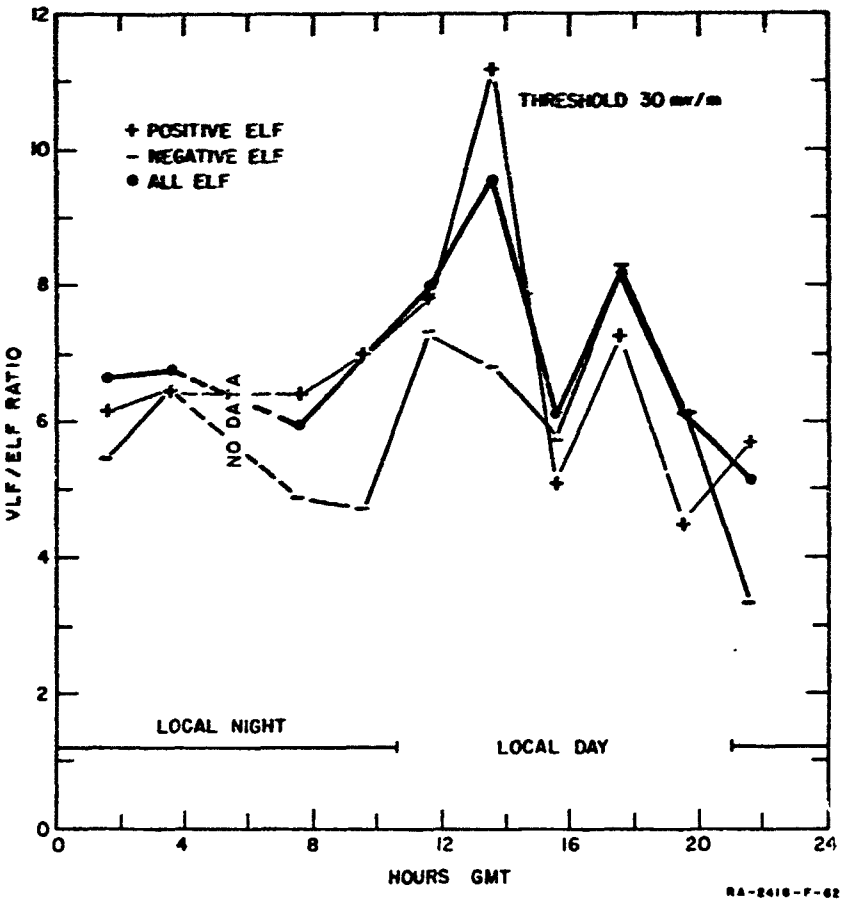

FIG. VII-2

DIURNAL VARIATION OF VLF/ELF RATIO, ST. JOHNS, NEWFOUNDLAND
JANUARY 1959

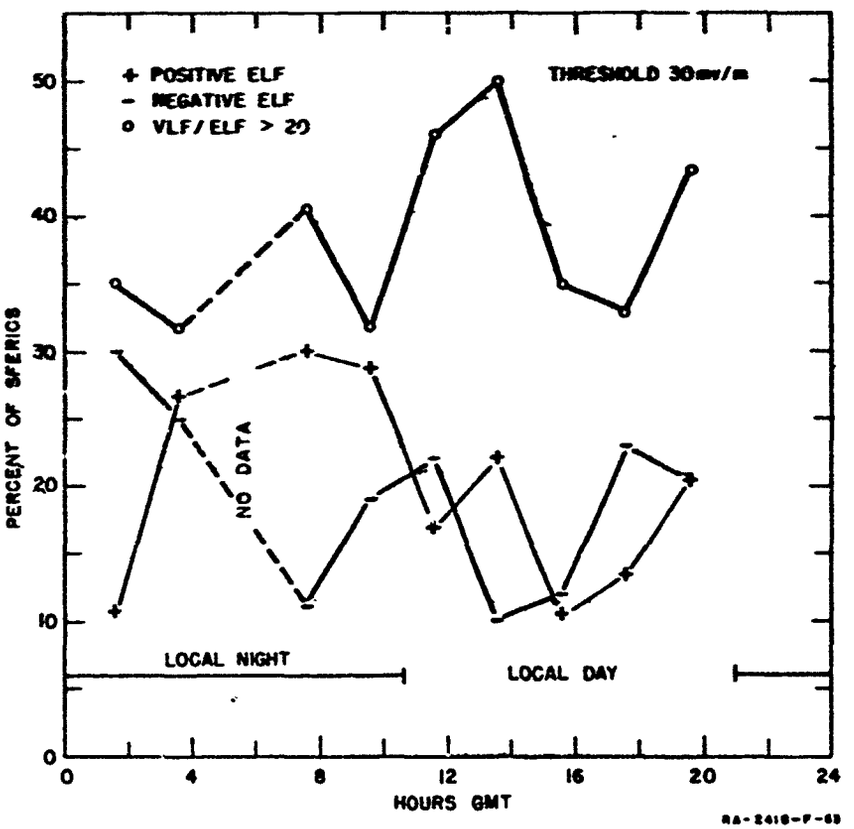

FIG. VII-3

DIURNAL VARIATION OF ELF POLARITY, ST. JOHNS, NEWFOUNDLAND
JANUARY 1959

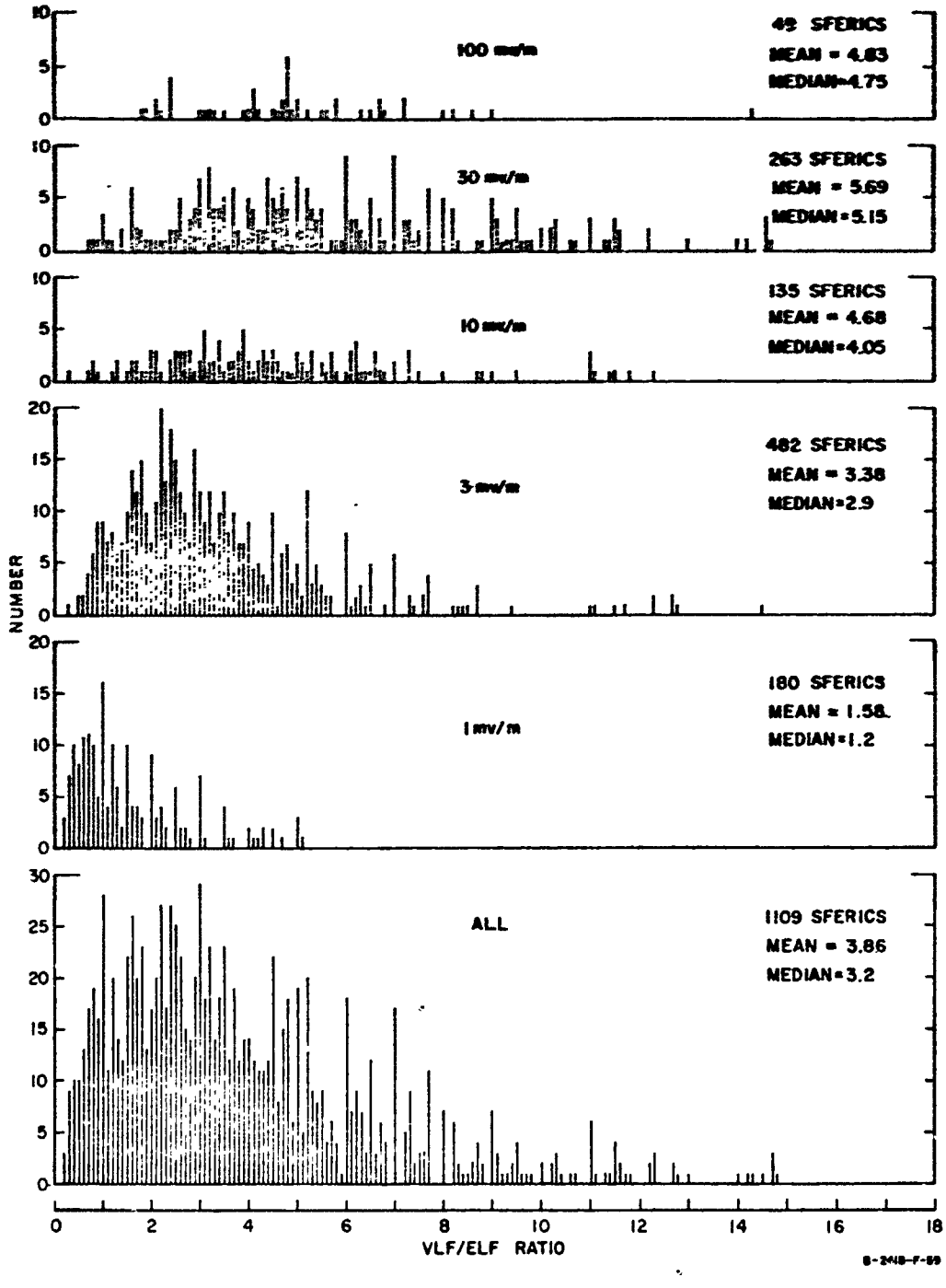

FIG. VII-4

DISTRIBUTION OF VLF/ELF RATIO, THULE, GREENLAND
SEPTEMBER 1958

The VLF/ELF ratio is approximately log-normal in distribution. The mean and median values of the VLF/ELF ratio as a function of VLF threshold are shown in Fig. VII-5, which indicates that as VLF threshold (amplitude) increases the mean and median VLF/ELF ratio increases. The data at 100 mv/m threshold is based on only 49 sferics and is not considered statistically reliable. A possible explanation of this VLF/ELF ratio increase with VLF amplitude can best be seen by looking at Fig. VII-6 which shows three typical sferics received at St. Johns, Newfoundland, and at Thule, Greenland. The upper two sferics originated in the Caribbean area and contain ELF components. These two sferics are typical and indicate that in arctic regions ELF is not attenuated as much as VLF. This difference in VLF and ELF propagation attenuation means that closer to the sferic source the VLF/ELF ratio increases. Referring again to Fig. VII-5, we see that the VLF/ELF ratio is increased when VLF threshold is increased, and increased threshold means decreased observing range. Thus, the mean VLF/ELF ratio is a function of the geographic location of the collection point with respect to the sferic activity centers throughout the world.

B. A Note Concerning ELF Propagation

In addition to the apparent decrease in propagation attenuation for ELF over VLF, Fig. VII-6 shows another phenomenon. For the same sferic from the Caribbean, the initial excursion of the ELF component reverses polarity in propagating from St. Johns to Thule. This reversal may or may not be an actual phase reversal since the method of recording both ELF and VLF in the same channel tends to hide any ELF component that occurs during the VLF portion of the sferic. However, the sferics shown in Fig. VII-6 are typical of all sferics received at St. Johns and Thule. Although the data obtained have limitations, they do indicate that further measurements should be made to determine whether this apparent ELF phase reversal is an actual reversal, indicating a possible ELF propagation anomaly.

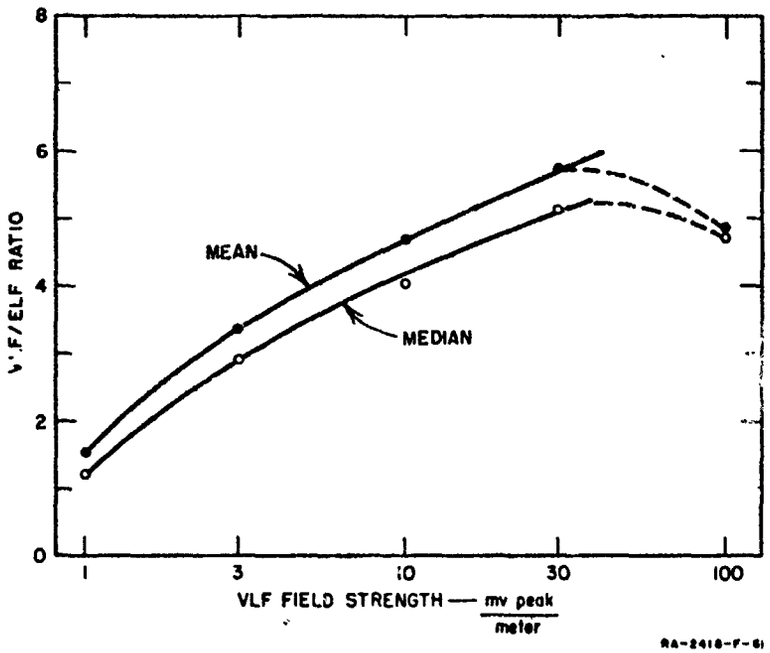

FIG. VII-5

VLF/ELF RATIO AS FUNCTION OF SIGNAL AMPLITUDE, THULE, GREENLAND
SEPTEMBER 1959

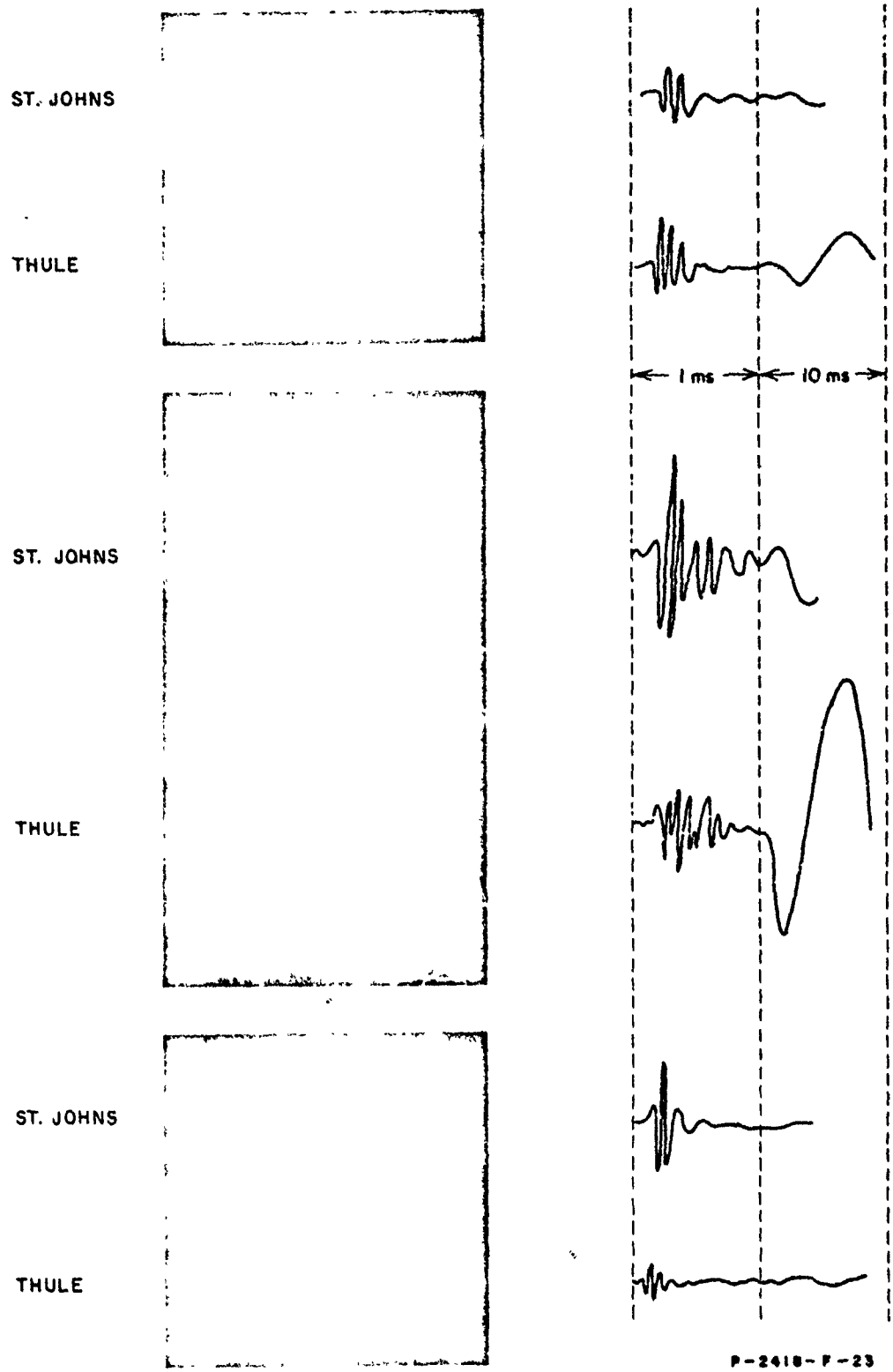

FIG. VII-6

ELF WAVEFORMS

VIII SOME OBSERVATIONS ON VLF PROPAGATION

The sferic data collected at the sferic monitoring stations at Fairbanks, Alaska, at Thule, Greenland, and at St. Johns, Newfoundland, contain a great potential for better understanding VLF propagation in Arctic regions. Data applicable to VLF propagation studies are: (1) relative received peak amplitudes as a function of geographic sferic source location, (2) spectral analysis of 3- to 30-kc sferic waveforms over known propagation paths, (3) atmospheric noise spectrum in the 12- to 20-kc frequency range as recorded by the scanning receiver, and (4) received amplitude and direction-of-arrival of keyed-CW VLF stations.

These studies were beyond the scope of the present program. However, some preliminary observations to indicate the potential information available on VLF propagation are given in the hope that the data collected in the future can be utilized to better understand VLF propagation in Arctic regions.

A. Relative Received Peak Amplitude

As indicated in Sec. VI, the geographic sources of some 3,200 sferics have been located in all regions of the Northern Hemisphere. Spectral analysis of these sferics could provide propagation attenuation data as a function of frequency from 3 to 30 kc for various paths in the Arctic, but time and effort were not available to do this. However, the peak received amplitudes of the 3,200 sferics, whose source locations were known, were normalized to a received unity amplitude at Thule, and are shown in Fig. VIII-1 for the various areas of the Northern Hemisphere. The numbers shown are average normalized received peak amplitudes for Fairbanks, Thule, and St. Johns respectively. The question mark symbol indicates that no data are available. Figure VIII-1 indicates that propagation attenuation over sea water is approximately 2 db/1000 km, over land it is 4 db/1000 km, and over Arctic tundra and ice, it is 6 to 8 db/1000 km.

B. Propagation Over Specific Arctic Paths

Comparison of sferics propagated along a path through two monitoring stations provides propagation data for specific paths in the Arctic. Figures VIII-2 and VIII-3 show sferics propagated along the Fairbanks-Thule and St. Johns-Thule paths, respectively. Peak amplitude comparisons give a peak amplitude down 61 percent for propagation from Fairbanks to Thule and down 24 percent from St. Johns to Thule.

Additional sferics were analyzed for peak amplitude attenuation and gave the following average percentage attenuation for the paths listed:

Fairbanks to Thule	48 percent using 51 sferics
Thule to Fairbanks	32 percent using 20 sferics
St. Johns to Thule	26 percent using 22 sferics

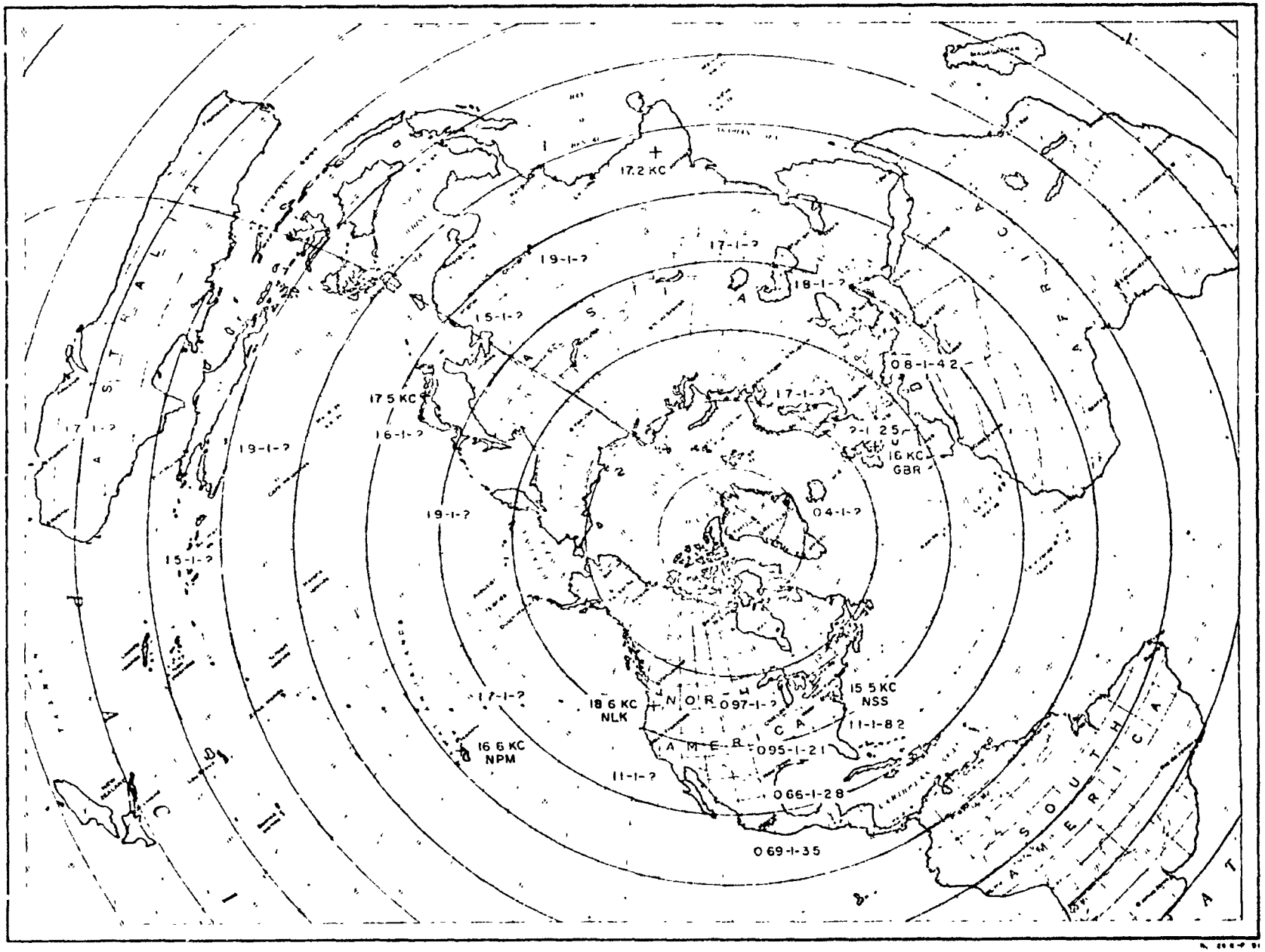

FIG. VIII-1 RELATIVE RECEIVED PEAK AMPLITUDE GEOGRAPHIC DISTRIBUTION

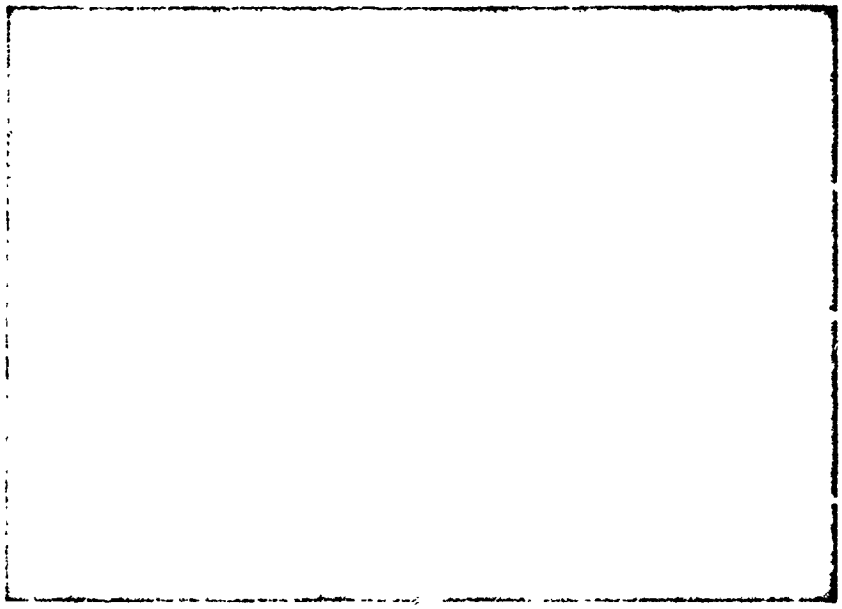

FAIRBANKS, ALASKA – 66 mv/m

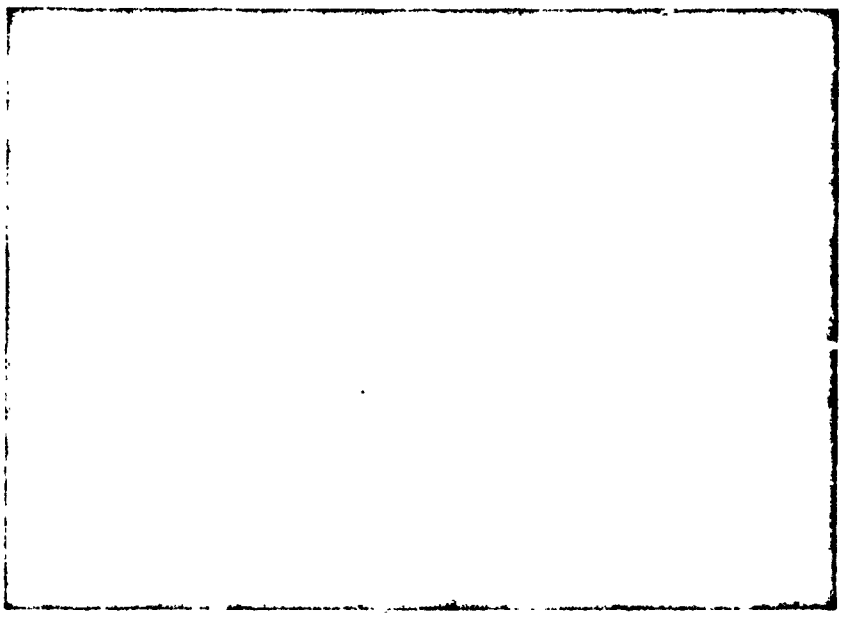

THULE, GREENLAND - 40 mv/m

P-2418-F-92

FIG. VIII-2

SFERIC PROPAGATED ALONG FAIRBANKS-THULE PATH

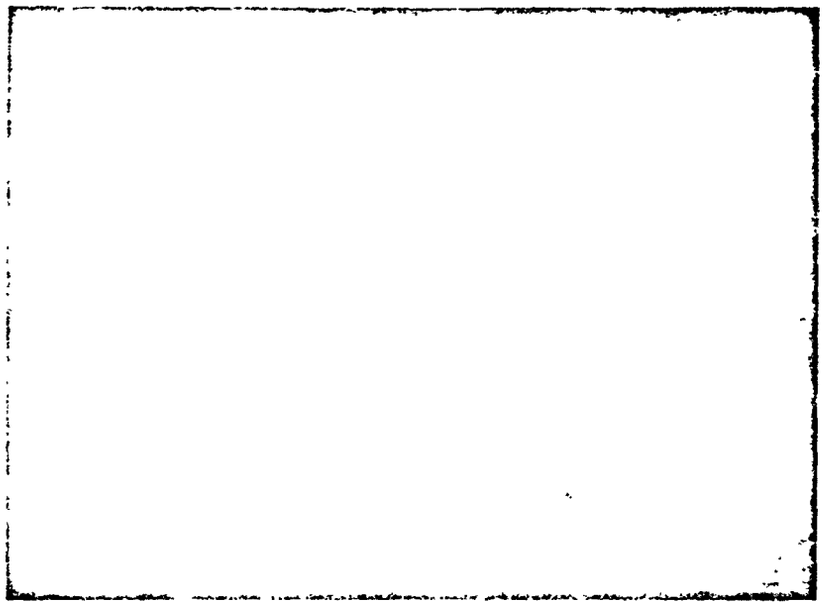

ST. JOHNS, NEWFOUNDLAND – 110 mv/m.

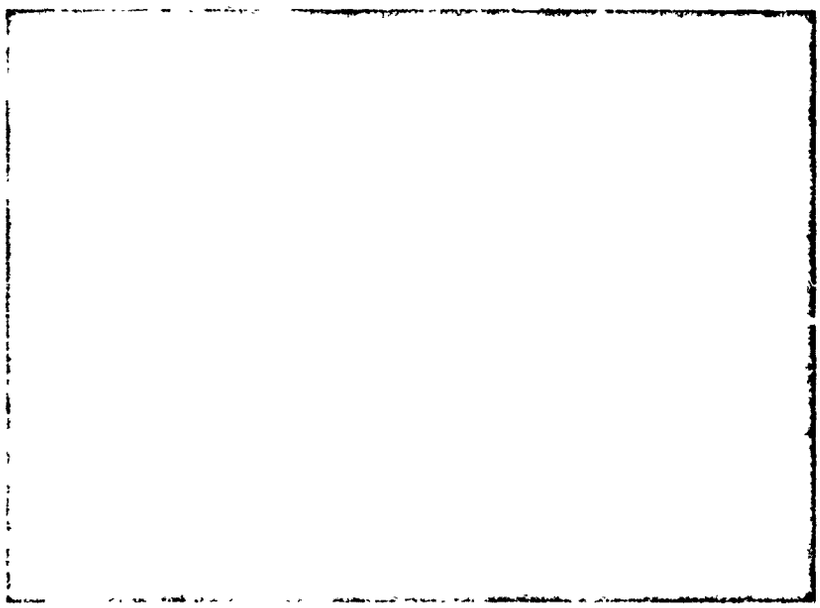

THULE, GREENLAND – 26 mv/m

P-2418-F-93

FIG. VIII-3

SFERIC PROPAGATED ALONG ST. JOHNS-THULE PATH

The above data indicate a difference in peak amplitude attenuation in propagation from Fairbanks to Thule compared to Thule to Fairbanks. While spectral analysis of these sferics was not performed, it is believed that this difference in peak amplitude attenuation is due to differences in spectral content of the two sferic sources. However, it is possible that for a particular frequency, attenuation is not identical for both directions. Comparison of Figs. VIII-2 and VIII-3 indicates differences in the spectral content of the sferics shown, although the exact nature of the spectral content cannot be determined without further analysis.

C. Atmospheric Noise Spectrum

The scanning receiver data presented in Appendix F present the average 12- to 30-kc spectrum of atmospheric noise as received at Fairbanks, Thule, and St. Johns. These data show the average 12- to 30-kc sferic spectrum for the intervals indicated. Some obvious facts can be seen. The sferic amplitude spectrum in general decreases with increasing frequency, with occasional peaks at approximately 15 and 25 kc. The month-to-month spectrum variation at each sferic monitoring station is a function of average distance to sferic source centers, direction of major activity, and possible variations in propagation. A detailed analysis of the direction-of-arrival distributions in Appendix D, sferic source locations from waveform and DF film and from integrated DF film as shown in Sec. VI, and the scanning receiver records might explain the spectrum variations and indicate the effects of Arctic propagation in the 12 to 30 kc frequency range.

D. VLF Station Reception

The scanning receiver recorded the presence--and to a certain degree the received amplitude--of several keyed-CW VLF stations between 15 and 21 kc. The frequency and location of the VLF stations received are shown on Fig. VIII-1. The received signal amplitudes were sensitive to signal duty cycle, as unknown, and since the scanning receiver time-sampled each signal at random times at each sferic monitoring station, reliable amplitude data were not obtained and therefore are not presented in this report. However, a review of the data on VLF stations did not indicate any obvious attenuation anomalies in the Arctic. The scanning receiver records are available for further analysis.

As is indicated in Appendix H, direction of arrival of keyed-CW VLF station signals were recorded from time to time. These data indicate that VLF propagation via the ionosphere may be dependent upon the alignment of the propagation path with the earth's magnetic field. This possible phenomenon is discussed in Appendix H.

IX CORRELATION WITH GEOPHYSICAL DATA

A. Solar Influence

Activity on the sun reacts in a complex manner with the earth's ionosphere and earth's magnetic field to affect long-range terrestrial propagation.[4] Solar activity, in the form of sunspots and flares, emit wave and particle radiations. Wave radiation traveling at the speed of light penetrates the sunlit portion of the earth's ionosphere and causes, among other things, a short-term enhancement of the D layer. Particle radiation, requiring one to two days to travel from the sun to the vicinity of the earth, reacts with the earth's ionosphere and magnetic field, causes magnetic storms, and influences aurora.

B. Sunspot Number and Magnetic Index

Relative sunspot number is reported as American R_A,[5] and Zurich Provisional R_Z for each day. R_A, and R_Z are approximately equivalent. Magnetic index, K_p, is averaged for the entire earth for each 3-hour interval of each day. Relative sunspot numbers and magnetic index were available for the entire operating period of the sferic monitoring stations and were plotted for correlation with the 10 mv/m sferic rate and RMS noise level at 15 and 25 kc for each sferic monitoring station. No correlation was found.

The lack of correlation could be due to the forms of data used. Sferic data were obtained by an omnidirectional system that did not have either an all-daytime or an all-nighttime propagation path. The magnetic index, K_p, is a world-wide average measure of magnetic activity and does not necessarily apply to the paths over which the major sferic activity was propagated for each station.

C. Solar Flares

The effects of solar flares upon the ionosphere are reported as sudden cosmic noise absorption (SCNA), sudden enhancements of Atmospherics (SEA), and solar noise bursts at 18 Mc (Burst). SEA is the effect of solar wave radiation causing enhancement of the D-layer. This enhancement normally lasts for 1/2 to 2 hours and is monitored by observing atmospherics at 27 kc.

---

[4] For a rather simplified discussion of solar effects, see M. A. Ellison, The Sun and Its Influence, (The MacMillan Co., New York, 1955).

[5] Geophysical data were obtained from monthly bulletins CRPL-F-178, "Part A--Ionospheric Data," and "Part B--Solar-Geophysical Data," National Bureau of Standards, Boulder, Colorado

SEA data were available for September and October, 1958, during which time only two occurences of major importance were recorded at 1640 to 1715 GMT and 1920 to 2020 GMT, 13 October 1958. Scanning receiver records were available from Thule, and St. Johns, for these periods. The records did not show an increase at the starting times of each SEA. Data from the scanning receiver records at 15 and 25 kc for RMS noise level and for keyed-CW VLF stations that were received are shown in Fig. IX-1. A definite correlation based upon this single sample cannot be made since the magnitude of signal level variations shown are commonly observed when a SEA is not reported. As stated before, keyed-CW VLF station signal amplitude is sensitive to duty cycle of signal and time of sample.

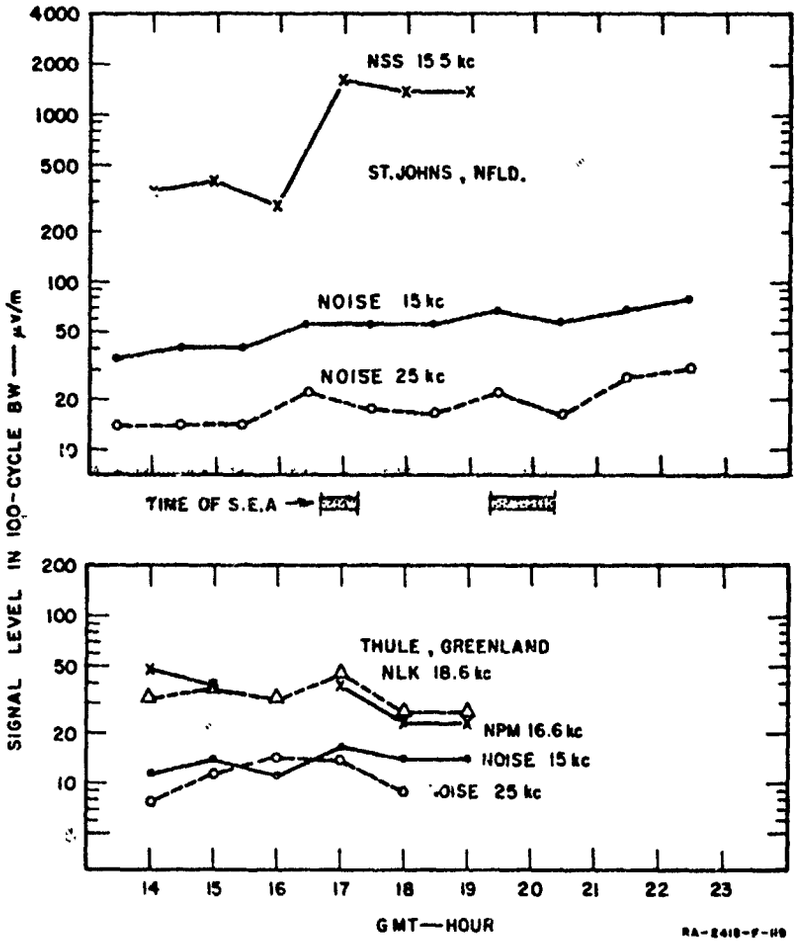

FIG. IX-1

SCANNING RECEIVER DATA DURING SOLAR FLARE, 13 OCTOBER 1958

ACKNOWLEDGMENT

The author acknowledges with gratitude the assistance of many persons in the Radio Systems Group who contributed greatly to the work reported herein. In particular, the site operators--R. B. Daniel at Fairbanks, Alaska, A. H. Selby at Thule, Greenland, and E. W. Green at St. Johns, Newfoundland--repeatedly performed the seemingly impossible to meet operating schedules and solved unforeseen difficulties in the Arctic winter.

Data reduction, a thankless, tedius task, was performed efficiently and with minimum direction by H. V. Prentiss, W. F. Mullen, R. MacKinnon, Helen Thompson, and Barbara J. Cribbins.

The author wishes to thank J. H. Priedigkeit, R. A. Nelson, and L. R. Tepley for their assistance in the technical operation of the program and in preparation of this report.

Appendix A

INSTALLATION

Preceding page blank

INSTALLATION

1. Site Selection

Sites for installation of the SRI Sferics Monitoring System were selected to satisfy the following criteria:

(1) Sites in the North American continent were to be utilized to determine sferic activity in the Northern Hemisphere with best coverage on the land masses.

(2) Sites were to be on, inside, and outisde the Arctic Circle and auroral zone to evaluate Arctic VLF propagation.

(3) Interference in the form of electrical power radiation was to be a minimum.

(4) Air Force bases were preferred to minimize logistic support problems.

Two site survey teams were used to find locations in the Arctic that satisfied the above criteria. Team One surveyed sites at Ft. Barrow and Fairbanks, Alaska, and selected Fairbanks as the site that most nearly satisfied the above criteria.

Team Two surveyed sites at Thule, Greenland and at various locations in Newfoundland, during April and May 1958. Sites at Thule AFB, Greenland, on South Mountain and at an abandoned receiver site at Pepperrell AFB, St. Johns, Newfoundland, were selected.

2. Fairbanks, Alaska

The site at Ladd AFB, Fairbanks, Alaska is approximately 100 miles south of the Arctic Circle and is in the auroral zone. The geographical location is latitude 64° 55'N and longitude 147° 40'W. Installation was made in an undeveloped area approximately one-quarter mile from military housing barracks (see Fig. A-1). Base coordinates were N 294000, E 304200. An aero-medical laboratory was the only other building in the immediate area.

The equipment was housed in a 33-foot commercial house trailer which was heated by electrical heaters to satisfy fire regulations. Electrical power was available at a pole 50 feet from the trailer and was extended to the trailer by cable lying on the surface of the ground.

The 30-foot crossed-loop antenna was erected 100 feet east of the trailer, and aligned to true North by correcting a magnetic compass, since sighting Polaris is impossible in July at this latitude. Base Air Installation personnel, under the direction of the SRI installation engineer, were used to align the antenna.

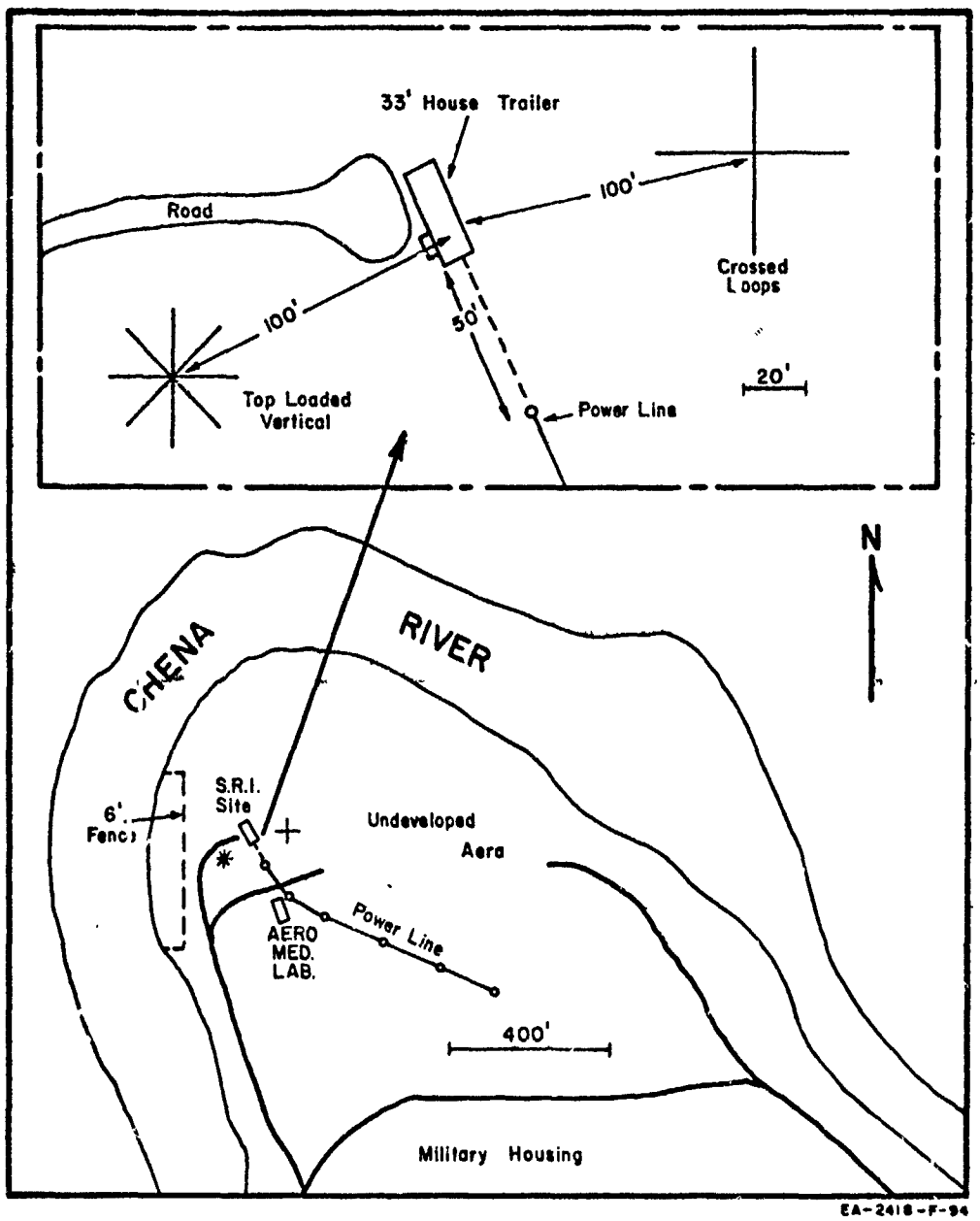

FIG. A-1

INSTALLATION AT FAIRBANKS, ALASKA

The 30-foot, top-loaded, vertical antenna was erected 100 feet west of the trailer on a 40-foot, chicken-wire ground screen. Antenna capacitance was measured as 375 micromicrofarads. Capacitance of the coaxial cable leading to the vertical antenna was 1,930 micromicrofarads.

Upon completion of the installation at Ladd AFB on 22 July 1958, electrical interference was measured as 1 volt per meter, center to peak, at 60 cycles and 0.1 volt per meter, center to peak, at 180 cycles. Higher harmonics of electrical power interference were approximately 70 millivolts per meter, center to peak. These measurements did not agree with those made on 20 March 1958 by a site survey team. The electrical power interference measured by the site survey team was 15 millivolts per meter, center to peak. This difference was not considered to be abnormal since the installation required electric power lines not present when the site survey was made.

3. Thule, Greenland

The site at Thule AFB, Greenland is inside both the Arctic Circle and the auroral zone, at latitude 76° 31'N and longitude 68° 48'W. Installation was made on South Mountain, about 2 miles south of the main base area (see Fig. A-2). Base coordinates were N 31600 E 27400. South Mountain is used by several other installations, the nearest being a corner reflector and two rhombic antennas 1,700 feet from the SRI installation. Site elevation is approximately 700 feet above sea level and about 450 feet above the main base area.

The equipment was housed in a standard, movable, Air Force, arctic building positioned approximately 400 feet south of the existing road with a floor area of approximately 600 square feet. Electric heat was used. Electric power was supplied by the Base from an existing power line 400 feet north of the road. Electric power lines were installed from the existing power line to the building. The electric power distribution system on South Mountain is laid on the ground inside pipes. A 30-kilowatt gasoline motor generator for standby electrical power was housed along the Base power line approximately 200 feet from the building containing the SRI Sferics Monitoring System.

The 30-foot crossed-loop antenna was erected 150 feet south of the building and was aligned to True North by correcting a magnetic compass and sighting known existing land marks.

The 30-foot top-loaded vertical antenna was erected 300 feet south of the building on an existing ground screen consisting of 36 radials, each 200 feet in length. Vertical antenna capacitance was measured as 370 micromicrofarads. The vertical antenna coaxial cable was RG-13U, and its capacitance was 7,100 micromicrofarads.

Interference at Thule AFB consisted of a high-power radio station just above the 30 kilocycle upper limit of SRI sferics monitoring system. A trap was installed in the vertical and DF systems to reduce this

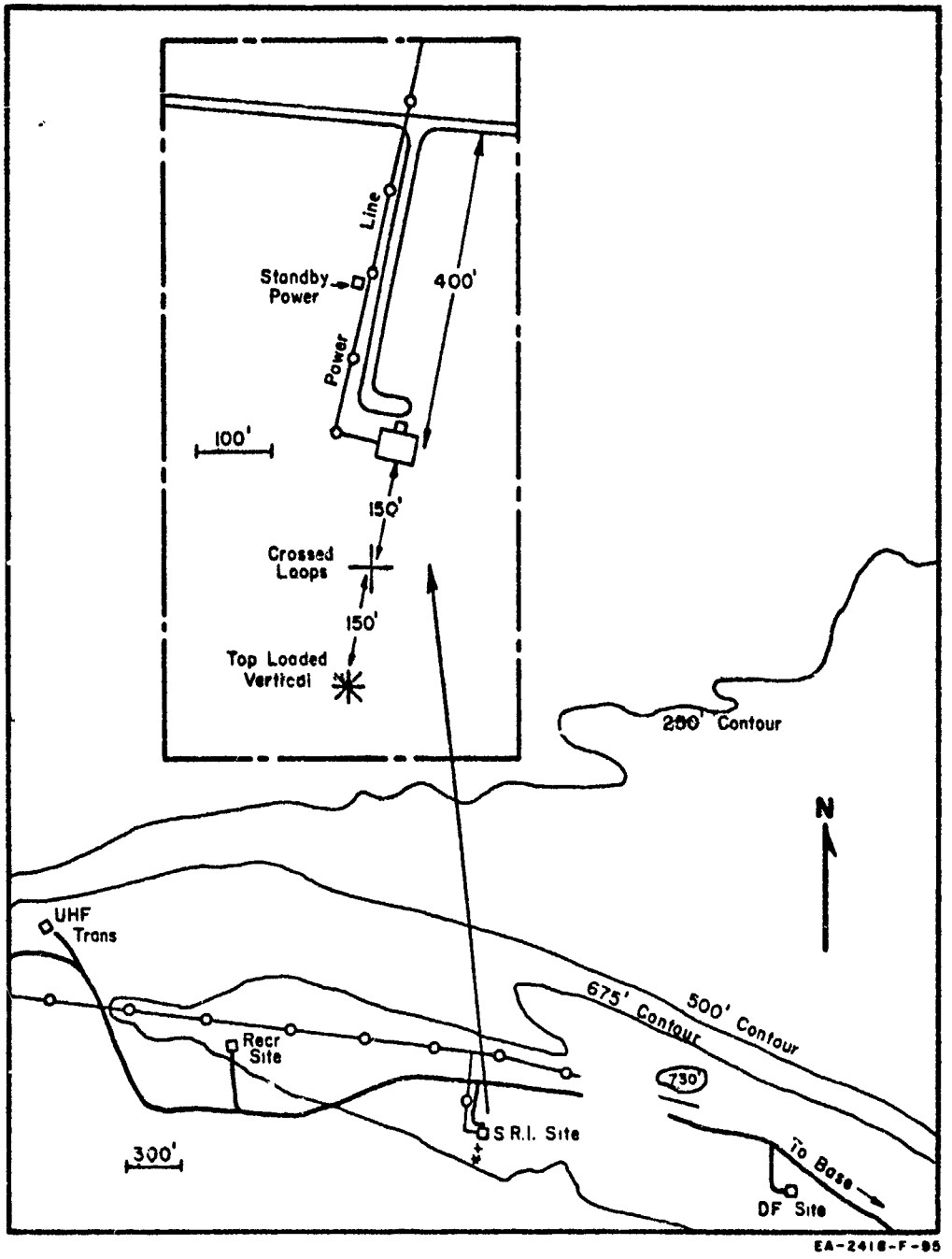

FIG. A-2

INSTALLATION AT THULE, GREENLAND

interference by 80 db below the system midband gain. This reduced the interference from the radio station to less than an equivalent field strength of 0.5 millivolt per meter, center to peak.

Interference from the electrical power and its harmonics after installation was measured as 45 millivolts per meter, center to peak, using Base electric power. Using standby power, the interference was 5 millivolts per meter, center to peak.

4. St. Johns, Newfoundland

The site at Pepperrell AFB, St. Johns, Newfoundland, is outside both the Arctic Circle and the auroral zone. The geographic location is latitude 47° 37'N and longitude 52° 47'W. Installation was made at the unused receiving site, Snelgrove, some 5 miles NE of Pepperrell AFB (see Fig. A-3). Three buildings and a fire watch tower are on the site. Snelgrove is the highest hill in the area at an elevation of 756 feet. The terrain is rocky and hilly, has numerous ponds, and forms a peninsula with sea water on the west, north, and east sides. The coast line, which is a 400- to 800-foot cliff, is 4 miles west, 12 miles north, and 6 miles east of Snelgrove.

The equipment was located in the center section of one unused building 520 feet west and 40 feet below the peak of the hill. Oil heaters were used. Electrical power was commercially available on an existing line on poles entering the site from the south.

The 30-foot crossed-loop antenna was erected on sloping ground approximately 180 feet from the equipment and was aligned to True North by sighting Polaris.

The 30-foot top-loaded vertical antenna was erected east of the equipment on an existing ground screen consisting of 36 radials each 150 feet in length. The ground screen is on a leveled area. Two additional ground screens are located approximately 300 feet south of the antennas. Vertical antenna capacitance was measured as 440 micromicrofarads. The vertical antenna coaxial cable was RG-13/U and its capacitance was 9500 micromicrofarads.

Interference from electrical power and its harmonics were measured as less than 3 millivolts per meter, center to peak.

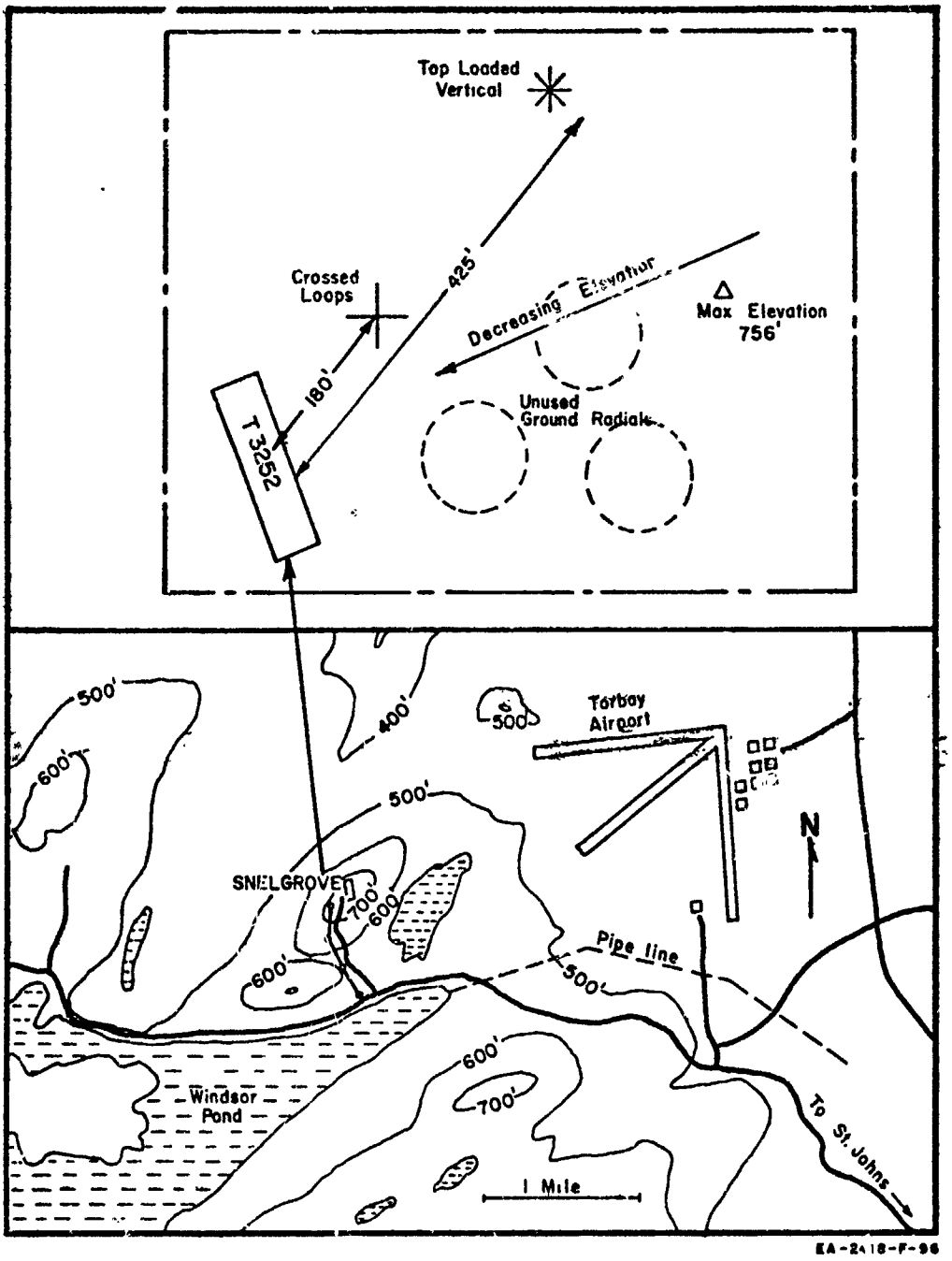

FIG. A 3

INSTALLATION AT ST. JOHNS, NEWFOUNDLAND

Appendix B

AVAILABLE SAGERIC DATA

AVAILABLE SFERIC DATA

1. Introduction

The SRI Sferic Monitoring System was used to collect data on atmospheric noise (sferics) from August 1958 through March 1959 at Fairbanks, Alaska, at Thule, Greenland, and at St. Johns, Newfoundland.

Several forms of data recordings were collected.

a. Waveform and DF Film

Individual sferic 3- to 30-kc waveforms and instantaneous direction of arrival were recorded on continuous-running 35mm photographic film.

b. Integrated DF Film

The direction of arrival of all sferics received in a fixed time interval was recorded on individual frames of 35mm photographic film.

c. Events Counter

The number of sferics exceeding fixed field strengths for each quarter of the GMT day were recorded on Veeder-Root counters and manually recorded each day.

d. Scanning Receiver

The RMS noise level in a 100-cycle bandwidth, as a function of frequency from 12 to 30 kc, was recorded using a scanning receiver and a pen recorder.

2. Waveform and DF Film

Waveform and DF films were collected on a schedule designed to sample all parts of the GMT day and all seasons. In general, waveform and DF film was collected in at least four 5-minute samples in a 4-hour period each and every day, and the schedule was advanced 2 hours per day so that in twelve days' time film samples for all parts of the GMT day were obtained. Figures B-1 and B-2 indicate the periods each day when waveform and DF film was collected, in unison, at all three stations. Film was collected daily at the times and thresholds indicated in Table B-1 through B-5. The times shown in Figs. B-1 and B02 and in Tables B-1 through B-5 are GMT times and indicate scheduled operation. At various times, and for various reasons, one or more of the stations were not operating as scheduled. The major periods when complete data were not obtained are indicated in Fig. B-1 prior to September 13, 1958, when the entire three-station system was not in operation, and in Fig. B-2 during February 1959, when St. Johns was not in operation. Periods when individual five-minute film runs were missed are not indicated, since this occurred for only a very small percentage of the total number of film runs.

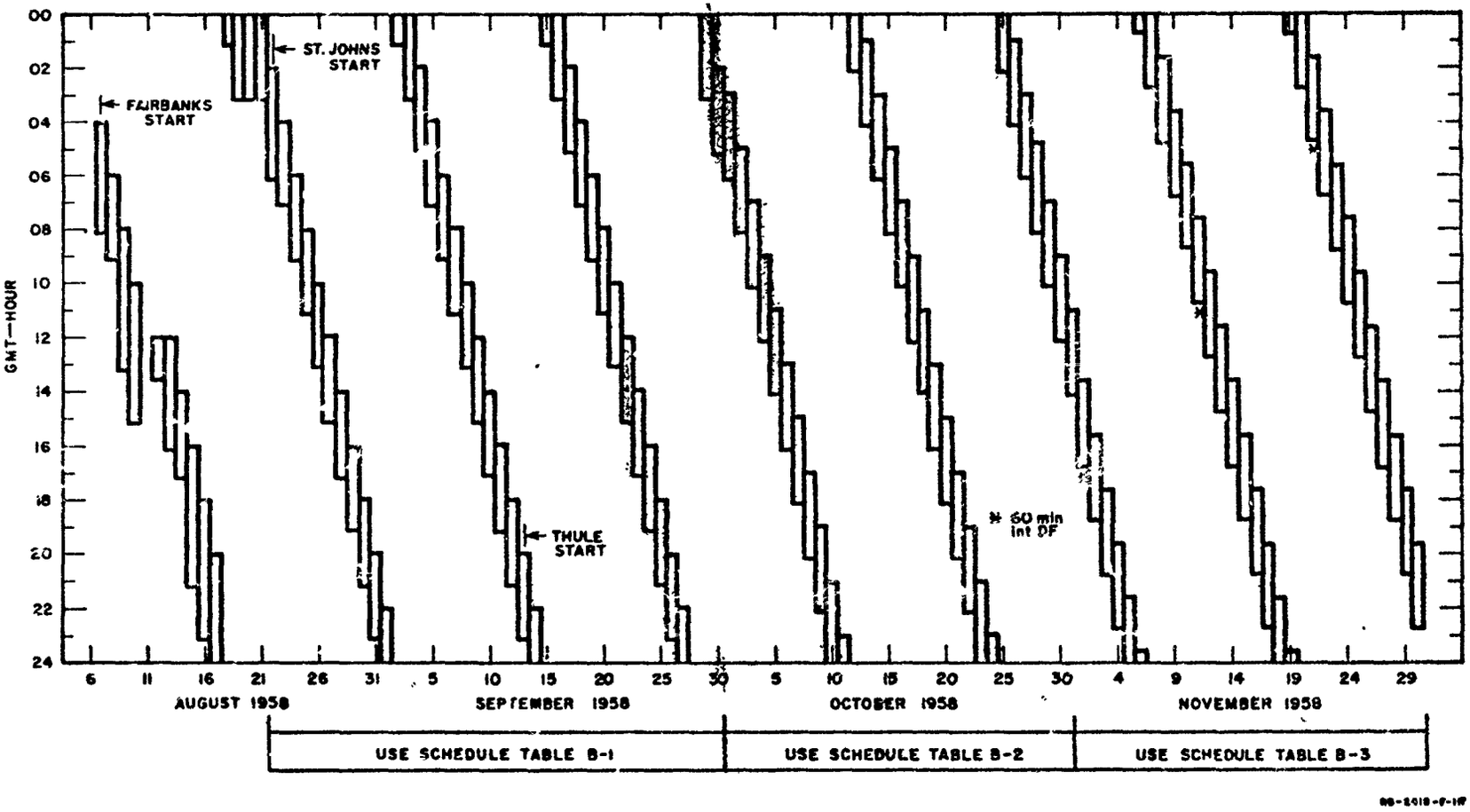

FIG. B-1

FILM OPERATING SCHEDULE AUGUST 1958 TO NOVEMBER 1958

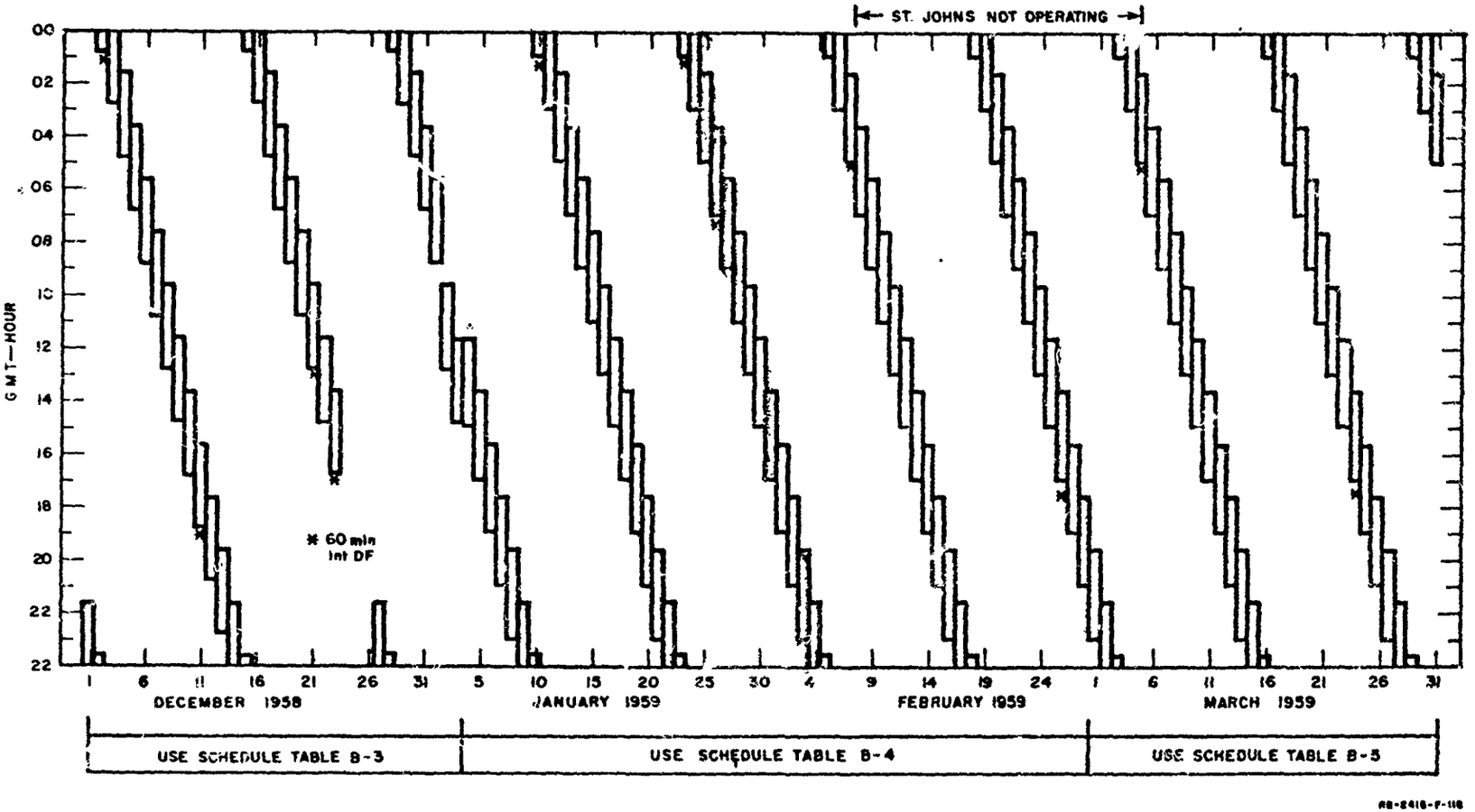

FIG. B-2

FILM OPERATING SCHEDULE DECEMBER 1958 TO MARCH 1959

Table B-1

DAILY WAVEFORM AND DF FILM SCHEDULE

21 to 30 September 1958

RUN NUMBER	START TIME GMT	STOP TIME GMT	THRESHOLD MV/M			FILM SPEED INCH/SEC.
			FAIRBANKS	THULE	ST. JOHNS	
1	00:00*	00:05	**			1
2	01:00	01:05				1
3	02:00	02:05				1
4	03:00	03:05				1

*Times shown are for 21 August 1958. Advance schedule two hours each day.

**Threshold selected by site operator as function of activity. Starting 20 September 1958 thresholds selected by site operators on threshold schedule similar to that shown in Table B-2.

Table B-2

DAILY WAVEFORM AND DF FILM SCHEDULE

1 to 31 October 1958

RUN NUMBER	START TIME GMT	STOP TIME GMT	THRESHOLD MV/M			FILM SPEED INCH/SEC.
			FAIRB.	NKS THULE	ST. JOHNS	
1	02:59:50*	03:05:10	6	3**	30	1
2	03:59:50	04:05:10	20	30	100	1
3	04:59:50	05:05:10	60	100	300	1
4	05:59:50	06:05:10	6	3	30	1

*Times shown are for 1 October 1958. Advance schedule two hours each day.

**Thresholds at Thule and St. Johns at various times were 10 db above scheduled thresholds.

Table B-3

DAILY WAVEFORM AND DF FILM SCHEDULE

1 November 1958 to 3 January 1959

RUN NUMBER	START TIME GMT	STOP TIME GMT	THRESHOLD MV/M			FILM SPEED INCH/SEC.
			FAIRBANKS	THULE	ST. JOHNS	
1	13:34:50*	13:40:10	3	10	10	1
2	14:34:50	13 40:10	10	30	30	1
3	15:34:50	13:40:10	30	100	100	1
4	16:34:50	13:40:10	3	10	10	1

*Times shown are for 1 November 1958. Advance schedule two hours each day.

Table B-4

DAILY WAVEFORM AND DF FILM SCHEDULE

4 January to 28 February 1959

RUN NUMBER	START TIME GMT	STOP TIME GMT	THRESHOLD MV/M			FILM SPEED INCH/SEC.
			FAIRBANKS	THULE	ST. JOHNS	
1	11:34:50*	11:40:10	10	30+	30	1
2**	11:44:50	11:50:10	30	100	100	1
3	12:29:50	12:50:10	100	300	300	1/8
4	13:29:50	13:50:10	100	300	300	1/8
5	14:29:50	≈14:50	100	300	300	1/8

*Times shown are for 4 January 1959. Advance schedule two hours each day.

**Run number 2 delayed 5 minutes from this schedule from 18 January 1959 through 28 February 1959 to miss WWV silent period.

+Threshold of Thule identical to Fairbanks from 4 February through 28 February 1959.

Table B-5

DAILY WAVEFORM AND DF FILM SCHEDULE

1 to 31 March 1959

RUN NUMBER	START TIME GMT	STOP TIME GMT	THRESHOLD MV/M			FILM SPEED INCH/SEC.
			FAIRBANKS	THULE	ST. JOHNS	
1	19:34:50*	19:40:10	10	10	30	1
2	19:49:50	19:55:10	30	30	100	1
3	20:04:50	21:10	100	100	300	1/8
4	20:29:50	21:35	10	10	100	1
5	22:29:50	22:55	30	10	10	1

*Times shown are for 1 March 1959. Advance schedule two hours each day.

From 7 August 1958 through 31 March 1959, 285 hundred-foot rolls of film were obtained at Fairbanks, Alaska. This film contains waveform and DF data on individual sferics that occurred in approximately 150 hours of total time.

From 13 September 1958 through 31 March 1959, 251 hundred-foot rolls of film were obtained at Thule, Greenland. This film contains waveform and DF data on individual sferics that occurred in approximately 133 hours of total time.

From 22 August 1958 through 31 March 1959, 251 hundred-foot rolls of film were obtained at St. Johns, Newfoundland. This film contains waveform and DF data on individual sferics that occurred in approximately 107 hours of total time.

The films listed above, 787 hundred-foot rolls, have been cataloged and filed and are available for future reference or use.

3. Integrated DF Film

During the intervals between the waveform and DF film runs indicated in Figs. B-1 and B-2, approximately 22 hours per day, integrated sferic direction-of-arrival data were collected. A 10-minute integrating time per film frame was normally used. Occasionally, a 60-minute integrating time was used to indicate directions with small sferic activity. The 60-minute integrating times are indicated on Figs. B-1 and B-2.

The integrated DF records are included in the correct time sequence on the 787 rolls of film listed above. Approximately 55,000 frames of integrated DF sferics patterns were obtained corresponding to 9,180 hours of recording time.

4. Events Counter

The events counter recorded the number of sferics exceeding fixed field strengths each quarter of the GMT day (00-06, 06-12, 12-18, and 18-24 hours GMT). The thresholds (field strength) used were 1, 10, 100, 1,000, and 10,000 millivolts per meter center to peak.

Events counters were in operation at Fairbanks, Alaska, from 1 December 1958 through 31 March 1959; at Thule, Greenland, from 16 September 1958 through 23 November 1958, and from 3 January through 31 March 1959; and at St. Johns, Newfoundland, from 22 August through 11 September 1958, from 1 October 1958 through 31 January 1959, and from 5 through 31 March 1959.

5. Scanning Receiver

The output of a scanning receiver was recorded on a pen recorder calibrated in RMS field strength in a 100-cycle bandwidth. The frequency scanning cycle was 12 to 30 kc and back to 12 kc in a one-hour

period. The data obtained was RMS atmospheric noise level in a 100-cycle bandwidth and approximate signal level of VLF stations in the 12- to 30-kc frequency band. The VLF station field strength is approximate since the unknown duty cycle and the random manner in which the receiver encountered each signal caused the receiver output to vary although the amplitude of the received signal may have been constant. However, the records do indicate approximately when each VLF station was receivable above the atmospheric noise at each sferic monitoring station.

Each roll of recorder paper at each station contains approximately three days of data. Scanning receiver records were obtained at Fairbanks, Alaska from October 1958 through March 1959; at Thule, Greenland from 20 September 1958 through 31 March 1959; and at St. Johns, Newfoundland from 24 August 1958 through 7 February 1959, and from 4 through 31 March 1959.

6. Miscellaneous Data

In addition to the sferic data collected, operational data were recorded at each sferic monitoring station. These data were:

(1) Time standard stability

(2) Local reception of WWV, WWVH, and JJY (all frequencies) as Poor, Fair, or Good

(3) Local outside temperature and known local storm conditions as obtained from the local Air Force weather service.

Appendix C

CALIBRATION AND PERFORMANCE MEASUREMENTS

CALIBRATION AND PERFORMANCE MEASUREMENTS

1. Introduction

The SRI Sferics Monitoring System incorporated internal calibration circuits for periodic calibration of (1) the sferic waveform and DF film, (2) the events counter, (3) the scanning receiver, and (4) the time standard. These calibrations were used on the following schedule:

(1) Waveform and DF film--daily on the first roll of film

(2) Events counter--at least once each month and whenever data deviated from daily normal

(3) Scanning receiver--once on each roll of recorder paper (approximately every 3 days)

(4) Time standard--daily if WWV reception was reliable.

The calibration procedure used for the data-recording system was based upon a calculated effective height for the vertical antenna and measured capacitance of the vertical antenna and coaxial line. The capacitance was re-measured periodically.

An engineer visited each site every three months to verify calibration procedures and system characteristics.

2. Vertical Antenna Effective Height

The vertical antenna used for the SRI Sferics Monitoring System is a 30-foot tower with eight 22-foot top-loading elements at a downward angle of 45 degrees (see Fig. C-1). The tower is triangular, 6 inches on a side, and is mounted on a 4-inch base insulator. The top-loading elements are 3/16-inch guy wires electrically attached to the top of the tower, with insulators 22 feet from the tower.

The effective height of the antenna was computed by calculating the capacitance of the antenna. The capacitance of the tower[6] is

$$C_T = \frac{7.36\ m}{\log \frac{2m}{d} - K}\ \mu\mu f$$

[6] Terman, Radio Engineers Handbook, (McGraw-Hill Book Co., Inc., New York City, 1943) pp. 114-116.

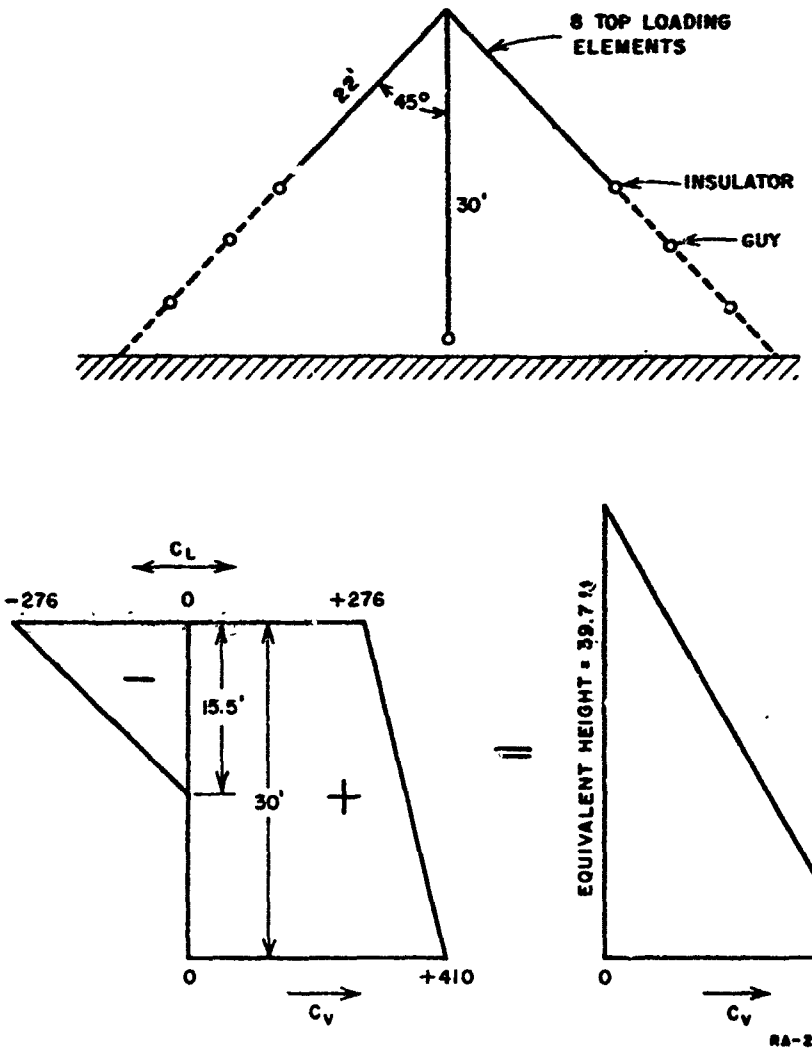

FIG. C-1

VERTICAL ANTENNA EQUIVALENT HEIGHT

where m = tower height = 30 feet

d = tower diameter = 0.5 foot

K = constant, a function of base insulator height divided by m = 0.43

$C_T = 134$ μμf .

The capacitance of the top-loading elements[6] was calculated using the horizontal wire formula at 22.5 feet (the center height of each element), and a length of 15.5 feet (the horizontal component of each element):

$$C_L = nl \frac{7.354}{\log \frac{4h}{d'} + 8C'} \text{ μμf}$$

where n = number of elements = 8

l = horizontal length = 15.5 feet

h = height above ground = 22.5 feet

d' = diameter = 0.0156 foot

C' = insulator capacitance, estimated at 4 μμf .

Then $C_L = 276$ μμf .

Thus, the total antenna capacitance, C_v, is

$$C_v = C_T + C_L = 410 \text{ μμf} .$$

Using the procedure indicated in Fig. B-1, the top-loaded vertical antenna is equivalent to an unloaded vertical antenna 39.7 feet high. The effective height for an electrically short vertical antenna is one-half the height of the antenna. Therefore, the effective height (he) of the SRI Sferics Monitoring System vertical antenna is approximately 20 feet or six meters.

3. Calibration Circuit

The calibration circuit (see Fig. C-2) used in the SRI Sferics Monitoring System was designed to induce a calibration signal, either a sine wave or a simulated sferic, equivalent to 10 millivolts per meter center-to-peak into the vertical antenna circuit and directly

[6] Terman, Radio Engineers Handbook, (McGraw-Hill Book Co., Inc., New York City, 1943) pp. 114-116

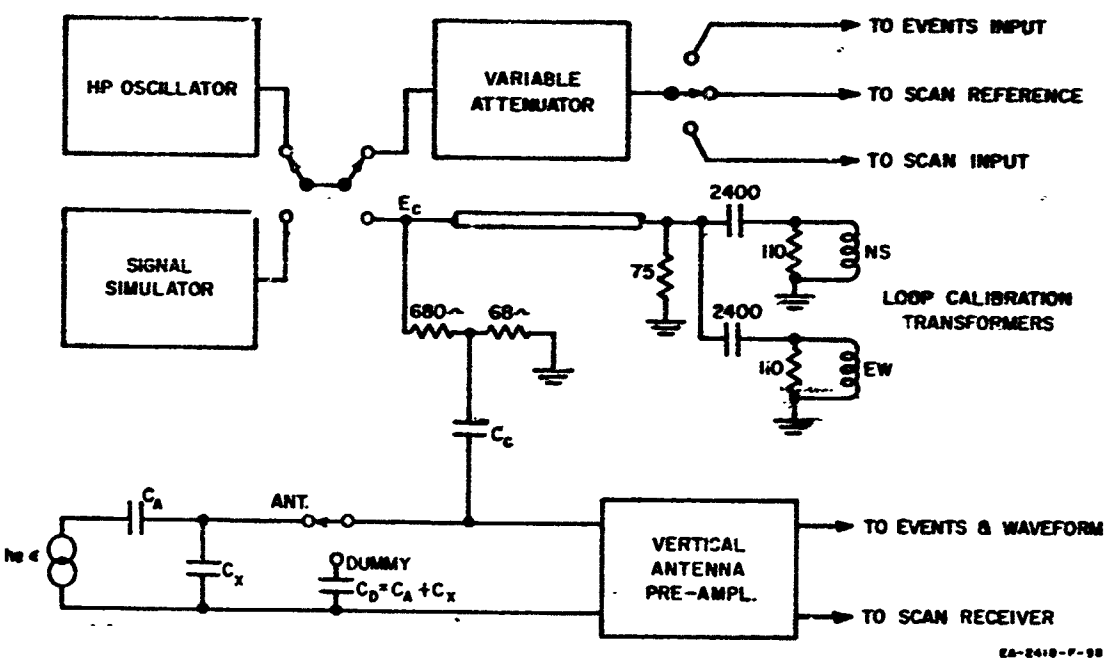

FIG. C-2

SIMPLIFIED CALIBRATION CIRCUIT

into the loop antennas. C_c was selected as a function of the vertical antenna capacitance, C_A, and for a calibration input signal E_c, equal to one volt center to peak:

$$C_c = \frac{11\ he\ E}{E_c} C_A$$

$$= 0.726\ C_A$$

for $E = 10$ mv/m center to peak

$he = 6.6m$*.

A dummy antenna, C_D, was provided so that the vertical antenna could be disconnected during calibration. The individual values used in the calibration circuit on each site were:

	C_X	C_A	C_D	C_c
Fairbanks, Alaska	1930**	375	2300	270
Thule, Greenland	7100	370	7500	270
St. Johns, Newfoundland	9500	440	10000	320

The coupling network and the loop calibration transformers were designed to induce a signal into the loop antenna approximately equal to 10 millivolts per meter center-to-peak and 90 degrees out of phase with the input calibration signal.

4. Waveform and DF Film

The waveform and DF film was calibrated daily and the calibration signal recorded on the film. The calibration circuit described above was used to inject a simulated sferic into the system. Vertical channel gain was adjusted to trigger the threshold circuit. Vertical channel gain was increased 10 db and the display gain (oscilloscope) was adjusted to scribe marks. Loop channel gains were adjusted to a 45 degree pattern

---

*The effective height of the vertical antenna was originally calculated in error as 6.6 meters. Corrected calculation is 6 meters. The error was not discovered in time to be incorporated in this report without excessive expense. Effective height of 6.6 meters is used in this report since the exact effective height based upon field measurements is not known. It is estimated that actual effective height would be between 5 and 6 meters.

**C_X at Fairbanks, Alaska, was increased by 4700 micromicrofarads with a fixed capacitor so that the over-all gain of all three systems was alike; thus, calibration procedures were identical.

with a prescribed length. Three recordings were then made with vertical channel and DF channel gains at threshold, 10 db above threshold, and 20 db above threshold. Variations in daily adjustments were used as indications of trouble.

Approximately once a month the over-all bandpass characteristics of the vertical channel and the DF channels were measured. A typical result is shown in Fig. C-3.

5. Events Counter

The events counter recorded the number of sferics exceeding fixed trigger levels. Calibration was accomplished by measuring the magnitude of the calibration signal at the input to the events counter. With this magnitude of input signal the 10 mv/m center-to-peak counter circuit was adjusted to trigger. By increasing the input to the events counter in 20-db steps, the remaining counter circuits were adjusted.

The simulated sferic signal at 5-cps rate was used to check the event-counting rate to ensure that multiple counts per sferic were not recorded.

6. Scanning Receiver

The scanning receiver was calibrated in RMS volts in two ways. A one-millivolt RMS, 25-kc sine wave was sampled on the increasing frequency portion of each scan and the receiver input was grounded once each scan. This calibration was used to ensure that receiver gain and noise level were constant with time.

In addition, the recorder was calibrated in RMS millivolts per meter by measuring the receiver input when a one-volt RMS sine-wave calibration signal was injected into the calibration circuit. This measured voltage was then used at various frequencies in the 12- to 30 kc band to calibrate the recorder. Calibration was accomplished while the tuning mechanism was in operation by setting the calibration frequency just ahead of the tuning. The above calibration was repeated in 20-db amplitude steps throughout the useful range of the receiver.

7. Time Standard

The SRI Sferics Monitoring System incorporated a battery operated frequency standard to operate a wall clock, camera clock, events counter timing, and scanning-receiver recorder drive. The entire system was maintained on GMT by aligning the frequency standard one-second output with WWV or WWVH one second "ticks," allowing for the propagation time difference. The propagation times used were

WWVH to Fairbanks, Alaska	16.5 milliseconds
WWV to Fairbanks, Alaska	17.5 milliseconds
WWV to Thule, Greenland	14 milliseconds
WWV to St. Johns, Newfoundland	7 milliseconds .

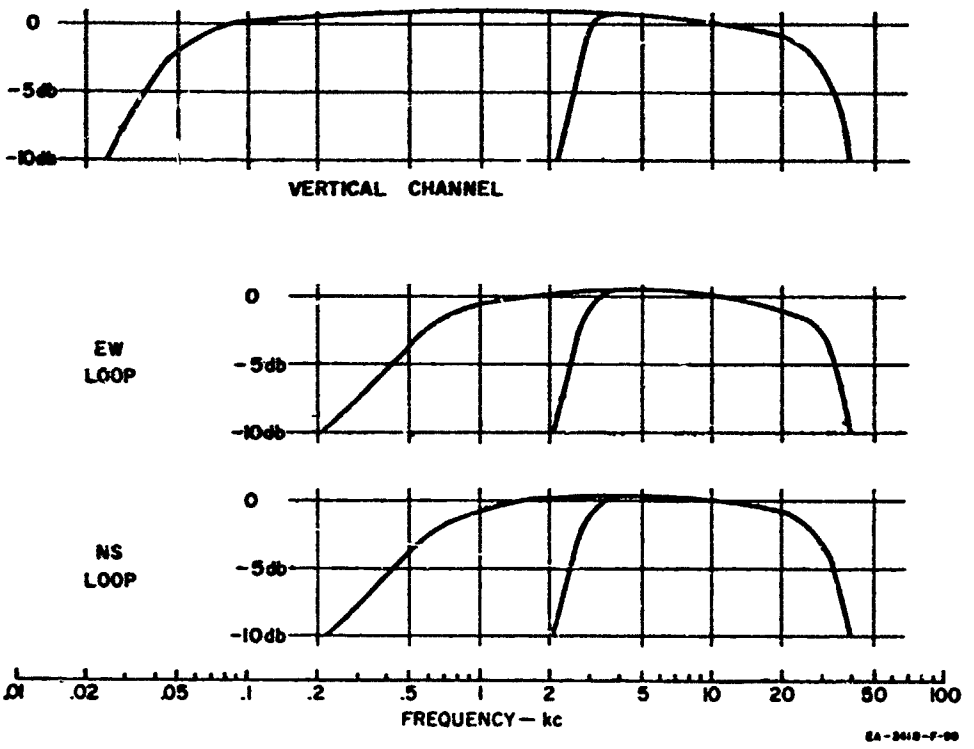

FIG. C-3

SFERIC SYSTEM FREQUENCY RESPONSE

The timing system was compared with WWV or WWVH daily at either midday or midnight when propagation was more or less consistent. Corrections to the frequency standard were made when long-term drifts were indicated from the daily comparisons.

The accuracy of the timing system for time difference measurements was determined from sferics propagated along a common great circle path through two stations. Figure C-4 shows a typical sferic propagated along the Fairbanks-Thule path. The time difference measures 9.8 milliseconds as compared to a calculated propagation time of 9.33 milliseconds. Thus, for this example the timing system accuracy for time difference measurements is 0.47 millisecond. Figure C-5 shows the distributions of time difference measurements for the Fairbanks-Thule and St. Johns-Thule paths. The samples used were taken from all months of operation and indicate a time difference accuracy of approximately 1 millisecond.

8. Sferic Amplitude Corrections

During data reduction, amplitude calibration of the waveform film was assumed to be as indicated by each station operator. Measurements on each system were used to verify or correct the assumed calibrations. The following are corrections that were applied to the recorded and analyzed data prior to preparation of this report. THESE CORRECTIONS HAVE BEEN APPLIED TO THE DATA PRESENTED IN THIS REPORT and are thus applicable only to the original recorded data in unanalyzed form.

a. Fairbanks, Alaska

Prior to 4 November 1958, a calibration procedure was used that did not utilize the built-in calibration circuit. An attenuator was used to inject a signal at the vertical-antenna input to the preamplifier with the antenna and coaxial line removed. An effective signal strength was then calculated. Recalculation indicates that the film records at Fairbanks, Alaska, prior to 4 November 1958 must be multiplied by 0.88 to obtain corrected amplitude.

In addition, from 4 November 1958 through 6 March 1959, in the standard calibration procedure for the waveform and DF film, the calibration signal injected was 1.2 volts center to peak. Thus, for this period at Fairbanks, Alaska, film records were multiplied by 1.2 to obtain corrected amplitude.

b. Thule, Greenland

The calibration procedure as outlined above was used starting on 4 October 1958. For the period 4 October through 22 November 1958, C_c was 253 micromicrofarads and the calibration input voltage was 0.7 volt center-to-peak, due to an incorrectly thrown switch. Thus, the film records at Thule, Greenland, for this period were multiplied by 0.66 to obtain corrected amplitude. Film calibration was correct for all other periods during operation at Thule, Greenland.

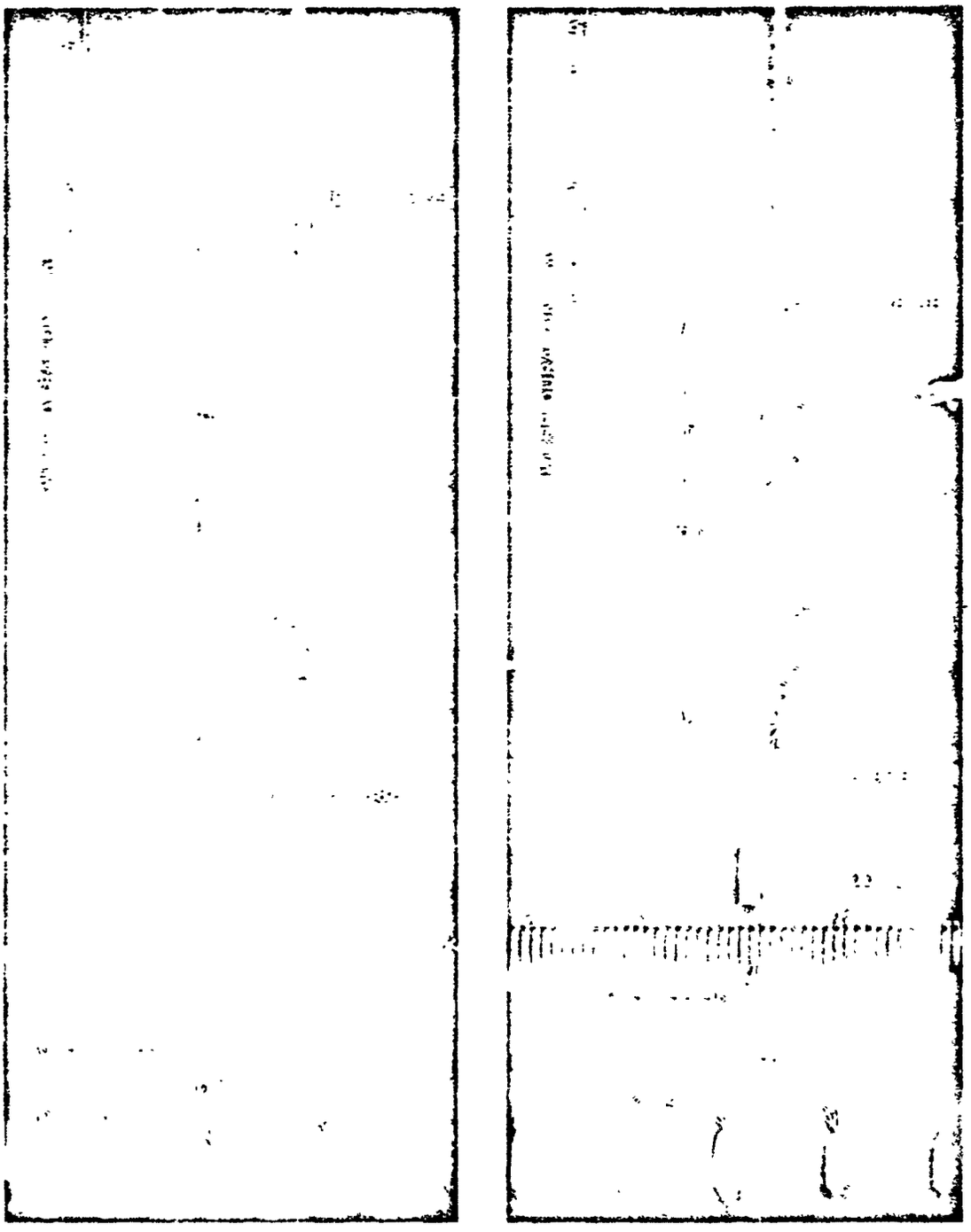

THULE, GREENLAND FAIRBANKS, ALASKA

TIME DIFFERENCE = 10:37:38.9883 - 10:37:38.9785 = 9.8 ms
CALCULATED TIME DIFFERENCE = 9.33 ms

P-2418-F-65

FIG. C-4

MEASUREMENT OF TIMING ACCURACY, 12 NOVEMBER 1958

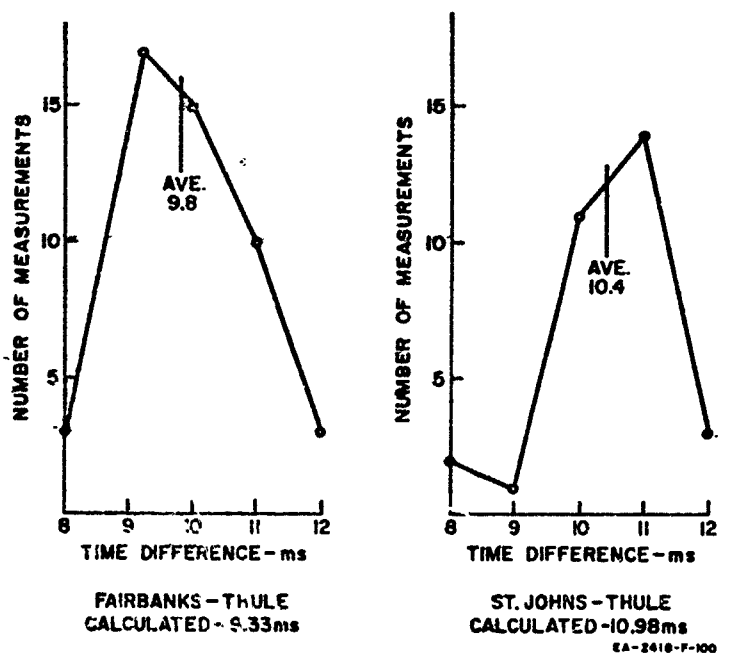

FIG. C-5

TIME MEASUREMENT ACCURACY

c. St. Johns, Newfoundland

The calibration procedure outlined above was used throughout operation; however, a calibration input signal of 1.1 volts center-to-peak was used on all film calibrations prior to 6 March 1959. Prior to this date the film records at St. Johns, Newfoundland, were multiplied by 1.1 to obtain corrected amplitude.

9. Direction-of-Arrival Corrections

The crossed-loop antennas were aligned North-South true, and East-West true. These antennas were connected through identical amplifiers to the vertical and horizontal plates of the oscilloscope so that North was at the end of the waveform trace. As viewed on the processed film placing the timing marks at the bottom (see Fig. C-4) North is up, South is down, East is to the right, and West is to the left. This is identical to normal directional presentations on maps. This direction-of-arrival presentation was used on all film data taken at Fairbanks, Thule, and St. Johns except as follows. At St. Johns, on films P-1 through P-14 (20 August 1958 to 3 September 1958) and from waveform data on film P-21 through integrated DF's on film P-26 (10 to 17 September 1958), the North-South and East-West loop antenna displays were reversed, changing the directional display on the processed film so that East is up, West is down (toward the timing lights), North is to the right, and South is to the left.

10. Scanning Receiver Amplitude Corrections

As indicated above, the scanning receiver records were calibrated in RMS field strength. These calibrations for 10 microvolts per meter as a function of frequency are shown in Fig. C-6. A single calibration curve for Fairbanks, Alaska and St. Johns, Newfoundland are shown, since calibration varied less than one recorder division throughout the operating period.

On 23 February 1959 repairs were required on the scanning receiver at Thule, Greenland. The repairs changed the scanning receiver calibration as indicated by the two curves shown in Fig. C-6 for Fairbanks, Alaska.

The 10-microvolt-per-meter calibrations shown in Fig. C-6 apply to the 1- and 100-microvolt-per-meter calibrations by subtracting and adding, respectively, 13 recorder divisions to the recorder scales shown for Fairbanks and Thule and 14 recorder divisions to the recorder scale shown for St. Johns. These extensions to other signal levels are shown on Fig. C-6 and are linear in db.

In addition, prior to 4 November 1958 the vertical antenna loading capacitance including the coaxial cable at Fairbanks, Alaska, was increased from 4300 to 7000 micromicrofarads to standardize operating conditions. This change requires that prior to 4 November 1958 at

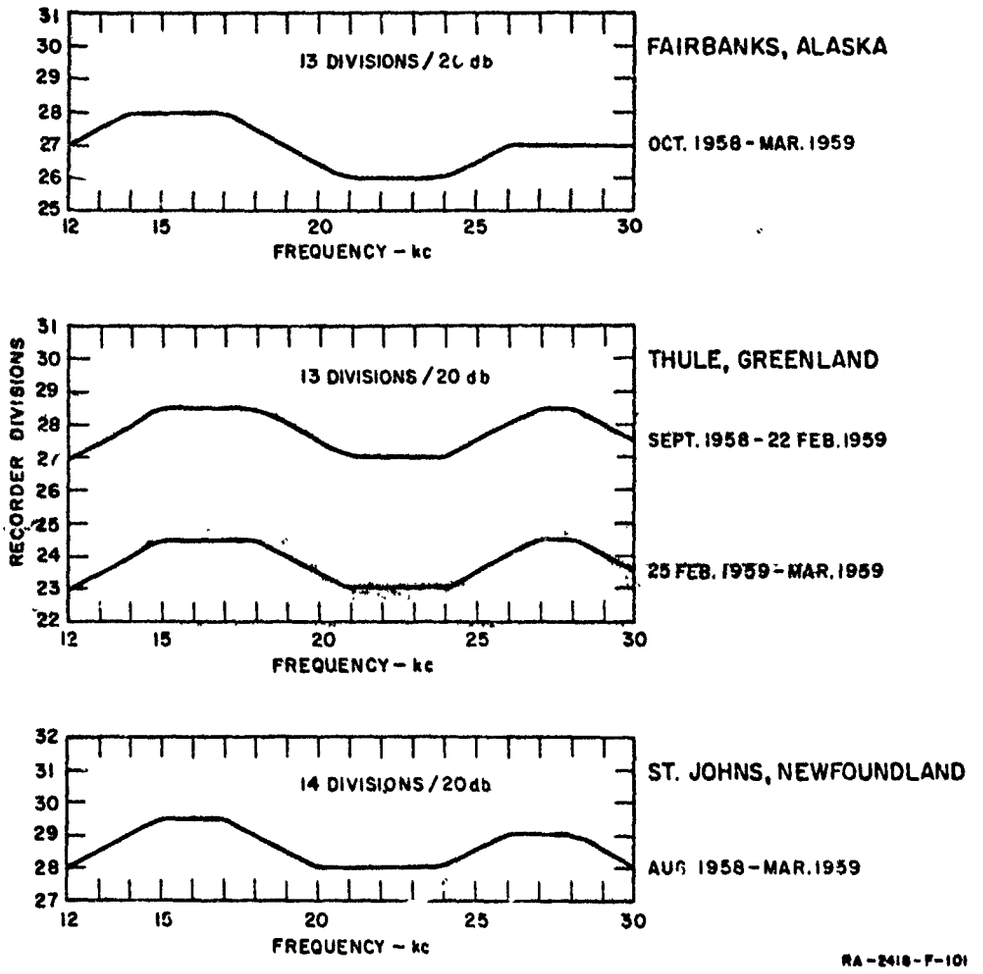

FIG. C-6

SCANNING RECEIVER CALIBRATION AT 10 μv PER METER

Fairbanks, Alaska, the scanning receiver recorded RMS noise levels must be multiplied by 0.615 to obtain corrected field strength.

THE ABOVE CORRECTIONS HAVE BEEN APPLIED TO THE SCANNING RECEIVER DATA PRESENTED IN THIS REPORT and thus apply only to original records.

Appendix D

AMPLITUDE AND DIRECTION-OF-ARRIVAL DISTRIBUTIONS

AMPLITUDE AND DIRECTION-OF-ARRIVAL DISTRIBUTIONS

The broadband (3 to 30 kc) waveform and the instantaneous direction of arrival of individual sferics were recorded on 35mm film on the schedule and at the thresholds indicated in Appendix B. Direction of arrival was obtained from the first 300-microsecond portion of each sferic recorded. (See Technical Report 1 on this contract for a description of equipment.) The waveform recording system had a dynamic amplitude range of 20 db and was calibrated in millivolts per meter, center to peak.

The film collected was sampled, and data for each sferic in the sample were entered on individual IBM cards. For each month, and for each station, equal time-duration samples uniformly distributed throughout the GMT day were processed. With the operating schedule as indicated in Appendix B, data from 12 consecutive days were required to obtain each monthly sample for processing. The data collected on the same days at all sites were used when possible.

The sferic parameters entered on IBM cards were as follows:

(1) Receiving date and time (GMT)

(2) Maximum center-to-peak amplitude in millivolts per meter

(3) Direction of arrival to the nearest 10 degrees

(4) Waveform type (see Fig. III-1).

The data presented in this appendix are the waveform amplitude and direction-of-arrival data that have been entered on approximately 90,000 IBM cards; they present only 18 hours of the approximately 390 hours of film collected at the three sites between mid-August 1958, and 31 March 1959. However, the 18 hours of film processed onto IBM cards form approximately 30 percent of the film records available at the system thresholds selected for processing.

Figures D-1 through D-8 show the amplitude distributions for sferics received at Fairbanks, Alaska, at Thule, Greenland, and at St. Johns, Newfoundland, for the months of August 1958 through March 1959. Amplitude distribution is defined as the number of sferics per second exceeding a specified field strength (threshold) as a function of threshold. A separate distribution curve for each quarter of the GMT day is shown and the number of seconds of film analyzed to obtain each distribution curve are shown. The waveform amplitude corrections indicated in Appendix C have been applied.

Figures D-9 through D-16 show the direction of arrival distributions for each amplitude distribution shown in Figs. D-1 through D-8, respectively. Again sferic rate is the number of sferics per second exceeding a fixed threshold.

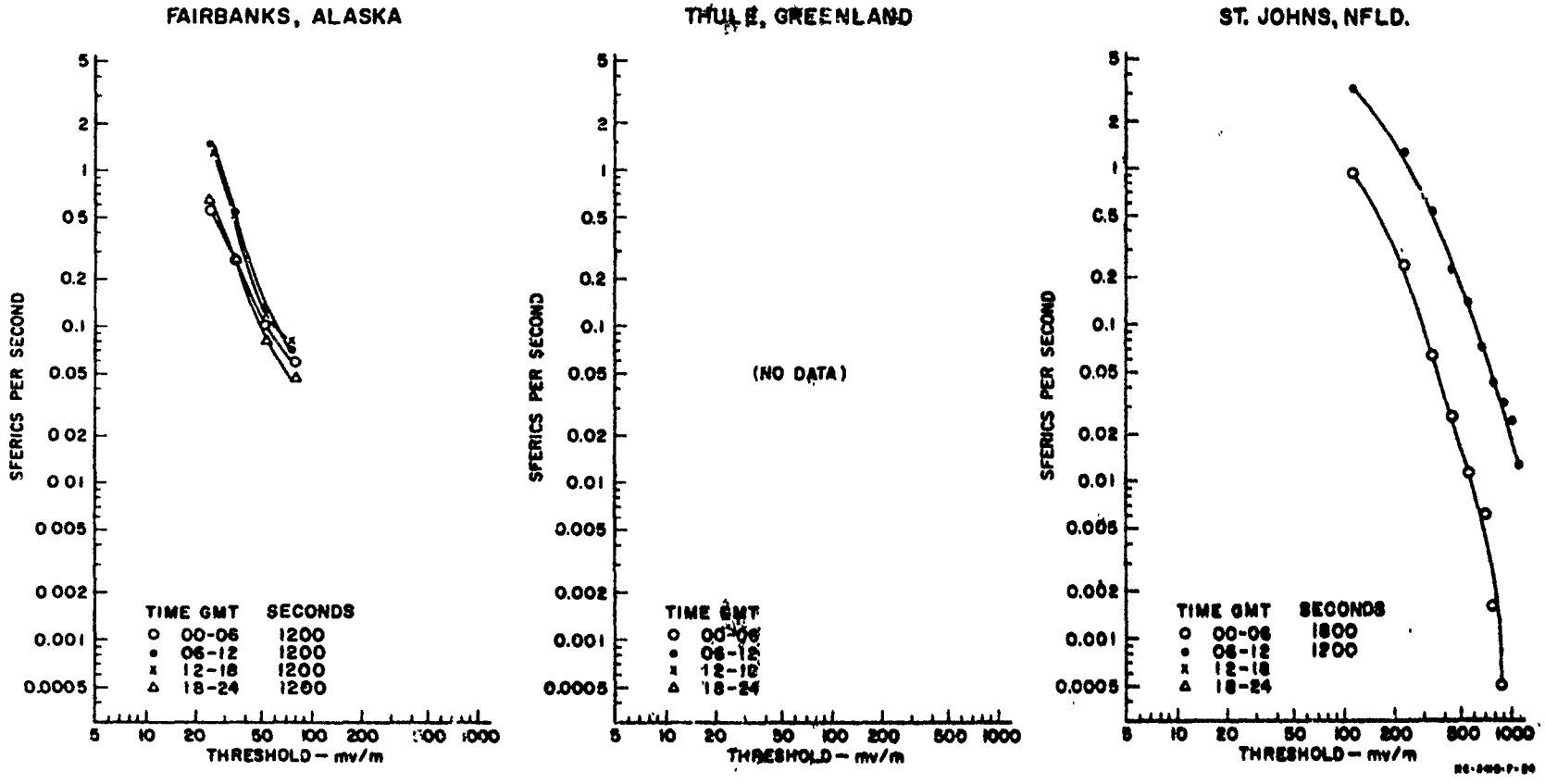

FIG. D-1

SFERIC AMPLITUDE DISTRIBUTION—AUGUST 1958

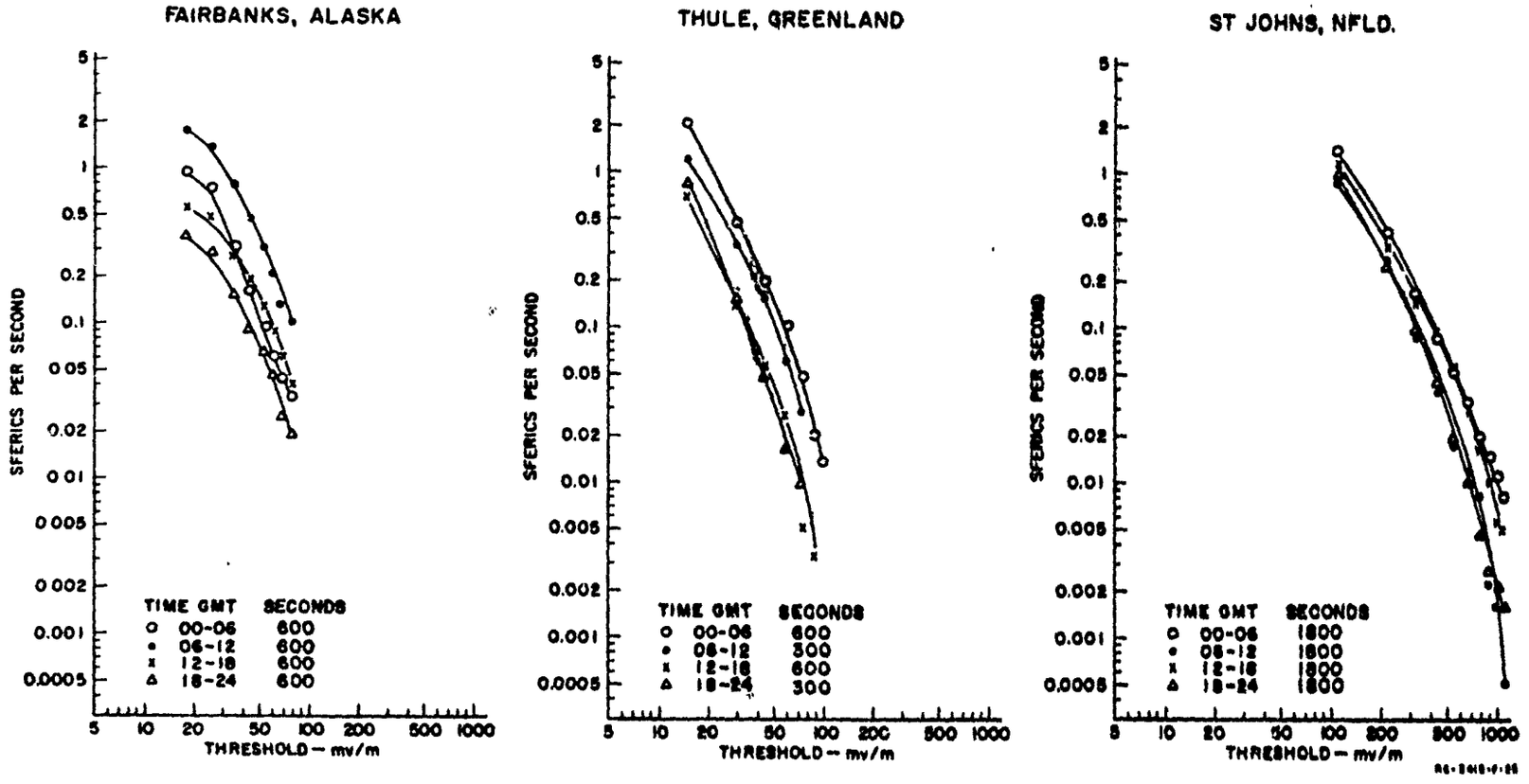

FIG. D-2

SFERIC AMPLITUDE DISTRIBUTION — SEPTEMBER 1958

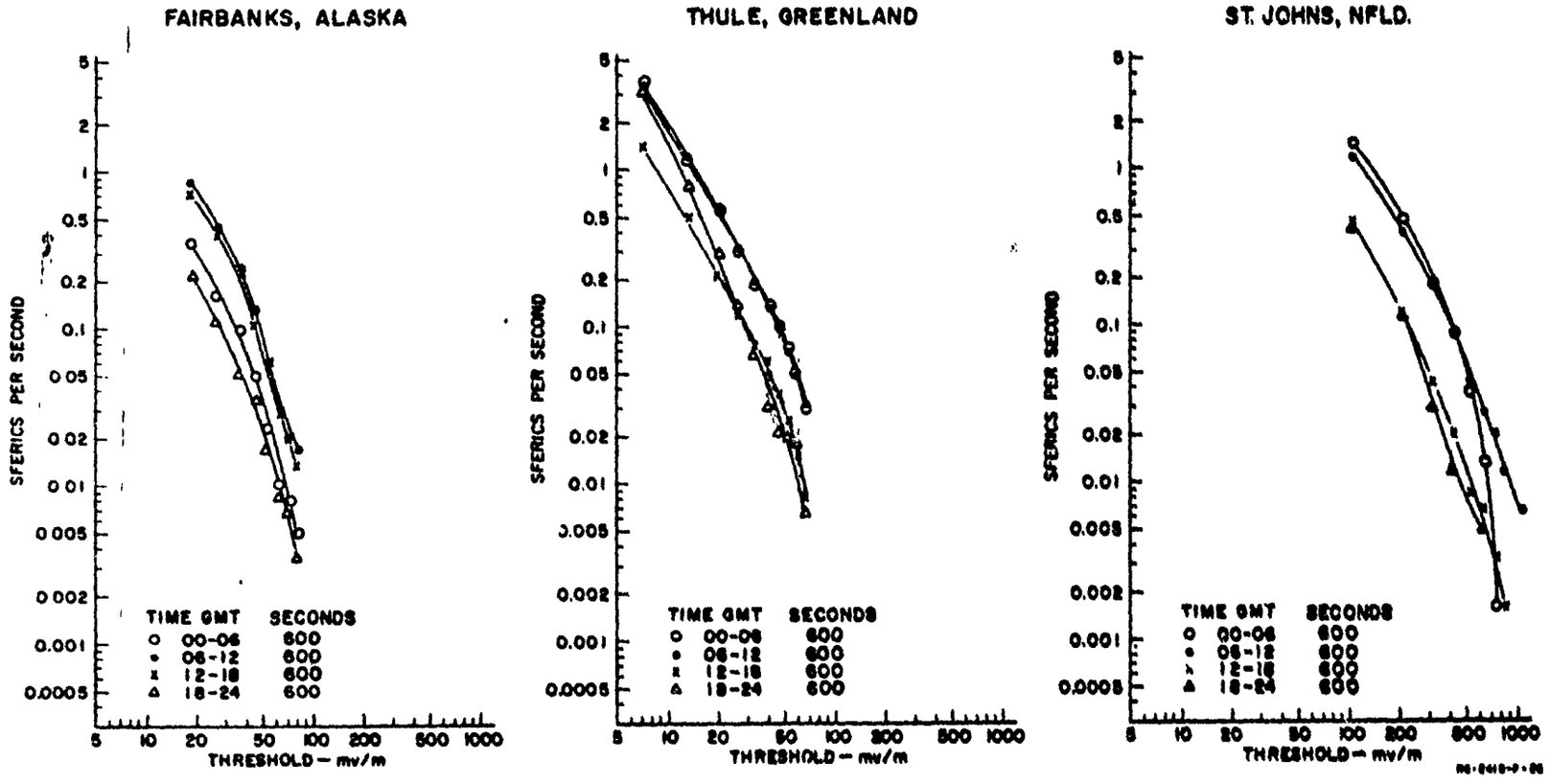

FIG. D-3

SFERIC AMPLITUDE DISTRIBUTION — OCTOBER 1958

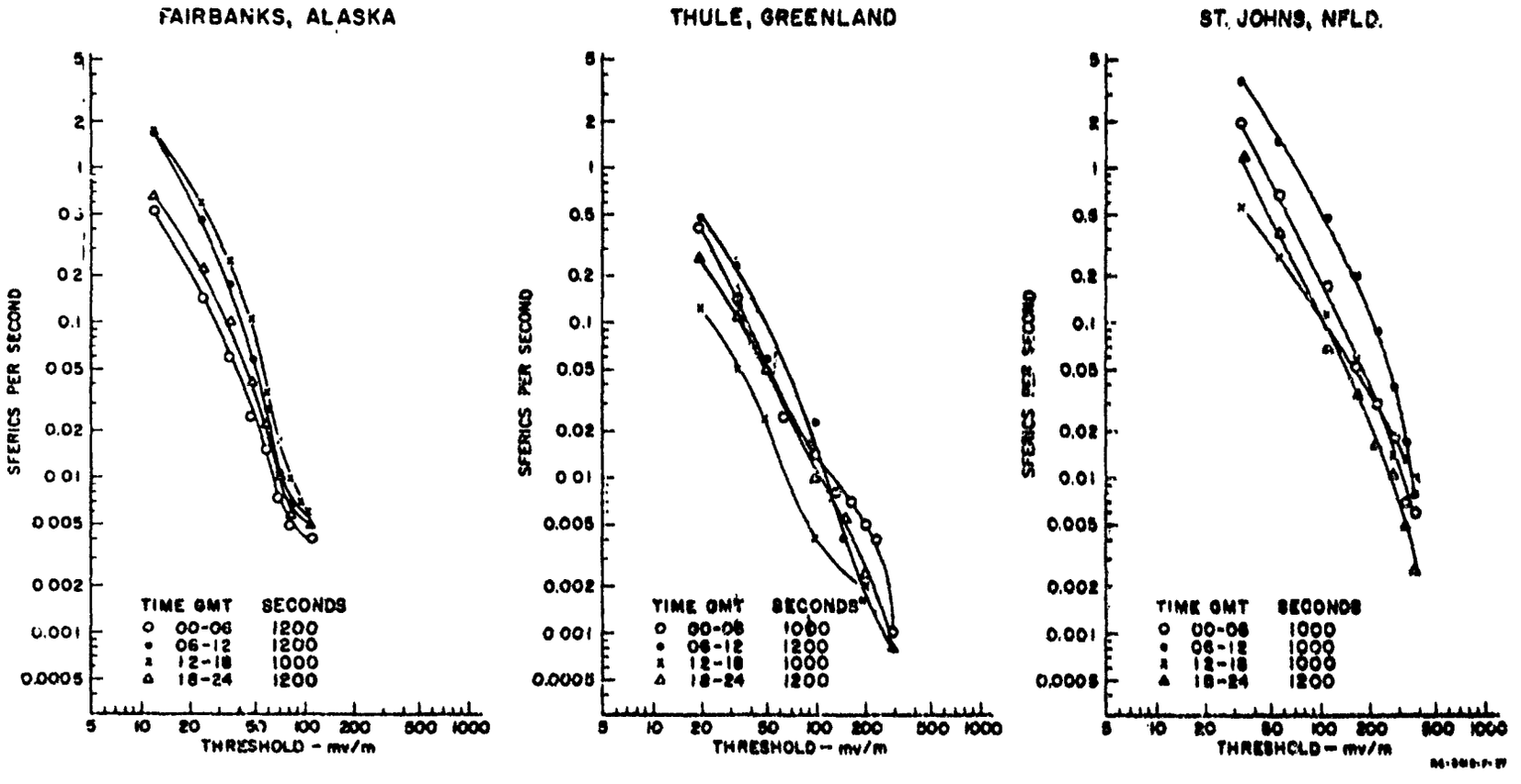

FIG. D-4

SFERIC AMPLITUDE DISTRIBUTION — NOVEMBER 1958

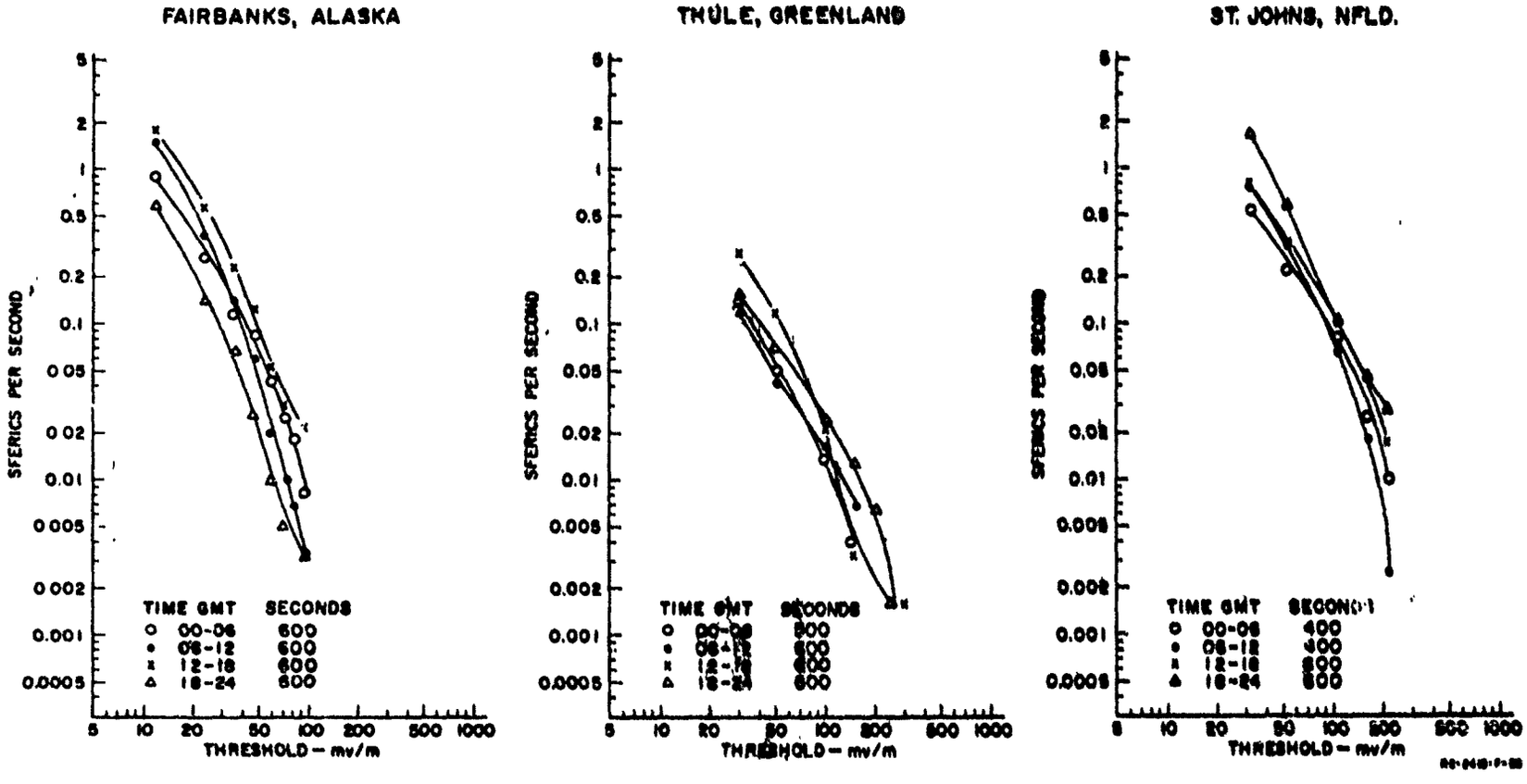

FIG. D-5

SFERIC AMPLITUDE DISTRIBUTION — DECEMBER 1958

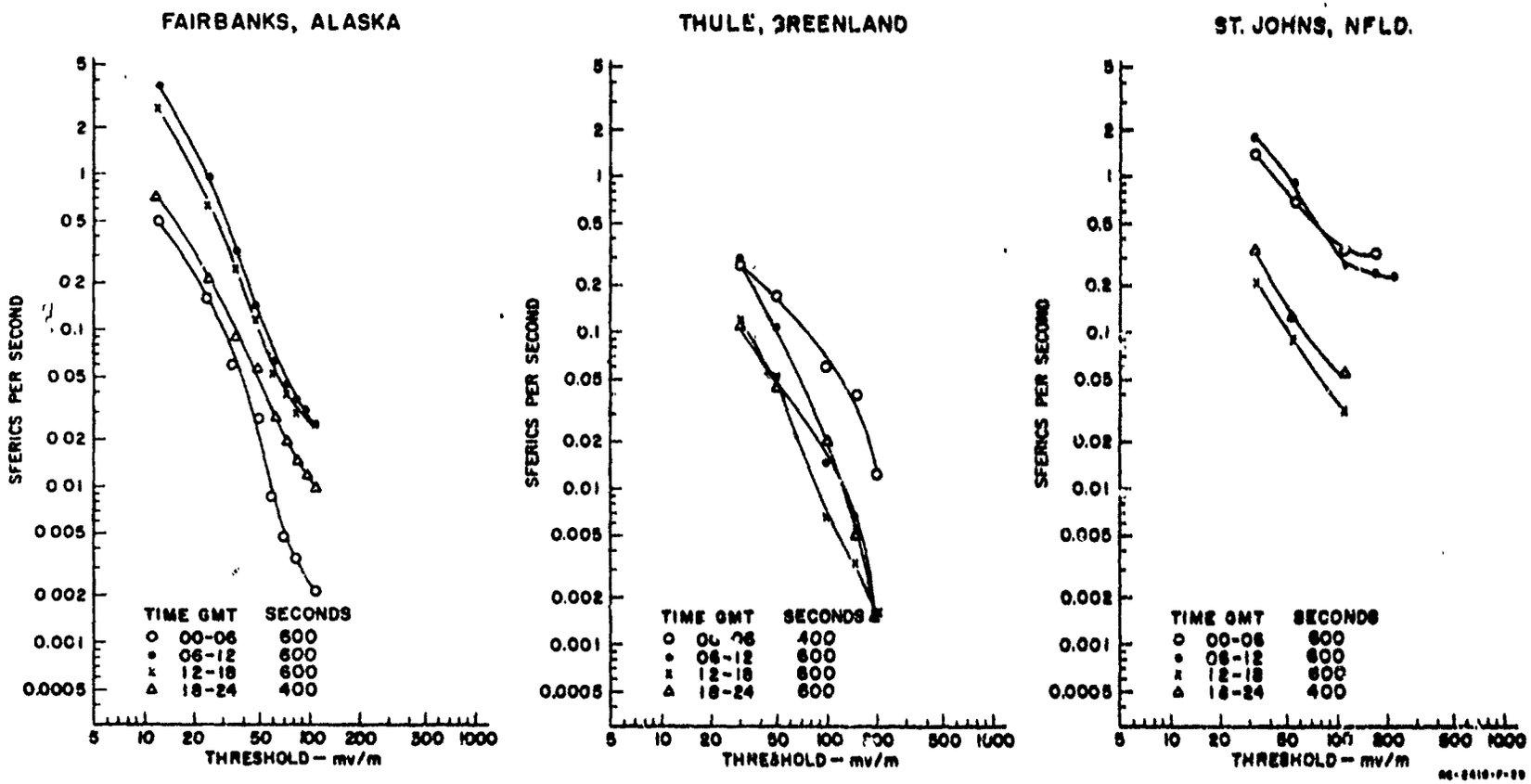

FIG. D-6

SFERIC AMPLITUDE DISTRIBUTION—JANUARY 1959

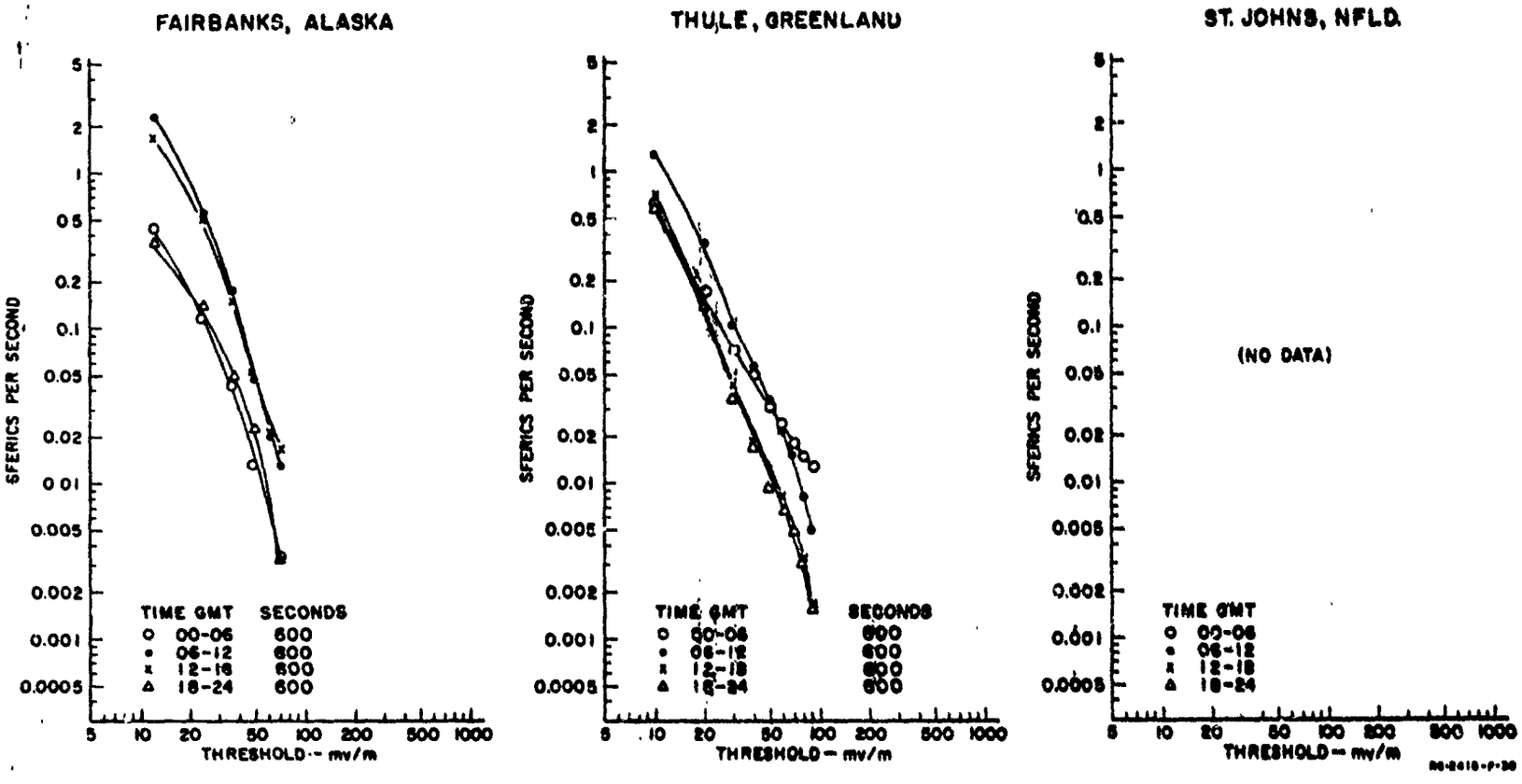

FIG. D-7

SFERIC AMPLITUDE DISTRIBUTION—FEBRUARY 1959

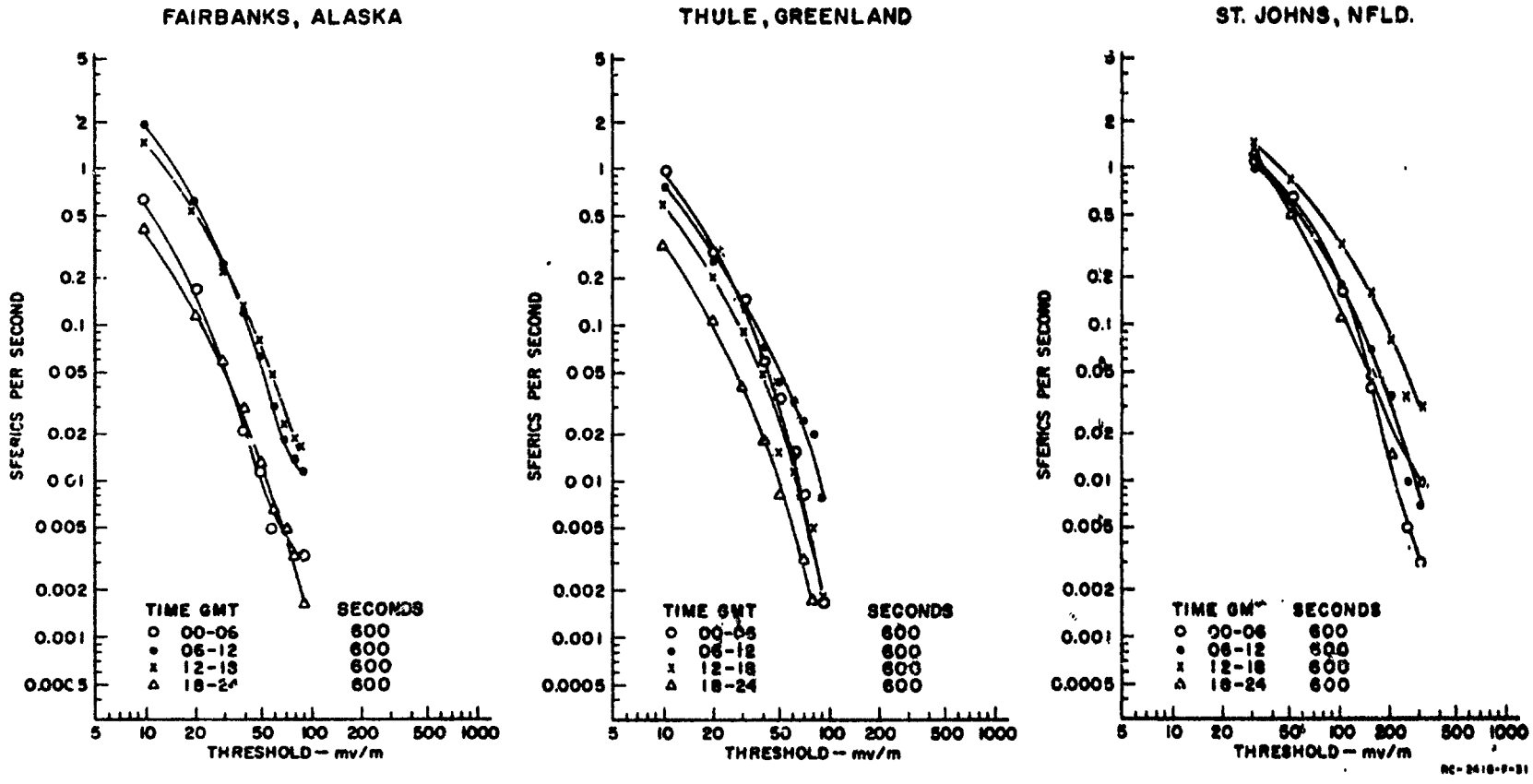

FIG. D-8

SFERIC AMPLITUDE DISTRIBUTION—MARCH 1959

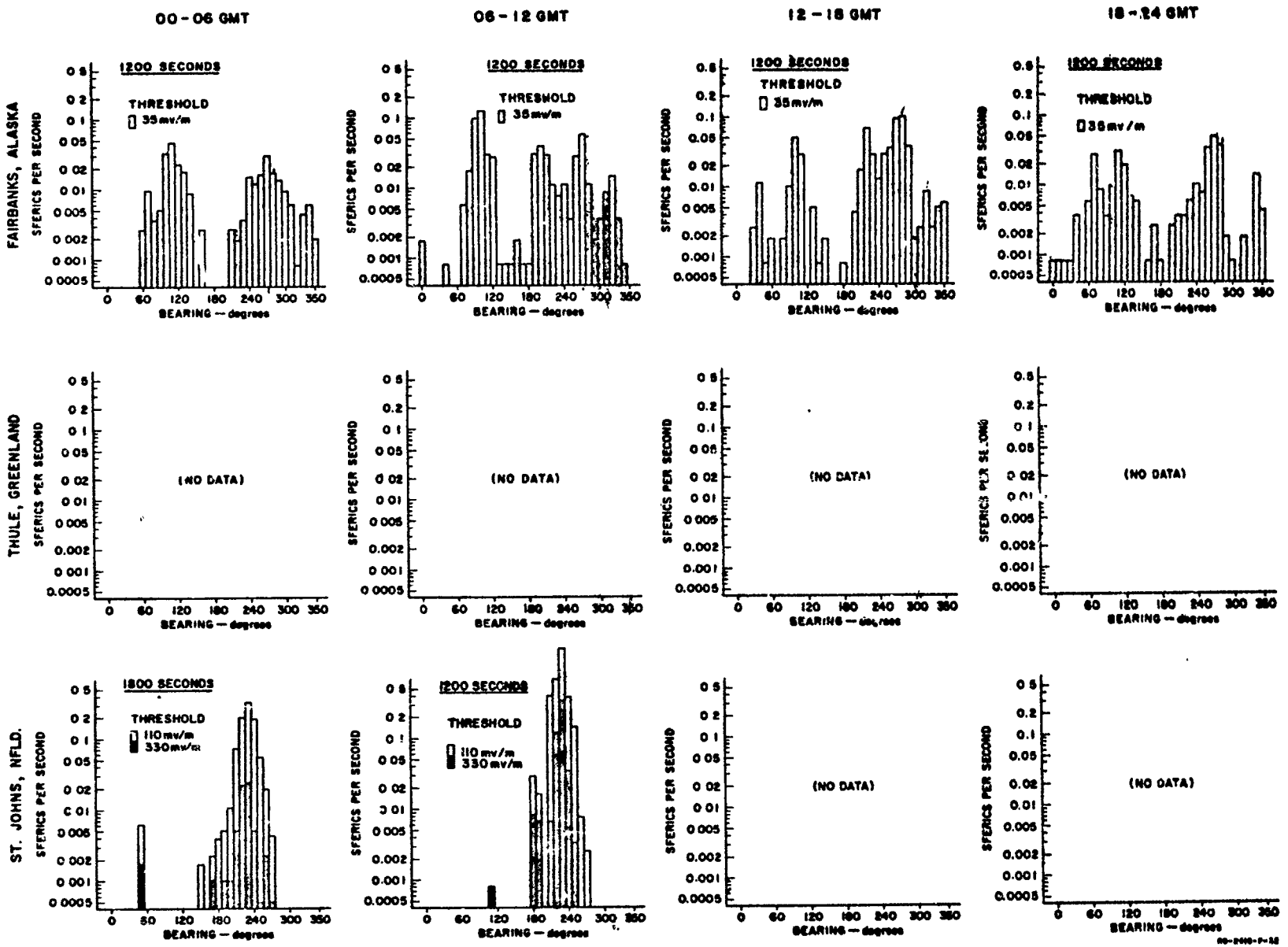

FIG. D-9

DIRECTION-OF-ARRIVAL DISTRIBUTION — AUGUST 1958

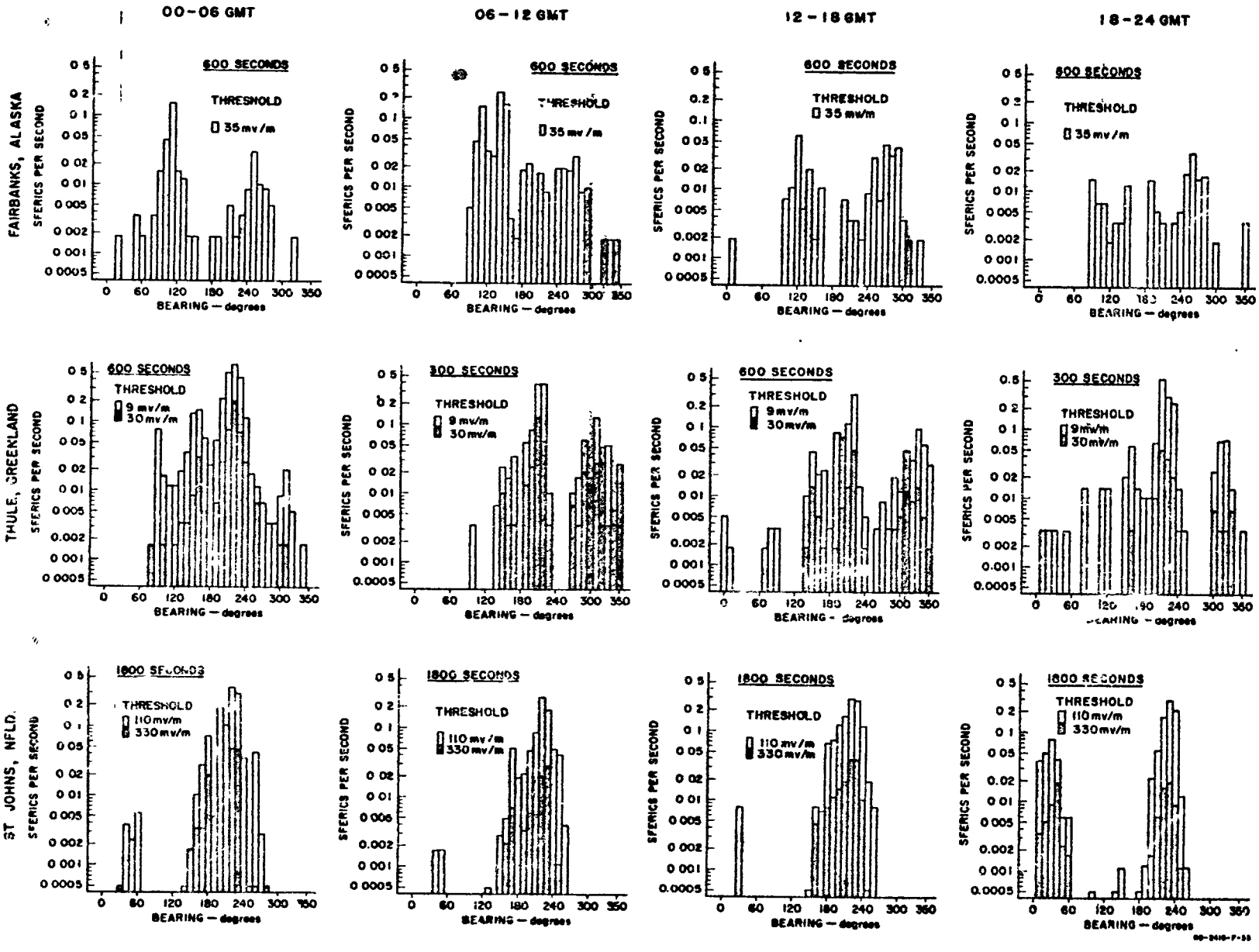

FIG. D-10

DIRECTION-OF-ARRIVAL DISTRIBUTION— SEPTEMBER 1958

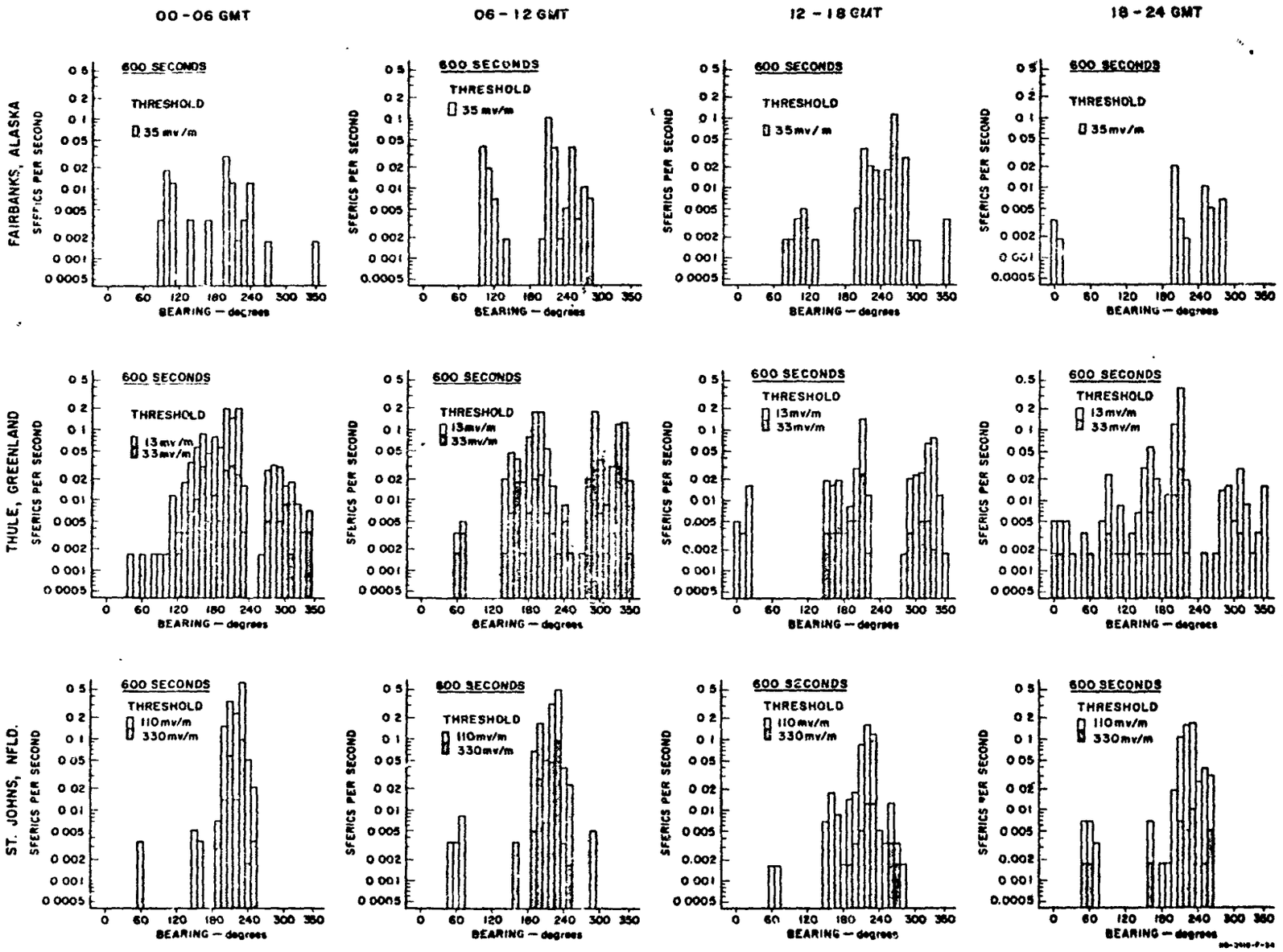

FIG. D-11

DIRECTION-OF-ARRIVAL DISTRIBUTION—OCTOBER 1958

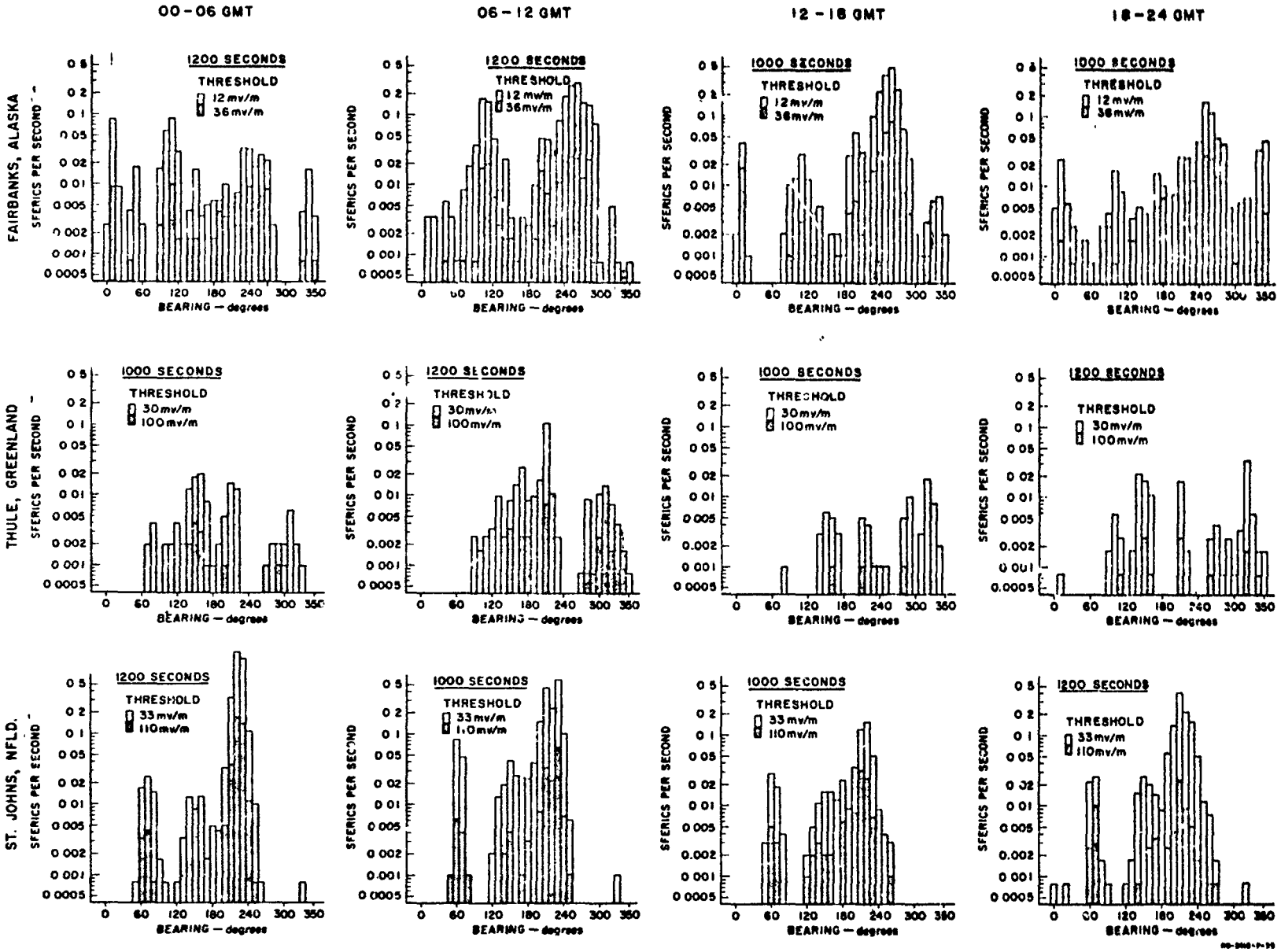

FIG. D-12

DIRECTION-OF-ARRIVAL DISTRIBUTION—NOVEMBER 1958

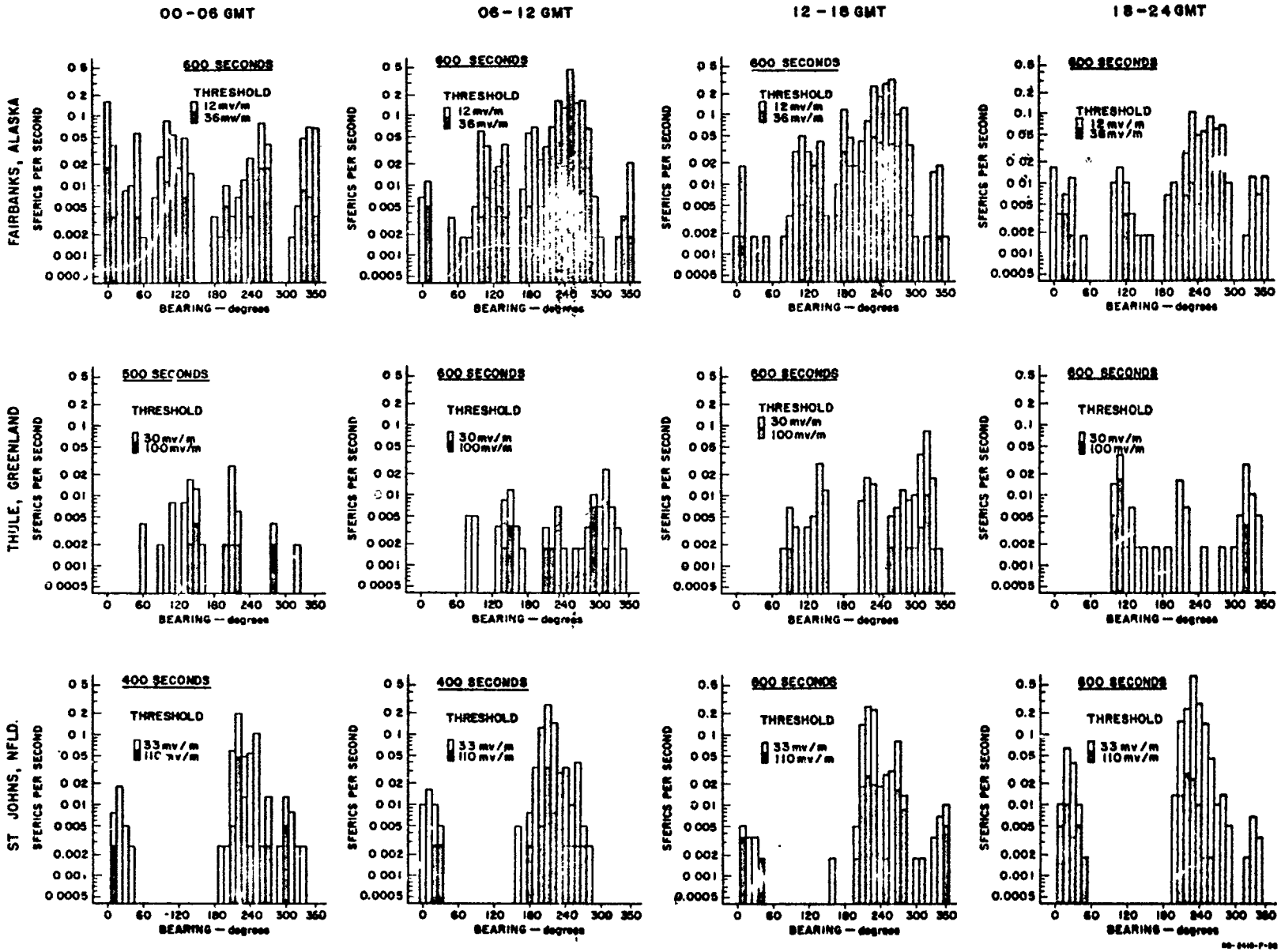

FIG. D-13

DIRECTION-OF-ARRIVAL DISTRIBUTION — DECEMBER 1958

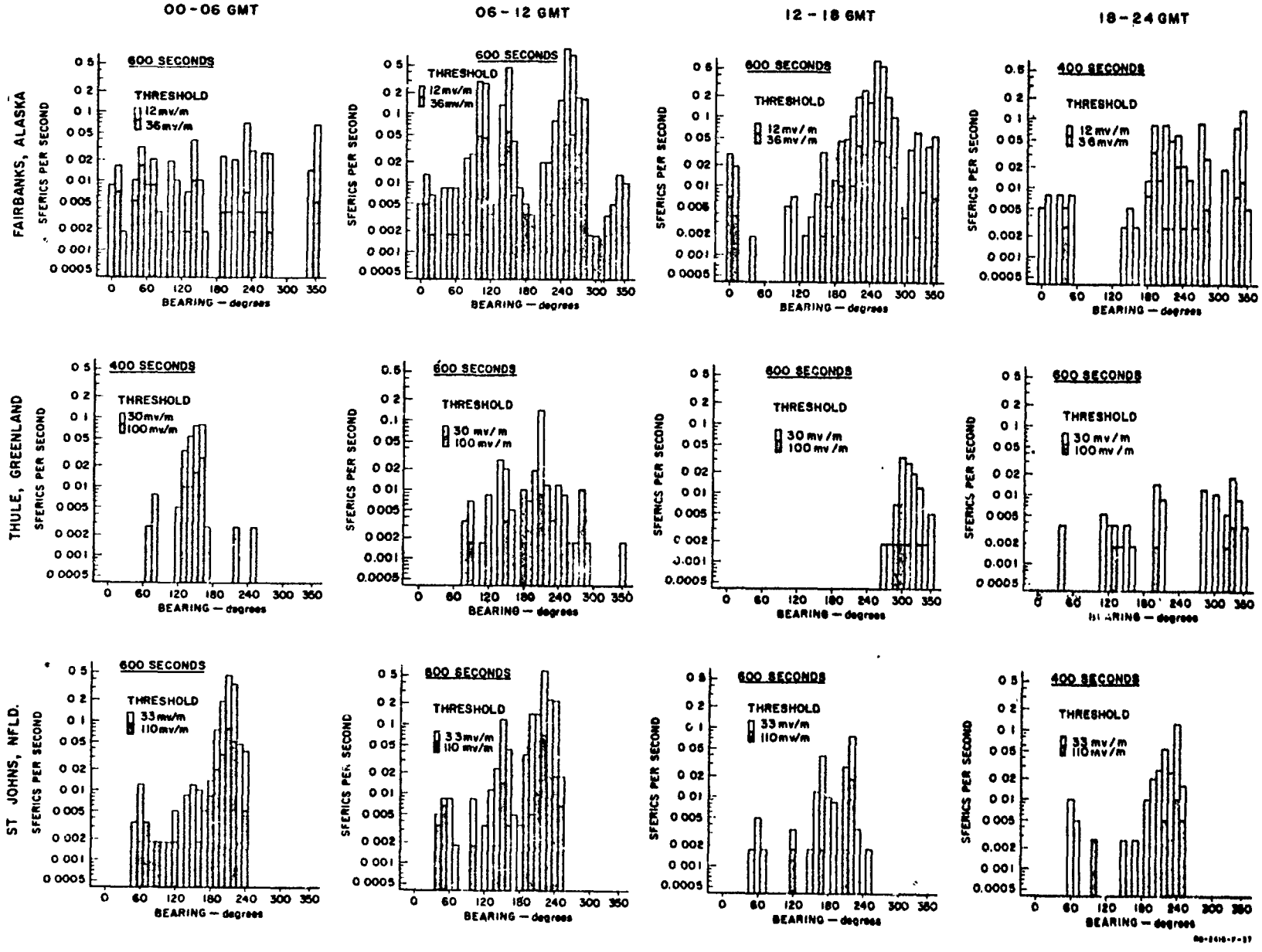

FIG. D-14

DIRECTION-OF-ARRIVAL DISTRIBUTION—JANUARY 1959

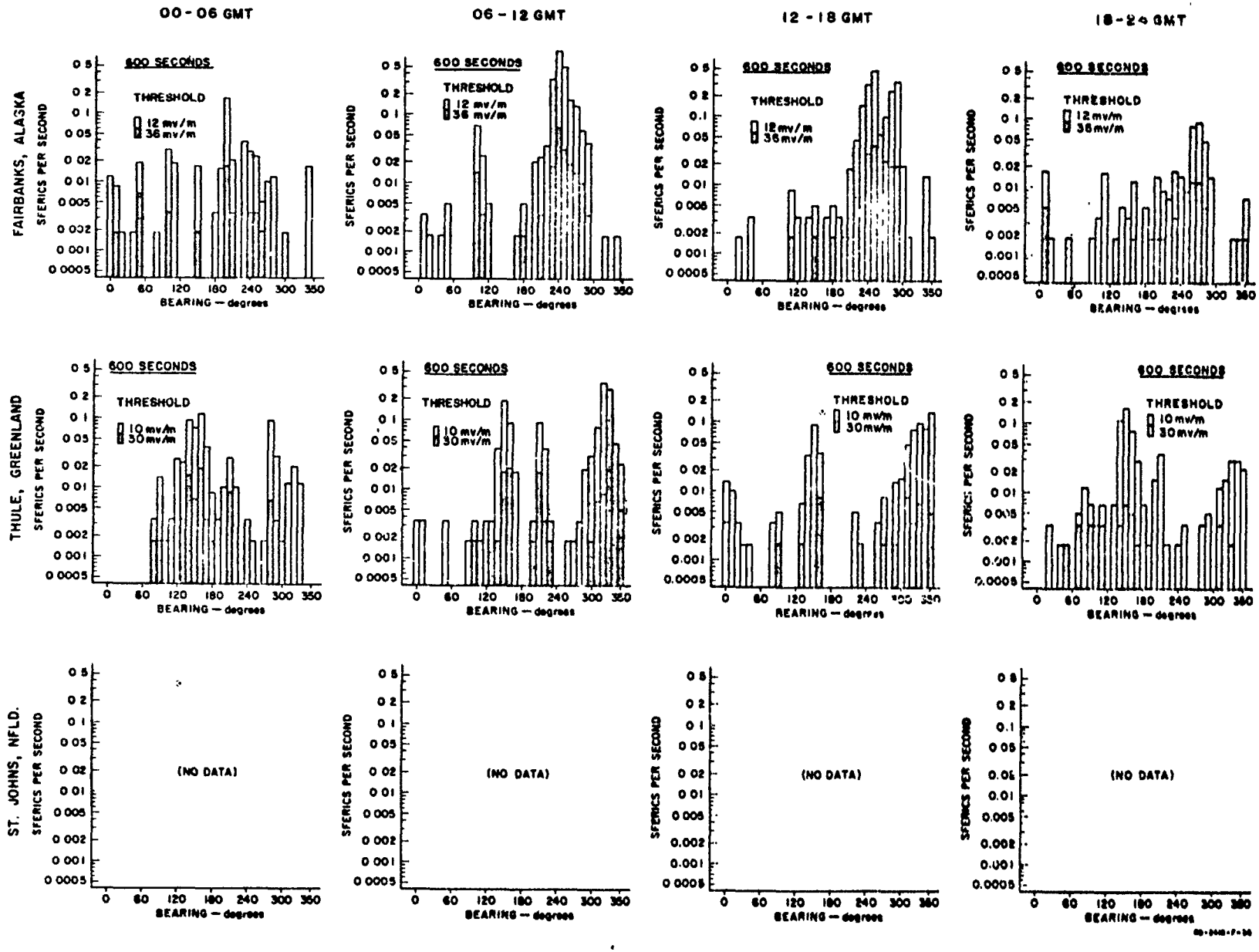

FIG. D-15

DIRECTION-OF-ARRIVAL DISTRIBUTION — FEBRUARY 1959

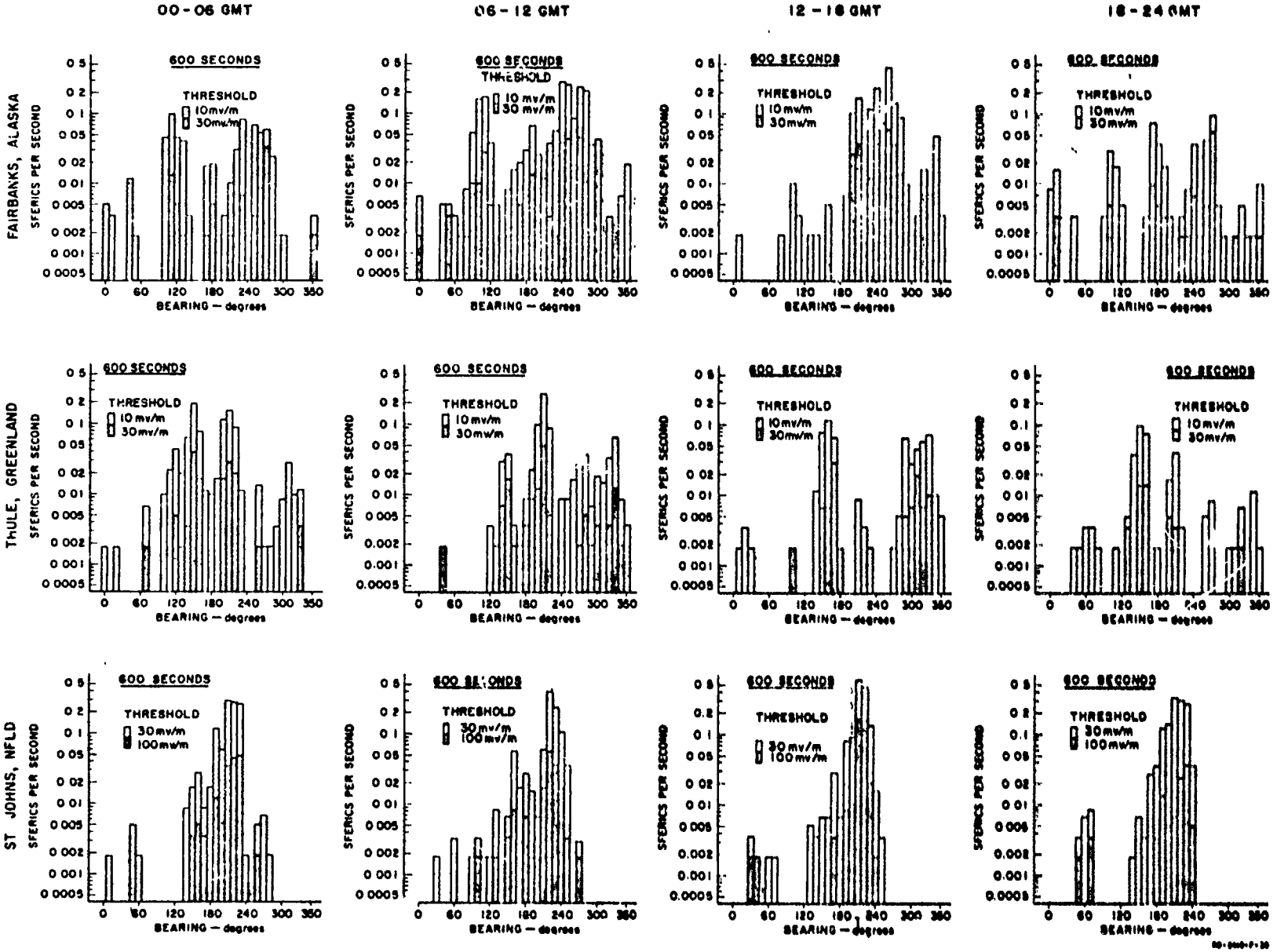

FIG. D-16

DIRECTION-OF-ARRIVAL DISTRIBUTION — MARCH 1959

Appendix E

EVENTS COUNTER

EVENTS COUNTER

Veeder-Root counters were used to record continuously the number of sferics exceeding pre-set leve. of field strengths in each quarter of the GMT day, (00-06, 06-12, 12-18, and 18-24 hours GMT) at Fairbanks, Alaska, at Thule, Greenland, and at St. Johns, Newfoundland. Four fixed field-strength levels at 20-db intervals were used. The Veeder-Root counters were preceded by electronic decade dividers so that either 10 or 100 sferics were required to register a single count on the counters. The number from the counters were manually recorded every day except when bad weather made station operation impossible or when equipment troubles were encountered.

The counters were set to trigger at either 1, 10, 100, and 1000 millivolts per meter, center to peak, or 10, 100, 1000, and 10,000 millivolts per meter, center to peak, depending upon the amount of activity at each station. Since the sferic monitoring stations were, in general, monitoring distant sferic activity, the highest level counters registered only one or two counts per quarter GMT day. Occasionally a false count was recorded on all counters at the quarter-day switching intervals; thus, the highest level counter data were not considered to be reliable and are not presented in this appendix.

Figures E-1 through E-4 show 10- and 100-millivolt-per-meter events-counter data collected at Fairbanks, Alaska, for December 1958 through March 1959. Prior to December 1958, there was "spike" electrical interference that caused the events counter to be unreliable. This interference was found to be due to a faulty theormstat in an adjacent laboratory, and was eliminated in late November of 1958. The sferics per second for each quarter GMT day are shown as different symbols in the figures. The dashed line in the figures indicates that data were collected for that period and were averaged into the proper quarter-GMT-day data point following the interval. The blank periods on the figures indicate that no data were obtained.

Figures E-5 through E-10 show 1, 10, and 100 millivolt-per-meter events-counter data collected at Thule, Greenland, from mid-September 1958 through March 1959. The 100-millivolt-per-meter counter was inoperative during November 1958, and all counters were inoperative during December 1958, due to equipment trouble.

Figures E-11 through E-16 show 10 and 100 millivolt-per-meter and 1 volt-per-meter events counter data collected at St. Johns, Newfoundland, from late August 1958 through March 1959. Equipment troubles prevented collection of data between 12 and 30 September 1958. The station at St. Johns, Newfoundland, was not in operation during February of 1959, due to bad weather.

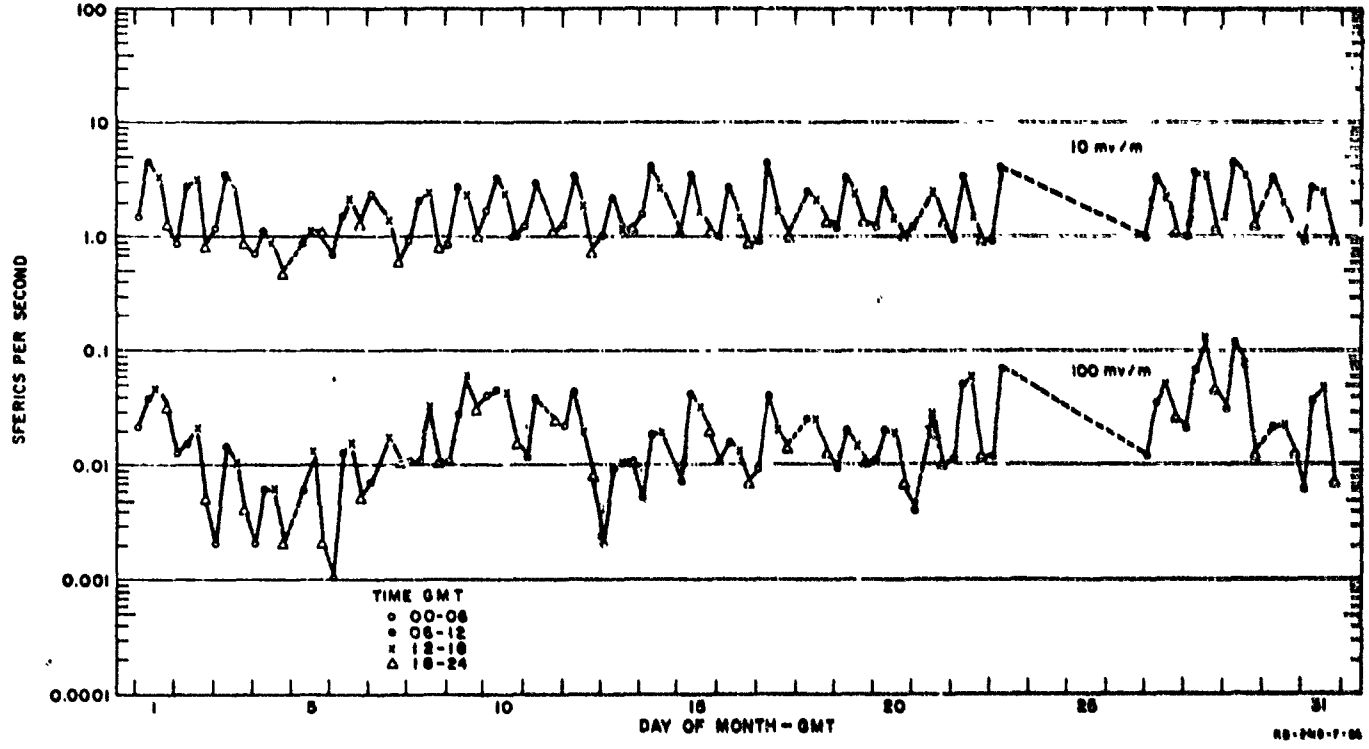

FIG. E-1

SFERICS PER SECOND AT FAIRBANKS, ALASKA—DECEMBER 1958

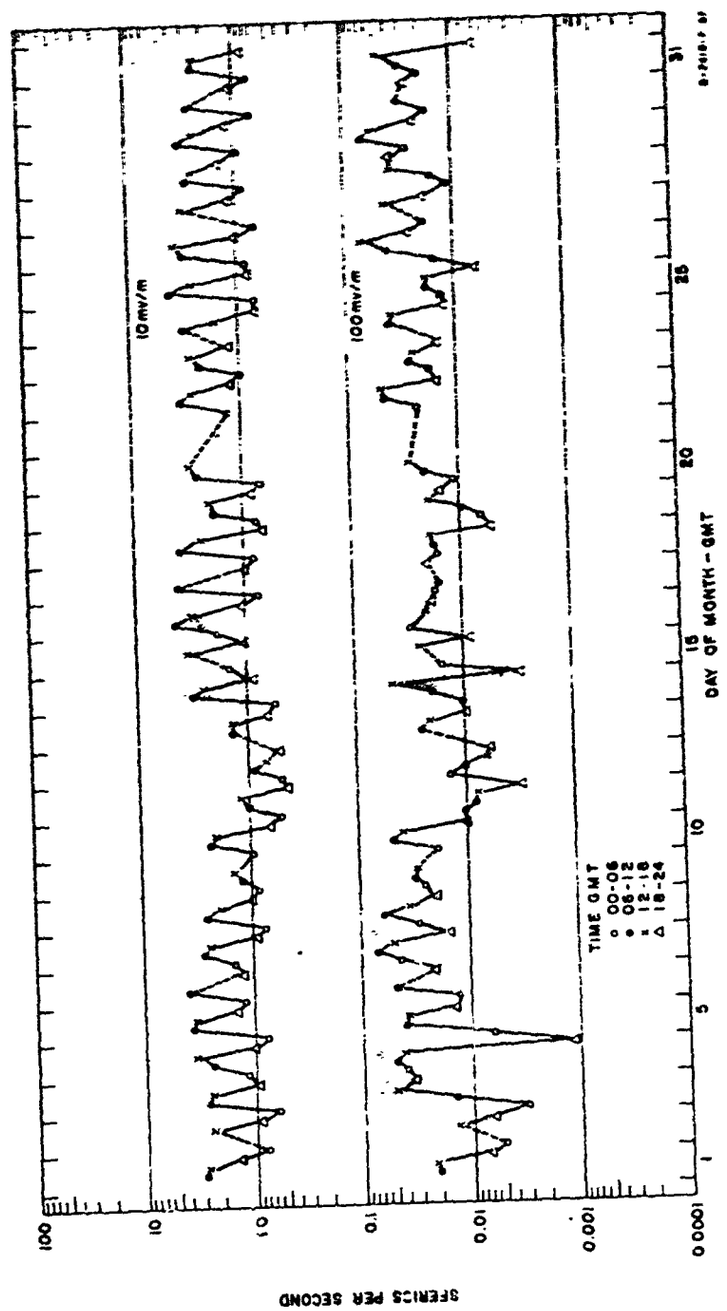

FIG. E-2
SFERICS PER SECOND AT FAIRBANKS, ALASKA—JANUARY 1959

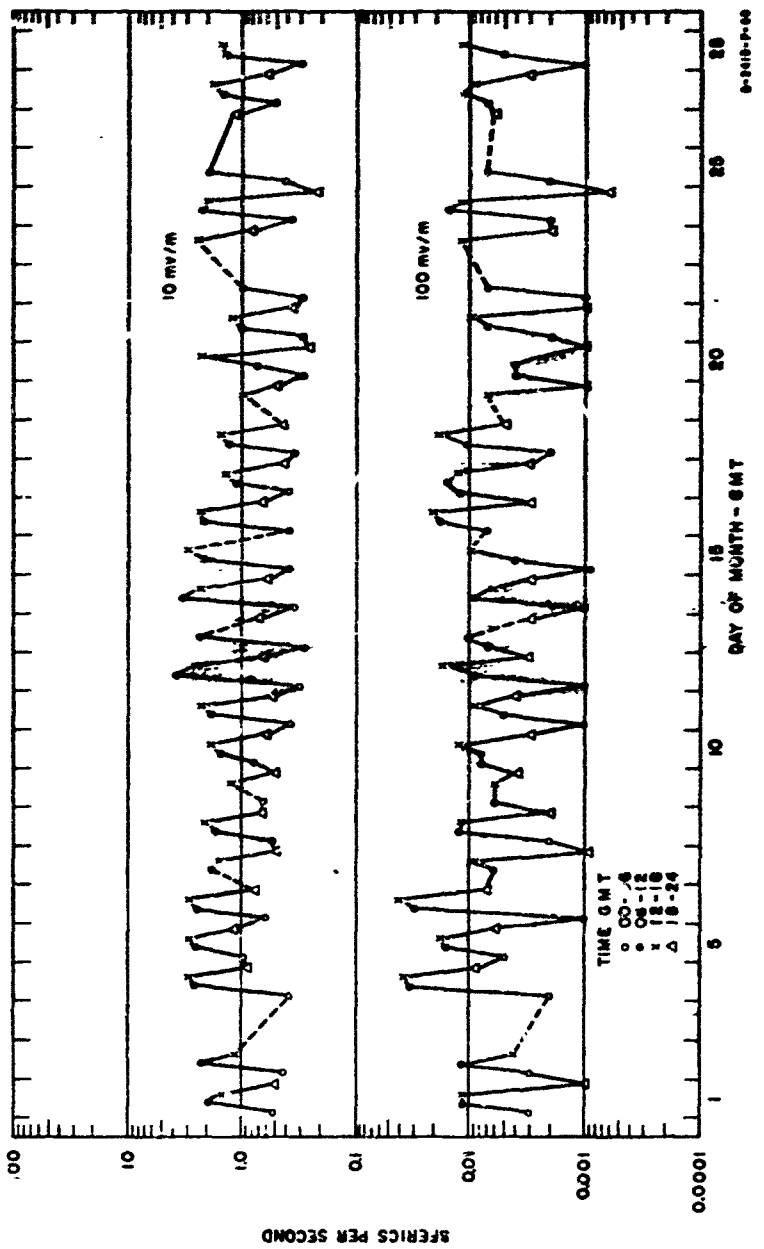

FIG. E-3

SFERICS PER SECOND AT FAIRBANKS, ALASKA — FEBRUARY 1959

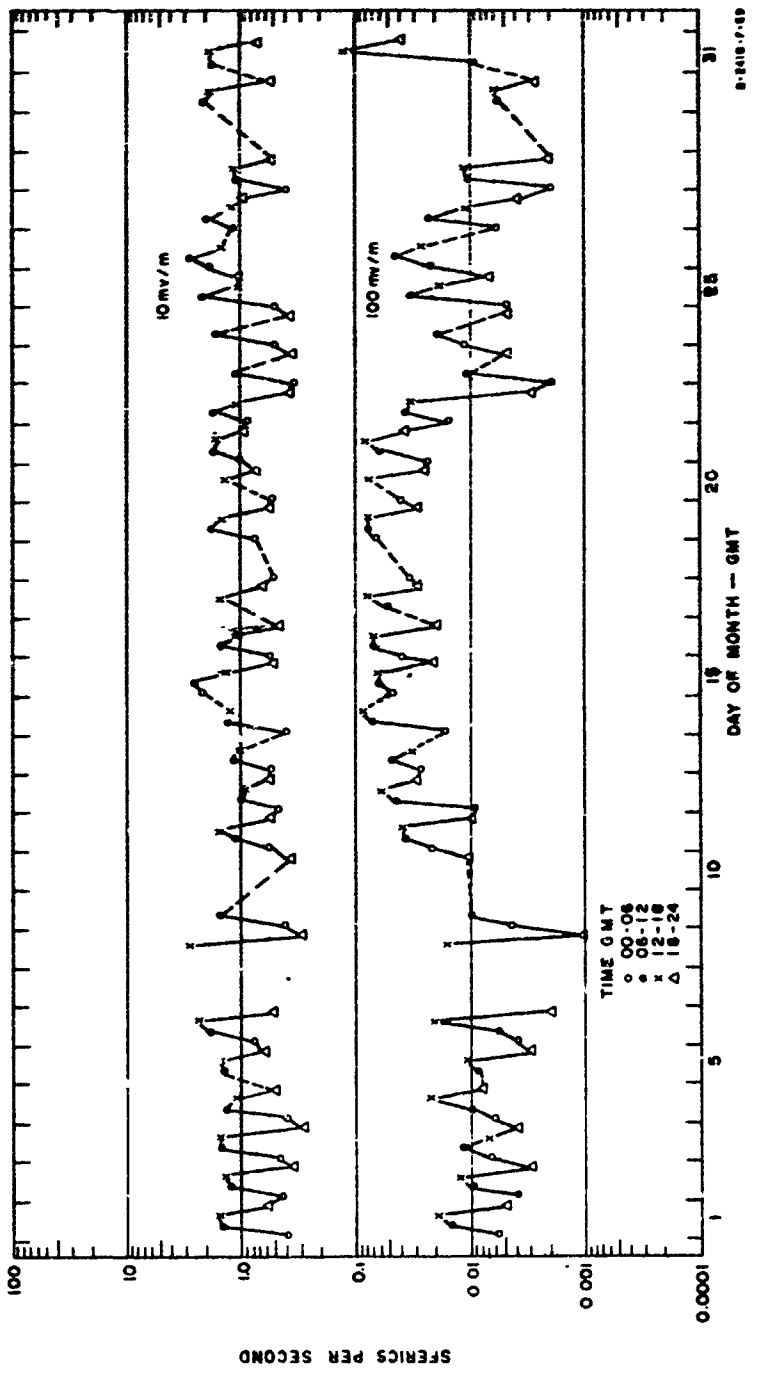

FIG. E-4

SFERICS PER SECOND AT FAIRBANKS, ALASKA—MARCH 1959

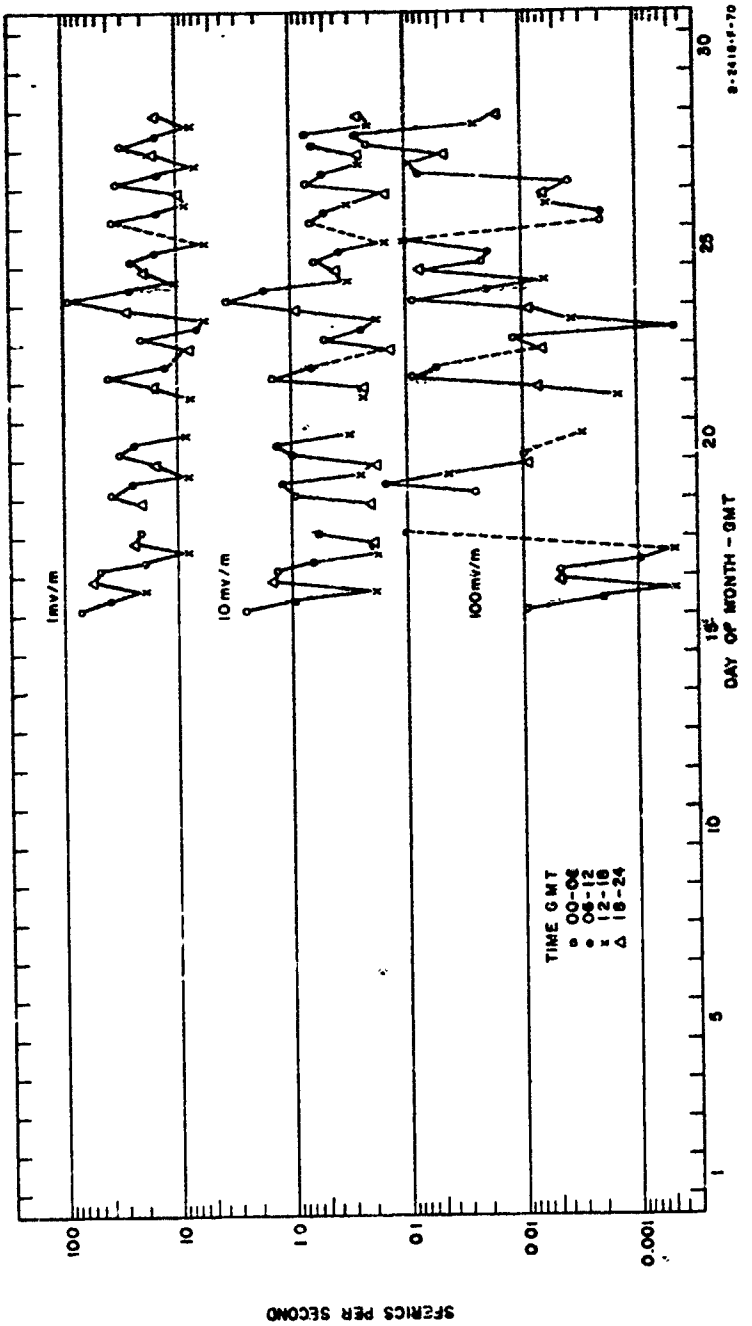

FIG. E-5

SFERICS PER SECOND AT THULE, GREENLAND—SEPTEMBER 1958

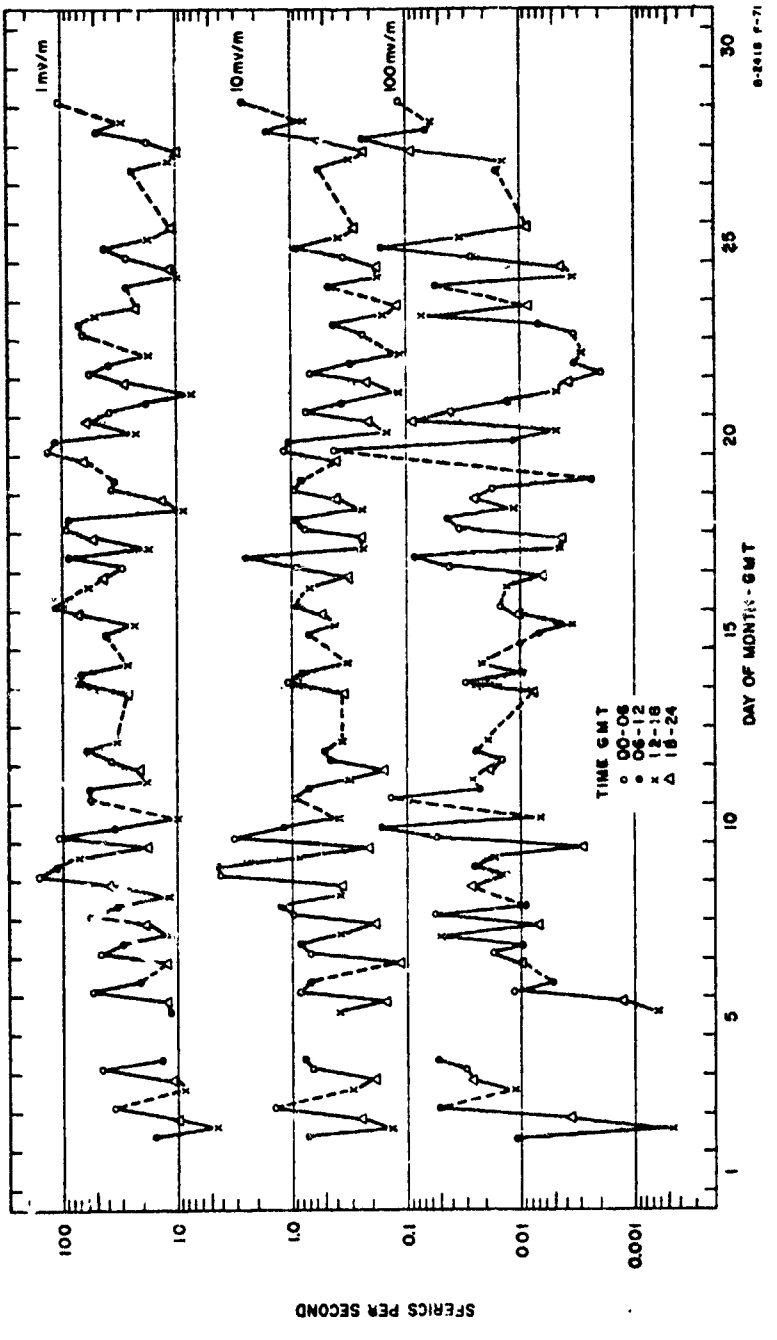

FIG. E-6

SFERICS PER SECOND AT THULE, GREENLAND—OCTOBER 1958

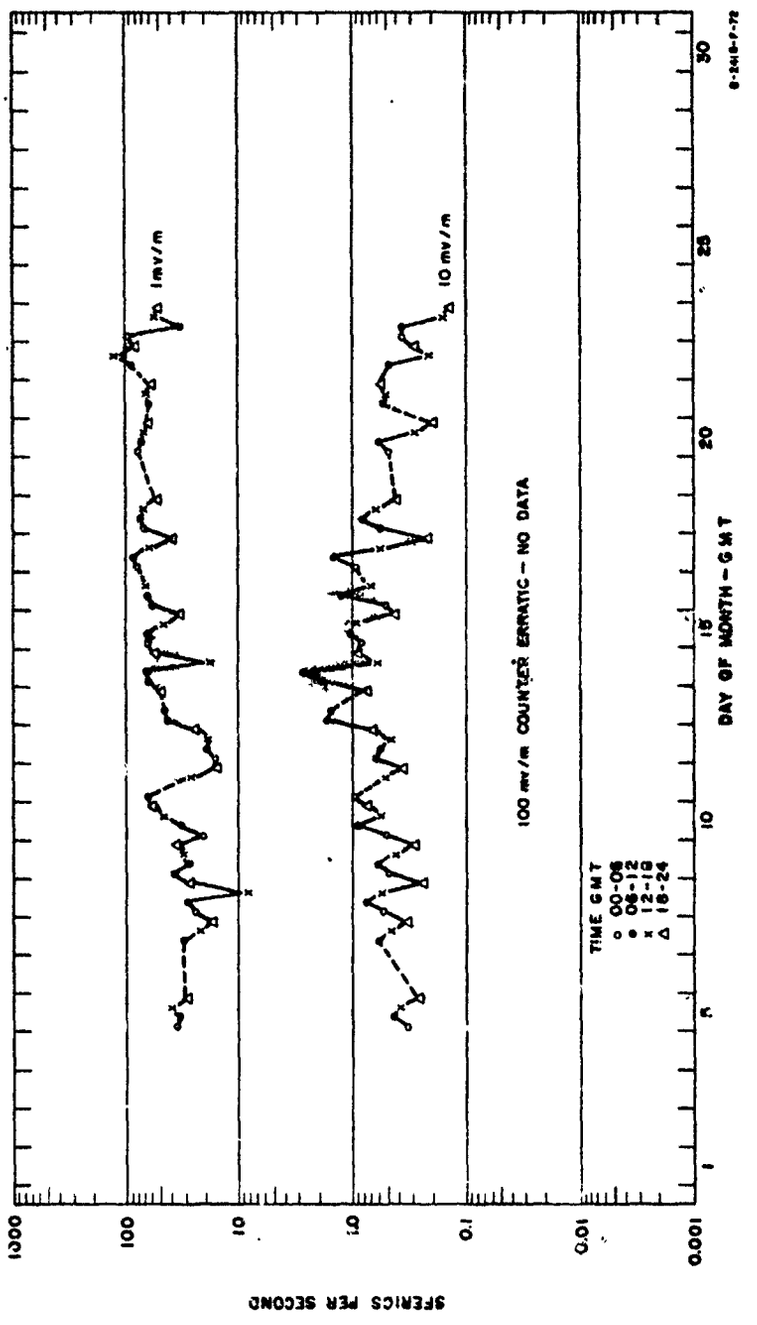

FIG. E-7

SFERICS PER SECOND AT THULE, GREENLAND—NOVEMBER 1958

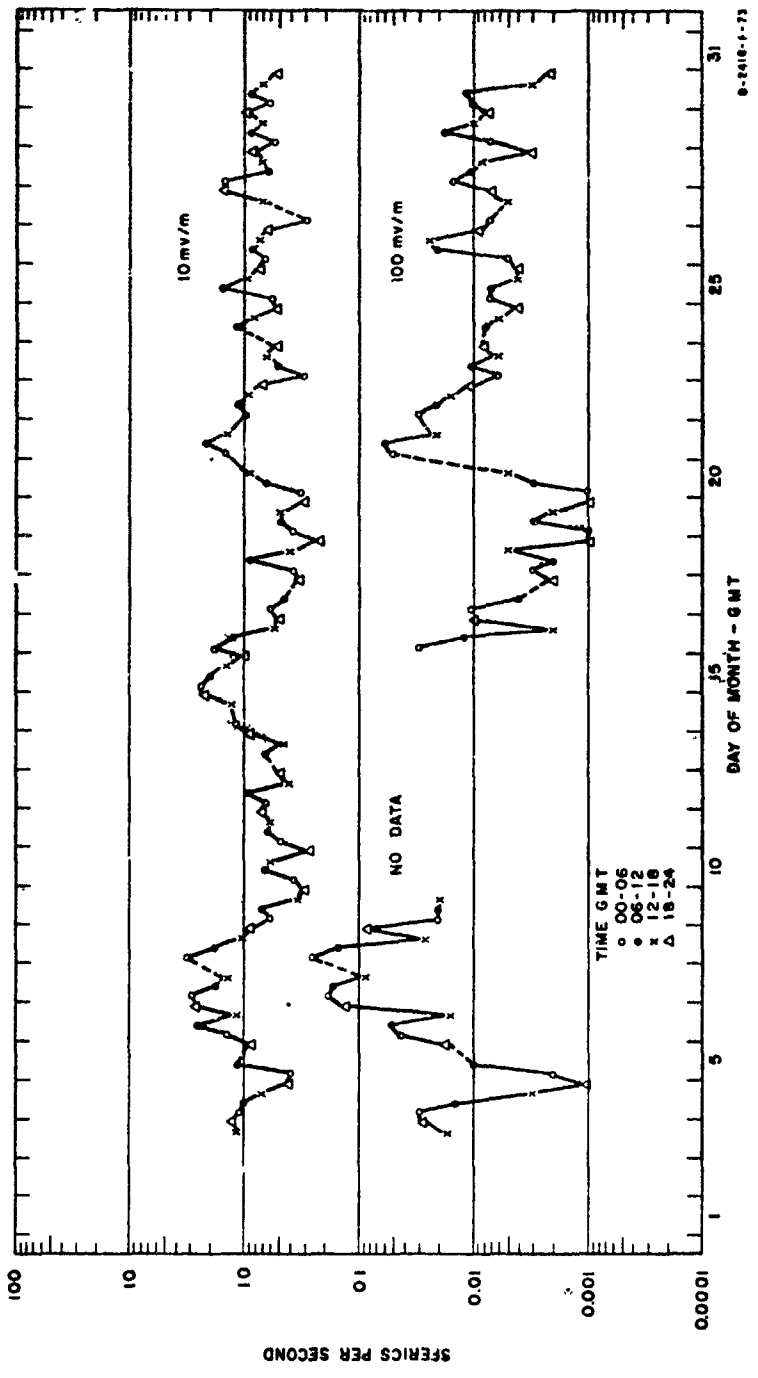

FIG. E-8

SFERICS PER SECOND AT THULE, GREENLAND—JANUARY 1959

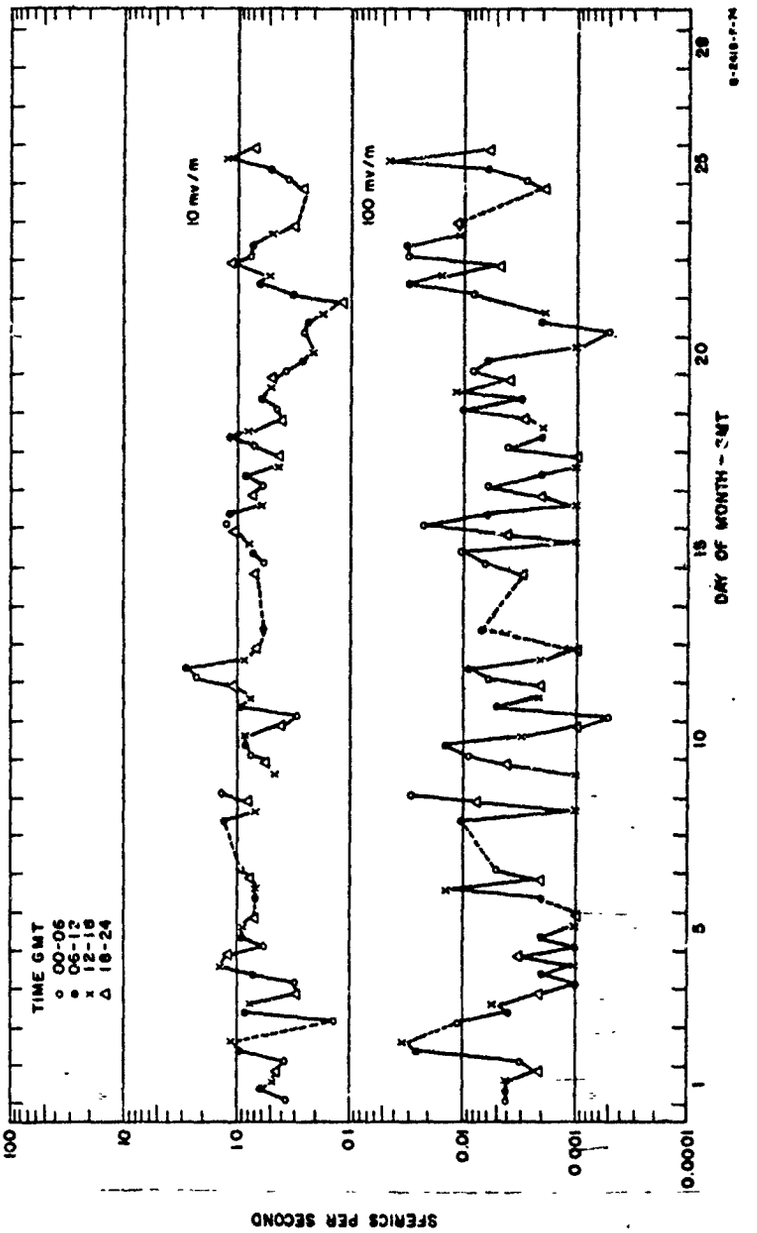

FIG. E-9

SFERICS PER SECOND AT THULE, GREENLAND—FEBRUARY 1959

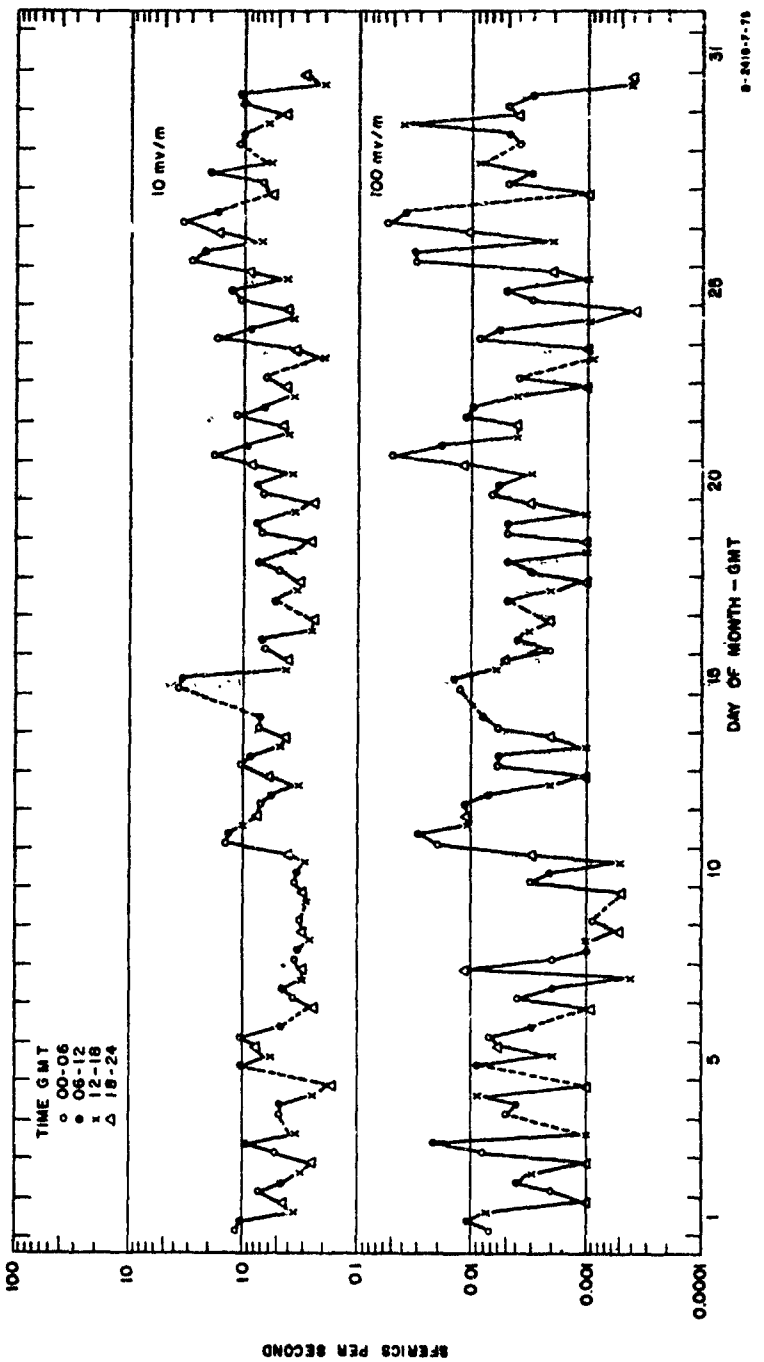

FIG. E-10

SFERICS PER SECOND AT THULE, GREENLAND—MARCH 1959

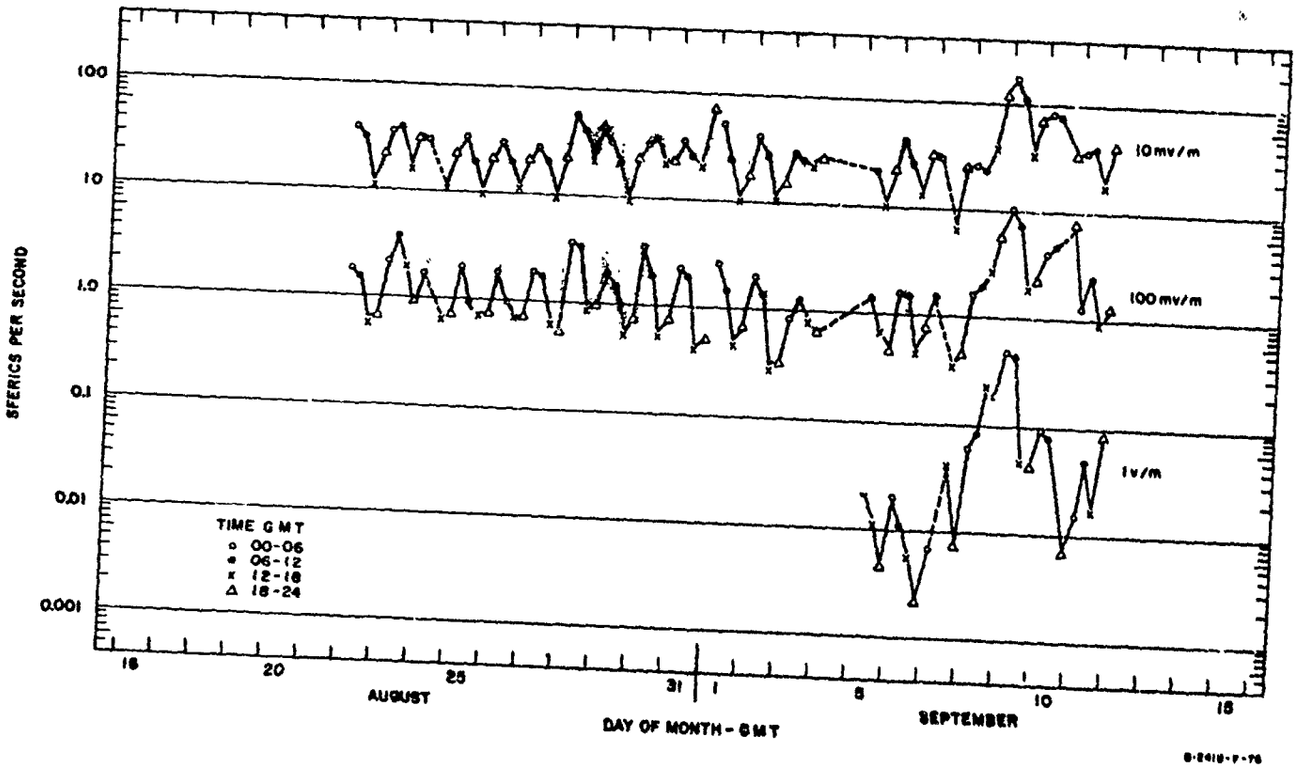

FIG. E-11

SFERICS PER SECOND AT ST. JOHNS, NEWFOUNDLAND — AUGUST TO SEPTEMBER 1958

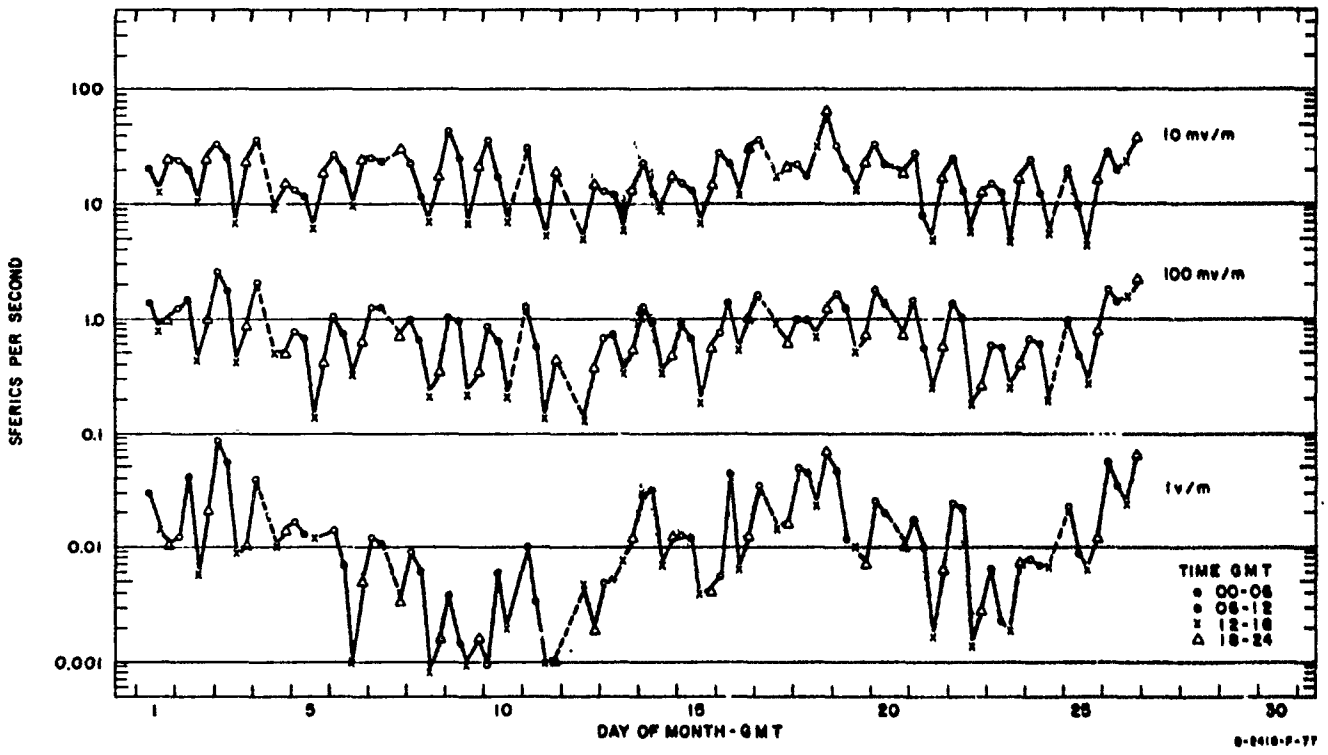

FIG. E-12

SFERICS PER SECOND AT ST. JOHNS, NEWFOUNDLAND—OCTOBER 1958

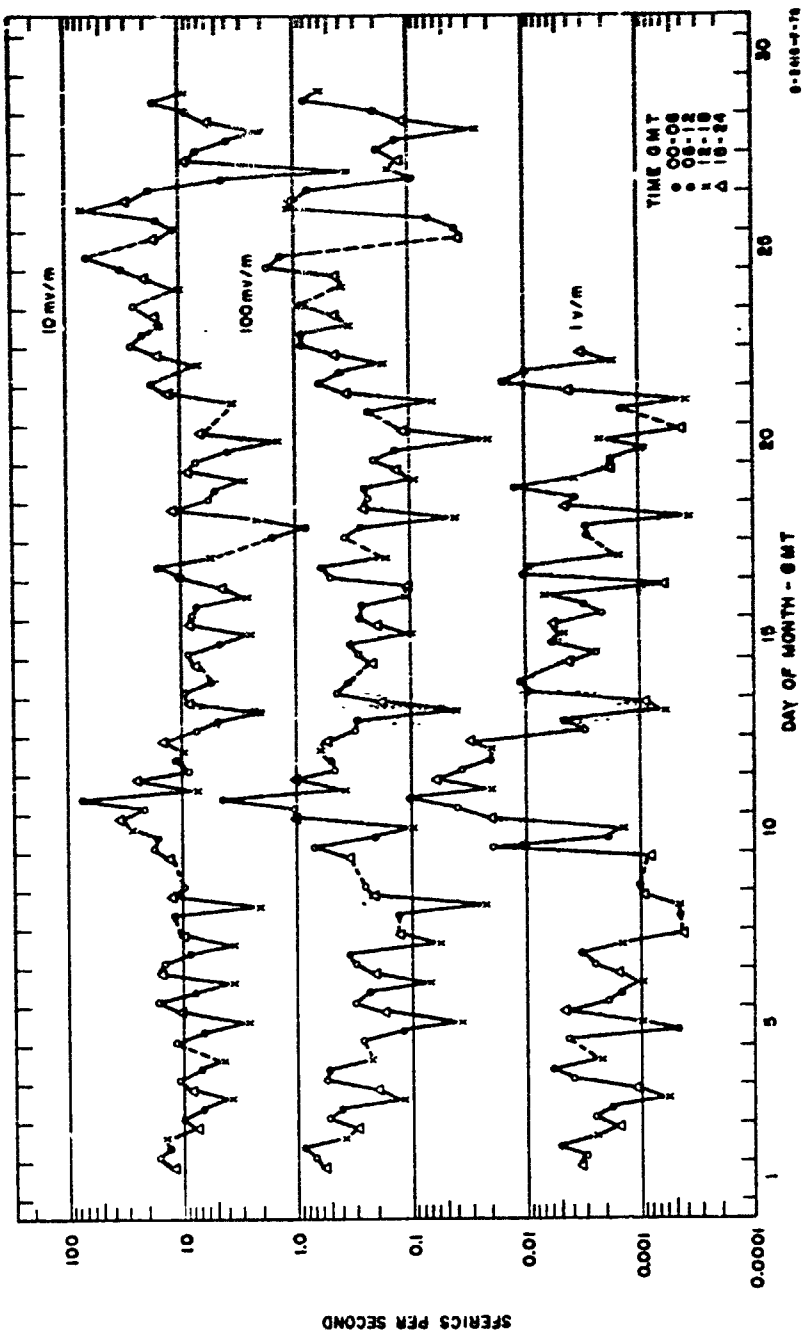

FIG. E-13

SFERICS PER SECOND AT ST. JOHNS, NEWFOUNDLAND—NOVEMBER 1958

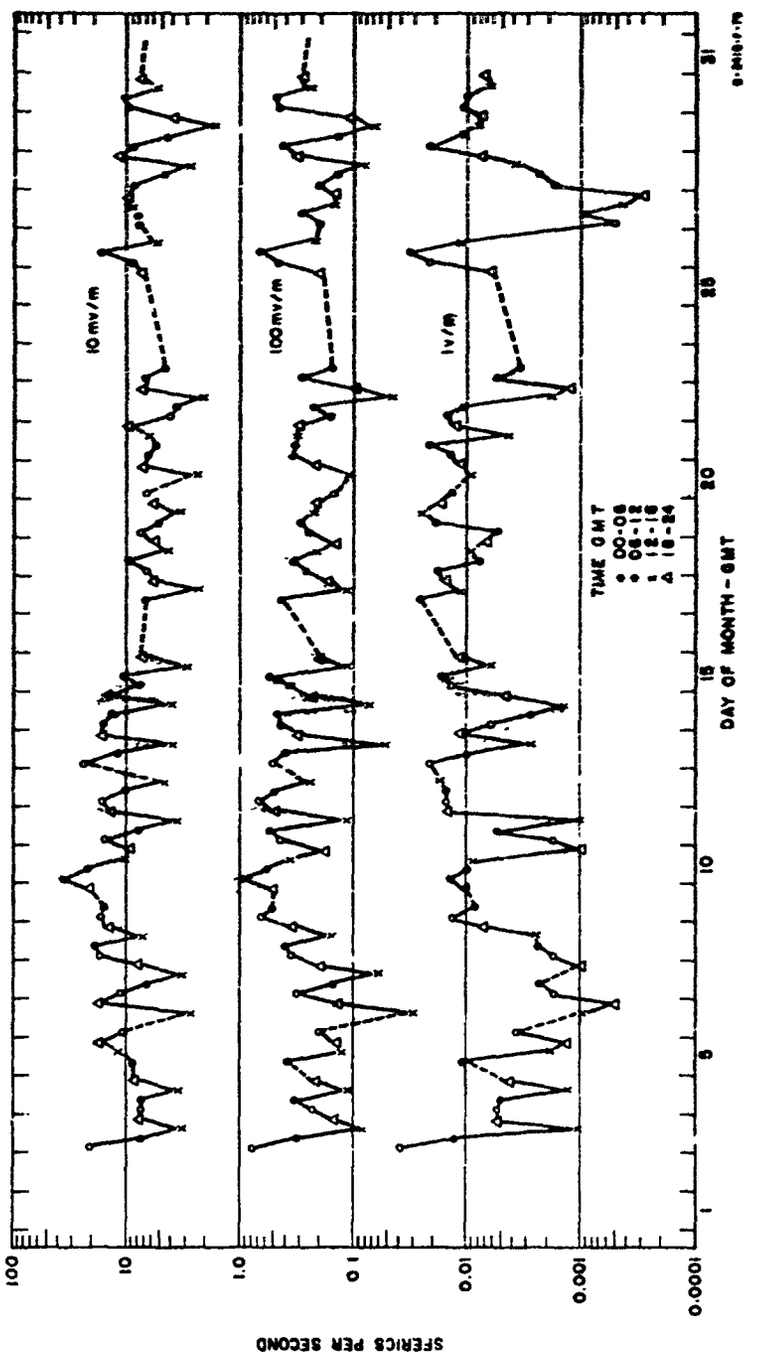

FIG. E-14

SFERICS PER SECOND AT ST. JOHNS, NEWFOUNDLAND — DECEMBER 1958

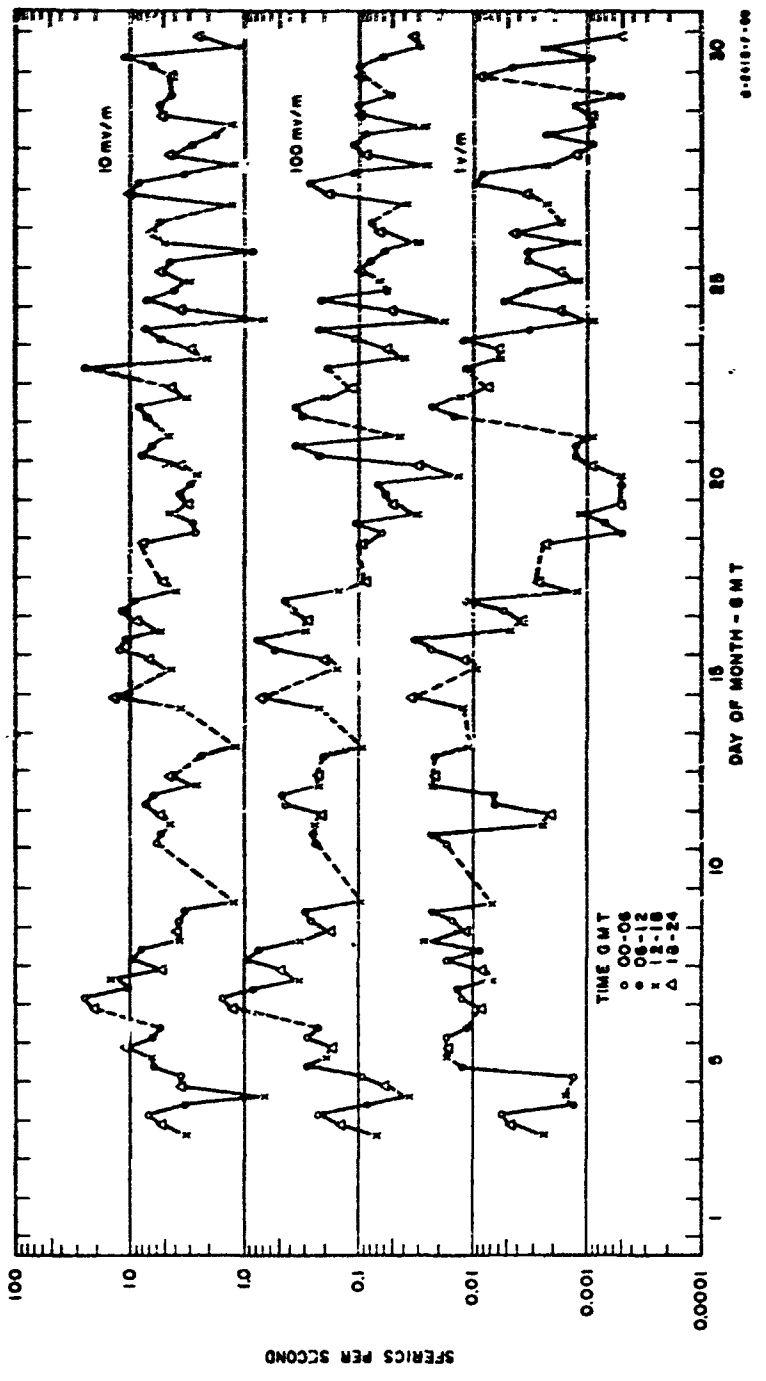

FIG. E-15

SFERICS PER SECOND AT ST. JOHNS, NEWFOUNDLAND—JANUARY 1959

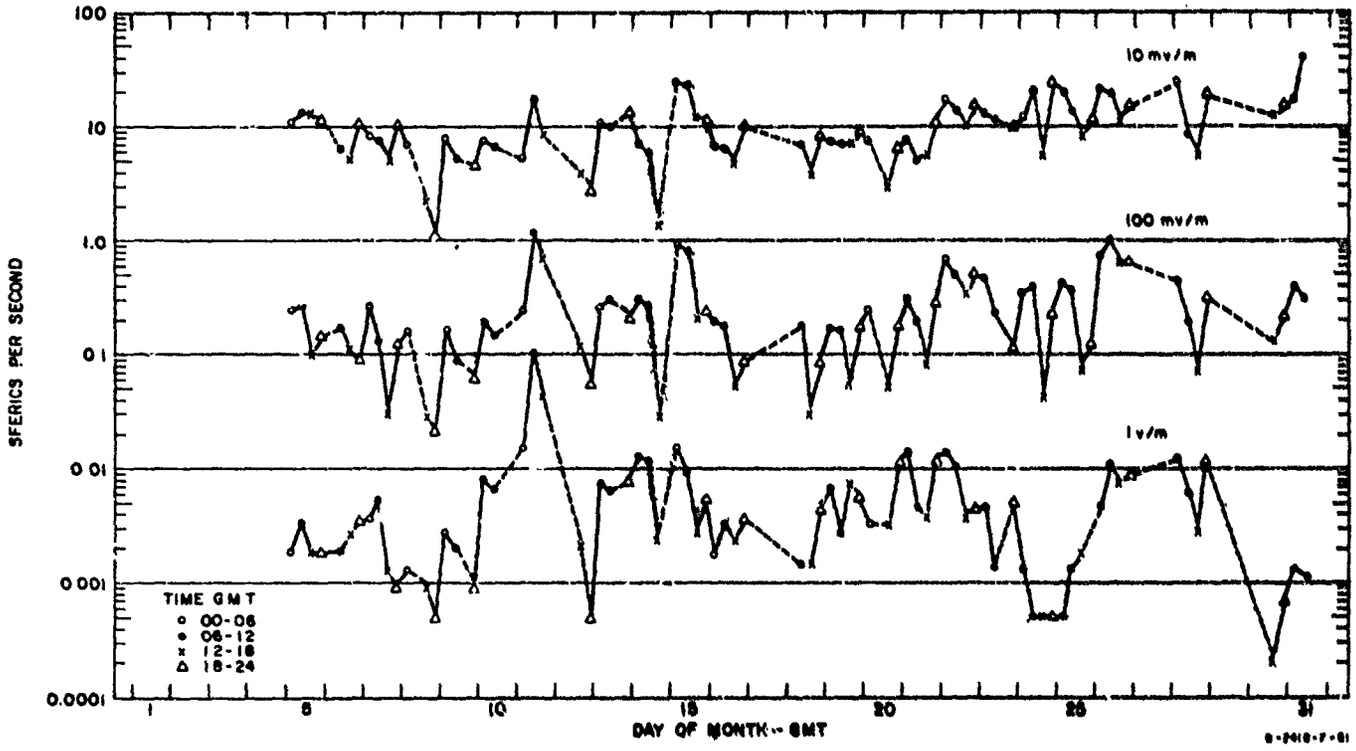

FIG. E-16

SFERICS PER SECOND AT ST. JOHNS, NEWFOUNDLAND — MARCH 1959

Appendix F

RMS NOISE SPECTRUM--12 TO 30 KC

Preceding page blank

RMS NOISE SPECTRUM--12 TO 30 KC

The RMS field strength of atmospheric noise as a function of frequency was continuously recorded by a scanning receiver at each sferic monitoring station. The scanning receiver had a 100-cycle bandwidth at the 3-db-down points, and tuned from 12 kc to 30 kc and back to 12 kc in one hour. Thus, each frequency in the receiver tuning range was scanned twice each hour.

The recording system used was a pen recorder, sensitive linearly in db to the average receiver output voltage, which in a narrow bandwidth is approximately equal to the RMS value of the receiver output voltage. The scanning receiver system was calibrated in RMS field strength.

The scanning receiver records (pen recordings) collected at Fairbanks, Thule, and St. Johns were analyzed by manually recording the RMS noise field strength as a function of frequency at 0300, 0900, 1500, and 2100 hours GMT. These hours were selected as mid-points in each quarter day. Noise level was read at each kilocycle on the increasing frequency scanning cycle. Half-month averages and minimum-maximum values of RMS noise level as a function of frequency are presented in this appendix.

Scanning receiver records were collected at Fairbanks from 18 October 1958 through 31 March 1959 and are presented for each month in Figs. F-1 through F-6.

Scanning receiver records were collected at Thule from 20 September 1958 through 31 March 1959 and are presented for each month in Figs. F-7 through F-13.

Scanning receiver records were collected at St. Johns from 1 September 1958 through 7 February 1959 and for 4 to 8 March 1959 and are presented in Figs. F-14 through F-19.

Each figure, in general, presents the data from each station for each month. The averaged curve is a smoothed curve. The minimum and maximum recorded values for each frequency are shown as a series of dots.

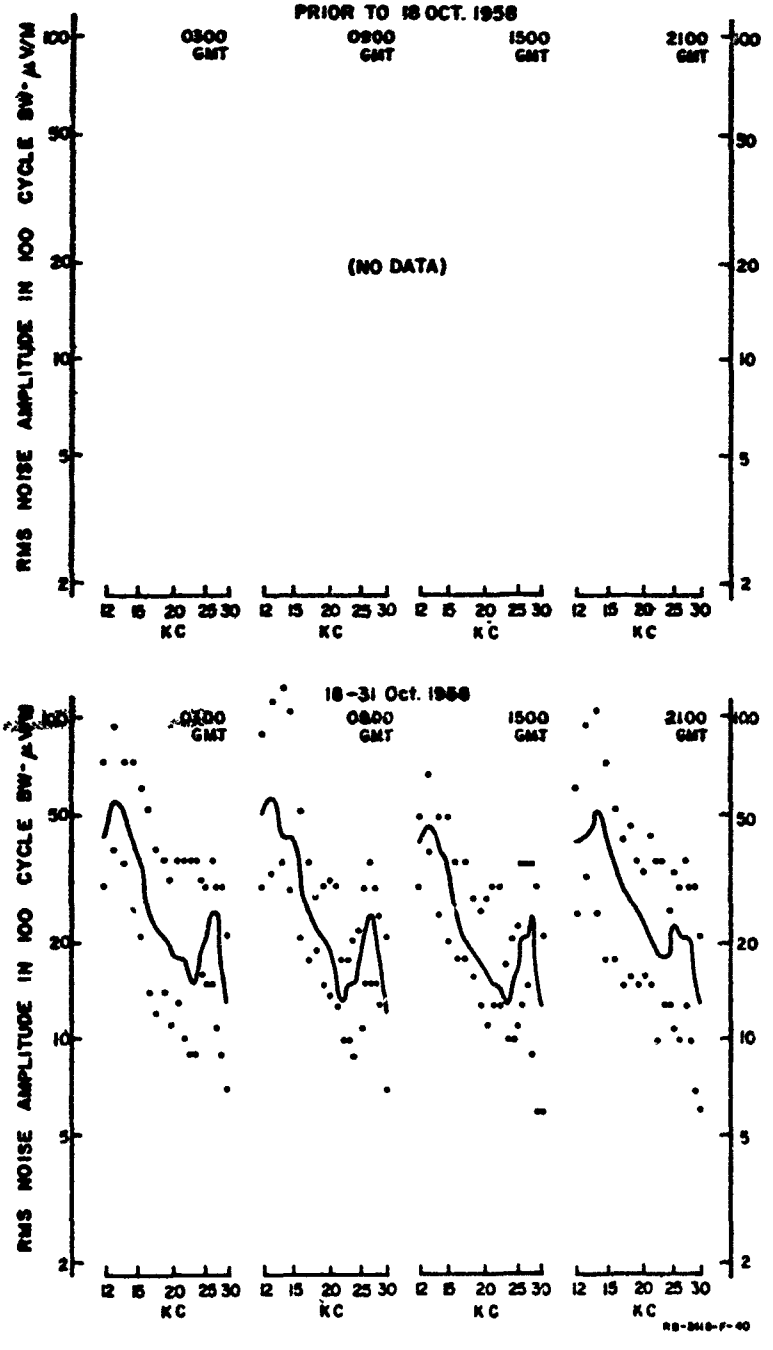

FIG. F-1

RMS NOISE SPECTRUM AT FAIRBANKS, ALASKA—OCTOBER 1958

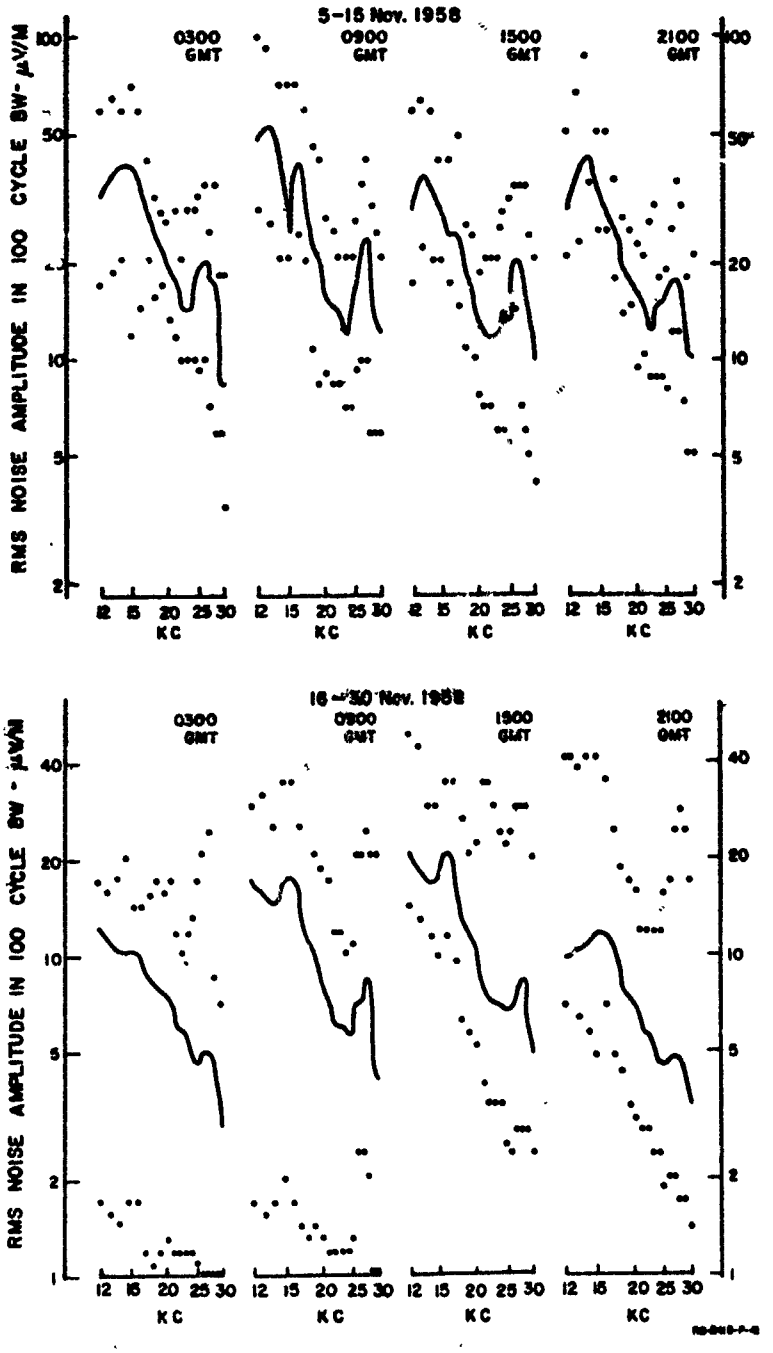

FIG. F-2

RMS NOISE SPECTRUM AT FAIRBANKS, ALASKA—NOVEMBER 1958

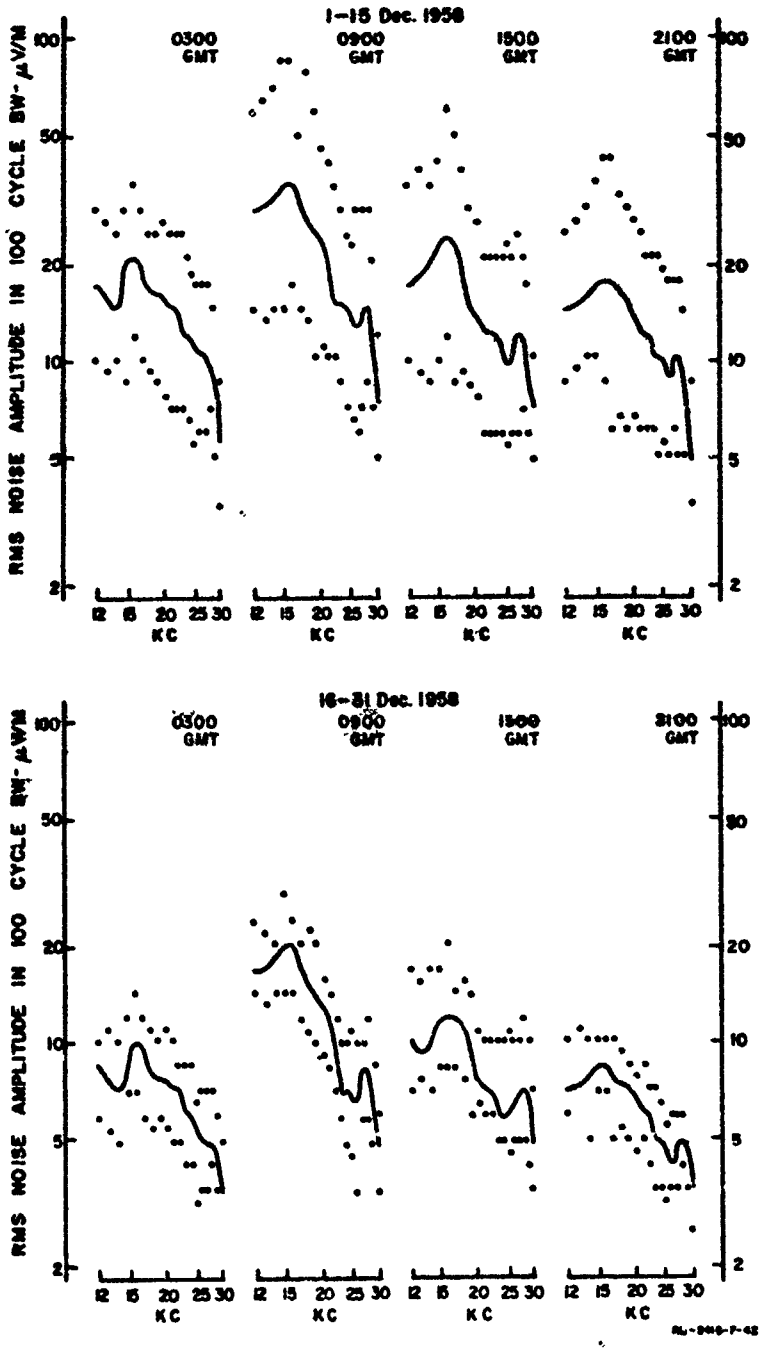

FIG. F-3

RMS NOISE SPECTRUM AT FAIRBANKS, ALASKA—DECEMBER 1958

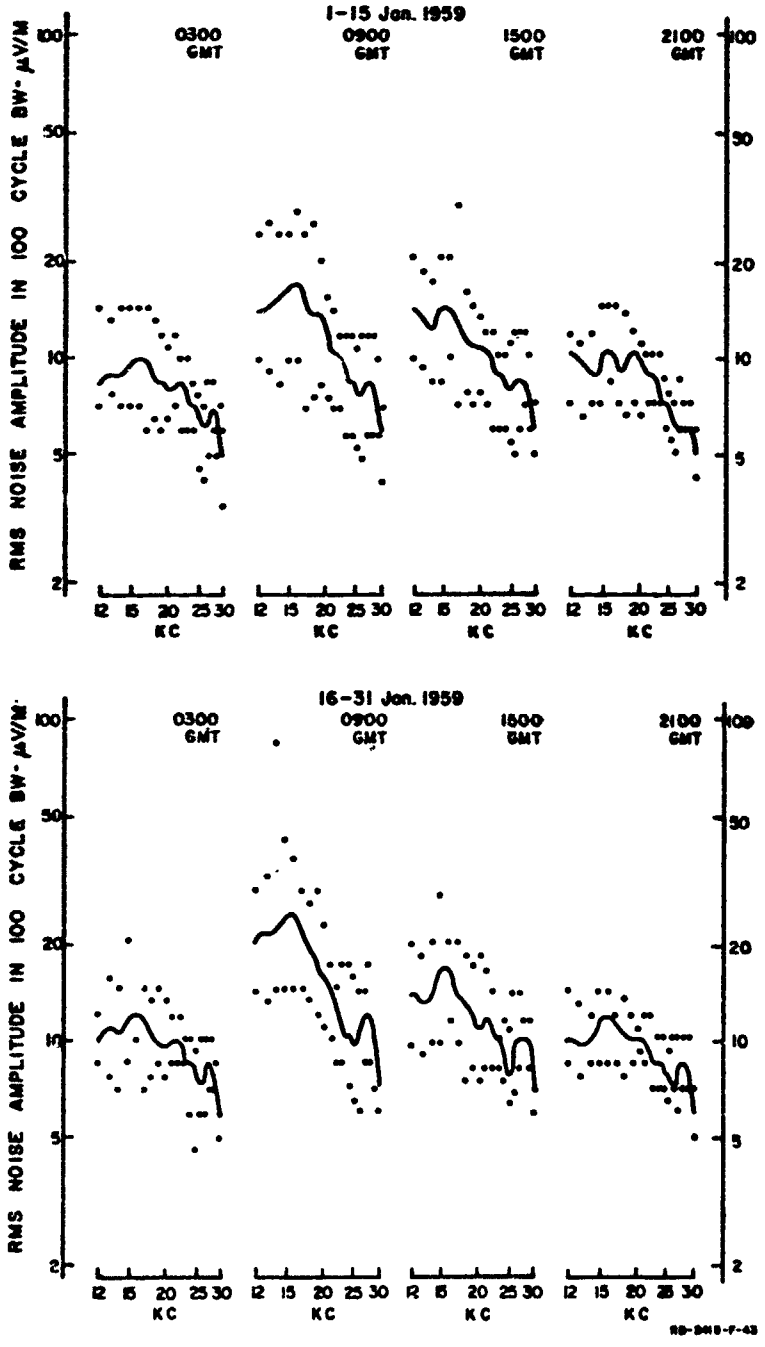

FIG. F-4

RMS NOISE SPECTRUM AT FAIRBANKS, ALASKA—JANUARY 1959

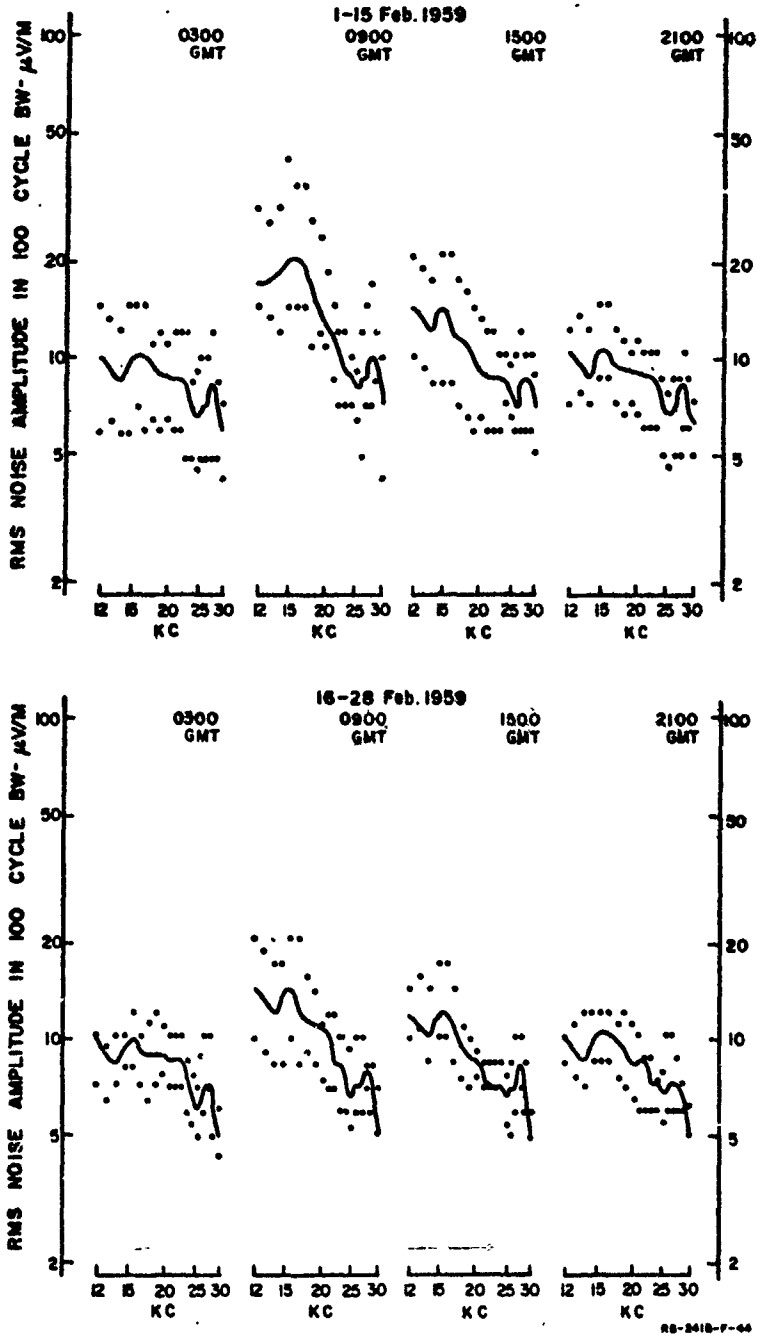

FIG. F-5

RMS NOISE SPECTRUM AT FAIRBANKS, ALASKA—FEBRUARY 1959

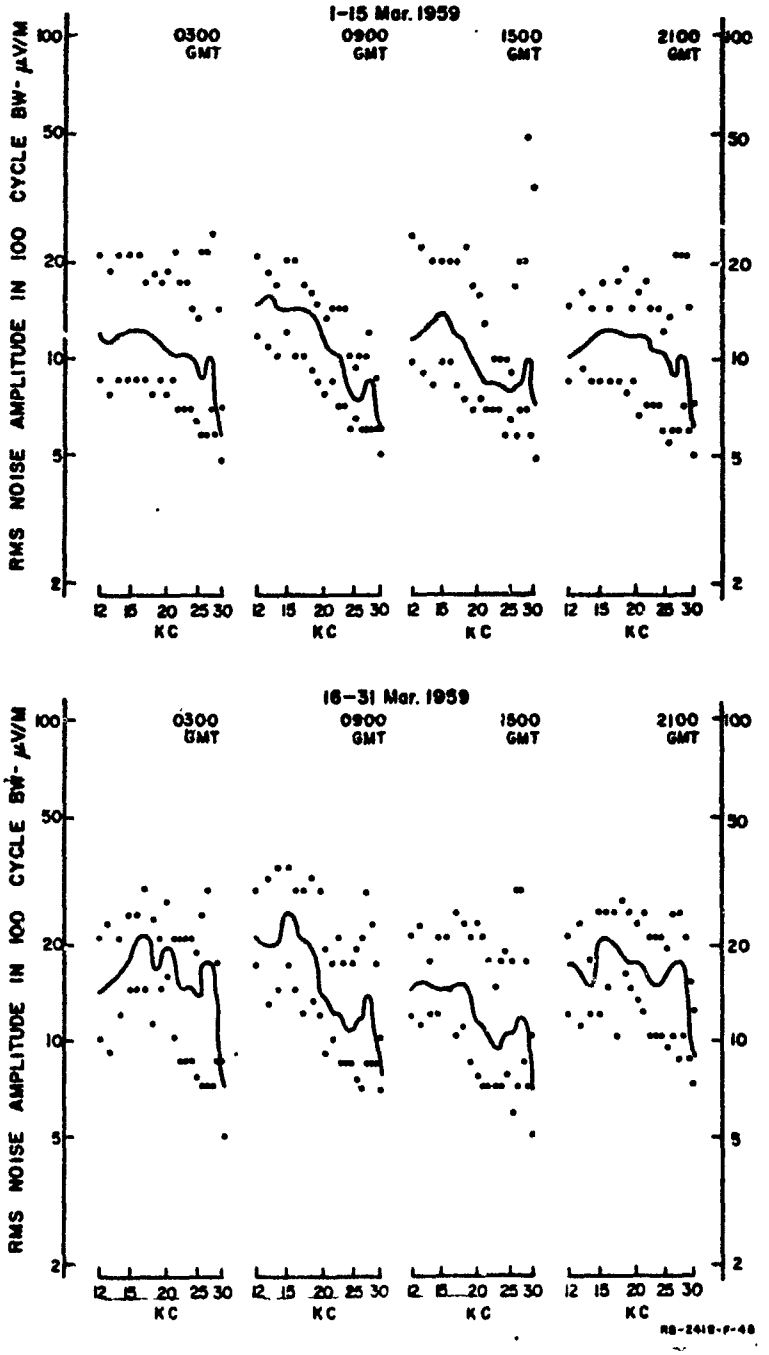

FIG. F-6

RMS NOISE SPECTRUM AT FAIRBANKS, ALASKA—MARCH 1959

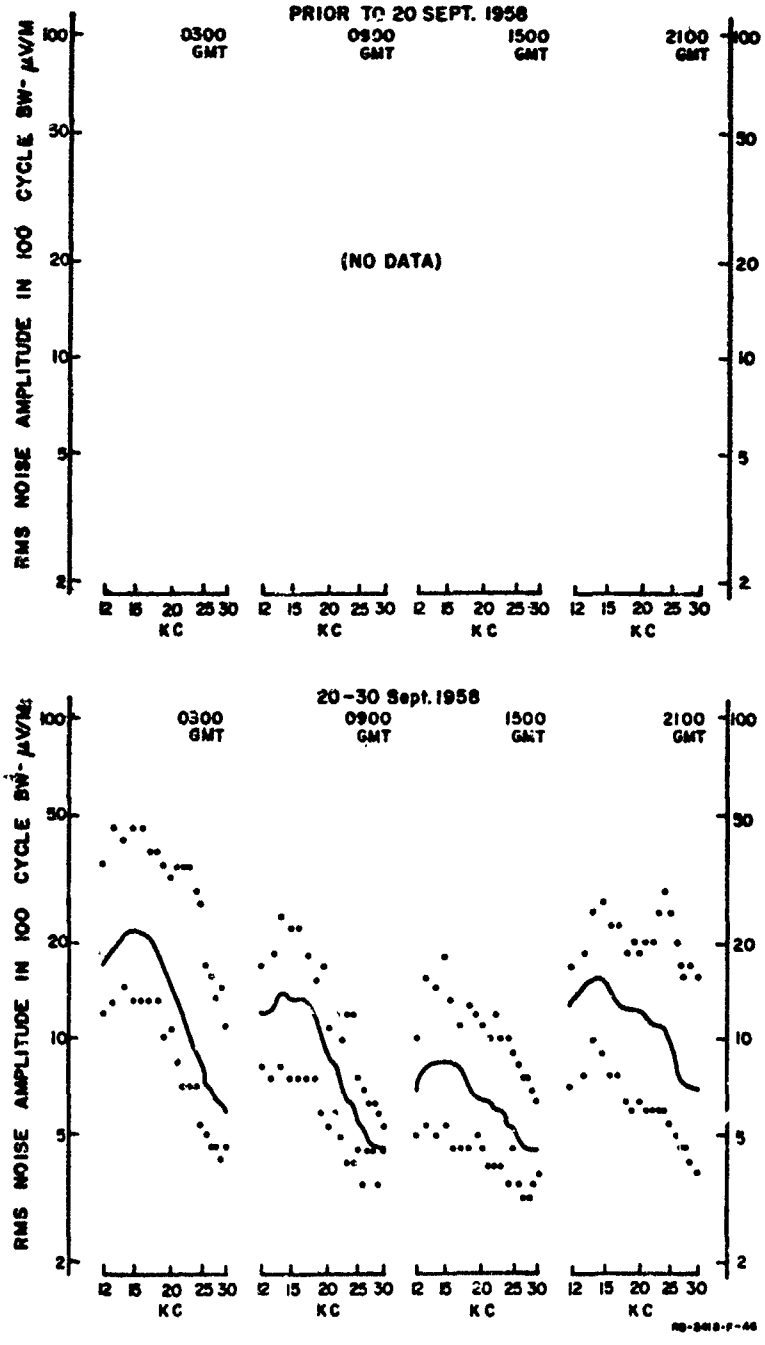

FIG. F-7

RMS NOISE SPECTRUM AT THULE, GREENLAND — SEPTEMBER 1958

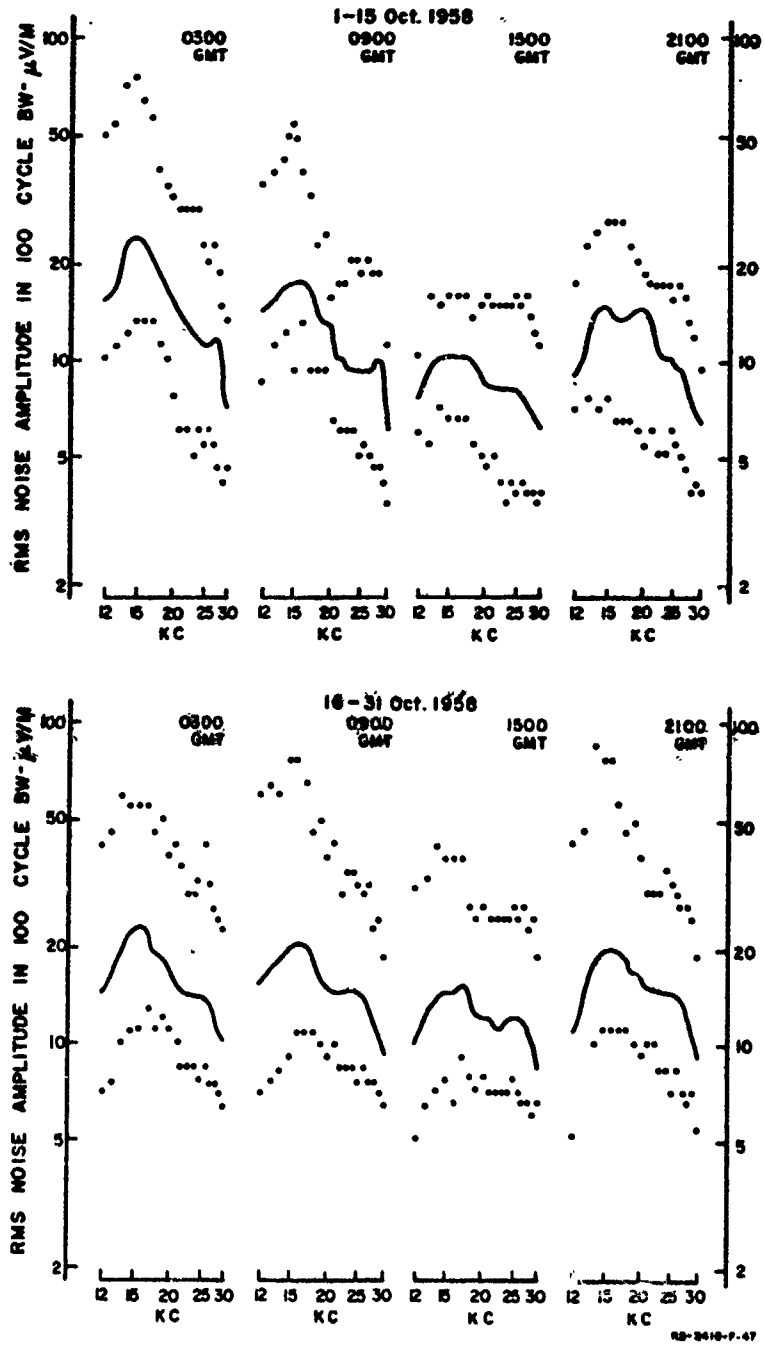

FIG. F-8

RMS NOISE SPECTRUM AT THULE, GREENLAND—OCTOBER 1958

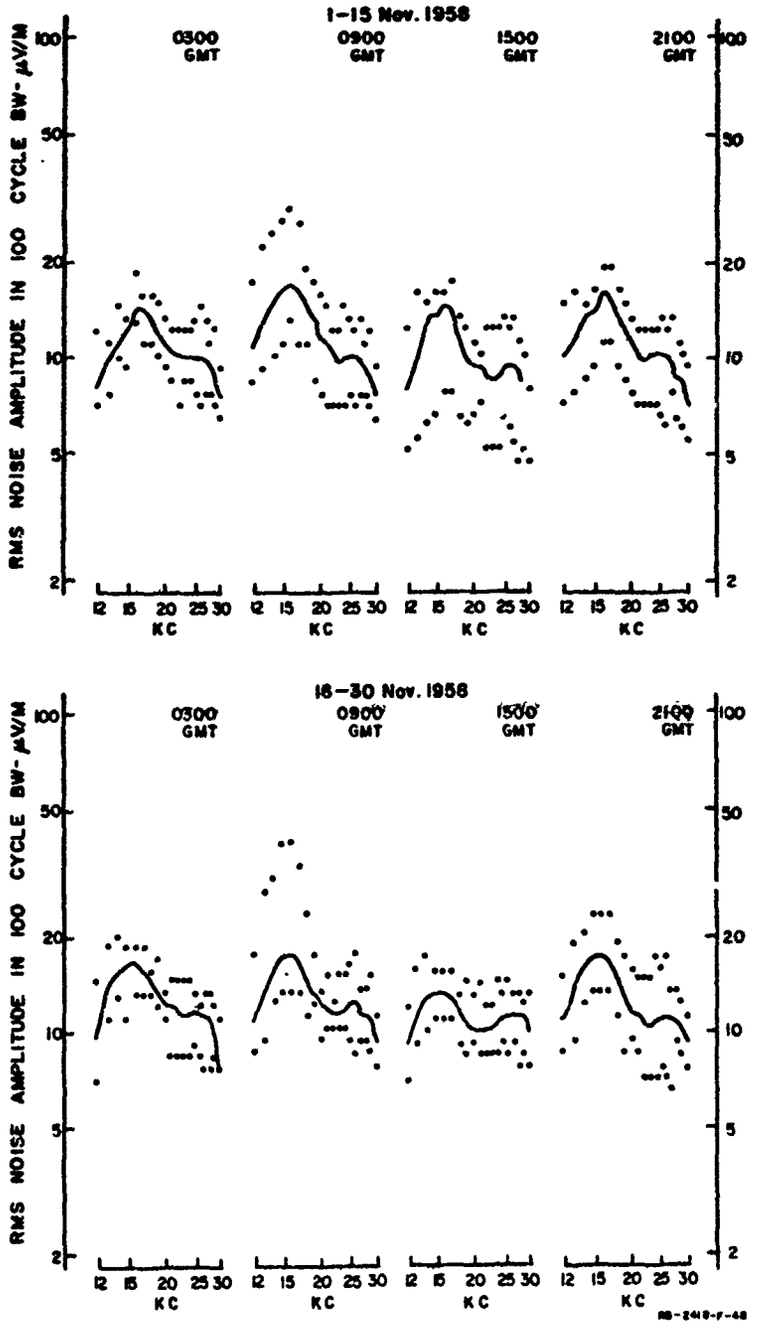

FIG. F-9

RMS NOISE SPECTRUM AT THULE, GREENLAND — NOVEMBER 1958

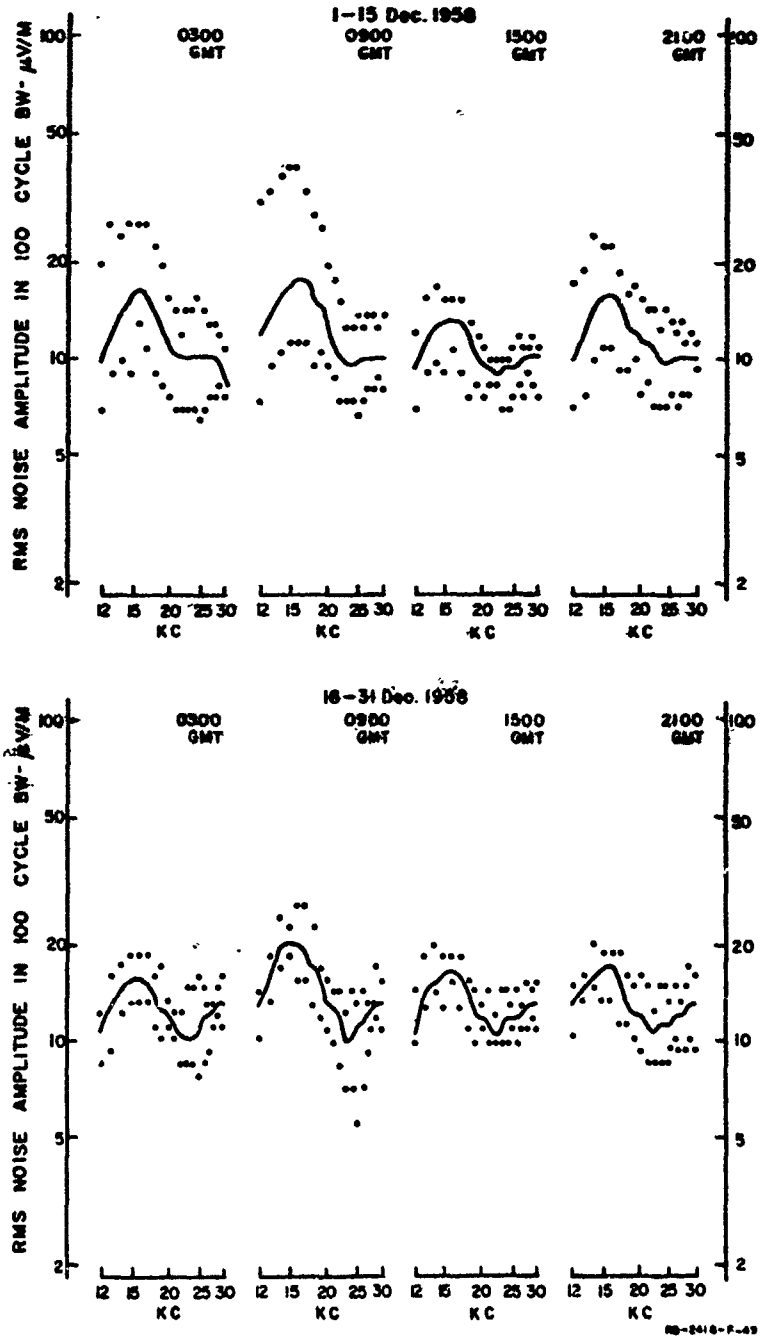

FIG. F-10

RMS NOISE SPECTRUM AT THULE, GREENLAND — DECEMBER 1958

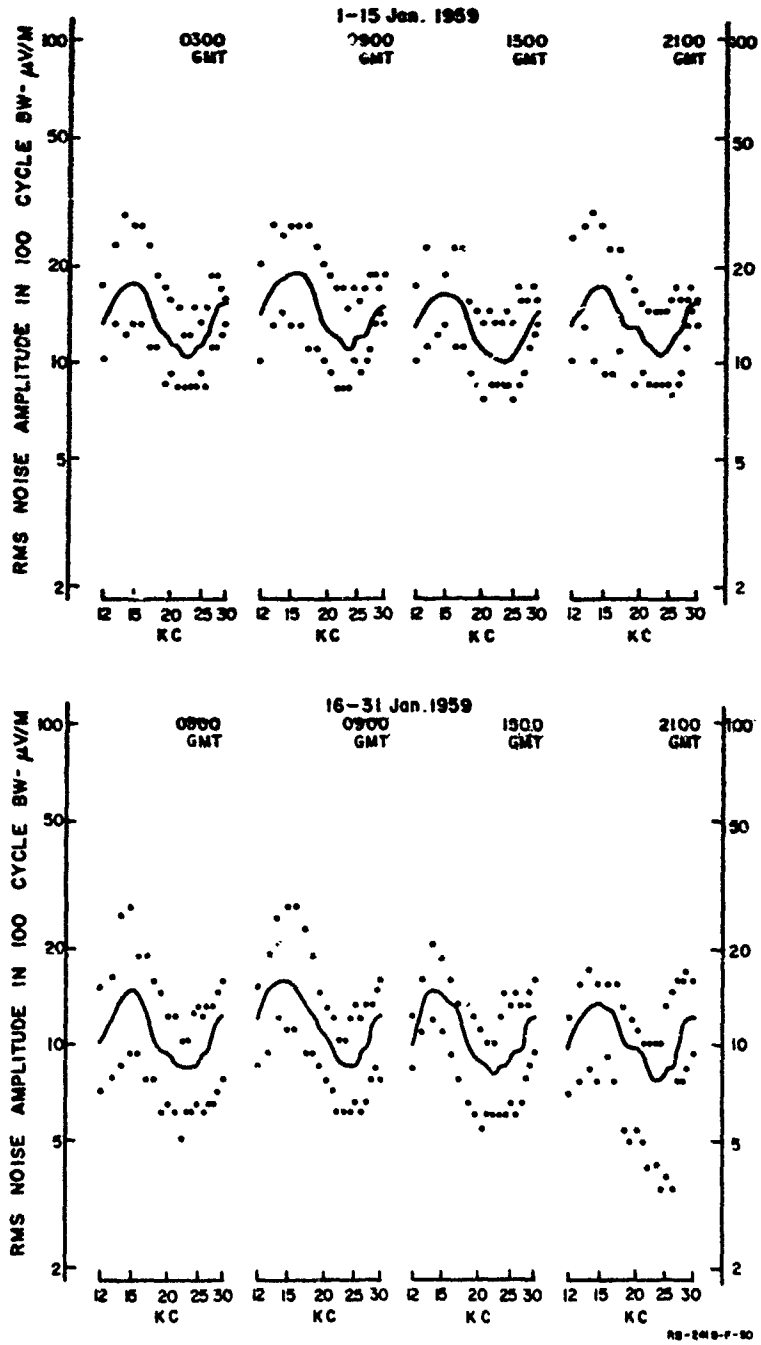

FIG. F-11

RMS NOISE SPECTRUM AT THULE, GREENLAND—JANUARY 1959

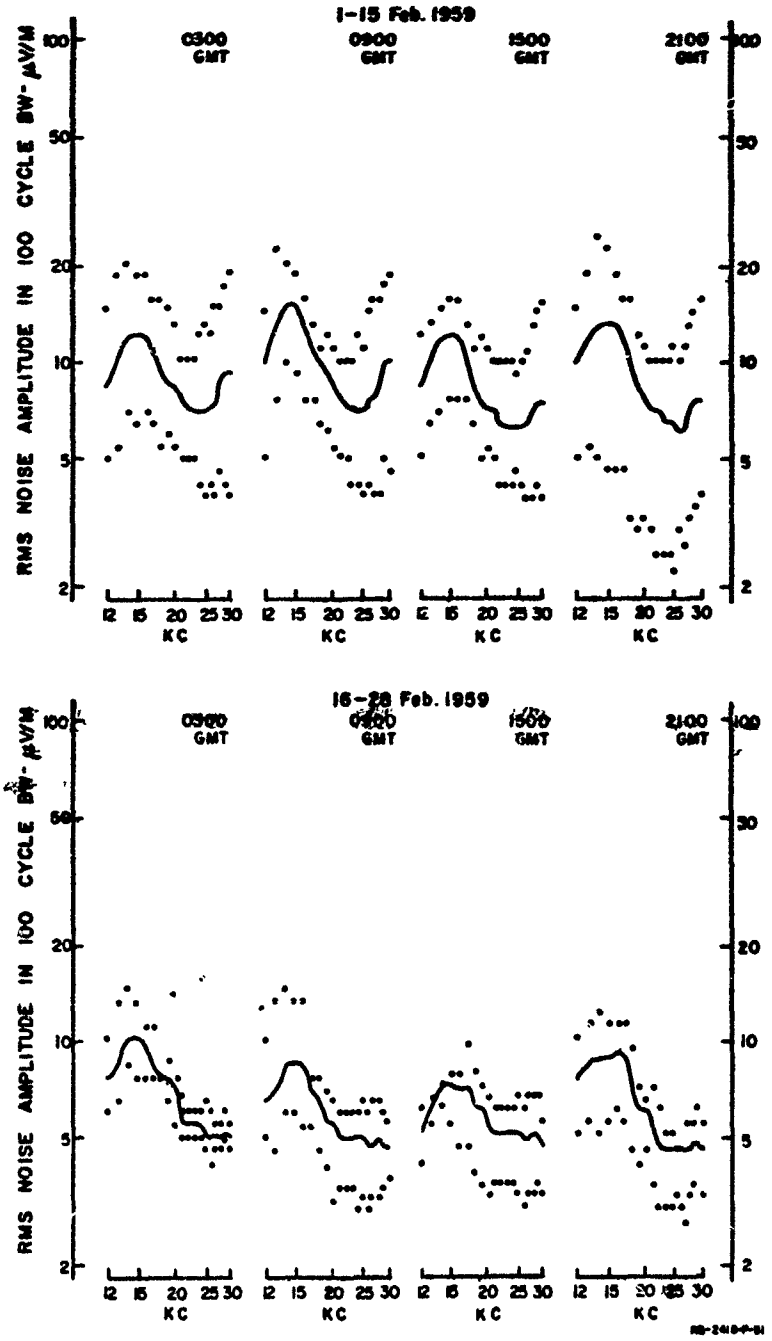

FIG. F-12

RMS NOISE SPECTRUM AT THULE, GREENLAND—FEBRUARY 1959

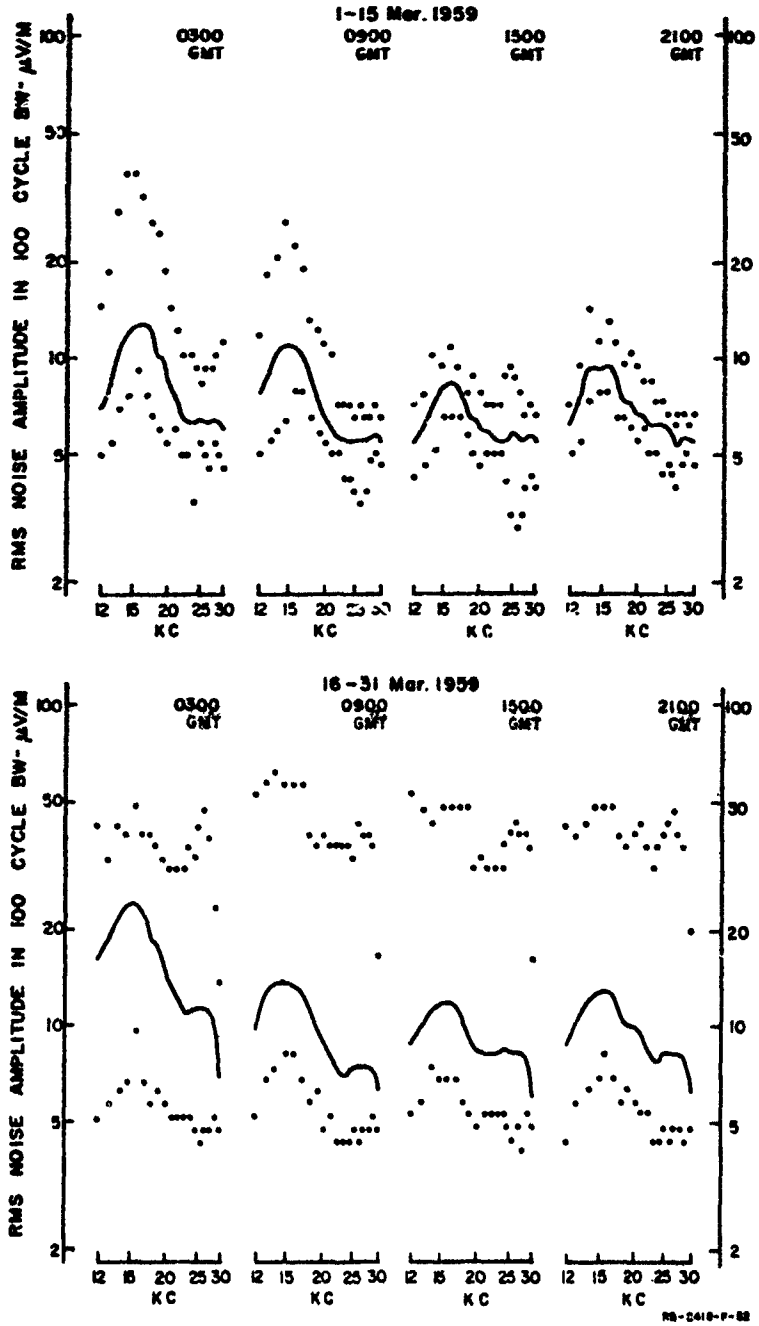

FIG. F-13

RMS NOISE SPECTRUM AT THULE, GREENLAND—MARCH 1959

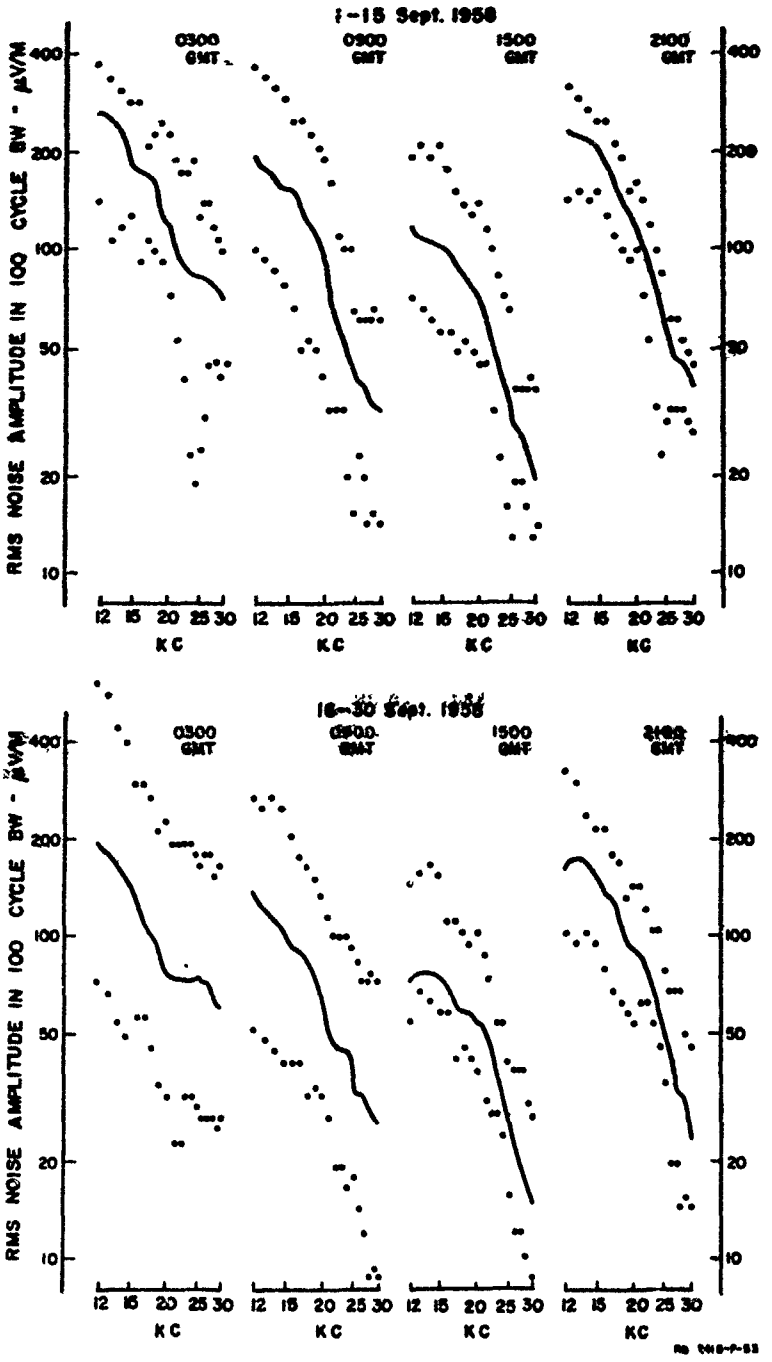

FIG. F-14

RMS NOISE SPECTRUM AT ST. JOHNS, NEWFOUNDLAND—SEPTEMBER 1958

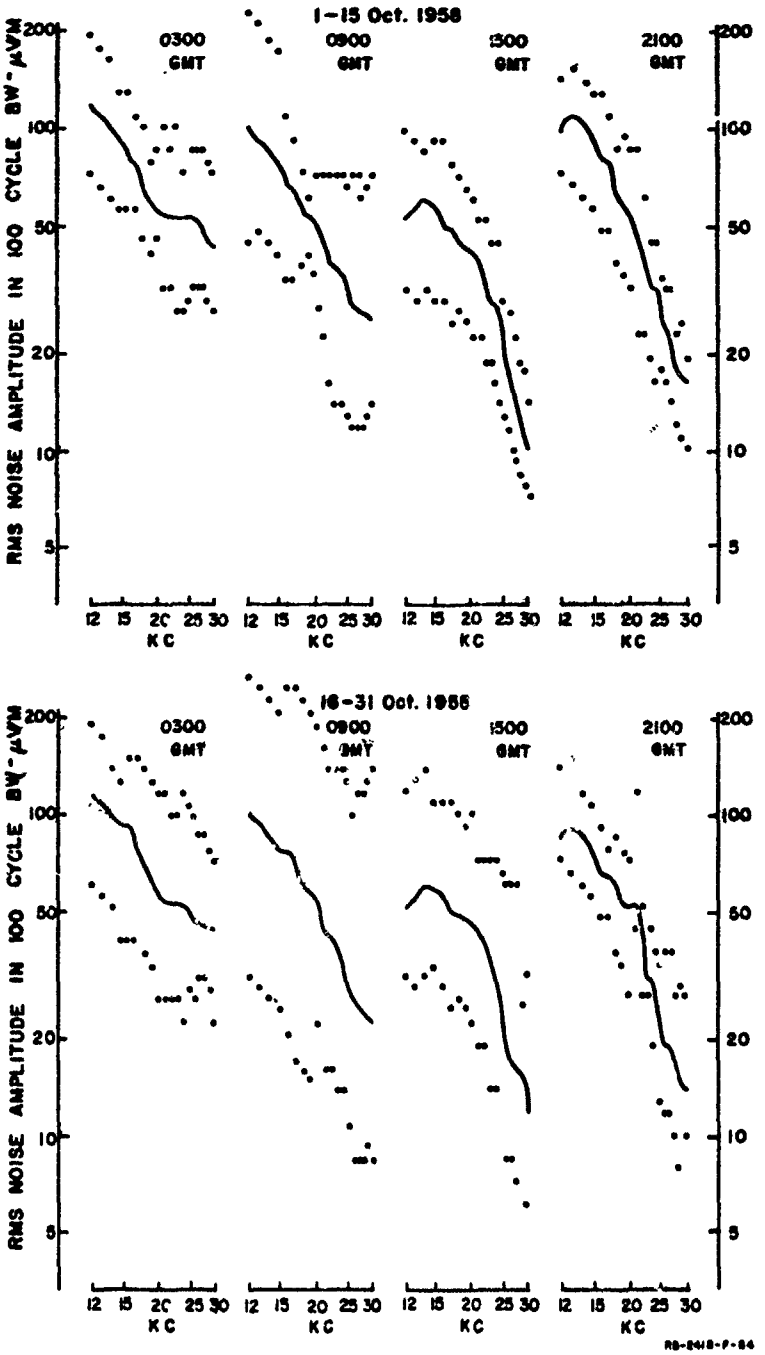

FIG. F-15

RMS NOISE SPECTRUM AT ST. JOHNS, NEWFOUNDLAND — OCTOBER 1958

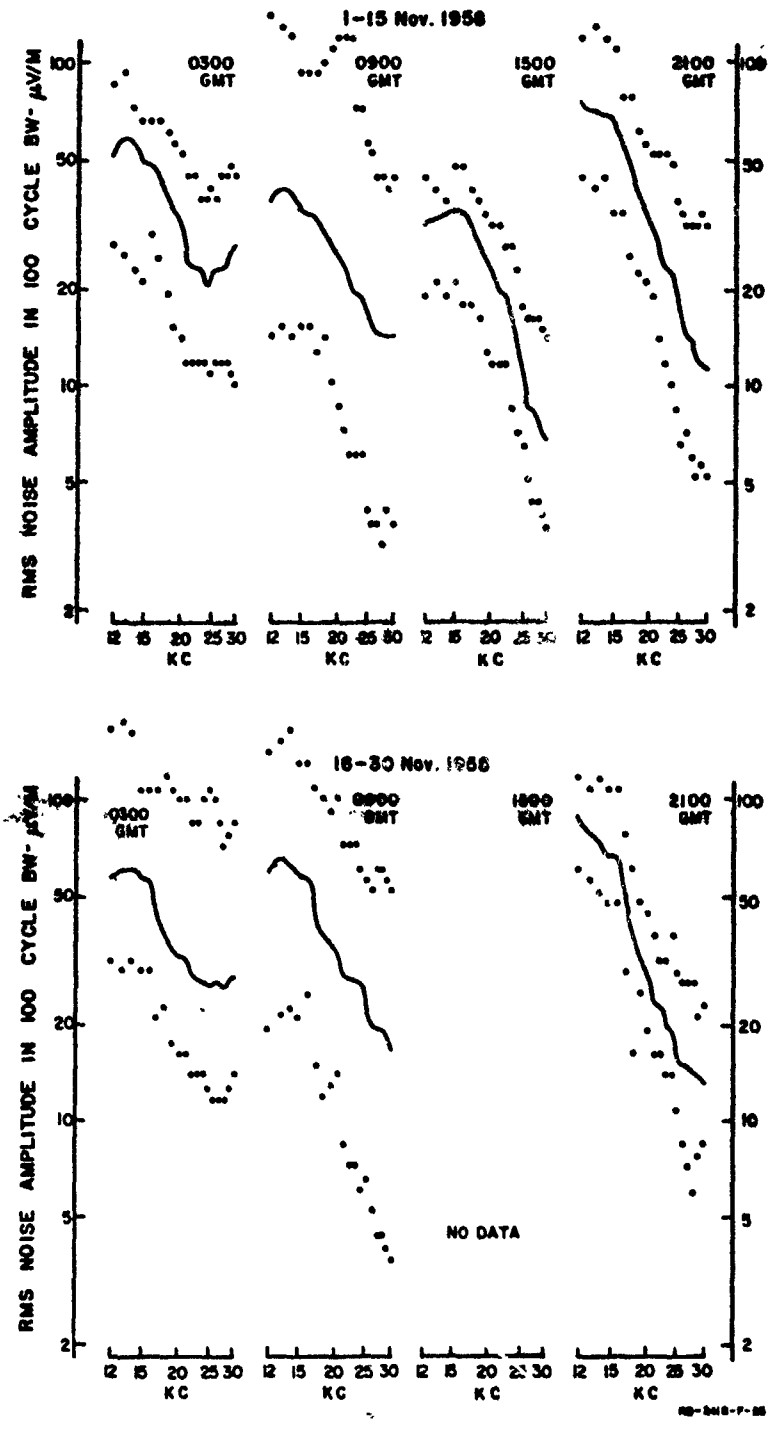

FIG. F-16

RMS NOISE SPECTRUM AT ST. JOHNS, NEWFOUNDLAND—NOVEMBER 1958

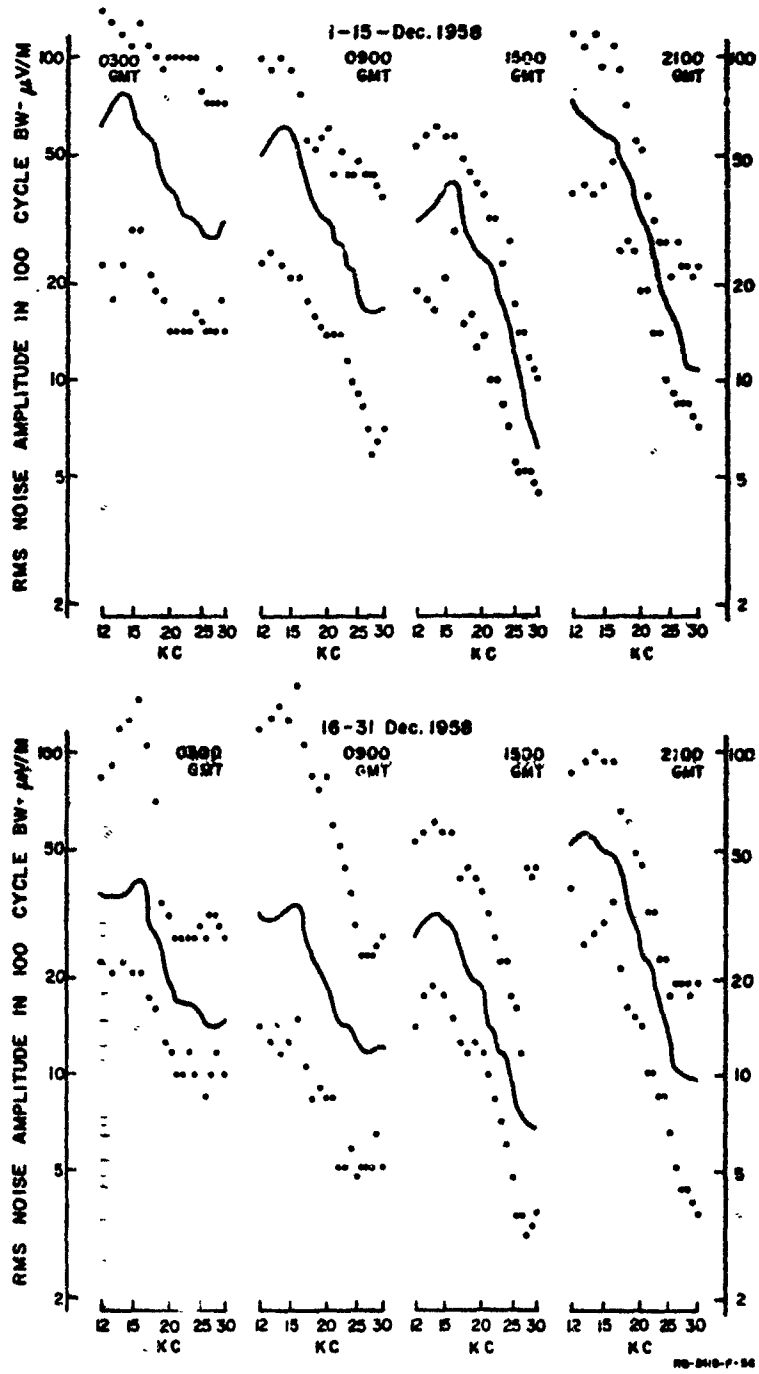

FIG. F-17

RMS NOISE SPECTRUM AT ST. JOHNS, NEWFOUNDLAND — DECEMBER 1958

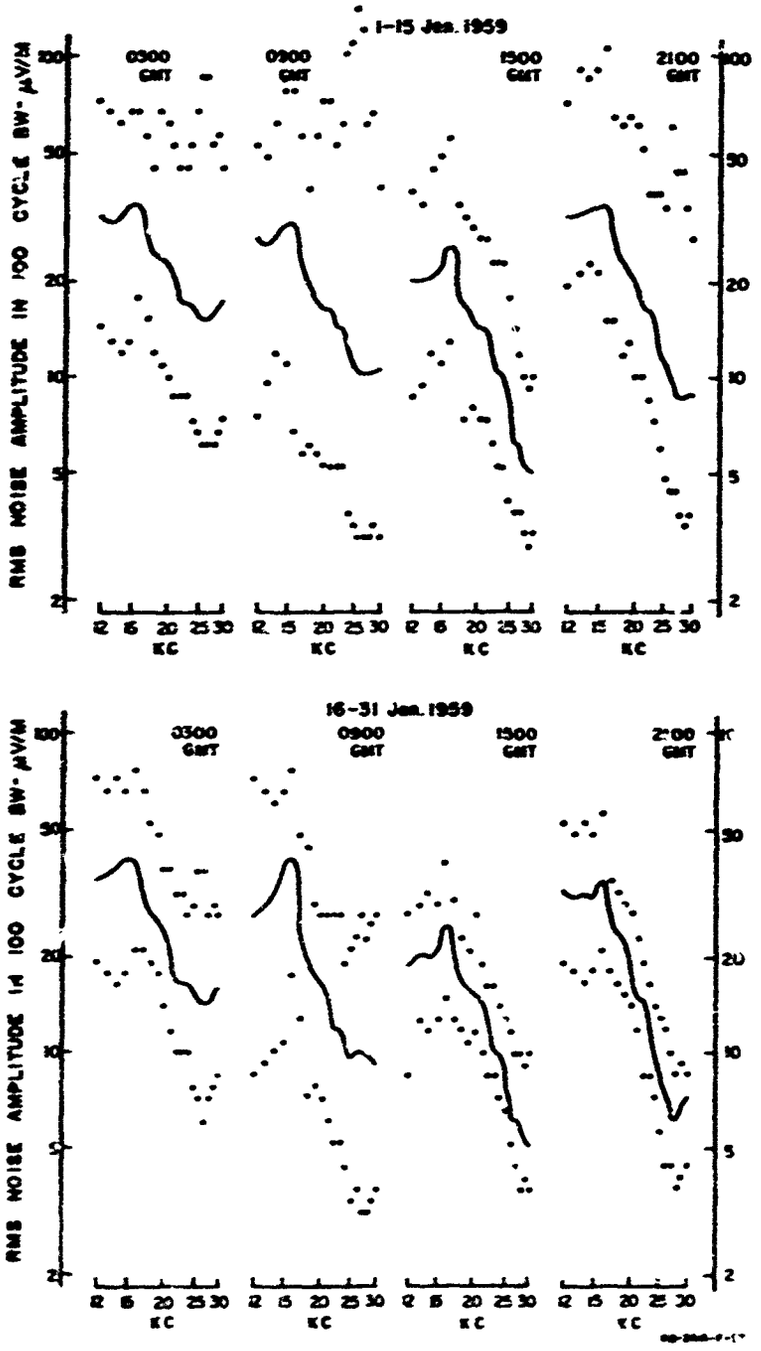

FIG. F-18

RMS NOISE SPECTRUM AT ST. JOHN'S, NEWFOUNDLAND—JANUARY 1959

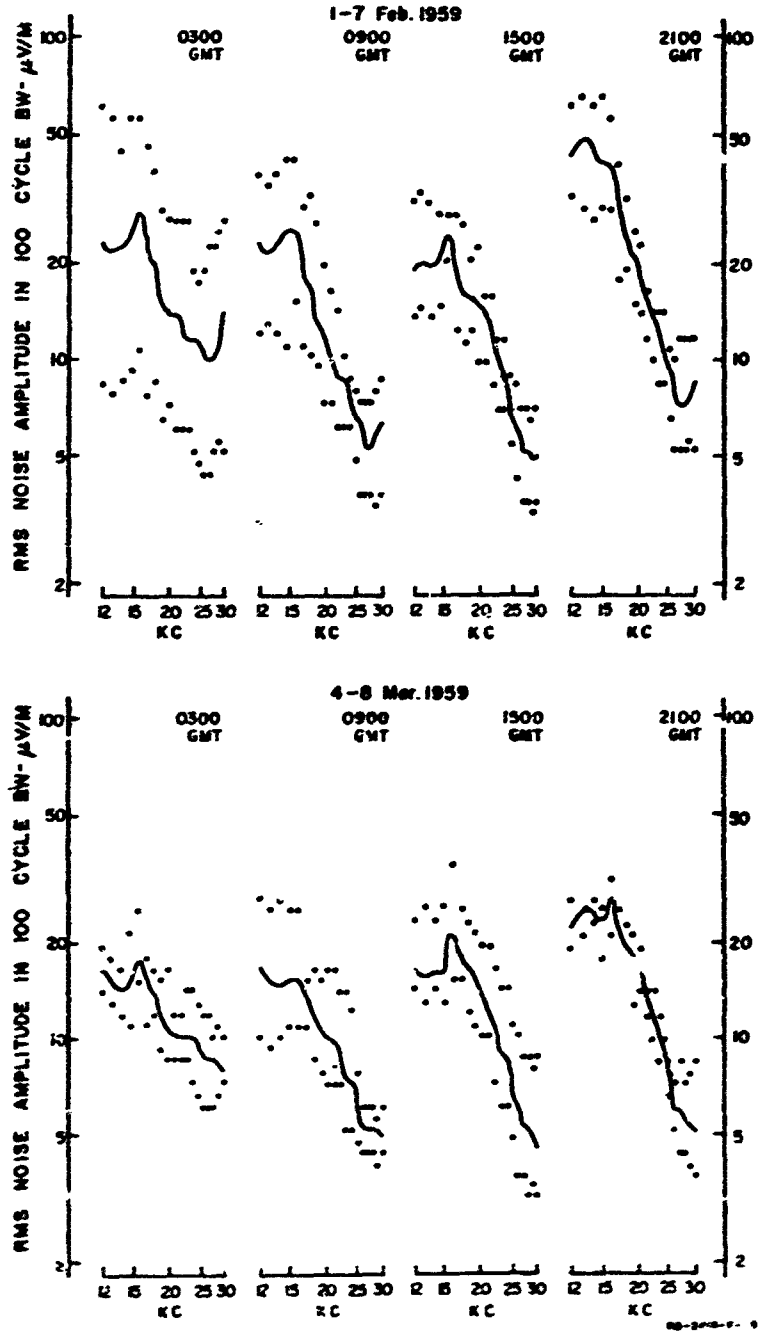

FIG. F-19

RMS NOISE SPECTRUM AT ST. JOHN'S, NEWFOUNDLAND
FEBRUARY TO MARCH 1959

Appendix G

INTEGRATED DF

INTEGRATED DF

The SRI Sferic Monitoring System was used to obtain direction-of-arrival data during the periods between the waveform-and-DF-film runs indicated in Appendix B. Direction-of-arrival information for individual sferics exceeding fixed field strengths was recorded on single frames of 35mm film. The film was automatically advanced in intervals of 10 minutes except on rare occasions when a one-hour interval was used to indicate directions with minimum activity. Each film frame indicates the directions at which sferic activity was observed for one specific time interval. These data are called integrated DF.

Figures G-1 through G-12, show integrated DF records from Fairbanks, Alaska, from Thule, Greenland, and from St. Johns, Newfoundland, for September 1958, November 1958, January 1959, and March 1959. The time interval for each frame is 10 minutes and the system trigger threshold is indicated on each figure. In each figure one 10-minute sample is shown for each GMT hour and the approximate GMT time is shown below each frame. The solid line under the time indicates local night, and the dashed line indicates local twilight.

The integrated DF data presented in this appendix are less than 0.6 percent of all data of this type that were collected. The data presented, however, were selected to show the typical average activity for each month for each station and, thus, represents more than 0.6 percent of the information available for integrated DF film.

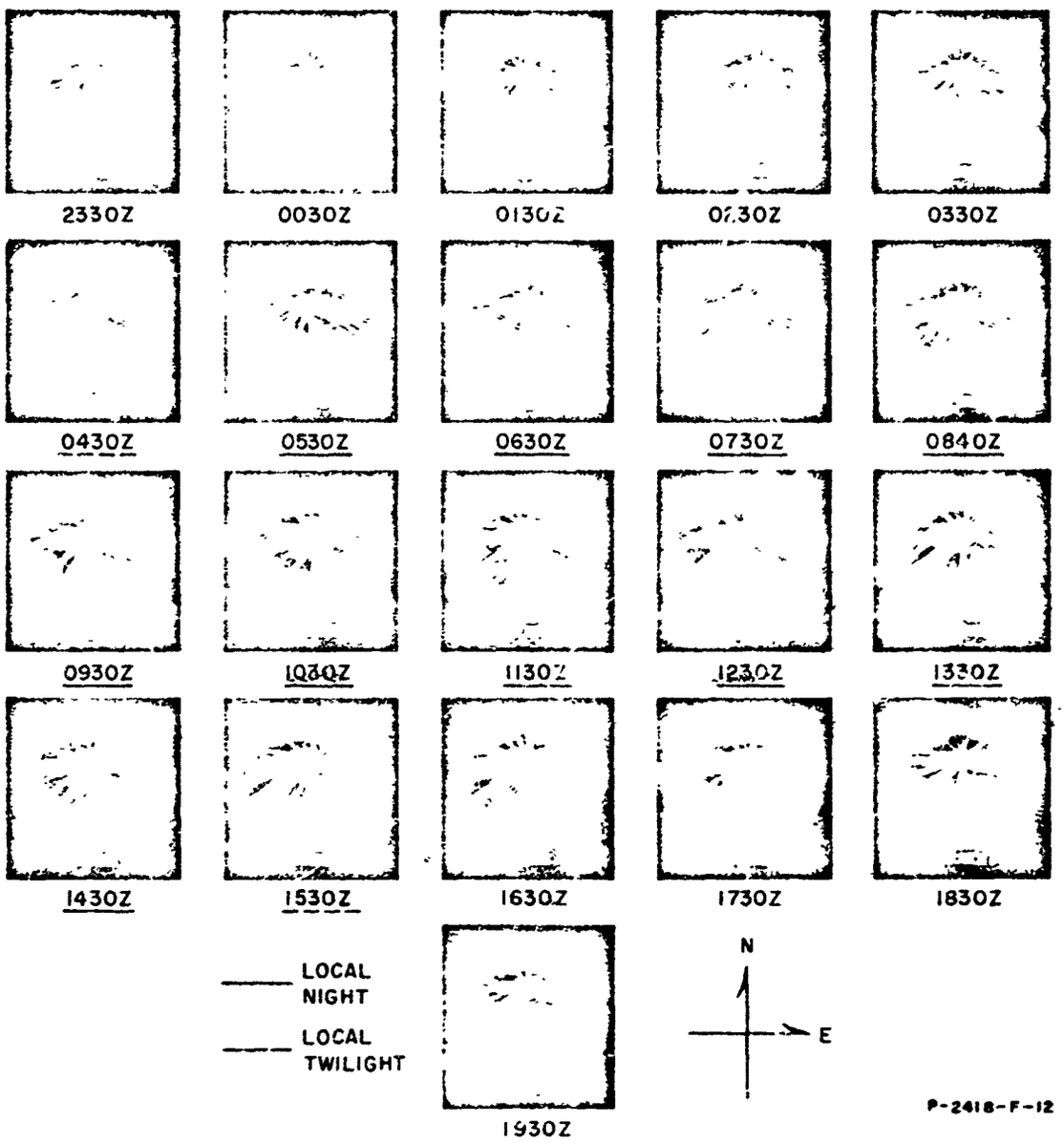

FIG. G-1

TEN MINUTES INTEGRATED DF AT FAIRBANKS, ALASKA — 25-26 SEPTEMBER 1958

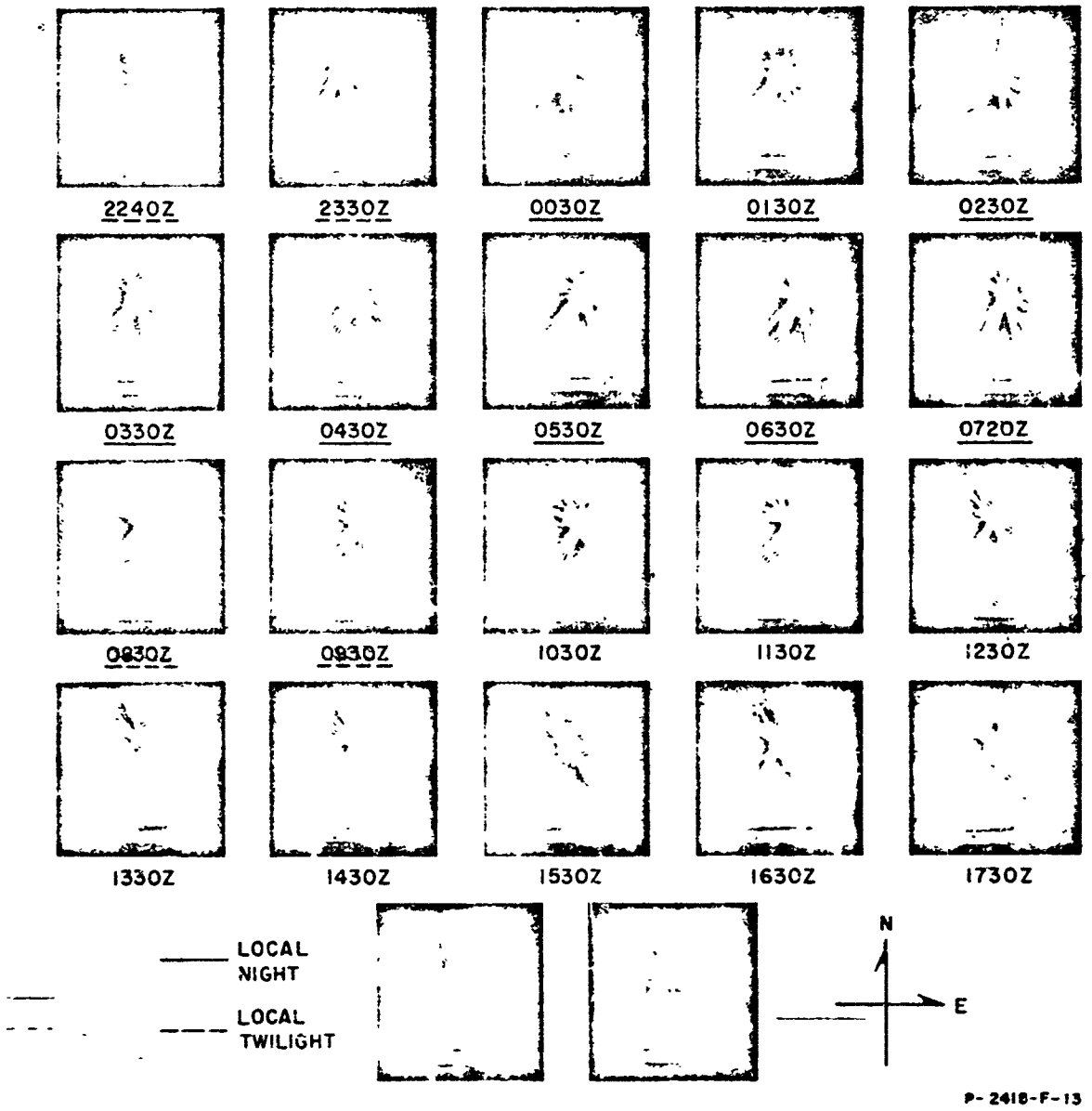

FIG. G-2

TEN-MINUTES INTEGRATED DF AT THULE, GREENLAND—25-26 SEPTEMBER 1958—10 mv/m

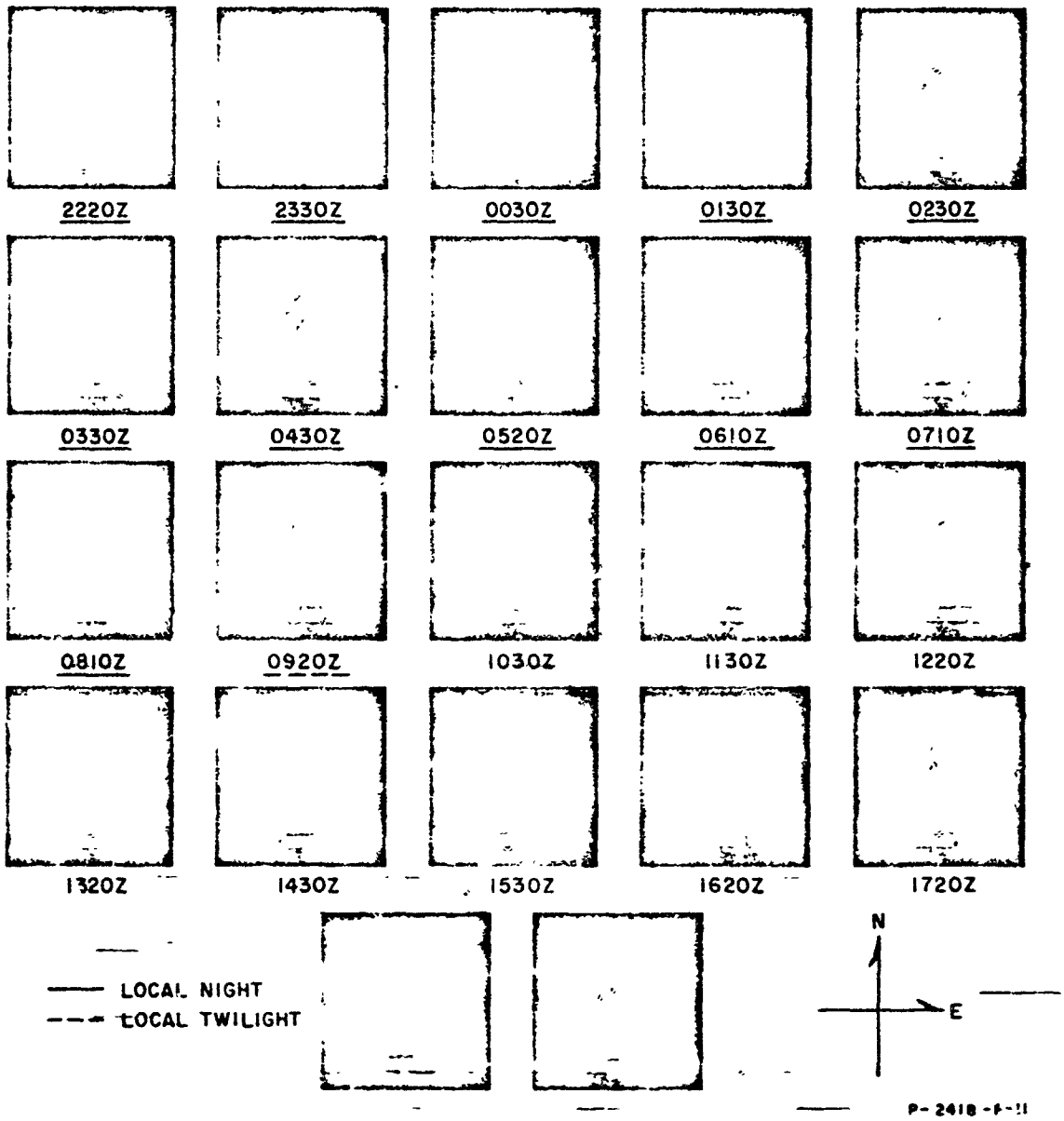

FIG. G-3

TEN MINUTES INTEGRATED DF AT ST. JOHNS, NEWFOUNDLAND—25-26 SEPTEMBER 1958—100 mv/m

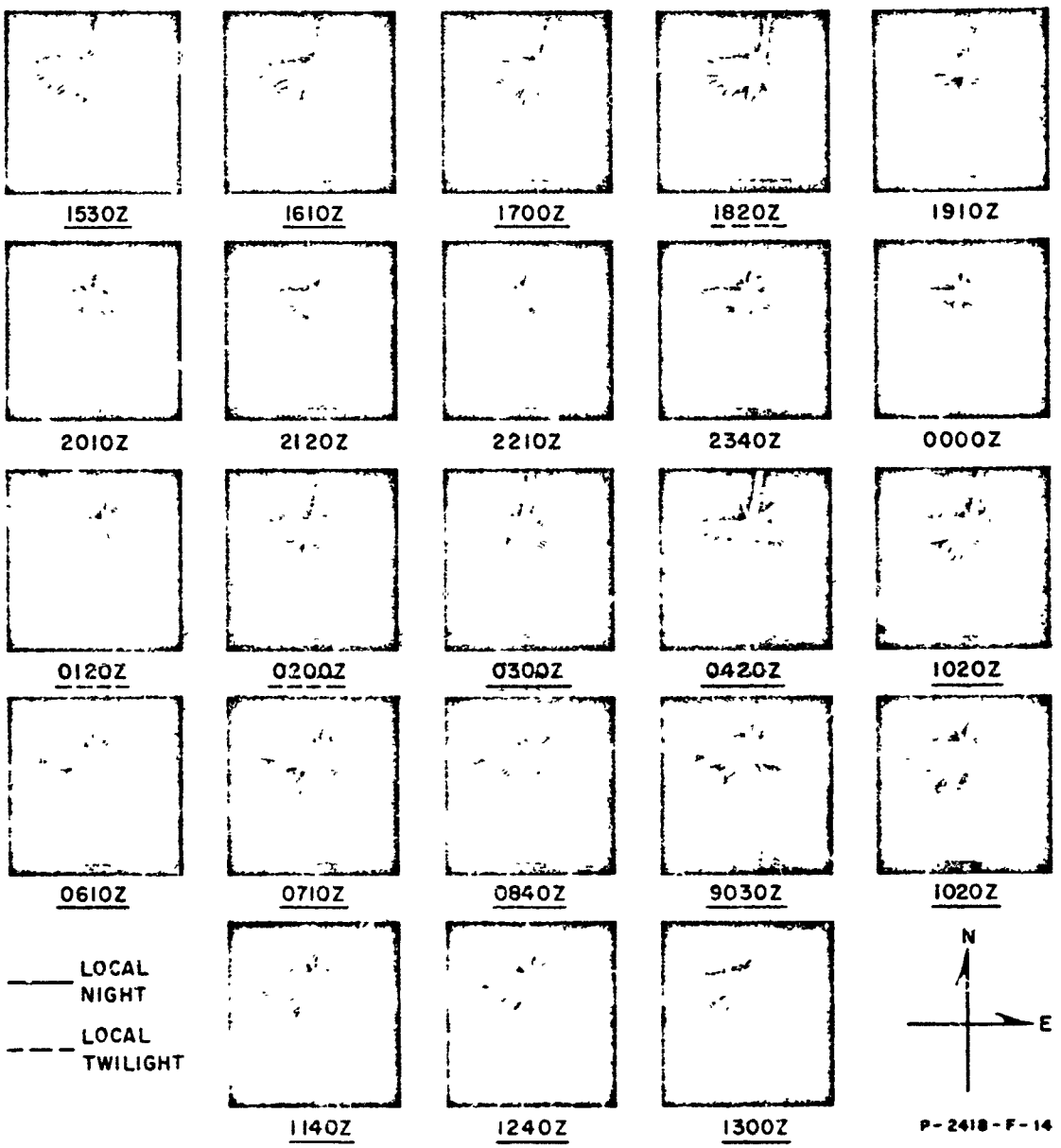

FIG. G-4

TEN MINUTES INTEGRATED DF AT FAIRBANKS, ALASKA—13-14 NOVEMBER 1958—10 mv/m

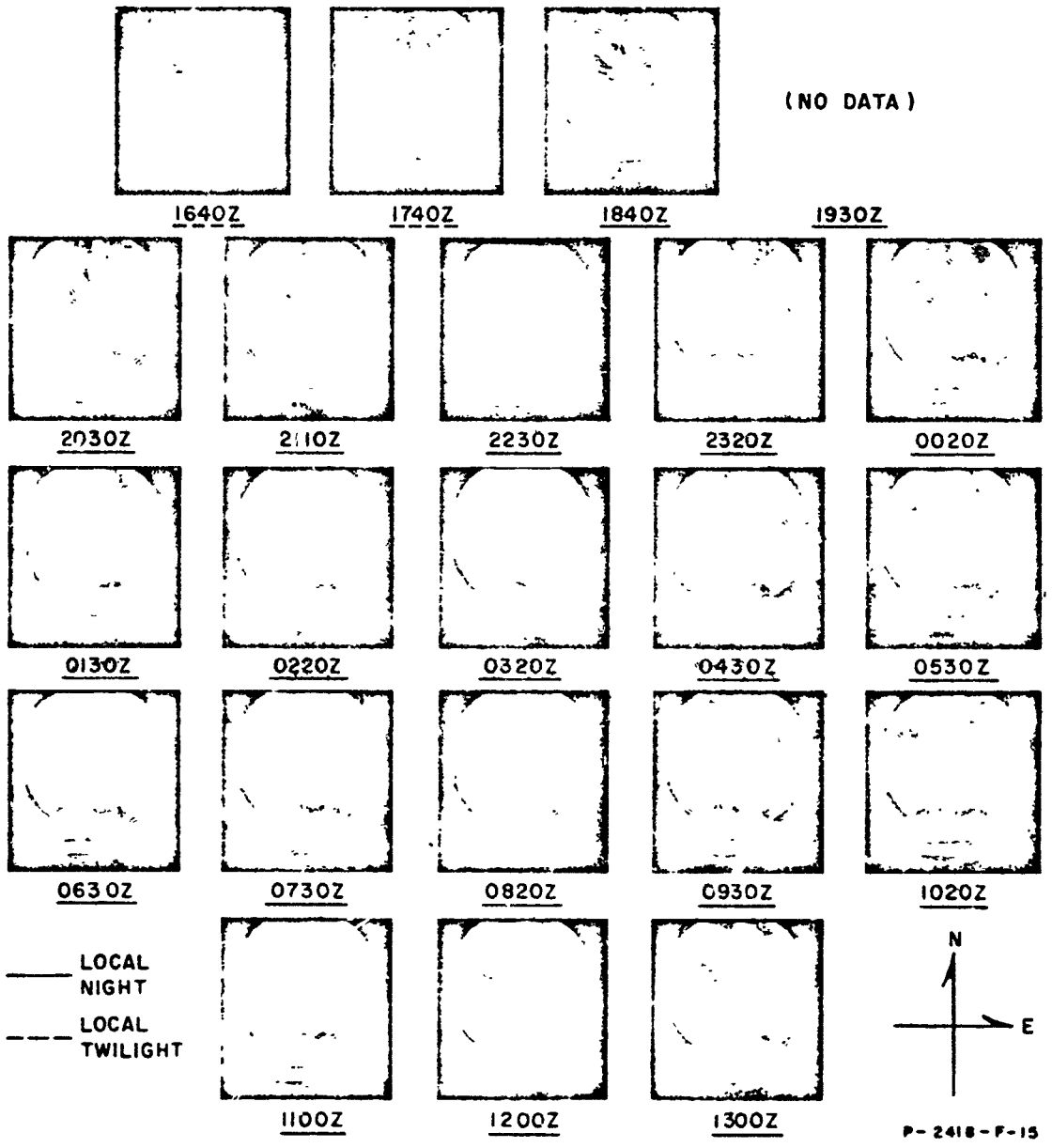

FIG. G-5

TEN MINUTES INTEGRATED DF AT THULE, GREENLAND — 13-14 NOVEMBER 1958 — 10 mv/m

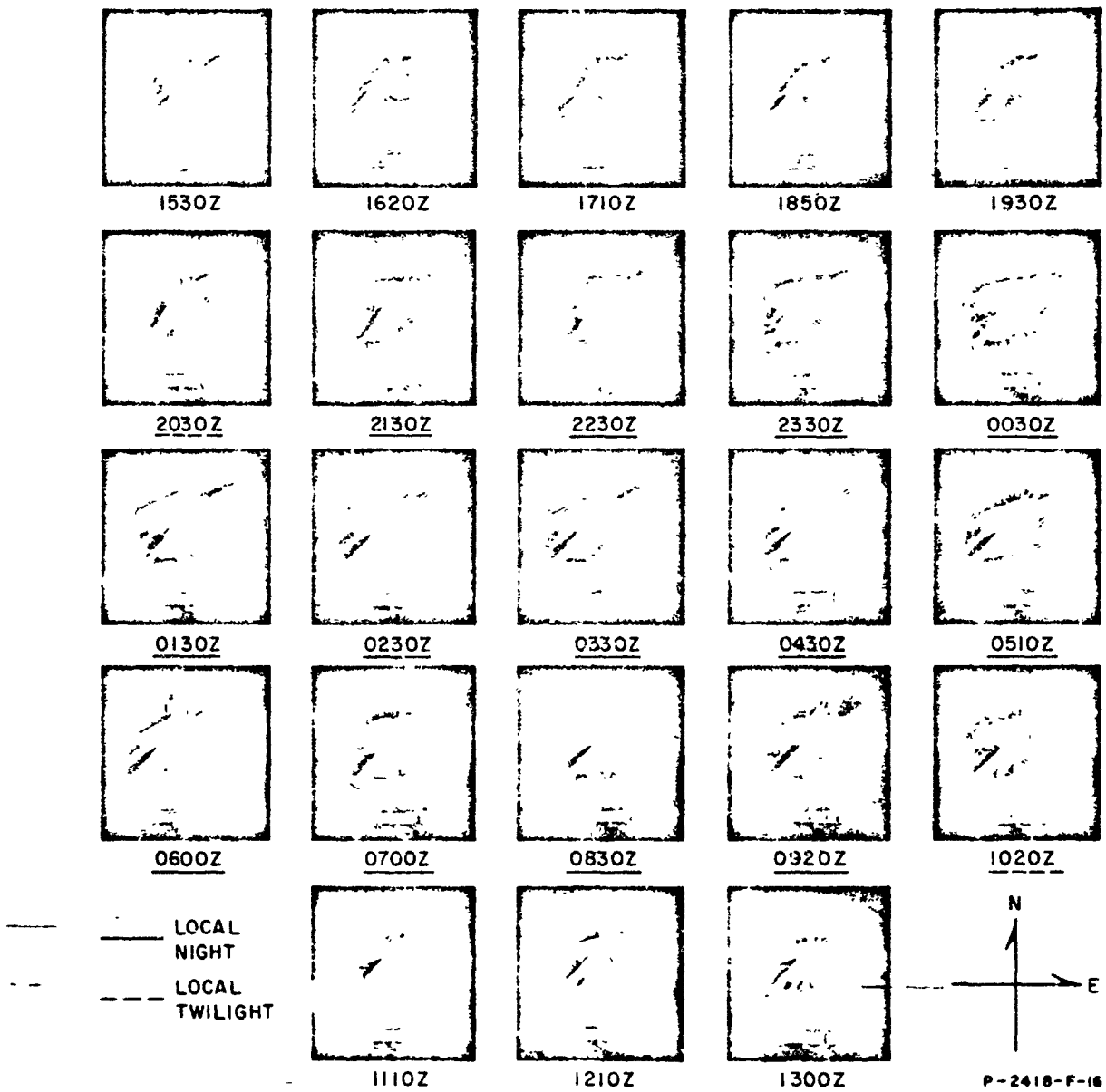

FIG. G-6

TEN MINUTES INTEGRATED DF AT ST. JOHNS, NEWFOUNDLAND — 13-14 NOVEMBER 1958 — 100 mv/m

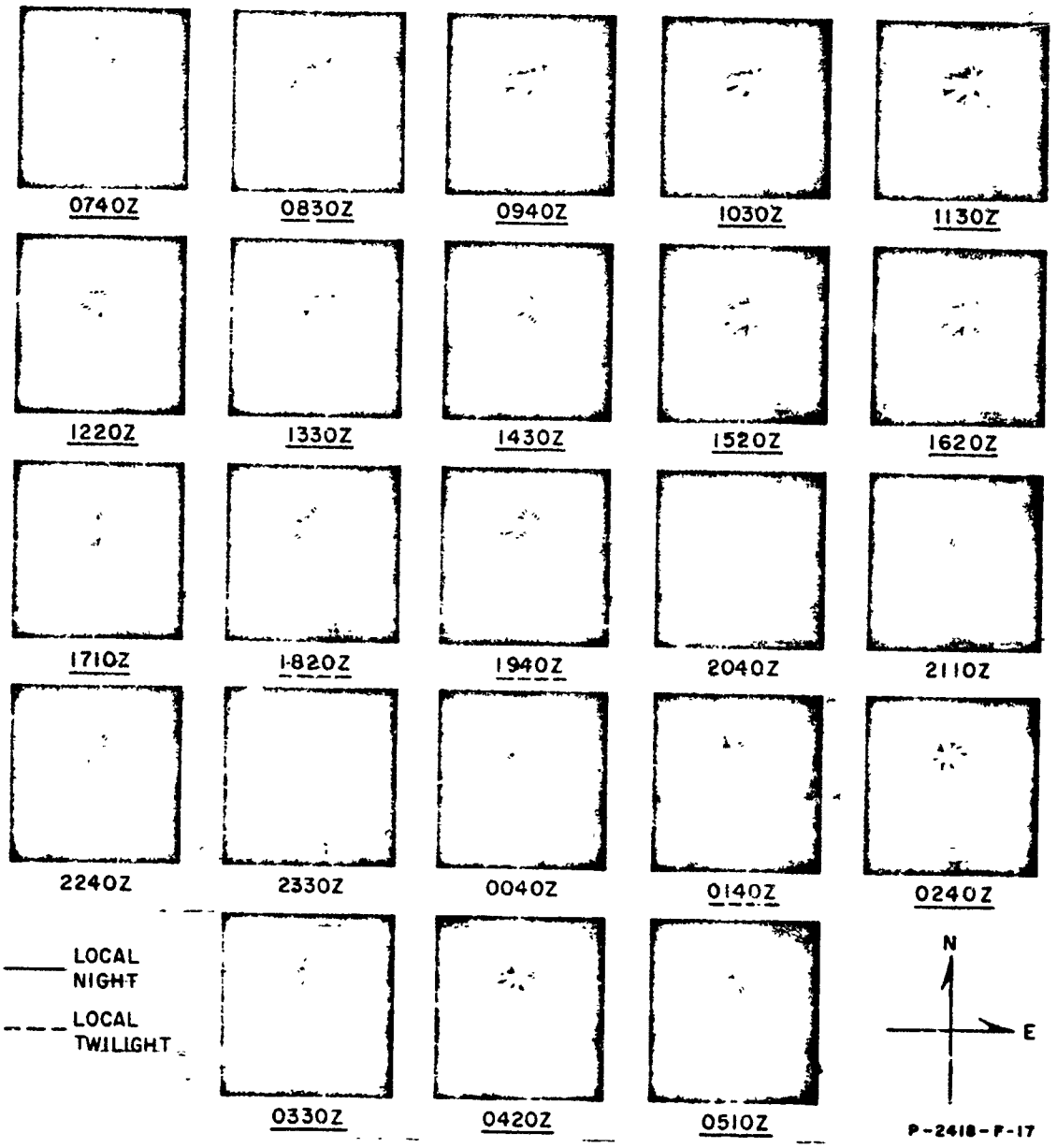

FIG. G-7

TEN MINUTES INTEGRATED DF AT FAIRBANKS, ALASKA—13-14 JANUARY 1959—10 mv/m

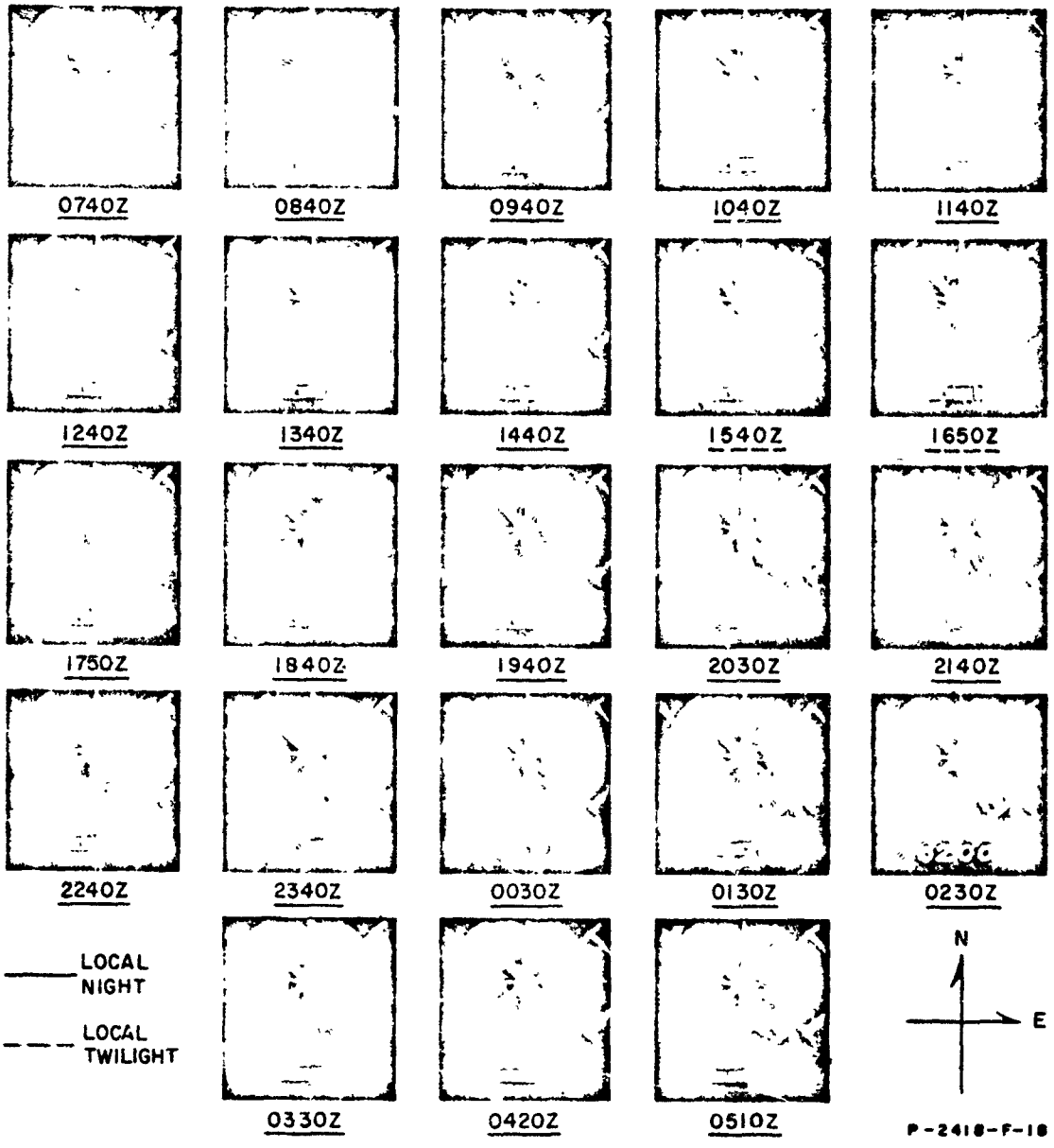

FIG. G-8

TEN MINUTES INTEGRATED DF AT THULE, GREENLAND—13-14 JANUARY 1959—10 mv/m

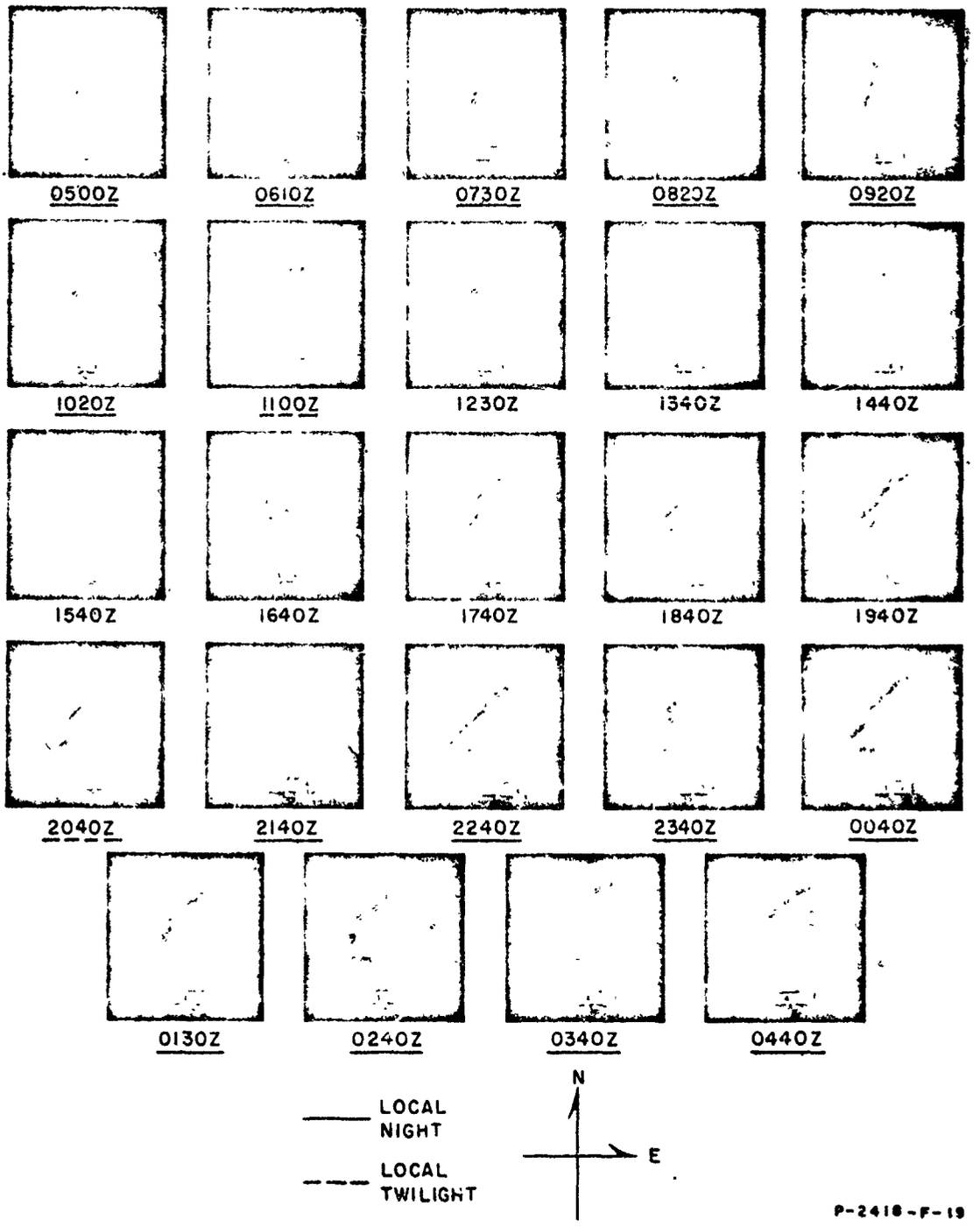

FIG. G-9

TEN MINUTES INTEGRATED DF AT ST. JOHNS, NEWFOUNDLAND—13-14 JANUARY 1959—100 mv/m

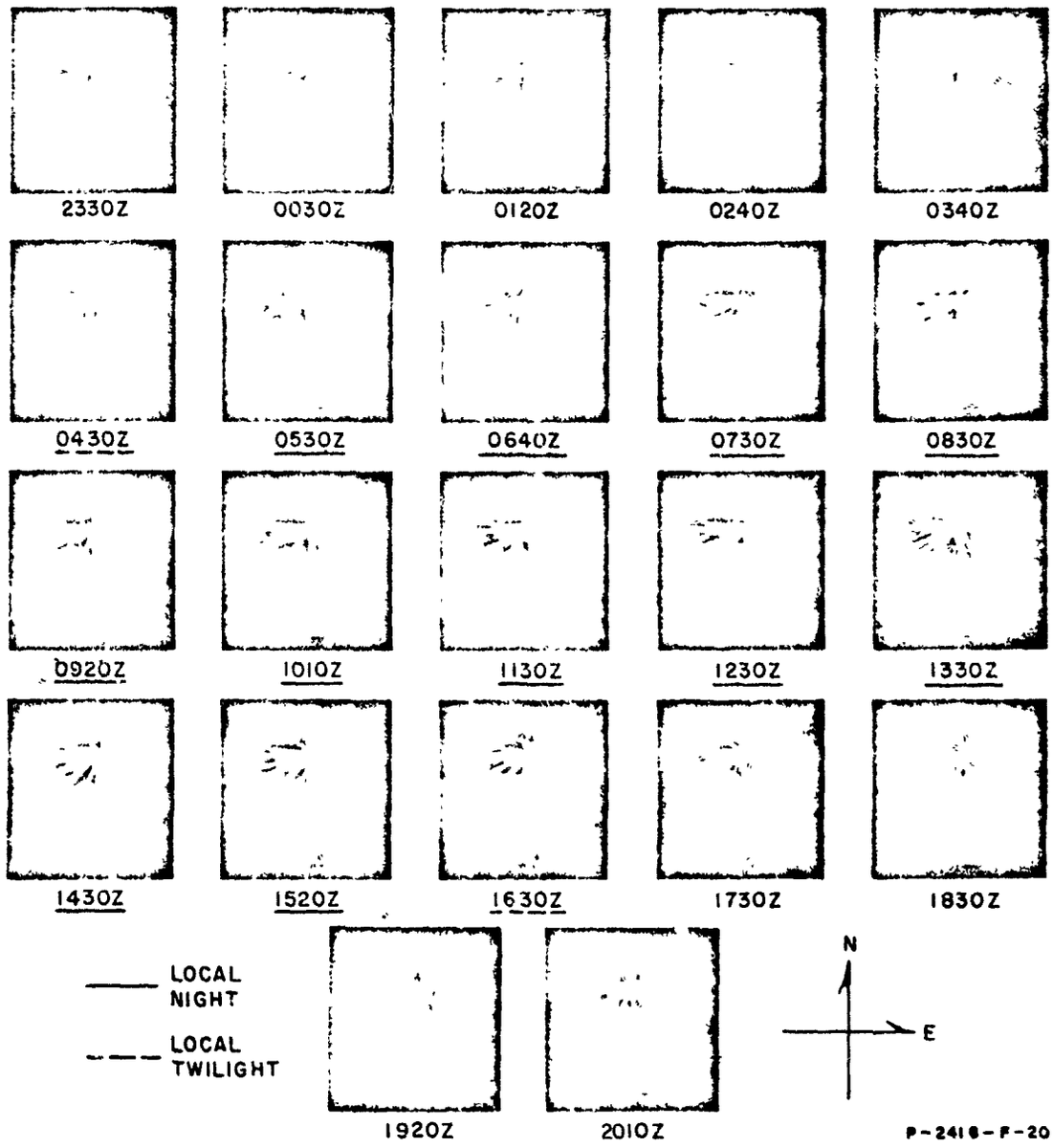

FIG. G-10

TEN MINUTES INTEGRATED DF AT FAIRBANKS, ALASKA—14-15 MARCH 1959—10 mv/m

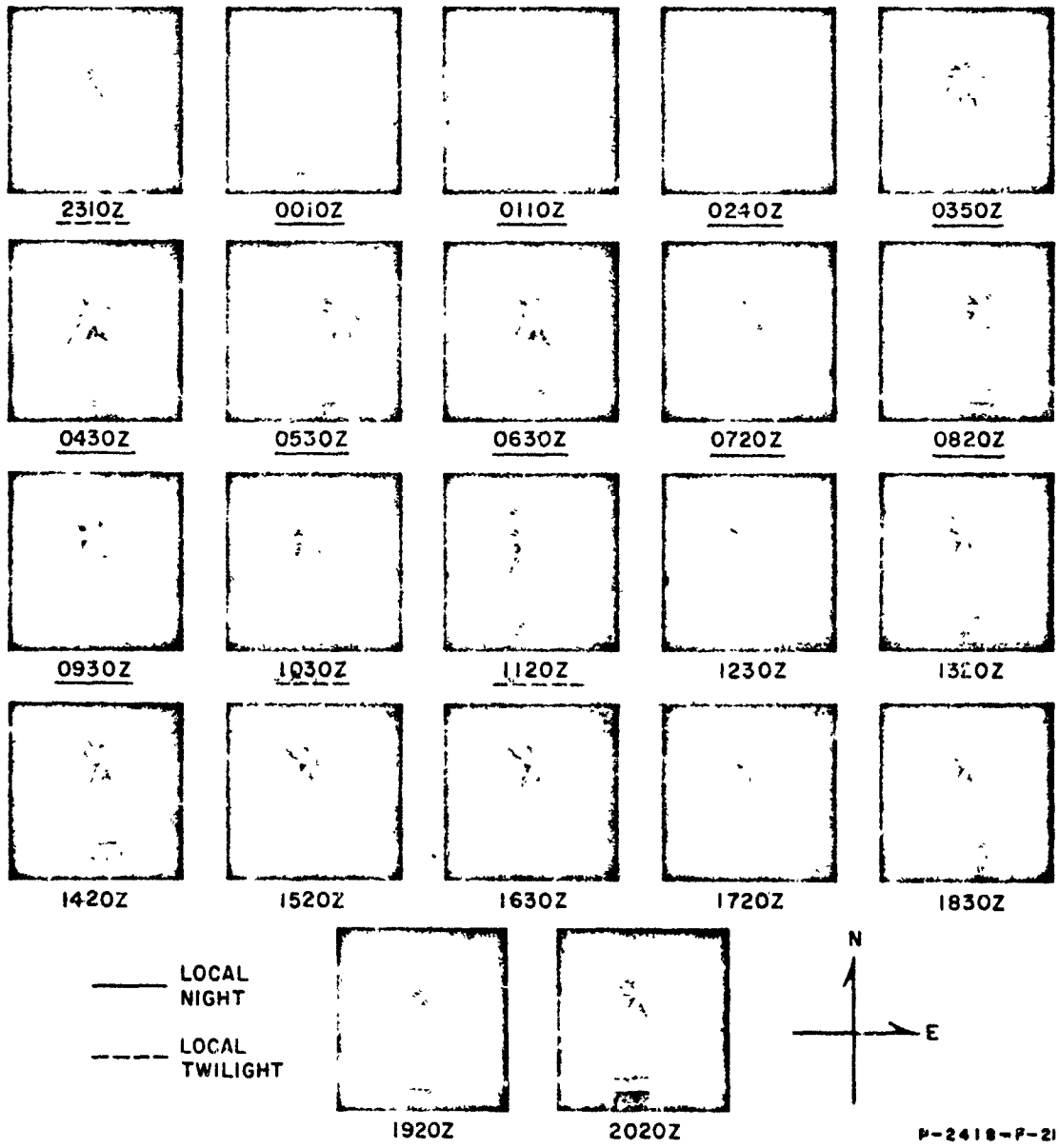

FIG. G-11

TEN MINUTES INTEGRATED DF AT THULE, GREENLAND—14-15 MARCH 1959—30 mv/m

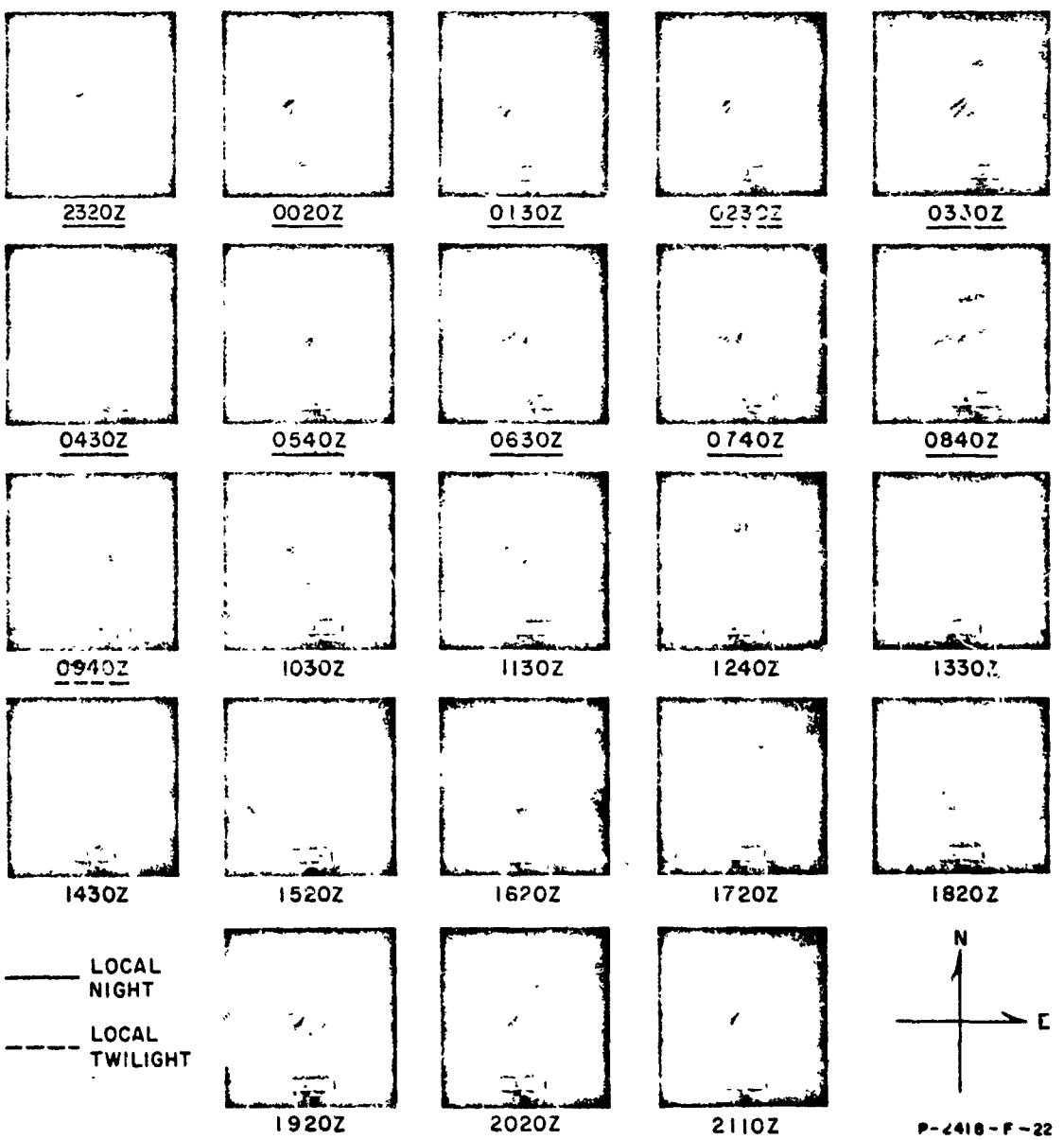

FIG. G-12

TEN MINUTES INTEGRATED DF AT ST. JOHNS, NEWFOUNDLAND—14-15 MARCH 1959—10 mv/m

Appendix H

DIRECTION-OF-ARRIVAL ACCURACY

DIRECTION-OF-ARRIVAL ACCURACY

The direction of arrival of sferics was measured using crossed loop antennas which are sensitive to cross polarization of the received wavefront.* The magnitude of the error caused by cross polarization becomes more apparent when redundant source location data, in the form of a third direction-of-arrival station, are utilized. In general, sferic source locations, when determined from a three-station direction-of-arrival net. are a triangular area and not a fixed point. Assuming the error to be normally distributed, the actual source location has a 90 percent probability of being within this fix triangle.

Direction-of-arrival error can be divided into error due to (1) the mechanics of the system (2) anomalies adjacent to the receiving station; i.e., hills, buried pipes, power lines, etc., and (3) propagation distortion in the wavefront. System error due to antenna alignment, calibration and film reading was approximately ±1.5 degrees. Source location accuracy can be measured by recording the angle required at each station to "close" the fix triangle assuming the direction-of-arrival from the other two stations to be correct. This closing angle indicates the magnitude of the fix accuracy and is a function of the combined error from all three stations. Average closing angle and the 10 and 90 percent points on the distributions for typical areas in the Northern Hemisphere are listed in Table H-1. In the Gulf of Mexico area, for example, the average fix triangle includes the Gulf of Mexico east and west and extends from Chicago to the Pacific Ocean just south of Central America.

As stated before, error in terms of closing angle required direction-of-arrival from three monitoring stations. Less than 500 of the sferics that were recorded and analyzed could be used to determine direction-of-arrival accuracy by closing angle. Thus, with these limited data, diurnal and seasonal variations were not discernible. In addition, site errors (local anomalies) using sferics could not be determined since the sferic activity recorded was limited to three or four geographic locations.

In an effort to better understand the DF errors indicated by recording sferics at three Arctic monitoring stations, direction-of-arrival data on various keyed-CW VLF stations were obtained by modifying the sferic monitoring system to have a narrow tunable bandwidth--approximately 200 cycles at the 3-db-down points. The results of these measurements are listed in Table H-2. Diurnal variation based upon a single day's data was detectable; however, diurnal variation was meaningless when all data from various days were used.

---

*The effect of skywave contamination was minimized by utilizing only the first 300 microseconds of the received signal for direction-of-arrival.

Table H-1

CLOSING ANGLE

APPROXIMATE AREA		FAIRBANKS	THULE	ST. JOHNS
1. Gulf of Mexico	10%	0°	0°	0°
	Ave.	+20°	-12°	+28°
	90%	+40°	-25°	+55°
2. North Atlantic	10%	+ 9°	- 9°	+38°
	Ave.	- 2°	+ 2°	- 8°
	90%	-13°	+13°	-60°
3. Europe	10%	- 5°	+ 4°	-20°
	Ave.	+ 4°	- 4°	+15°
	90%	+13°	-13°	+50°
4. China Sea	Ave.	7°	- 5°	+12°

Table H-2

VLF STATION DF DATA

RECEIVING STATION	VLF STATION	TRUE BEARING	RECORDING BEARING RANGE
Fairbanks, Alaska	NLK-18.6 kc Washington	129°	108° to 154°
	NPM-16.6 kc Honolulu	193°	182° to 202°
	17.5 kc Yosami, Japan	274°	265° to 280°
Thule, Greenland	GBR 16.0 kc England	95°	78° to 92°
	NSS 15.5 kc Annapolis	191°	180° to 198°
	NLK 18.6 kc Washington	245°	243° to 259°
	NPM 16.6 kc Honolulu	272°	268° to 285°
	17.5 kc Yosami, Japan	337°	322° to 340°
St. Johns, Newfoundland	GBR 16.0 kc England	62°	48° to 67°
	NSS 15.5 kc Annapolis	254°	230° to 268°

In general, the direction-of-arrival data in Table H-2 indicate errors compatible with the closing angle data, and do indicate a fair amount of uncertainty as to source location when monitored at large distances with a crossed loop antenna system. While the form of data presentation used in Table H-2 does not show it, one interesting generality can be made regarding direction-of-arrival accuracy. Propagation paths aligned with the earth's magnetic field were more predictable as to repeatability of DF measurements and did tend to have less error-indicating possibly interaction between the earth's magnetic field and reflection from the ionosphere. NLK Washington and NPM Honolulu, as received at Fairbanks, Alaska, are a good example of this possible phenomenon.

Appendix I

WAVEFORM AND DF FILM IBM FORMAT

WAVEFORM AND DF FILM IBM FORMAT

Data from individual sferics as recorded on the waveform and DF film were placed upon individual IBM cards so that machine processing could be used. Data from approximately 90,000 sferics were recorded in this manner and the cards are available for additional processing. The IBM card format and data recorded were as follows:

DATA RECORDED		IBM COLUMN	REMARKS
Station Location		1	1 - Fairbanks 2 - Thule 3 - St. Johns
Film Number	Hundreds	2	Films at each station number sequentially
	Tens	3	
	Units	4	
Date (GMT) Month	Tens	5	
	Units	6	
Day	Tens	7	
	Units	8	
Year	Tens	9	
	Units	10	
Received Hour	Tens	12	Time recorded to only nearest 10 seconds. Col 18, 19, and 20 reserved for milli-seconds
Time (GMT)	Units	13	
Minutes	Tens	14	
	Units	15	
Seconds	Tens	16	
	Units	17	
Direction of Arrival in Degrees	Hundreds	24	Col 26 not used for majority of data. Y in Col 24 indicates no DF
	Tens	25	
	Units	26	
System Threshold in mv/m	10 Thousands	27	Blank columns to be read as zero
	Thousands	28	
	Hundreds	29	
	Tens	30	
	Units	31	
Center-to-Peak Amplitude in mv/m	Units	35	Col 39 Y indicates no waveform, X indicates off scale
	10 Thousands	36	
	Thousands	37	
	Hundreds	38	
	Tens	39	

(continued)

DATA RECORDED	IBM COLUMN	REMARKS
Waveform Type	40	1 - Ordinary 2 - Smooth 3 - Peaky 4 - Precusor with Sferic 5 - Precusor without Sferic 8 - Transient 9 - Quasi-CW

BIBLIOGRAPHY

Since VLF propagation and the investigation of atmospheric noise is not a new topic for study, the literature contains a wealth of data on these subjects. The following are some of the publications that were used in part to establish a background for this study.

1. F. Adcocks and C. Clarke, "The Location of Thunderstorms by Radio Direction-Finding," Proc. IEE (London) 94 (1947).

2. P. W. A. Bowe, "The Waveforms of Atmospherics and the Propagation of Very Low Frequency Radio Waves," Philosoph. Mag. 42, No. 325 (February 1951).

3. K. G. Budden, "The Propagation of a Radio-Atmospheric," Philosoph. Mag. 42 (1951).

4. K. G. Budden, "The Propagation of a Radio Atmospheric II," Philosoph. Mag. 43, No. 346 (November 1952).

5. K. E. Budden, "The Reflection of Very Low Frequency Radio Waves at the Surface of a Sharply Bounded Ionosphere with Superimposed Magnetic Field," Philosoph. Mag. 42 (1951).

6. F. W. Chapman and R. C. O. Marcario, "Propagation of Audio-Frequency Radio Waves to Great Distances," Philosoph. Mag. 177 (May 19, 1956).

7. M. W. Chiplonkav and V. N. Athavale, "Simultaneous Recordings of Atmospherics on Four Different Frequency Bands in the Low Frequency Region," Jour. Atmos. and Terrest. Phys. 13 (1958).

8. D. C. Crombie, A. H. Allan, and M. Newman, "Phase Variations of 16 kc/s Transmissions from Rugby as Received in New Zealand," Proc. IEE (London) 105, Part B, Paper 2562R (May 1958).

9. F. F. Gardner, "The Use of Atmospherics to Study the Propagation of Very Long Radio Waves," Philosoph. Mag. 41 (1950).

10. J. Harwood, "Atmospheric Radio Noise of Frequencies Between 10 kc/s and 30 kc/s," Proc. IEE (London) Part B, Paper 2619R (May 1958).

11. F. Hepburn, "Interpretation of Smooth Type Atmospheric Waveform," Jour. Atmos. and Terrest. Phys. 14 (1959).

12. H. G. Hopkins and B. G. Pressey, "Current Direction-Finding Practice," Proc. IEE (London) Paper 2579R (March 1958).

13. H. G. Hopkins and L. G. Reynolds, "An Experimental Investigation of Short Distance Ionosphere Propagation at Low and Very Low Frequencies," Proc. IEE (London) Paper 1600R (1953).

14. F. Horner, "Radio Direction Finding," Wireless Engineer 30, 8 (August 1953).

15. F. Horner, "The Accuracy of the Location of Sources of Atmospherics by Radio Direction Finding," Proc. IEE (London) 101, Part III, No. 74, Paper 1709 (November 1954).

16. F. Horner and C. Clarks, "Some Waveforms of Atmospherics and Their Use in the Location of Thunderstorms," Jour. Atmos. and Terrest. Phys. 7, pp. 1-13 (1955).

17. F. Horner and J. Harwood, "An Investigation of Atmospheric Radio Noise at Very Low Frequencies," Proc. IEE (London) Part B, Paper 2147R (November 1956).

18. F. Horner, "The Measurement of Atmospheric Noise," Annals of IGY, Vol. III, Parts II, III, and IV (1957).

19. F. Horner, "The Relationship Between Atmospheric Radio Noises and Lightning," Jour. Atmos. and Terrest. Phys. 13, pp. 140-154 (1958).

20. J. R. Johler and L. C. Walters, "Transmission of a Ground Wave Pulse Around a Finitely Conducting Spherical Earth," National Bureau of Standards Report 5566 (17 April 1958).

21. H. L. Jones, "A Sferic Method of Tornado Identification and Tracking," Bull. Amer. Meteorol. Soc. 32 (December 1951).

22. Atsushi Kimpara, "The Waveform of Atmospherics in Daytime," URSI Proceedings, Vol. VIII (1950).

23. Atsushi Kimpara, "Origin of Atmospherics in the Far East," URSI Proceedings, Vol. VIII (1950).

24. Atsushi Kimpara, "Correlation of Atmospherics with Weather Phenomena," URSI Proceedings, Vol. VIII (1950).

25. F. A. Kitchen and K. W. Tremellen, "A Review of Present Knowledge of the Ionospheric Propagation of Very Low, Low, and Medium Frequency Waves," Proc. IEE (London), Paper 1463R (December 1952).

26. Myron G. H. Ligda, "The Radar Observation of Lightning," Jour. Atmos. and Terrest. Phys. 9, Nos. 5/6, pp. 329-346 (1956).

27. R. G. Stansfield, "Statistical Theory of Direction Finding," Proc. IEE (London)

28. B. A. P. Tantry and R. S. Srivastava, "Waveforms of Atmospherics with Superimposed Pulses Recorded with an Automatic Atmospheric Recorder," Jour. Atmos. and Terrest. Phys. 13, pp. 38-42 (1958).

29. B. A. P. Tantry and R. S. Srivastava, "Polarization of Atmospheric Pulses Due to Successive Reflections from the Ionosphere," Jour. Geophys. Res. 63, 3 (September 1958).

30. J. R. Wait, "On the Mode Theory of VLF Ionospheric Propagation," National Bureau of Standards Report 5022 (10 October 1956).

31. J. R. Wait, "An Extension to the Mode Theory of VLF Ionospheric Propagation," National Bureau of Standards Report 5091 (3 June 1957).

32. J. R. Wait, "The Propagation of VLF Pulses to Great Distances," National Bureau of Standards Report 5513 (3 September 1957).

33. J. R. Wait, "A Study of VLF Field Strength Data--Both Old and New," National Bureau of Standards Report 6000 (August 20, 1958).